Spring 2015

Impact of biogenic volatile organic compounds on peroxyacetyl nitrate production in the southeast United States

Christopher John Groff
Purdue University

Graduate School Form 30
(Updated 11/20/2014)

PURDUE UNIVERSITY
GRADUATE SCHOOL
Thesis/Dissertation Acceptance

This is to certify that the thesis/dissertation prepared

By Christopher J. Groff

Entitled IMPACT OF BIOGENIC VOLATILE ORGANIC COMPOUNDS ON PEROXYACETYL NITRATE PRODUCTION IN THE SOUTHEAST UNITED STATES

For the degree of Master of Science

Is approved by the final examining committee:

Paul B. Shepson

Peter T. Kissinger

Timothy Zwier

To the best of my knowledge and as understood by the student in the Thesis/Dissertation Agreement, Publication Delay, and Certification/Disclaimer (Graduate School Form 32), this thesis/dissertation adheres to the provisions of Purdue University's "Policy on Integrity in Research" and the use of copyrighted material.

Paul B. Shepson

Approved by Major Professor(s): _____

_____

Approved by: R. E. Wild 04/17/2015

Head of the Department Graduate Program Date

IMPACT OF BIOGENIC VOLATILE ORGANIC COMPOUNDS ON PEROXYACETYL NITRATE PRODUCTION IN THE SOUTHEAST UNITED STATES

A Thesis

Submitted to the Faculty

of

Purdue University

by

Christopher John Groff

In partial Fulfillment of the

Requirements of the Degree

of

Master of Science

May 2015

Purdue University

West Lafayette, Indiana

In loving memory of AFG and MJG, I know you would have been proud.

ACKNOWLEDGMENTS

I have found without the help of many, the production of this thesis would not have been possible. To my advisor, Dr. Paul Shepson, I thank you for all the guidance you have shared with me. During my toughest times in graduate school you showed me how to pick myself up and to never give up on myself. I would also like to thank my fellow group members for their support and friendship throughout my years at Purdue. To Dr. Kevin McAvey, Dr. Joel Rindelaub and Fulizi Xiong, I owe my deepest gratitude for their leadership and expertise that was essential to finishing this thesis. To Angela Raso and Olivia Salmon, thank you for our conversations that helped keep an anti-social graduate student sane. To my committee members, Dr. Timothy Zwier, Dr. Peter Kissinger and Dr. Hillka Kentamaa, thank you for your time and input on this thesis.

Special thanks go to several of my advisors from my undergraduate institution, Purdue University Calumet. To Dr. Harold (Hal) Pinnick and Dr. Alan Szeto, my undergraduate academic advisors, I thank you both for your continued support in my academic and professional life. Also, to Jon Aros, thank you for your encouragement and showing me that one can follow their aspirations beyond the classroom. The support I received from my undergraduate institution was essential to my success in graduate school, and I look forward to future conversations with all of you!

I am forever indebted to two very special people in my life. I would not be where I am today without the upbringing my parents provided me. You both have sacrificed so much to help me achieve my goals, and I am grateful for everything I have been able to enjoy so far because of that. To my brothers, I am sorry I was the spoiled little brother that I was. I admit, in writing, that I became extremely skilled at avoiding yard work at your expense. However, not everyone has two older brothers to look up to and I thank you for always being there and supporting me as the two best friends I could ever have. When I'm rich and famous, I will try to repay you both for the laborious struggles you faced in our youth, pun intended.

Finally, to my fiancée, Mariah, thank you for being my inspiration to push forward every day of my life. I could never have reached my maximum potential without you. On to our next adventure together!

TABLE OF CONTENTS

Page

Page

LIST OF TABLES

Tables Page

LIST OF FIGURES

Figure Page

ABSTRACT

Groff, Christopher John. M.S., Purdue University, May 2015. Impact of Biogenic Volatile Organic Compounds on Peroxyacetyl Nitrate Production in the Southeast United States. Major Professor: Paul B. Shepson.

Our atmosphere is arguably the fundamental entity that has made life on Earth possible. Knowledge of the delicate nature of our atmosphere continues to spread as "green" initiatives promote awareness of human influence on the environment. However, many climate scientists fear that unless immediate mitigation occurs, the reversal of human impact on our planet will be impossible, leading to unknown consequence. Perturbations to natural processes are likely to cause drastic change to the planet as we know it and ultimately result in significant health issues. It is important to push the boundaries of our understanding of atmospheric processes with intent to reduce the impact human activity has already imposed. This work focuses on the production of peroxyacetyl nitrate (PAN), a compound known for its adverse effects on plant life and human health, in two parts; (1) using relative production ratios to calculate relative PAN production using a chemical tracer, and (2) application of an explicit chemical model in simulating relative production of PAN in a southeastern US forest environment.

Chapter two examines our current understanding of the isoprene photo-oxidation mechanism particularly in regards to the formation of two peroxyacyl nitrates: PAN and

MPAN. A relationship when production is greater than loss processes between MPAN and PAN was found to be relatively constant throughout the experiment with a ratio of MPAN/PAN of 1.5 $\pm$ 19% RSD. This relationship can be used in ambient conditions to approximate isoprene contribution to PAN production, since MPAN is formed solely through isoprene oxidation. Absolute concentrations of isoprene nitrates and APNs are found to be significantly oversimulated. This shows an incomplete understanding of the isoprene oxidation mechanism and begs for continued studies to further our understanding of this chemical system.

Chapter three applied the observed ratio of MPAN/PAN within the chamber experiment to an ambient calculation to approximate isoprene contribution to PAN production in the SOAS campaign. Results show that an average of 44% ± 16% of PAN production results from the oxidation of isoprene. Further analysis using a 0-D ambient model show isoprene contributes 50-70% to PAN production, which statistically is not different from calculations using MPAN/PAN ratio from chamber experimentation.

Chapter four reflects on the results of this study to provide insight to the future of the field. Suggestions for future studies to improve understanding of the PAN mechanism are presented, as well as suggestions for future ambient modeling with a transport model.

CHAPTER 1: INTRODUCTION

1.1 Earth's Atmosphere and Global Radiative Balance

If we were able to condense the Earth's atmosphere to standard temperature and pressure (STP), the thickness of Earth's atmosphere would be approximately 8 km. Considering the mean radius of Earth to be ~6,400 km, the atmosphere composes only ~0.125% of the mean radius. Despite its relatively small size, the atmosphere is an essential entity that makes all life on the planet is possible. The atmosphere's ability to sustain life can be attributed to Earth's atmospheric composition, which is unlike any known planetary body. Relative to Venus and Mars (our nearest planetary neighbors), Earth's atmosphere contains an extremely small amount of CO2 and comparatively large amounts of N2 and O2 [Holloway and Wayne, 2010]. However, it is this unique composition that accounts for the atmosphere's ability to absorb harmful radiation and prevent temperature fluctuations that would otherwise cause all life on Earth to perish.

Our planet is hospitable to life due to its ability to maintain temperatures in a narrow range about the global average of 14 ^{0} C [Jones et al., 1999]. The process that helps maintain hospitable temperatures is referred to as Earth's energy balance and it accounts for the balance between shortwave radiative energy received from the Sun and outgoing infrared (IR) long wave radiation escaping to space. Before the 1960s little about the energy balance was understood, as the ability to make direct observations was

limited. However, the onset of the space age created a breakthrough due to satellite remote sensory abilities. Among the first observations was a determination of the planet's albedo, or the ratio of outgoing flux of solar energy to incoming flux from the Sun, about 30% [Vonder Haar, 1971]. It is known that the atmosphere plays an integral role at maintaining surface temperatures due to its influence on the energy balance. Figure 1.1 illustrates the current understanding of Earth's Energy budget from 2000-2010. The term greenhouse effect, in relation to the energy budget, refers to the Earth's ability to absorb outgoing infrared radiation within the atmosphere by greenhouse gases such as H_2O and CO_2. A current estimation during the years of 2000-2010 reports an energy imbalance of 0.6 W/m^2, although the uncertainty associated with this value calls for improvements of methods for measuring individual heat fluxes. [Stephens et al 2012]. One thing is for certain, as greenhouse gases accumulate in the atmosphere, more radiative energy is absorbed and reflected back to the surface, resulting in higher temperatures. The current net increase in temperature is estimated to be rising at a rate of 0.15-0.20 ^{0} C every decade [Hansen et al 2010]. Figure 1.2 illustrates the increase of greenhouse gases over the past 200 years from Antarctic ice core data. There is a positive correlation between population growth and the increase in greenhouse gases. These increases are largely in part due to the onset of the industrial revolution and human combustion of fossil fuels [IPCC 2014].

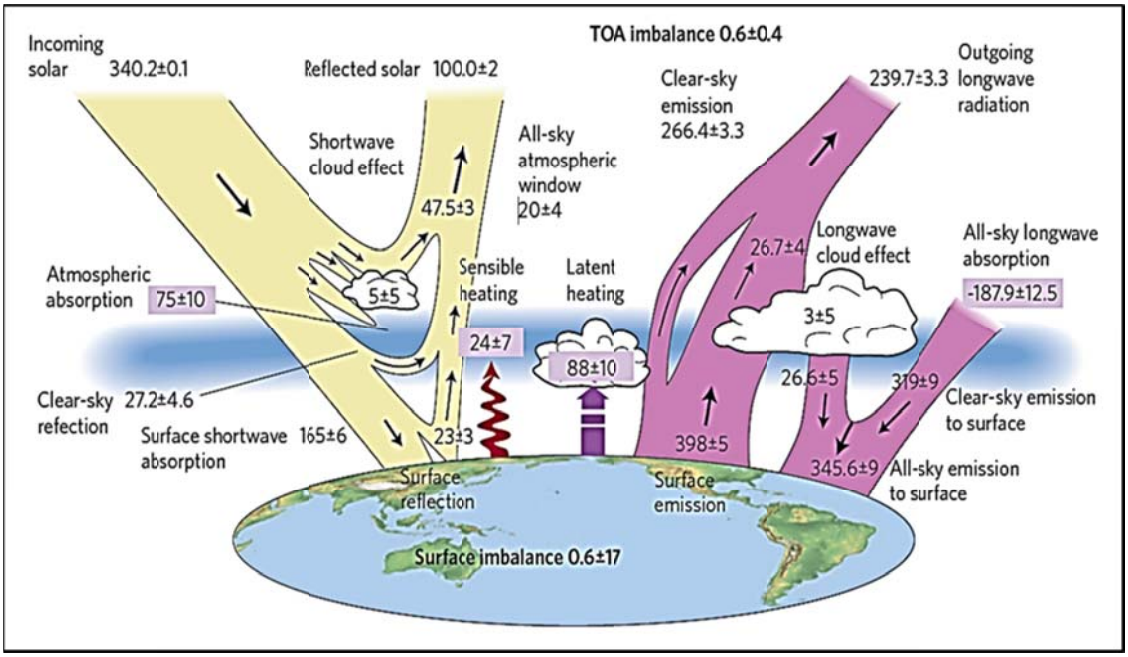

Figure 1.1 – Earth's energy budget for the years 2000-2010. Fluxes are presented with units of W/m^2 [Stephens et al 2012]

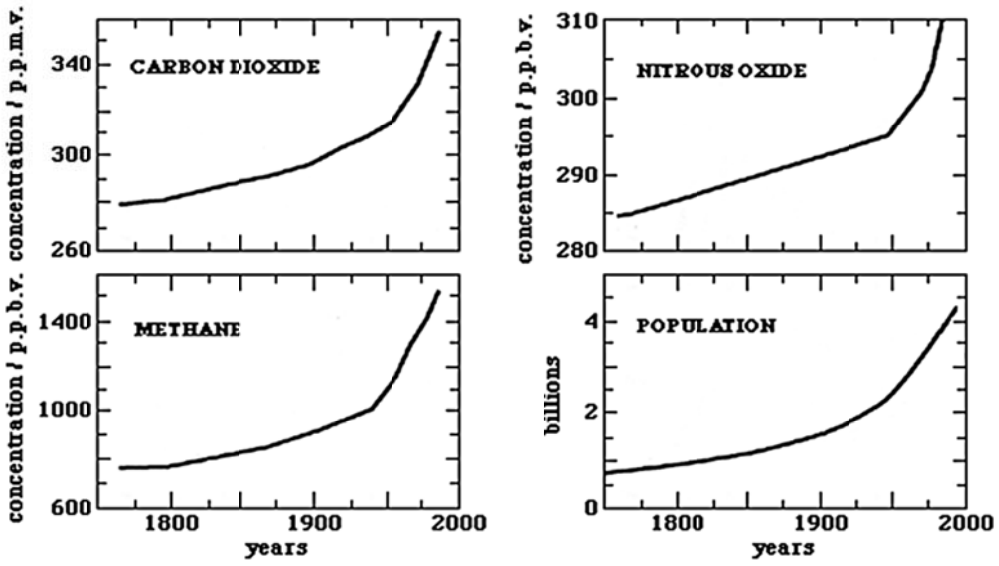

Figure 1.2 – Antarctic ice core data showing the increase in greenhouse gases over the past 200 years. The population trend is included for comparison [Lorius et al., 1992].

1.1.1 Atmospheric Layers

The Earth's atmosphere is comprised of multiple layers, which are characterized by increases or decreases in temperature as a function of pressure or altitude as indicated in Figure 1.3. Within the troposphere, atmospheric temperature tends to decrease with height except in the presence of a temperature inversion which is defined as the tropopause. This temperature inversion is caused by elevated warm air masses acting as a cap to prevent underling colder dense air from mixing upward. The warm air mass just above the tropopause in the stratosphere is caused by the exothermic chemical interactions of the ozone layer, discussed in further detail below. The increase in thermosphere temperature is due to absorbance of N_2 and O_2 and atomic species at wavelengths < 200 nm [Finlayson-Pitts and Pitts, 2000].

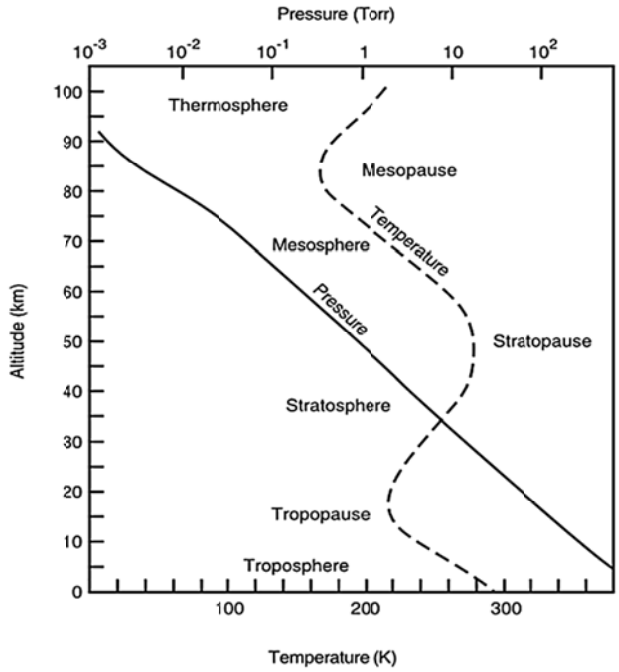

Figure 1.3 Depiction of atmospheric layers as a function of altitude and corresponding temperature and pressure [Finlayson-Pitts and Pitts, 2000]

The upper atmosphere can be characterized as all layers above the tropopause. The thermosphere layer is responsible for removing solar radiation at wavelengths below 200 nm. This is due to the strong absorption characteristics of N_2 and O_2 at these wavelengths. The stratosphere absorbs radiation of wavelengths 200-310 nm, due to the presence of ozone and some overlap of diatomic oxygen. This ozone maintains steady state concentration by a process known as the "Chapman cycle". The cycle as predicted by Sir Sydney Chapman is shown in Reactions 1.1 to 1.4 [Finlayson-Pitts and Pitts, 2000].

$$O_2 + h\nu \rightarrow 2O(^3P) \qquad (1.1)$$

$$O(^3P) + O_2 (+M) \rightarrow O_3 + \text{heat } (+M) \qquad (1.2)$$

$$O(^3P) + O_3 \rightarrow 2O_2 \qquad (1.3)$$

$$O_3 + h\nu \rightarrow O(^1D) + O_2 \qquad (1.4)$$

This band of ozone in the stratosphere is commonly referred to as the ozone layer. The upper atmosphere is vital in the process of eliminating harmful short wave radiation since wavelengths below 310 contain enough energy to break carbon-carbon bonds, e.g. those in DNA. The upper atmosphere's ability to remove radiation of less than 310 nm implies only chemical species that absorb at longer wavelengths than 310 nm are important to photochemistry in the troposphere.

Figure 1.4 illustrates the full spectrum of Earth's atmosphere to better illustrate the absorption properties of the atmosphere. Although diatomic oxygen and ozone are weak at absorbing in the infrared region, they are extremely efficient at absorbing harmful ultraviolet (UV) radiation (< 310 nm). On the contrary, greenhouse gases such as H_2O and CO_2 are effective at absorbing radiation in the IR region of the spectrum, but

do not absorb in the UV. These two systems work together to remove harmful radiation before it hits the planetary surface, as well work to maintain Earth's global average temperature.

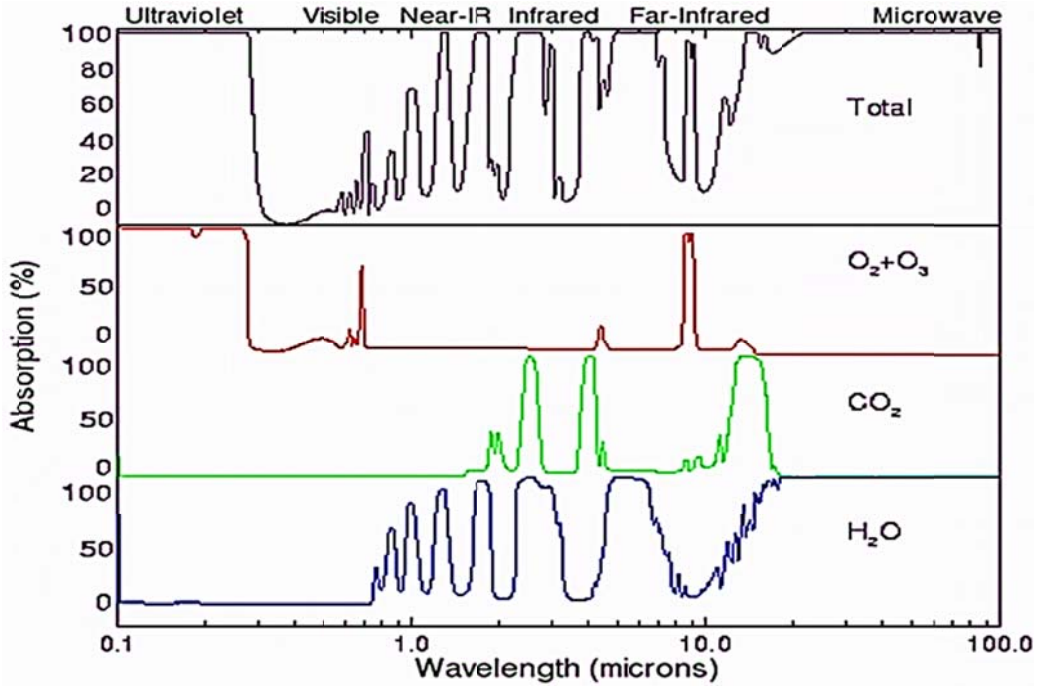

Figure 1.4 – Total and individual absorbance spectrum for several species found within the atmosphere with units of % absorbance. [Howard, 1959]

Due to our everyday experience close to the ground, we are most familiar with the layer of air that is nearest to the Earth's surface known as the troposphere. The troposphere is defined by two distinct layers, the boundary layer nearest to the surface and the free troposphere (also known as free atmosphere) above it. The atmospheric boundary layer (ABL) reacts to surface forces on a time scale of about 1 hour and is constrained by the surface and a temperature inversion 100 to 3,000 m above ground. There is a strong absorption effect of radiation at the Earth's surface, resulting in warmer

temperatures near the surface and a temperature decrease as a function of height known as a lapse rate (dry adiabatic lapse rate = ~10 K/km. This decreasing temperature gradient with altitude in the troposphere enables air masses to rise buoyantly as long as the measured lapse rate is equal to or exceeds the adiabatic lapse rate. This upward mixing allows chemical species to transport vertically within air parcels on a time period of a few hours to a few days to the tropopause. People are most familiar with this layer, as it is responsible for the local microclimates and wind patterns that are experienced on a day to day basis. Physical forcings within the ABL directly influence local chemistry due to transport, dilution effects, emission from vegetation or anthropogenic sources, and photochemistry via radiation. A complete description of the diurnal variation of the ABL is outlined in the next section.

1.1.2 Diurnal Variation of Atmospheric Boundary Layer

The ABL demonstrates a diurnal cycle due to the influence of solar radiation as illustrated in Figure 1.5. During midday, the ABL reaches a maximum height correlating strongly to solar radiation heating the surface. Surface warming and interaction with the Earth's surface create turbulent and buoyant forces that vertically mix air parcels within the boundary layer, known as the convective mixed layer. Decline in solar radiation at the end of day results in the subsidence of the ABL height and formation of a smaller (and less defined) nighttime stable boundary layer (SBL, ~100 m) due to the emission of heat from the surface. The formation of a new boundary layer causes an isolated air mass between the capping inversion and nighttime SBL to form, referred to as the residual layer. Nighttime meteorological processes are not well understood and are significantly

more difficult to constrain due to less predictable turbulent events. After sunrise, the residual layer breaks up and mixes downward as the surface is heated and the ABL begins to grow. The ABL height varies from about 1 km to 6 km dependent on time of year and geographical location [Stull, 1988].

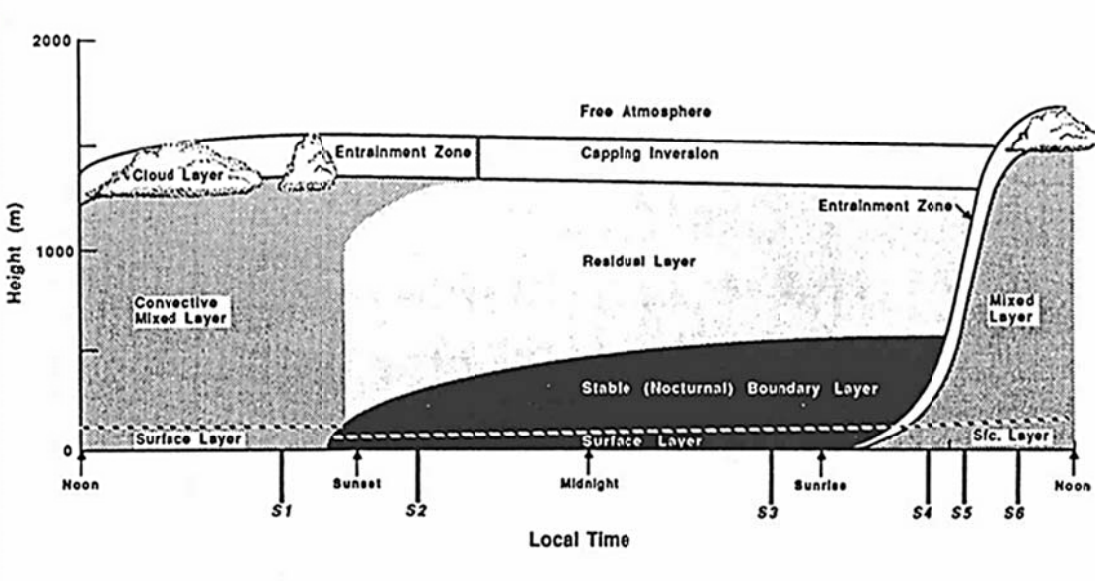

Figure 1.5 – Illustration of the diurnal evolution of the ABL [Stull, 1988].

The BL is important to air quality since it is here that various biogenic and anthropogenic pollutants can accumulate. Escaping the BL via means of vertical mixing can take anywhere from hours to days. Therefore, chemical species with lifetimes on the order of days to months can experience long range transport throughout the troposphere. This transport process leads to cases in which species that are longer lived influence chemistry in remote areas with varying effect. Instances like this make mitigation and

policy enforcement difficult since the origin of these long lived chemical species are often difficult to determine.

1.2 Ozone and Reactive Nitrogen

Ozone, although vitally important to absorb harmful radiation in the upper atmosphere, can be harmful to human and plant health when near-surface concentrations are high [Tilton, 1989]. Ozone is known to be a respiratory irritant, causing decreased lung function and exacerbation of chronic respiratory conditions (e.g., asthma) during short term exposure [Bell et al., 2004]. Ozone exposure to vegetation is known to have damaging effects due to oxidation chemistry in the presence of ozone [Hewitt and Kok, 1991].

There are only two known sources of ozone within the troposphere, transport of stratospheric ozone and production from gas phase reactions [Terao et al., 2008]. Downward mixing from the stratosphere contributes only ~9% to the total tropospheric ozone concentration [Wang et al., 1998]. Therefore, the majority of tropospheric ozone is due to gas phase chemical processes. NO_2 in the atmosphere is anthropogenic in nature mainly formed from combustion of fossil fuels, with a minor natural component due to lightning and biomass burning [Finlayson-Pitts and Pitts 2000]. Reaction 1.5 involving NO_2 photolysis is the dominant source of ozone within the troposphere, via production of $O(^3P)$ which can subsequently react with O_2 to form ozone as seen previously in Reaction 1.2. However, the resulting NO can also react with ozone, leading to no net ozone production (Reaction 1.6).

$$NO_2 + h\nu \rightarrow O(^3P) + NO \quad (1.5)$$

$$NO + O_3 \rightarrow NO_2 + O_2 \quad (1.6)$$

In addition to ozone, the HO_2 radicals and organic peroxy radicals (RO_2) also convert NO to NO_2 (Reactions 1.6-1.7).

$$NO + HO_2 \rightarrow NO_2 + O_2 \quad (1.7)$$

$$NO + RO_2 \rightarrow NO_2 + RO\cdot \quad (1.8)$$

These reactions can then be followed photolysis of NO_2 via Reaction 1.5 and the resulting $O(^3P)$ can react with diatomic oxygen to form ozone (Reaction 1.2). In the case of Reactions 1.6-1.7, a net ozone production occurs since ozone destruction was not required to convert NO to NO_2.

Despite the health implication near surface ozone presents, it is a vital part of the natural self-cleaning process of the atmosphere. During ozone photolysis (Reaction 1.4), the production of $O(^1D)$ can result in the reformation of ozone via Reactions 1.9 and 1.3 or react in the present of water vapor to produce hydroxyl (OH) radicals as seen in Reaction 1.11.

$$O(^1D) + M \rightarrow O(^3P) \quad (1.9)$$

$$O_3 + h\nu \rightarrow O_2 + O(^1D) \quad (1.10)$$

$$O(^1D) + H_2O \rightarrow 2\cdot OH \quad (1.11)$$

Reactions 1.11-1.12 demonstrate how volatile organic compounds (VOCs, shown as RH) can react with OH radicals in the presence of oxygen to produce RO_2. Recall from Reaction 1.7 that RO_2 radicals have the oxidative ability to convert NO to NO_2.

$$RH + \cdot OH \rightarrow R\cdot + H_2O \qquad (1.11)$$

$$R\cdot + O_2 \rightarrow RO_2 \qquad (1.12)$$

Ozone photolysis has the potential of producing two OH radicals. In the presence of VOCs, an OH radical has the potential of producing two new NO_2 molecules. The first NO_2 is produced when the resulting RO_2 is converted to an alkoxy radical ($RO\cdot$) via Reaction 1.8. Alkoxy radicals are known to release HO_2 upon rearrangement, thus potentially producing a second NO_2 molecule via Reaction 1.7. These NO_2 molecules can result in the production of two ozone molecules, the only way a net ozone production is possible within the troposphere. The limiting reagent in this system in a forest environment where VOC concentrations are high is the concentration of NO. Therefore, understanding of NO_x concentrations and transport is vitally important due to the implications on the impact of tropospheric ozone concentrations.

1.3 Isoprene

Understanding that VOCs play an integral role in tropospheric ozone production, it is important to identify key compounds and the impact potential individual species have on local chemistry. Isoprene (C_5H_8, 2-methyl-1,3-butadiene) emitted from vegetation is identified as the most abundant non-methane BVOC found in the troposphere accounting for 44% of all naturally emitted BVOCs [Guenther et al., 1995]. Due to unsaturation within the molecule, it rapidly oxidizes in the atmosphere and therefore has a significant impact on ozone production and available reactive nitrogen within the troposphere [Atkinson and Ashmann, 1984]. Figure 1.6 shows that oxidation of isoprene leads to production of isoprene derived RO2 radicals which can convert NO

to NO2, effectively producing ozone. Alternately, oxidation products of isoprene are also involved in the production of organic nitrates which effectively acts as a NOx sink [Ziemann and Atkinson, 2012]. There is still disagreement on isoprene nitrate yields, with reported yield ranges varying between 4.4 to 15% [Tuazon and Atkinson, 1990; Chen et al., 1998; Chuong and Stevens, 2002; Patchen et al., 2007; Paulot et al. 2009; Lockwood et al., 2010; Xiong et al., 2015]. Therefore, isoprene's effectiveness as a reactive nitrogen sink is not fully understood. Chapter 2 explores the current understanding of the isoprene photo oxidation mechanism in relation to total measured data with an employed IN yield of 11% from a recent study [Xiong et al., 2015].

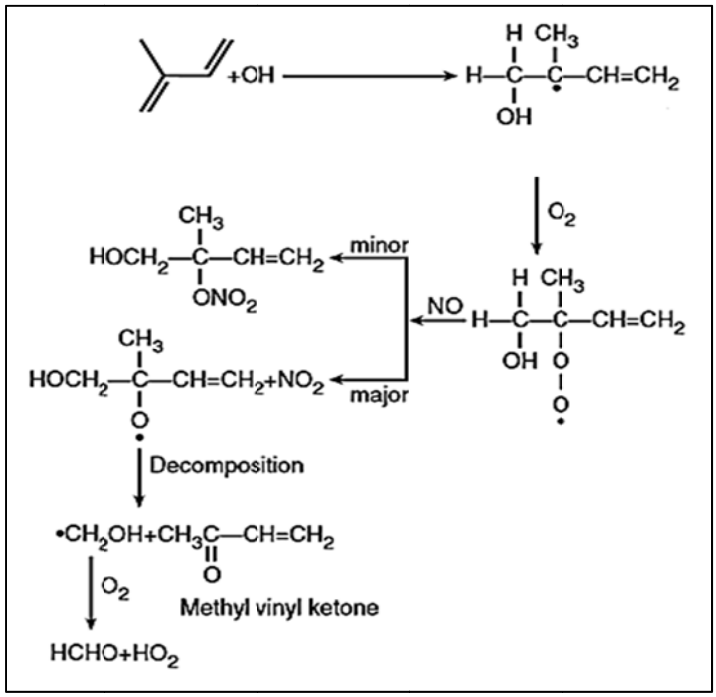

Figure 1.6 - Example isoprene and OH oxidation pathway. [Finlayson-Pitts and Pitts, 2000]

1.4 Peroxyacyl Nitrates

Organic nitrates can act as a sink for reactive nitrogen within the atmosphere. Understanding of these nitrates as a sink is imperative to understanding the influence to ozone production in the atmosphere. One class of organic nitrates, known as acyl peroxy nitrates ($RC(O)OONO_2$, APNs, also peroxyacyl nitrates), are known to be important due to their unique reactivity in the atmosphere. The decomposition of these compounds is highly temperature sensitive. Therefore, under lower temperatures (such as those at higher altitudes within the troposphere) APNs can act as a vehicle for long range transport of reactive nitrogen. Upon decomposition, NO_x is released back into the atmosphere, which can result in an enhanced production of ozone.

Perhaps the most important APN, peroxyacetyl nitrate ($CH_3C(O)OONO_2$, PAN) is estimated to make up ~80% of total APNs [Roberts et al., 2007]. The complication of understanding PAN formation resides within its precursor chemistry. Many VOCs in the atmosphere can oxidize to form the peroxyacetyl radical ($CH_3C(O)OO\cdot$, PA). Figure 1.7 shows the chemistry of several species thought to be important precursors to PAN production [LaFranchi et al., 2009]. Although PAN is a highly studied molecule due to the health implications it poses as a lachrymator, mutagen, as well as having phytotoxic properties [Stephens, 1969; Temple and Taylor, 1983; Kleindienst et al., 1990; Altshuller, 1993; Heddle et al., 1993], the relative contributions of explicit sources of PAN are not well understood. The fact that most VOCs in the atmosphere can decompose to form PA radicals poses an issue of identifying important contributors to local PAN production. Direct observation of local PAN production is additionally problematic, due to the potential of PAN background concentrations from long range transport. This thesis aims

to identify key precursors from local chemistry in a southeastern United States rural environment.

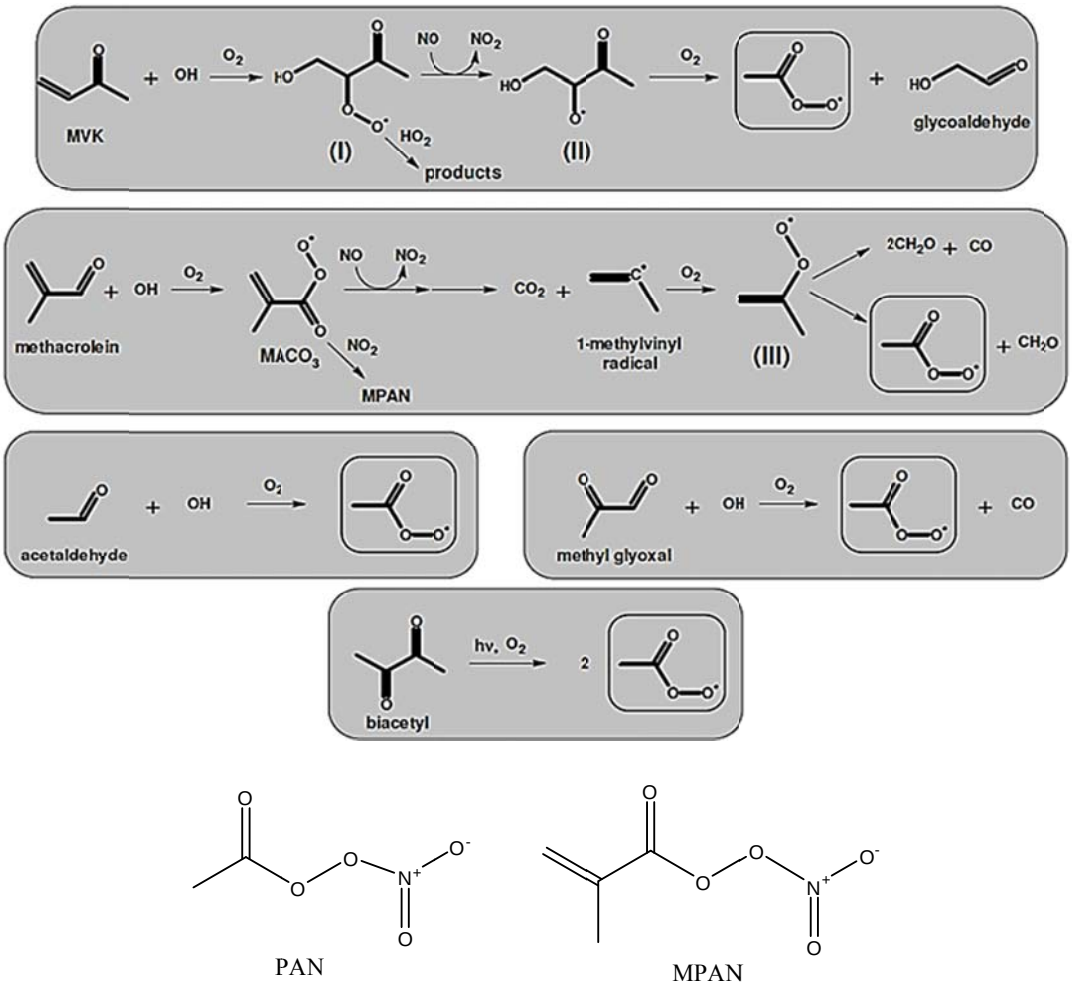

Figure 1.7 – Chemistry of several species leading to the formation of PA radicals [LaFranchi et al., 2009]. Structures of PAN and MPAN are also provided.

Another APN of interest for this study is methacryloyl peroxy nitrate ($CH_2C(CH_3)C(O)OONO_2$, MPAN). MPAN is known to be exclusively formed from the oxidation of methacrolein (MACR) as seen in Figure 1.7. With formation of MACR being exclusively due to oxidation of isoprene during the summer [Bertman and Roberts,

1991] this study addresses the potential of MPAN as a tracer for isoprene contribution to PAN production. The relationship between MPAN and PAN production via isoprene oxidation is explored further in chapter 2 through an isoprene/NO_x chamber photooxidation experiment carried out in May 2013. Using the observed production ratio, Chapter 3 demonstrates a simple calculation that allows an estimate of PAN production from isoprene in ambient conditions when concentrations of MPAN and PAN are both increasing.

1.5 Research Objectives

The objective of this thesis was to improve the understanding of PAN production within a mixed forested environment via 0-D simulations of VOC oxidation chemistry. We address this problem by asking the scientific question, what are the important precursors to PAN production within a forested environment in the southeast United States? This question is approached in two ways: 1) estimation of isoprene contribution to PAN production using MPAN as a tracer and 2) 0-D simulation of relative contribution to peroxyacetyl radicals using measured constraints.

Chapter two explores the relationship of the relative production of PAN and MPAN derived from a chamber study involving isoprene oxidation in the presence of NO_x. Several key species were monitored so that assessment of production and loss processes were possible. In order to evaluate the current understanding of the isoprene oxidation mechanism, a near-explicit 0-D photochemical box model was employed to simulate oxidation chemistry of isoprene within a photochemical reaction chamber. In addition to model validation, a relationship between MPAN and PAN production during

isoprene oxidation was observed and reproduced during simulations. We hypothesize that a relative PAN and MPAN production ratio during periods of isoprene oxidation can be assumed in ambient conditions in order to approximate relative isoprene contribution to total PAN production.

Chapter three aims to identify important precursors to PAN production within a southeastern US forested environment in conjunction with the SOAS field campaign. The MPAN/PAN production ratio established in Chapter 2 is employed to calculate a relative PAN production due to isoprene oxidation. Additionally, a modified 0-D model from Chapter 2 incorporates terpene oxidation chemistry for simulation of ambient conditions in an attempt to identify relative contributions to PAN production by isoprene, terpenes, acetone, and acetaldehyde. Discrepancies between simulated and calculated isoprene contribution to PAN production are explained through further analysis.

Chapter four briefly discusses the current state of atmospheric science related to PAN production, as well as provides suggestion of future work within the field.

CHAPTER 2: A STUDY OF PAN AND MPAN PRODUCTION DURING ISOPRENE PHOTO-OXIDATION, A COMPARISON BETWEEN MEASUREMENTS AND MODEL

2.1 Introduction

Isoprene (C_5H_8, 2-methyl-1,3-butadiene) is the non-methane biogenic volatile organic compound (BVOC) with the largest global emission. On a global scale, it is emitted at a rate of ~500 Tg C/yr, making up 44% of all global BVOC emissions [Guenther et al., 1995]. Oxidation of isoprene occurs at the gas kinetic limit with hydroxyl radicals (OH) [Atkinson and Ashmann, 1984], with subsequent oxidation products having a major influence on the chemistry within the atmospheric boundary layer [Biesenthal et al., 1997b]. Specifically, it is known that isoprene oxidation chemistry can have significant influence on ozone formation. In the presence of NO_x (NO_2 + NO), isoprene oxidation can lead to ozone production via Reactions 2.1-2.4. Some of the time isoprene reaction with NO_x can form an isoprene hydroxy nitrate (IN, or isoprene nitrate) compound, thus creating a sink for available NO_x as seen in Reaction 2.2b.

$$C_5H_8 + OH\ (+O_2) \rightarrow HOC_5H_8OO\cdot \qquad (2.1)$$

$$HOC_5H_8OO\cdot + NO \rightarrow HOC_5H_8O\cdot + NO_2 \qquad (2.2a)$$

$$HOC_5H_8OO\cdot + NO \rightarrow HOC_5H_8ONO_2\ \text{(isoprene nitrates)} \qquad (2.2b)$$

$$NO_2 + h\nu \rightarrow NO + O(^3P) \quad (2.3)$$

$$O(^3P) + O_2 \rightarrow O_3 \quad (2.4)$$

IN influence on ozone formation is dependent on the overall isoprene nitrate yield [Wu et al., 2007]. Reported values from 4.4 to 15% leave IN yields a continued topic of discussion [Tuazon and Atkinson, 1990; Chen et al., 1998; Chuong and Stevens, 2002; Patchen et al., 2007; Paulot et al. 2009; Lockwood et al., 2010; Xiong et al., 2015]. Therefore, IN influence on the sequestration of reactive nitrogen and inhibitor of ozone production is still not fully understood.

In addition to IN production, ozone is further influenced by isoprene oxidation via the production of peroxyacyl nitrates ($RC(O)OONO_2$, APNs), which can also lead to NO_x sequestration. These compounds have the ability, depending on their reactivity and overall stability, of acting as a long range transport vehicle for reactive nitrogen [Singh and Hanst, 1981]. Peroxyacyl nitrates are thermally sensitive species, which releases NO_2 in a unimolecular decomposition process (Reaction 2.5) that is exponentially temperature dependent [Kleindienst 1994], as shown in the Arrhenius expression (Equation 2.6).

$$RC(O)OONO_2 \leftrightarrow RC(O)OO\cdot + NO_2 \quad (2.5)$$

$$K_f = 2.52 \times 10^{16}\, e^{-13573/T}\ s^{-1} \quad (2.6)$$

Therefore, regions subject to lower NO_x conditions can be influenced by this release of NO_x, causing an enhancement in ozone production to occur. Understanding the production and loss processes for these species is fundamentally important for mitigation purposes in efforts to improve air quality.

For this study, we explore the relationship of two APNs, peroxyacetyl nitrate (PAN) and methacryloyl peroxy nitrate (MPAN). PAN is approximated to make up ~80% of total APNs within the atmosphere [Roberts et al., 2007]. It is a known lachrymator, cancer mutagen, and can be toxic to plant life [Stephens, 1969; Temple and Taylor, 1983; Kleindienst et al., 1990; Altshuller, 1993; Heddle et al., 1993; DeMarini et al., 2000]. The precursor chemistry for the production of PAN is very complicated, since most VOCs can oxidize to form the peroxy acetyl radical precursor (PA) [LaFranchi et al., 2009]. Figure 1.7 shows just five possible precursors thought to be important to PA radical production. In contrast, methacryloyl peroxy nitrate (MPAN) is known to formed exclusively through oxidation of methacrolein (MACR) shown in Figure 1.7 [Bertman and Roberts, 1991]. This unique formation property makes MPAN a potentially valuable tracer for isoprene oxidation chemistry since MACR is formed solely from oxidation of isoprene. In this chapter, we explore the possibility of using the relationship between the production of PAN and MPAN via isoprene oxidation to explore isoprene's role in PAN production.

2.1.1 Objectives

The objective of this experiment was to determine the relationship between the relative production of PAN and MPAN via photooxidation of isoprene within a photochemical reaction chamber. That isoprene-specific relationship can then be used to assess the isoprene contribution to PAN production in the ambient environment. We also aim to test our knowledge of the current isoprene oxidation mechanism with a near-explicit 0-D photochemical box model, and comparison to the chamber observation. This

mechanism is, to the best of our knowledge, the most up to date understanding of isoprene oxidation chemistry. To explore the mechanism performance, we compare overall simulated yields of INs and individual APNs measured during the experiment to measured concentrations. This comparison allows us to assess production and loss mechanisms for the species of interest for conditions with only one starting reactant and without the complexities of meteorology. Three simulation objectives were investigated: (1) the simulated total isoprene nitrate yield (2) the yield of PAN and MPAN within the system, and (3) determination of a production ratio between MPAN and PAN due to isoprene oxidation chemistry.

Figure 2.1 – Image of photochemical reaction chamber used for the May 2013 experiment [Costa, 2010].

2.2 Chamber Experimental

An isoprene/NO_x photo-oxidation experiment was conducted in May 5, 2013 in preparation for the Southern Oxidants and Aerosols Study field campaign. The photochemical reaction chamber (Figure 2.1) is a cylindrical 5.5 m^3 Teflon bag equipped with a mixing fan and UV lights as described in detail elsewhere [Chen et al., 1998; Espada et al., 2005; Lockwood et al., 2010; Rindelaub et al., 2015]. The spectral radiation output for the UV lamps is shown in Figure 2.2. Prior to the experiment, the chamber was flushed with hydrocarbon free air to remove contamination from previous experiments. Water was bubbled into the chamber under an ultra-pure air stream prior to experiments and water concentrations were monitored using a LICOR-7000 instrument. The relative humidity of the experiment was measured at 5%. Isoprene (3.38×10^{13} molecules/cm^3), nitric oxide (NO; 6.6×10^{12} molecules/cm^3) and nitrogen dioxide (NO_2; 5.1×10^{12} molecules/cm^3) were injected into the chamber along with a continuous 6 L/min flow of hydrocarbon free air to maintain pressure due to average instrument sampling. The reactants and products within the chamber were irradiated for approximately 4 hours, until ozone concentrations stopped increasing. Details of experimental chamber chemistry are explained further in Section 2.3.1 and 2.4.

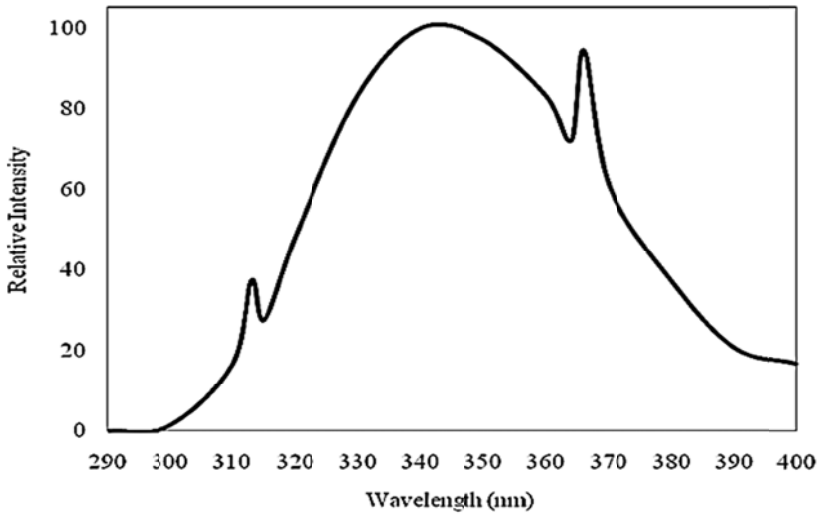

Figure 2.2 – Relative intensity vs. wavelength spectral output of UV solar simulator lamps.

2.2.1 Chamber Instrumentation

Isoprene measurements were obtained using a Shimadzu gas chromatograph equipped with a flame ionization detector (GC-FID), RTX-1 column (30 m, 0.53 mm i.d., 1.0 μm thickness) and isothermal oven temperature 155 deg. C [Chen et al., 1998]. A general schematic for the GC-FID is shown in Figure 2.3. Ozone concentrations were monitored using a UV absorption instrument from Thermo Environmental Instruments, Inc. (Model 49-003, Waltham, MD). Measurements of NO were obtained using a total reactive nitrogen instrument (TRENI), a NO chemiluminescence analyzer built with the assistance of the Jonathan Amy Facility for Chemical Instrumentation (JAFCI). NO is measured by detecting chemiluminescence of NO reaction with ozone via Reactions 2.7-2.8 using a photo multiplier tube (PMT) and a photon counting system.

$$NO + O_3 \rightarrow NO_2^* + O_2 \qquad (2.7)$$

$$NO_2^* \rightarrow NO_2 + h\nu \qquad (2.8)$$

The instrument can operate in several modes to also determine NO_y, NO_x, and NO_2 via their conversion to NO. For NO_2 measurements, NO_2 is converted to NO by a photolytic converter via Reaction 2.3. Total NO_x is then detected through Reactions 2.7-2.8 via PMT and a photon counting system. NO_2 measurements are defined as the difference between NO_x and NO concentrations. Total isoprene nitrates were measured using a chemical ionization mass spectrometer (CIMS) with operating procedures as described by Liao et al. [2011] and Xiong et al. [2015]. Individual peroxyacyl nitrates were measured using a custom gas chromatograph equipped with a Shimadzu GC mini-2 ^{63}Ni electron capture detector (GC-ECD) maintained at 55 deg. C, described in further detail in Pippin et al. [2001].

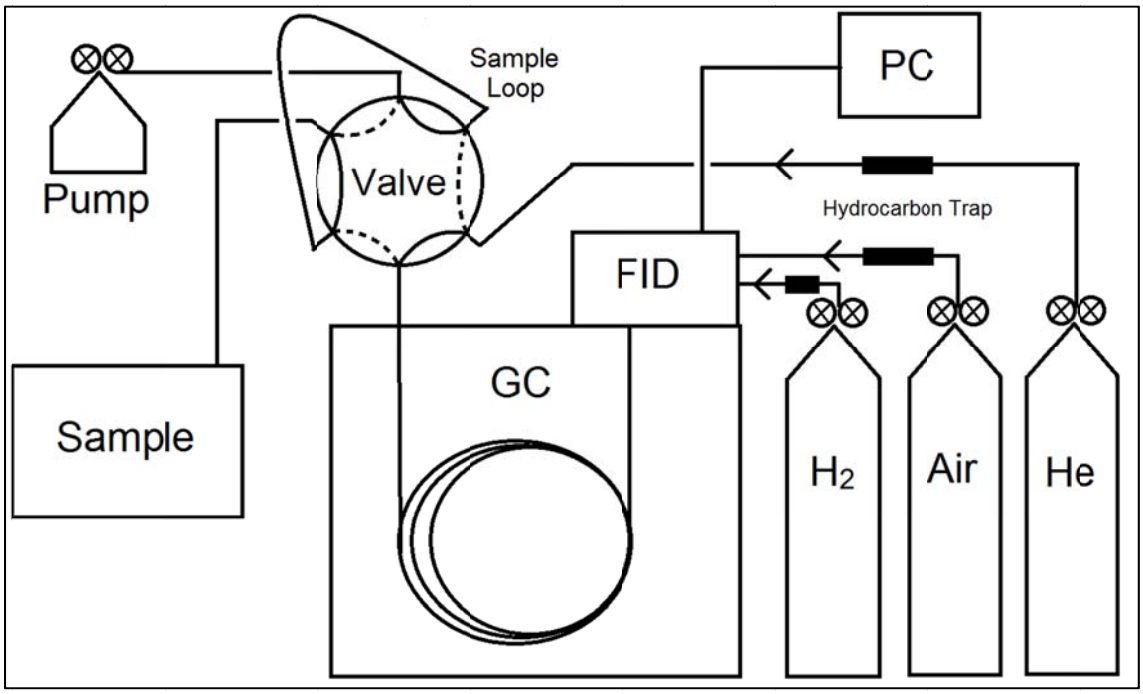

Figure 2.3 – General schematic for a gas chromatograph with flame ionization detector.

2.3 0-D Photochemical Model

A modified near-explicit photochemical models based on the Master Chemical Mechanism (MCM) v3.3 was generated to simulate a photochemical chamber experiment involving isoprene oxidation in the presence of NO_x. All simulations were processed using FACSIMILE, Version 4.2.50 (MCPA Software Ltd., Oxfordshire, UK). FACSIMILE is commercial software that solves a set of coupled ordinary differential equations (ODEs) using a predictor-corrector technique. The predictor-corrector process requires the program to predict solution vectors at the end of a defined time step, and then is corrected until the differential equations are satisfied by a few Newton iterations. The photochemical isoprene mechanism is a modified version of the isoprene subset available for download from the MCM v3.3 via website: http://mcm.leeds.ac.uk/MCM [Jenkin et al., 1997, and Saunders et al., 2003]. The model consists of 37 inorganic reactions, 1295 gas phase organic reactions, and 237 photolysis reactions. Appendix A provides a list of all reactions used in the isoprene oxidation mechanism. A general pathway for VOCs within the MCM subsets is outlined in a general reaction scheme of methane and 142 available NMVOCs' photochemical degradation as shown in Figure 2.4. Section 2.3.3 describes all modifications administered to the MCM v3.3 mechanism.

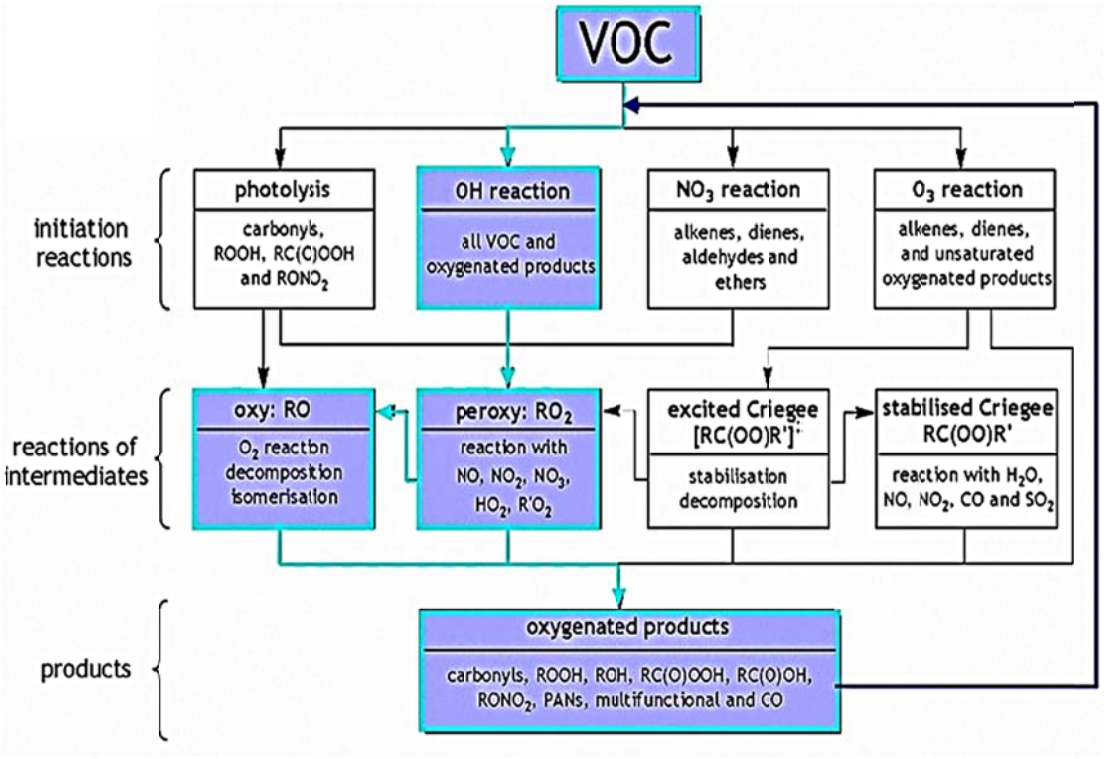

Figure 2.4 – General flow chart of VOC degradation within the MCM subsets. [Jenkin et al., 1997; Saunders et al., 2003]

2.3.1 General Reaction Scheme

As highlighted in Figure 2.4, much of the chemistry within the reaction chamber is dominated by the OH oxidation pathway due to its fast reaction rate relative to other oxidants. The OH oxidation is possible for all VOCs, either through hydrogen abstraction (alkanes) or addition to multiple bonds (alkenes, alkynes) as shown in Reactions 2.9-2.10.

$$CH_3CH_3 + OH \rightarrow CH_3CH_2\cdot + H_2O \qquad (2.9)$$

$$CH_2{=}CH_2 + OH \rightarrow \cdot CH_2CH_2\text{-}OH \qquad (2.10)$$

The resulting carbon centered radical can then react in the presence of oxygen to form a peroxy radical (RO_2).

NO_3 reactions also follow a similar process, although NO_3 reactions within the mechanism are limited to VOCs such as alkenes, dienes, aldehydes and ethers. In the case of alkenes and dienes, NO_3 adds across the double bond, ultimately forming a nitrogen containing RO_2. Hydrogen abstraction occurs in the case of aldehydes and ethers, resulting in the production of HNO_3. Simple examples of these reactions resulting in RO_2 production are shown in Reactions 2.11-2.12 respectively.

$$CH_2{=}CH_2 + NO_3 \ (+O_2) \rightarrow \cdot O\text{-}O\text{-}CH_2CH_2\text{-}ONO_2 \qquad (2.11)$$

$$CH_3CHO + NO_3 \ (+O_2) \rightarrow CH_3CH(O)\text{-}O\text{-}O\cdot \qquad (2.12)$$

Alkanes also react with NO_3, but the rate constants are several orders of magnitude slower than alkene + NO_3 reactions and are not considered significant for typical atmospheric conditions [Finlayson-Pitts and Pitts 2000]. Furthermore, in ambient conditions, NO_3 oxidation is restricted during daytime hours due to competition with NO_3 photolysis, which rapidly dissociates to NO_2 and $O(^3P)$. On the contrary, nighttime NO_3 concentrations become a significant oxidant for isoprene due to its rapid rate constant (6.96×10^{-13} cm^3 $molecules^{-1}$ s^{-1} at 298 K), and the absence of the competing photolysis reaction at night. Within the reaction chamber, NO_3 oxidation pathways are not expected to be significant due to rapid photolysis when exposed to the UV solar simulator lamps and analysis of nighttime isoprene oxidation through the NO_3 pathway is beyond the scope of this study.

Photolysis processes within the mechanism are limited to carbonyl compounds, ROOH, RC(O)OOH, and $RONO_2$ species, and result in the formation of RO_2 and alkoxy

radicals ($RO\cdot$). Peroxy radicals continue to react with oxidants (such as NO_x, NO_3, HO_2, and RO_2), degrading to form various oxygenated VOC (OVOC) products. Examples of these reactions are shown in Equations 2.13-2.17 for the peroxyacetyl (PA) radical, the precursor to PAN.

$$CH_3C(O)\text{-}O\text{-}O\cdot + NO_2 \leftrightarrow CH_3C(O)\text{-}O\text{-}O\text{-}NO_2 \text{ (PAN)} \quad (2.13)$$

$$CH_3C(O)\text{-}O\text{-}O\cdot + NO \ (+O_2) \rightarrow NO_2 + CH_3\text{-}O\text{-}O\cdot + CO_2 \quad (2.14)$$

$$CH_3C(O)\text{-}O\text{-}O\cdot + NO_3 \rightarrow NO_2 + CH_3\text{-}O\text{-}O\cdot + CO_2 \quad (2.15)$$

$$CH_3C(O)\text{-}O\text{-}O\cdot + HO_2 \rightarrow CH_3C(O)\text{-}O\text{-}OH + O_2 \quad (2.16)$$

$$CH_3C(O)\text{-}O\text{-}O\cdot + RO_2 \rightarrow RO\cdot + CH_3\text{-}O\text{-}O\cdot + CO_2 \quad (2.17)$$

These reactions are imperative to PAN chemistry since loss of PAN only occurs when peroxyacetyl radicals are destroyed, because reaction 2.13 is reversible. Alkoxy radicals are known to rearrange, decompose, or react in the presence of oxygen to produce carbonyl compounds as shown in Equation 2.18.

$$CH_3CH_2CH_2\text{-}O\cdot + O_2 \rightarrow CH_3CH_2CHO + HO_2 \quad (2.18)$$

The resulting HO_2 radical can go on to convert NO to NO_2 via Reaction 1.8, which can result in the net production of ozone (Reactions 2.3-2.4), and reproducing OH.

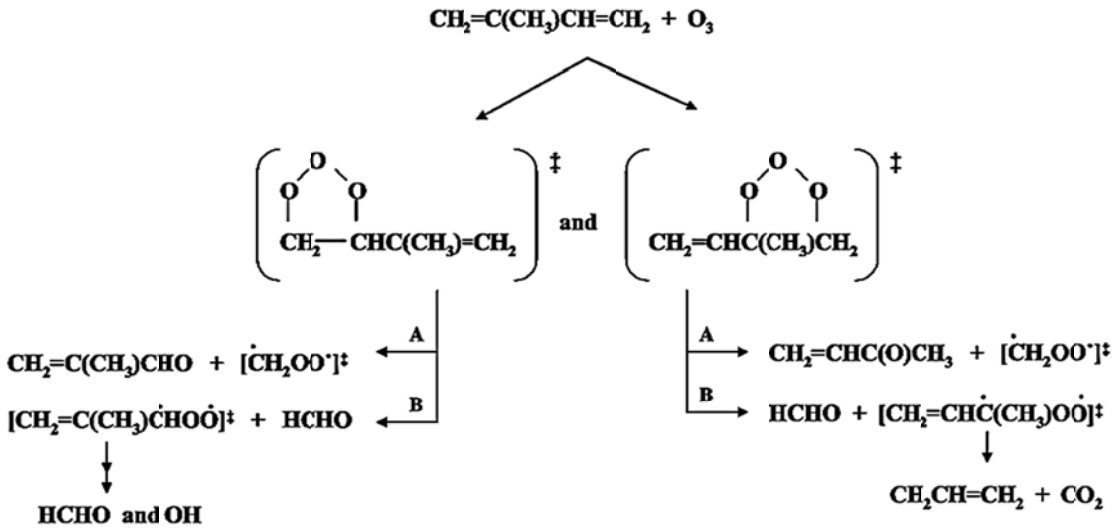

Figure 2.5 – The ozonolysis pathway of isoprene. Energy rich compounds are designated with the ‡ symbol. [Atkinson et al, 2006; Lockwood, 2008]

The ozonolysis pathway of unsaturated VOCs is also generalized in Figure 2.4. These reactions involve addition of ozone across a double bond as seen in the ozonolysis of isoprene in Figure 2.5. Rearrangement causes the formation of a carbonyl compound and an excited zwitterion known as a Criegee Intermediate (CI). These Criegee radicals can go through stabilization or decomposition to form various oxygenated products. It is important to note that Criegee radical chemistry is still in infancy stages, as most information of the intermediate is derived from theoretical calculations due to the difficulty of direct observations [Vereecken and Francisco, 2012]. However, recently these radicals have been detected and it is likely that future studies involving direct observations of Criegee intermediate reaction kinetics will impact understanding of ozonolysis in the atmosphere [Taatjes et al., 2014]. All oxidation processes involved in the MCM for each VOC are represented in detail until the formation of CO_2 or an organic

product that is already represented elsewhere in the mechanism. Table 2.1 lists all inorganic reactions included in the reaction scheme with their associated rate constants.

2.3.2 RO_2 Reactions

Peroxy radicals (RO_2) are treated with a modified approach using counters for each specific RO_2 compound. The issue with treating RO_2 reactions using counters within this mechanism is that counters are conserved since they do not directly react with any other chemical species. Using a strictly explicit approach to RO_2 chemistry is equally problematic. There are 95 individual RO_2 species in the isoprene mechanism, and 278 RO_2 species in the isoprene + terpene mechanism (Chapter 3). For each mechanism, this would equate to 9,025 and 77,284 permutation RO_2 reactions respectively if treated in a strictly explicit form for all $RO_2 + RO_2$ combinations. Instead, the sum of the concentration of all peroxy radicals is calculated at each integration step as a general counter term "RO_2." This RO_2 term is then multiplied by the second order rate constant of each RO_2 (specific) + RO_2 (counter) suggested by MCM to effectively create a pseudo-first order reaction rate constant for each specific RO_2 at each time step. Previous studies have demonstrated that a counter method for RO_2 reactions is equivalent to an explicit treatment of a similar mechanism [Lightfoot et al, 1992].

Table 2.1 – Inorganic reactions and rate constants used in all simulations. First order rate constants are expressed in units of (s^{-1}) and second order rate constants are expressed in units of ($cm^3 molecules^{-1} s^{-1}$).

Notation	Reaction	Rate Constant	Ref.
K1f	$O(^3P) + O_2 = O_3$	1.46×10^{-14}	IUPAC*
K2f	$O(^3P) + O_3 = O_2 + O_2$	8.00×10^{-15}	IUPAC*
K3f	$O(^1D) = O(^3P)$	7.10×10^{8}	IUPAC*
K4f	$O(^1D) + H_2O = OH + OH$	2.14×10^{-10}	IUPAC*
K5f	$O_3 + HO_2 = OH + O_2 + O_2$	2.00×10^{-15}	IUPAC*
K6f	$HO_2 + NO = NO_2 + OH$	8.50×10^{-12}	IUPAC*
K7f · 0.3	$HO_2 + NO_3 = NO_2 + OH + O_2$	4.00×10^{-12}	IUPAC*
K7f · 0.7	$HO_2 + NO_3 = HNO_3 + O_2$	4.00×10^{-12}	IUPAC*
K8f	$O_3 + OH = HO_2 + O_2$	7.30×10^{-14}	IUPAC*
K9f	$OH + HO_2 = HO_2 + H_2O$	1.11×10^{-10}	IUPAC*
K10f	$H_2O_2 + OH = HO_2 + H_2O$	1.70×10^{-12}	IUPAC*
K11f	$HO_2 + HO_2 = H_2O_2 + O_2$	1.75×10^{-12}	IUPAC*
K12f	$OH + H_2 = H_2O + HO_2$	6.70×10^{-15}	IUPAC*
K13f	$H + O_2 = HO_2$	9.47×10^{-11}	IUPAC*
K14f	$CO + OH = HO_2 + CO_2$	2.29×10^{-13}	IUPAC*
K15f	$HCO + O_2 = CO + HO_2$	5.20×10^{-12}	IUPAC*
K16f	$HCHO + NO_3 = HNO_3 + CO + HO_2$	5.50×10^{-16}	IUPAC*
K17f	$HNO_4 = HO_2 + NO_2$	0.316	IUPAC*
K18f	$OH + NO_3 = NO_2 + HO_2$	2.00×10^{-11}	IUPAC*
K19f	$CH_3O + O_2 = HO_2 + HCHO$	1.90×10^{-15}	IUPAC*
K20f	$O(^3P) + NO = NO_2$	5.01×10^{-11}	IUPAC*
K21f	$O(^3P) + NO_2 = NO + O_2$	9.90×10^{-12}	IUPAC*
K22f	$O(^3P) + NO_2 = NO_3$	2.30×10^{-11}	IUPAC*
K23f	$OH + NO = HONO$	3.31×10^{-11}	IUPAC*
K24f	$OH + NO_2 = HNO_3$	3.50×10^{-11}	IUPAC*
K25f	$HO_2 + NO_2 = HNO_4$	4.00×10^{-12}	IUPAC*
K26f	$OH + HONO = NO_2 + H_2O$	6.00×10^{-12}	IUPAC*
K27f	$OH + HNO_3 = NO_2 + H_2O$	1.50×10^{-13}	IUPAC*
K28f	$OH + HNO_4 = NO_2 + O_2 + H_2O$	3.20×10^{-12}	IUPAC*
K29f	$O_3 + NO = NO_2 + O_2$	1.80×10^{-14}	IUPAC*
K30f	$O_3 + NO_2 = NO_3 + O_2$	3.50×10^{-17}	IUPAC*

*Rate constants are consistent with IUPAC recommended values [Atkinson et al., 2006]

Table 2.1, Continued

Notation	Reaction	Rate Constant	Ref.
K31f	$NO_3 + NO = NO_2 + NO_2$	2.60×10^{-11}	IUPAC*
K32f	$NO_3 + NO_2 = N_2O_5$	1.90×10^{-12}	IUPAC*
K33f	$N_2O_5 = NO_2 + NO_3$	6.9×10^{-2}	IUPAC*
K34f	$NO_3 + NO_3 = NO_2 + NO_2 + O_2$	2.29×10^{-16}	IUPAC*
K35f	$N_2O_5 + H_2O = HNO_3 + HNO_3$	1.00×10^{-22}	IUPAC*
K36f	$NO_2 + NO_2 = HONO + HNO3$	1.2×10^{-17}	Adjusted+
KMT13	$CH_3O_2 + NO_2 = CH_3O_2NO_2$	2.03×10^{-7}	MCM#
KMT14	$CH_3O_2NO_2 = CH_3O_2 + NO_2$	5.89×10^{-12}	MCM#
KMT15	$C_2H_4 + OH =$ Products	7.71×10^{-12}	MCM#
KMT16	$C_3H_6 + OH =$ Products	2.58×10^{-11}	MCM#
KFPAN	$R(O)OO\cdot + NO =$ APN	8.7×10^{-12}	MCM#
KRO2HO2	Generic $RO_2 + HO_2$	2.28×10^{-11}	MCM#
KRO2NO3	Generic $RO_2 + NO_3$	2.3×10^{-12}	MCM#
KDEC	Generic Decomposition	1×10^{6}	MCM#
KNO3AL	Generic Aldehyde + NO_3	2.73×10^{-15}	MCM#
KAPHO2	Generic APNs + HO_2	1.39×10^{-11}	MCM#
KAPNO	Generic APNs + NO	1.98×10^{-11}	MCM#
KROPRIM	Generic Primary NO_2-$ORO\cdot + O_2$	9.14×10^{-15}	MCM#
KROSEC	Generic Secondary NO_2-$ORO\cdot + O_2$	9.14×10^{-15}	MCM#
KRO2NO	Generic RO_2 + NO	9.04×10^{-12}	MCM#

*Rate Constants are consistent with IUPAC recommended values [Atkinson et al., 2006].
+Desorption of HONO from walls is adjusted until inorganic chemistry is optimized (see Section 2.4).
#MCM rate constants are calculated using temperature dependent equations recommended by IUPAC [Atkinson et al., 2006].

2.3.3 Isoprene Chemistry

The framework for the isoprene mechanism used in this study is derived from the MCM isoprene subset. However, several modifications are included that are consistent with recent literature studies. Updates to the isoprene + OH oxidation pathway are explained in detail in Peeters et al. [2014] via the Leuven Isoprene Mechanism (LIM1). The mechanism accounts for additional OH cycling under "low" NO regions which were not present in previous mechanisms. Figure 2.6a and 2.6b illustrate the oxidation pathway that leads to formation of six isoprene RO_2 isomers. In addition to the inclusion of isoprene isomer chemistry from LIM1, oxidation mechanism information based on recent isoprene nitrate studies was included. This includes isoprene nitrate + OH/O_3 reaction rate constants [Lee et al., 2014], an IN yield of 11% [Xiong et al., 2015], and IN + OH products as detailed elsewhere [Paulot et al., 2009]. The isoprene + NO_3 product chemistry is consistent with the findings of Fan and Zhang [2004]. Finally, an updated rate constant for isoprene epoxydiols (oxidation product of isoprene, IEPOX) + OH is also included [Bates et al., 2014].

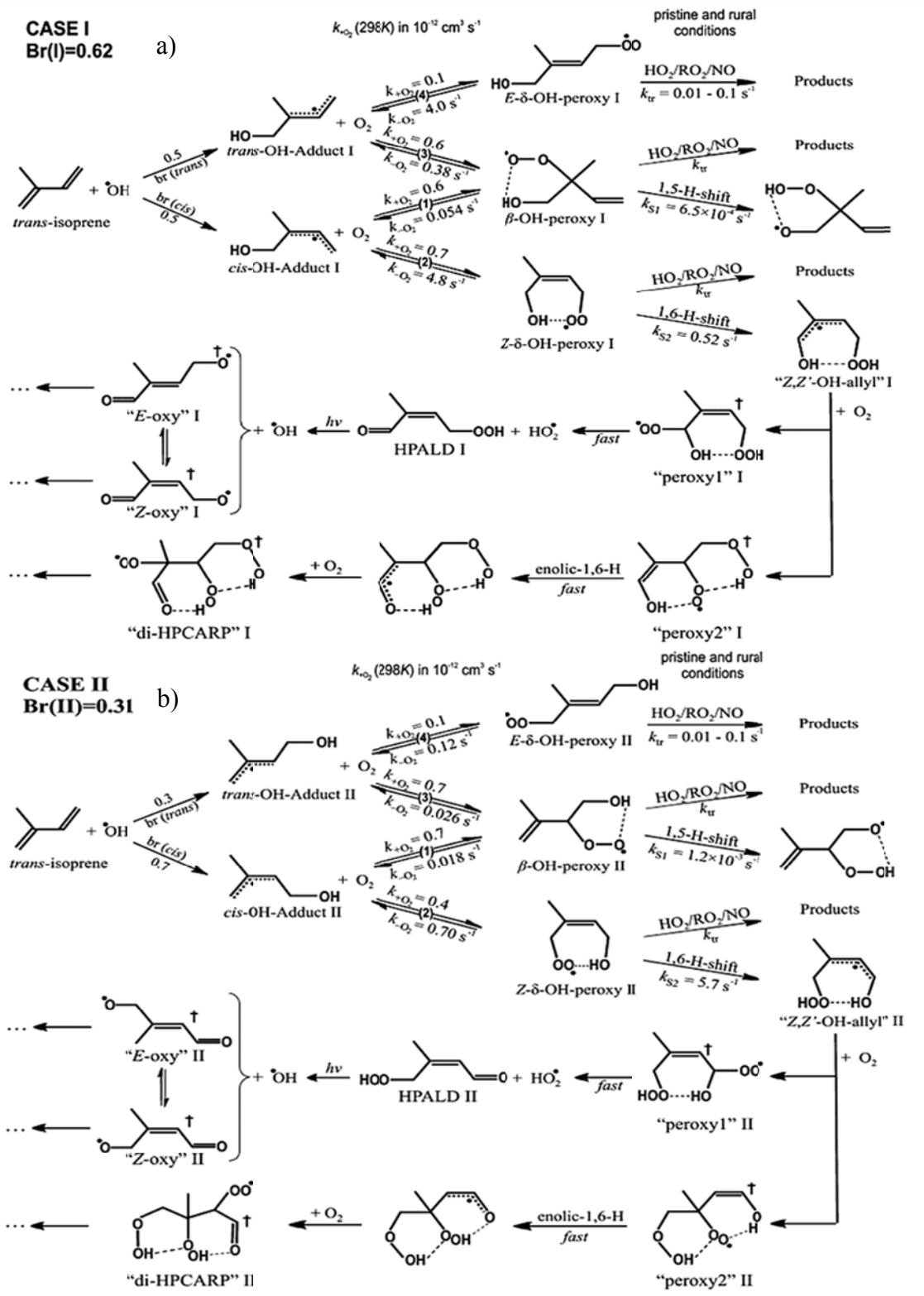

Figure 2.6 – Mechanism of isoprene oxidation in the presence of OH with a branching ratio of a) 0.62 and b) 0.31 [Peeters et al., 2014].

A 6 L/min dilution source was used throughout the experiment to make up for the rate of sampling. This was accounted for in simulations as a first order rate loss ($k = 1.82 \times 10^{-5}\ s^{-1}$). Within the chamber, photolysis rate constants were scaled to a measured $J(NO_2)$ using information via Saunders et al. [2003] and Equation 2.19.

$$J_x = \frac{\sum I_\lambda \cdot \sigma_{\lambda,x} \cdot \Phi_{\lambda,x}}{\sum I_\lambda \cdot \sigma_{\lambda,NO2} \cdot \Phi_{\lambda,NO2}} \cdot J_{NO2} \qquad (2.19)$$

J_x is the photolysis rate constant for the associated species and J_{NO2} is the measured value of $6.0 \times 10^{-4}\ s^{-1}$ ($\pm$ 3×10^{-5}, 1σ) within the reaction chamber. I_λ is the lamp intensity $\frac{\text{photons}}{\text{cm}^2\text{s}}$, σ_λ is the absorption cross section $\frac{\text{cm}^2}{\text{molecule}}$, and Φ_λ is the quantum yield, which are integrated over all wavelengths. Table 2.2 shows all J values used for the reaction chamber simulations. Note that J15 – J58 are photolysis rates used to describe a family of photodissociation reactions and are applied to similar chemical species. Table 2.3 lists the initial concentrations used for simulation of the May 2013 chamber experiment.

Table 2.2 – Calculated photolysis rates for the May 2013 chamber experiment (s^{-1}).

Notation	Photolysis Reaction	2013 Experiment
J1	$O_3 = O(^1D) + O_2$	2.53×10^{-6}
J2	$O_3 = O(^3P) + O_2$	2.96×10^{-5}
J3	$H_2O_2 = OH + OH$	5.27×10^{-7}
J4	$NO_2 = NO + O(^3P)$	6.00×10^{-4}
J5	$NO_3 = NO + O_2$	1.50×10^{-3}
J6	$NO_3 = NO_2 + O(^3P)$	1.03×10^{-2}
J7	$HONO = OH + NO$	5.66×10^{-4}
J8	$HNO_3 = OH + NO_2$	4.59×10^{-8}
J9	$HNO_3 = HONO + O(^1D)$	4.59×10^{-8}
J11	$HCHO = CO + HO_2$	2.18×10^{-6}
J12	$HCHO$ = Products	3.32×10^{-6}
J13	CH_3CHO = Products	3.24×10^{-7}

Table 2.2, Continued

Notation	Photolysis Reaction	2013 Experiment
J15	 → Products	1.33×10^{-6}
J17	 → Products	3.68×10^{-6}
J18	 → Products	5.67×10^{-7}
J19	 → Products	5.67×10^{-7}
J21	 → Products	4.08×10^{-8}
J22	 → Products	2.66×10^{-7}
J23	 → Products	9.18×10^{-7}
J24	 → Products	9.18×10^{-7}
J31	 → Products	3.75×10^{-6}
J32	 → Products	5.64×10^{-7}
J33	 → Products	1.86×10^{-6}
J34	 → Products	8.40×10^{-6}
J35	 → Products	1.80×10^{-5}
J41	 → Products	3.88×10^{-7}
J51	 → Products	7.75×10^{-8}
J53	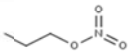 → Products	9.15×10^{-8}
J54	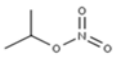 → Products	2.00×10^{-7}
J55	 → Products	5.61×10^{-7}
J56	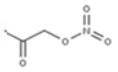 → Products	3.66×10^{-7}
J57	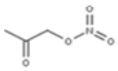 → Products	1.63×10^{-7}
J58	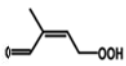 → Products	1.08×10^{-7}

Table 2.3 – Initial conditions used for the simulation of the May 2013 chamber experiment.

Parameter	2013 Experiment
Dilution Flow	6 L/min (kdil = 1.82 x 10^{-5} s^{-1})
C_5H_8	3.38 x 10^{13} molecules/cm^3
NO	6.59 x 10^{12} molecules/cm^3
NO_2	5.07 x 10^{12} molecules/cm^3
O_3	1.97 x 10^{10} molecules/cm^3
HONO	4.0 x 10^{10} molecules/cm^3
H_2O	3.33 x 10^{16} molecules/cm^3

2.4 May 2013 Results and Discussion

Figure 2.7 shows the measured and simulated concentrations of isoprene, NO_x and ozone during the May 5, 2013 chamber experiment. Water vapor was kept at a constant 5% RH (3.33 x 10^{16} molecules/cm^3) in the model, and initial isoprene and NO concentrations were constrained for simulations to measured values obtained during the experiment (3.38 x 10^{13} and 6.59 x 10^{12} molecules/cm^3 respectively). An average value for initial NO_2 concentration (5.07 x 10^{12} molecules/cm^3) using the first two data points from the experiment was constrained for simulation purposes due to the inexplicable sharp increase in NO_2 during the first 3 minutes of irradiation. Simulations of the NO conversion to NO_2 via RO_2/HO_2 reactions do not account for this increase alone.

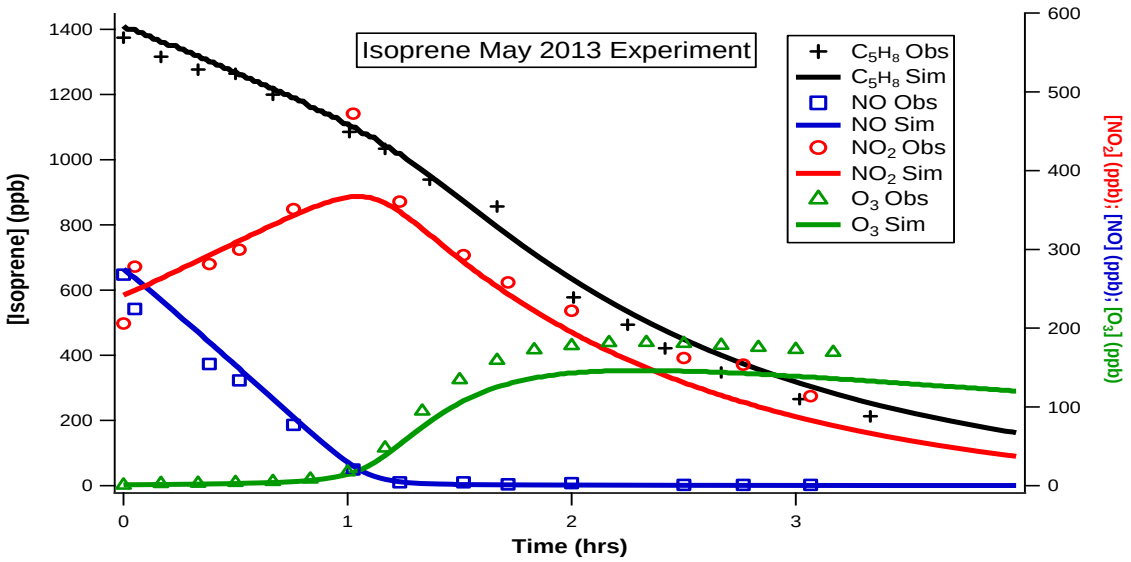

Figure 2.7 – Concentration vs. time for isoprene, NO_x, and ozone for the May 2013 chamber experiment. Symbols represent data collected from measurements, solid lines are simulated concentrations.

The initial isoprene decay is attributed to OH radical oxidation. The chamber experiment assumes that OH initiation is primarily from photolysis of nitrous acid (HONO). Photochemical chambers, such as the one at used in this experiment, are known to produce and desorb HONO from the walls of the vessel [Sakamaki and Akimoto, 1988; Rohrer et al., 2005; Zador et al., 2006] via the surface reaction shown in Reaction 2.20 [Zhou et al., 2002]. When exposed to radiation, HONO in the chamber photolyzes, producing NO and OH (Reaction 2.21).

$$2NO_2 \quad (+H_2O) \rightarrow \quad HONO + HNO_3 \qquad (2.20)$$

$$HONO \ (+h\nu) \rightarrow \quad \cdot OH + NO \qquad (2.21)$$

For this particular chamber, HONO production from the walls has not been previously measured. Therefore, an initial production rate constant for Reaction 2.20 and initial HONO concentration was adjusted until isoprene and NO decay, as well as NO_2

production were optimized for a best fit. In addition to the HONO parameters, an OH radical source was needed to account for the rapid decay of isoprene over time. The conditions that optimized agreement between experimental data and model simulated concentrations for isoprene and NO_x occurred with a second order rate constant for $K_{2.18}$ (relative to NO_2) of 1.2 x 10^{-17} $cm^3 molecules^{-1}$ s^{-1}, initial HONO concentration of 4.0 x 10^{10} molecules/cm^3 and an OH source effectively producing OH radicals at a rate of 5 x 10^8 molecules/cm^3s. This source likely reflects photochemical production of HONO on the walls during the experiment [Zhou et al., 2002]. The result of these parameter adjustments show measurement and simulated values to be within measurement uncertainty for isoprene and NO_x.

The first hour of the experiment is dominated by OH chemistry, since the presence of NO suppresses O_3 and NO_3 production. After about 1 hour, O_3 and NO_3 increase rapidly due to NO concentrations becoming negligible. Although the general profiles of ozone during the experiment are similar between measured and simulated values, ozone after t = 2 hours is under simulated by 18%. This discrepancy can be explained in part by the under simulation of NO_2 after t = 1 hr. At t = 2 hrs, NO_2 is similarly under simulated by 18% relative to measured data. Based on the agreement of simulated and experimental data for NO, it is likely that NO_2 sinks are over-predicted as opposed to a discrepancy in the inorganic chemistry, or it is possible that there is a wall source of NO_x, e.g. surface production of HONO, from deposited HNO_3. As discussed earlier, the loss of reactive nitrogen within the mechanism is due to organic nitrate sequestration as well as HNO_3 production. Therefore, it is likely that these sinks are over estimated.

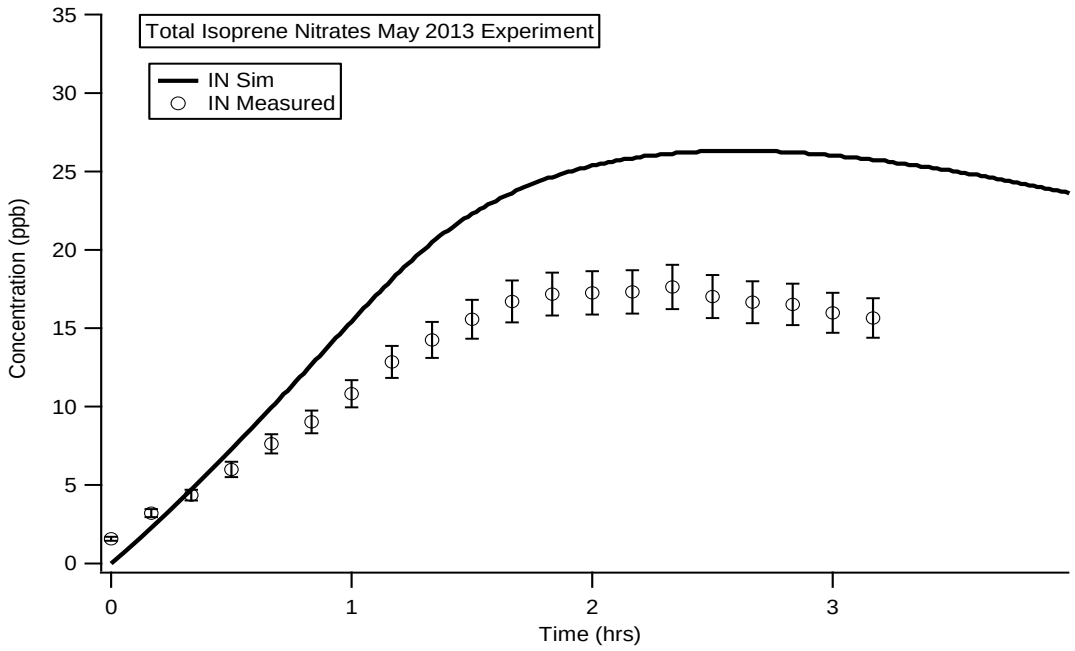

Figure 2.8 – Concentration vs. time for total isoprene nitrates. The lines represent simulated values and the symbols represent measurement data. An uncertainty of 8% for measured data is shown in error bars.

Total isoprene nitrates were also measured during the study. A recent study performed in our laboratory shows evidence of a total isoprene nitrate yield of 11%, which was utilized for these simulations (Xiong et al, 2015). Total isoprene nitrates are shown in Figure 2.8 to steadily increase with time during the experiment until approximately t = 2 hours. After two hours of isoprene oxidation, predictions from the model oversimulate isoprene nitrates by a factor of 1.8. The immediate divergence of simulated vs measured data suggests that production and loss processes within the current mechanism are not well understood. It is necessary to note that during this chamber experiment, the CIMS inlet was heated to a temperature of 100^0C. Regular operation of the CIMS during the SOAS campaign utilized standard operating procedures of heating the inlet line to only 50^0C. Therefore, the measurements could be biased low due to

thermal decomposition of IN during transfer into the CIMs. Further investigation of line loss due to heating of the inlet is necessary in the future to assess the extent to which this affects the IN concentration.

Comparison of measured and simulated peroxyacyl nitrates PAN and MPAN is illustrated in Figure 2.9. No significant production of peroxyacyl compounds occur during the first hour of the experiment. The fast reaction of the RO_2 precursors to peroxyacyl compounds with NO prevents significant increase in concentration until NO concentrations become low enough to favor the NO_2 reaction pathway. Reactions 2.11 and 2.12 illustrate these competing reactions. The simulated increase in PAN and MPAN occurs at the same time as the experimental observations, since simulated NO concentrations are in agreement with measured values. However, absolute concentrations for simulated and measured PAN and MPAN concentrations quickly diverge, as predicted PAN and MPAN exceeds observations by a factor of 1.5 and 1.9 respectively. There is large discrepancy between measured and simulated values, and the current mechanism presents simulations significantly different from previous studies that underpredicted PAN by 57% [Costa, 2010] and 40% [Carter and Atkinson, 1996]. It is worth noting that these two studies employed a significantly less detailed mechanism for their simulations, and likely were missing important sources of PAN precursors. Data obtained in the current simulation suggests that the current mechanism overpredicts source contributors to PAN and MPAN. This explanation is most likely since PAN loss processes are known to be dominated by thermal decomposition, which was constrained to the experimental temperatures for simulation, and the first order thermal decomposition rate constant is accurately known [Kleindienst et al., 1993]. Since PAN

loss processes rely on the destruction of the PA precursor, future work at assessing chemistry shown in Reactions 2.12-2.15 is necessary. A future study that monitors MVK and MACR would also be useful to identify sources of model disagreement involving first generation products, which are possibly oversimulated as well. Furthermore, study of MPAN decomposition due to reaction with NO_3 would help close the uncertainty of MPAN loss processes, since the unsaturated nature of the species suggest that reaction with NO_3 could potentially be important.

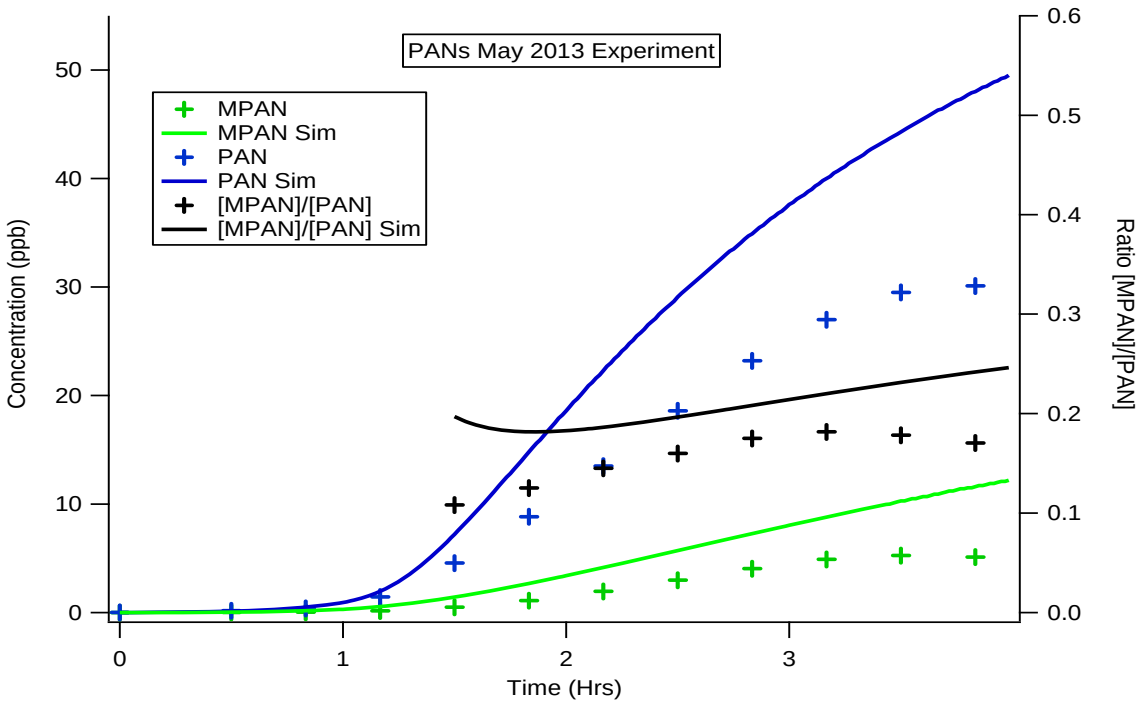

Figure 2.9 – Concentration vs. time for PAN and MPAN, and ratio of MPAN/PAN for the 2013 chamber experiment. Lines represent simulated values and symbols represent measurement data.

The relationship of MPAN and PAN production during the isoprene oxidation experiment was examined for potential application to ambient conditions. Figure 2.9

shows that the measured MPAN/PAN ratio remains relatively constant after t = 1.5 hours. The average ratio of MPAN/PAN for the measured data is 0.15 ± 0.03 RSD. Unlike the initial hour of the experiment, the chamber conditions after that point are influenced by multiple oxidants (NO, OH, O_3, and NO_3), which is similar to the complexity of ambient conditions seen during the SOAS campaign. There is a discrepancy of 33% between the simulated and observed MPAN/PAN concentration ratios, due to the greater bias to formation of MPAN within the model relative to PAN. However, using the observed [MPAN]/[PAN] ratio of 0.15 ± 0.03 from the measured chamber experiment data, a relationship between δMPAN/δPAN can be explored to approximate PAN production due to isoprene oxidation for ambient conditions. A detailed explanation of this calculation and application to ambient conditions are explained in the following chapter of this study.

2.5 Conclusions

Analysis of an isoprene photo-oxidation experiment has been presented and discussed in detail. A comparison between measurement and simulated data shows despite recent improvements to the current isoprene oxidation mechanism, there remains a need for further study of several reaction pathways of oxidation products formed from isoprene. An IN yield of 11% was used in simulations, consistent with a recent study [Xiong et al., 2015]. This yield caused simulated values to be overestimated by a factor of 1.8, suggesting an underestimation of organic nitrate loss processes.

The current state of APN chemistry via isoprene oxidation was also addressed, specifically in the case of production and loss processes of PAN and MPAN. There

continues to remain a discrepancy with the current mechanism information for the production of individual APN compounds. Both PAN and MPAN are over simulated by a factor of ~1.5 and ~2.3 respectively. This is likely due to a gap in understanding of the individual APN production mechanisms rather than direct APN loss processes. Loss processes are dominated by thermo decomposition processes for the conditions of this experiment, and are well constrained within the model. However, precursor chemistry to individual APNs that were unable to be monitored may be significantly oversimulated within the model. Future study measuring important first generation products such as MVK and MACR would be useful to identify initial model disagreement. These discrepancies between measured and modeled data can account for the under simulation of NO_2 concentrations within the model, which in turn helps explain the lower simulated values of O_3 concentrations. Therefore, the current mechanism overvalues the capacity of APNs to act as a NO_x sink.

An average MPAN/PAN ratio of 0.15 ± 0.03 RSD remains consistent in measured data after t = 1.5 hours. Although simulations fail to reproduce observed concentrations, the existence of a relatively constant ratio with a similar profile as measured between MPAN/PAN is evident for conditions when the rate of production is greater than rate of loss. We derive this relationship for use in ambient conditions to approximate the PAN production from isoprene oxidation. Details of this calculation and further analysis of this relationship will be discussed further in the subsequent chapter of this study.

CHAPTER 3: IMPACT OF BIOGENIC VOLATILE ORGANIC COMPOUNDS ON PAN PRODUCTION IN THE US SOUTHEAST

3.1 SOAS Field Campaign

This study was done in conjunction with the Southern Oxidant and Aerosol Study (SOAS, http://soas2013.rutgers.edu/) field campaign during the summer of 2013. Although much of the country has experienced an average increase in temperature, the southeastern United States region has cooled over the past century, as seen in Figure 3.1. Studies have hypothesized the influence of aerosols (particulate matter suspended in the atmosphere, or PM) derived from biogenic volatile organic compounds (BVOCs) as the cause for this anomaly [Goldstein et al., 2009]. The scientific community agrees that human activity adversely influences the atmosphere due to anthropogenic emissions, mostly through combustion of fossil fuels. However, the degree to which we influence atmospheric aerosol is still poorly understood. The SOAS campaign was initiated as a collaborative effort in the southeastern United States to address our understanding of oxidation processes of BVOCs in the presence of anthropogenic emissions, especially in regard to production of PM. For this study, the oxidation mechanism leading to peroxyacyl nitrates (APNs) formation was explored. APNs are important chemical species that influence the availability of reactive nitrogen in the atmosphere and will be discussed in detail in the following section.

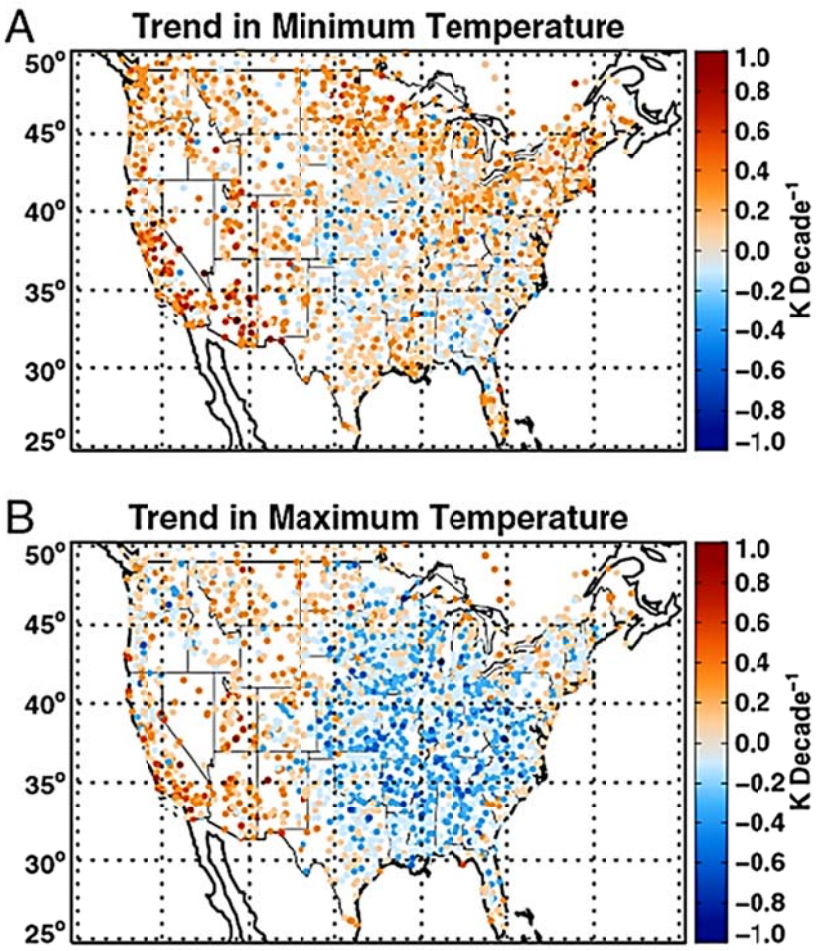

Figure 3.1 – Temperature trends for the United States from 1950-2006 a) minimum temperature and b) maximum temperature [Portmann et al., 2009].

3.1.1 Peroxyacyl Nitrates

Peroxyacyl nitrates ($RC(O)OONO_2$, APNs) are important chemical species within the atmosphere, making up a significant percentage of NO_y (sum of total reactive nitrogen) within the troposphere [Min et al., 2012]. Their unique thermodynamic properties allow them to be relatively long lived under cooler temperatures, acting as a vehicle for long range transport leading to the release of reactive nitrogen in warmer

remote areas [Singh and Hanst, 1981]. The Arrhenius expression for the temperature dependent dissociation of APNs is given in Equation 3.1 [Atkinson et al., 2006].

$$1.9 \times 10^{17}\, e^{(-14100/T)} \qquad \text{(For T = 280-330)} \qquad (3.1)$$

For a typical near surface temperature of 300 K, $K_{3.1} = 7.4 \times 10^{-4}$, while at 240 K (approximating the temperature at the top of the troposphere) $K_{3.1} = 5.8 \times 10^{-9}$. These two values correspond to a thermal lifetime of ~22 min and ~5 years, respectively. The release of reactive nitrogen can result, in the case of low NO_x environments, in an enhancement of ozone production. In addition to the implications of enhanced NO_x and ozone concentrations, APNs are known to cause health issues to plants and animals. This makes identifying chemical sources of APNs essential for control and mitigation purposes.

Peroxyacetyl nitrate (PAN, $CH_3C(O)OONO_2$) is the most abundant APN in the atmosphere, making up ~80% of total APNs [Roberts et al., 2007]. There have been many studies of this species due to its properties as a lachrymator, cancer mutagen, plant phytotoxin, and as a component of smog pollution causing respiratory issues [Stephens, 1969; Temple and Taylor, 1983; Kleindienst et al., 1990; Altshuller, 1993; Heddle et al., 1993]. However, a firm understanding of PAN precursor chemistry has proven elusive.

PAN is known to be formed by the reversible reactions (3.2a and b) of the peroxyacetyl radical (PA) in the presence of NO_2.

$$CH_3C(O)OO\cdot + NO_2 \rightarrow CH_3C(O)OONO_2 \qquad (3.2a)$$

$$CH_3C(O)OONO_2 \rightarrow CH_3C(O)OO\cdot + NO_2 \qquad (3.2b)$$

The complication of the formation of PAN arises from the fact that most VOCs within the atmosphere can degrade through various generations of oxidation products to form

the PA radical. Referring to Figure 1.7 shows several of the important precursors to PAN formation and their oxidation pathways to the formation of PA radicals [LaFranchi et al., 2009]. The relative contributions of these explicit sources are not well understood.

Previous studies have addressed the PA radical source issue in various complexity of chemical mechanism used. LaFranchi et al. [2009] uses a steady-state analysis of APNs to identify precursors within a Ponderosa Pine forest environment influenced by the Sacramento, CA urban plume. They approximated relative contributions of methyl vinyl ketone (MVK), methylglyoxal (MGLYOX), biacetyl (BIACET), methacrolein (MACR) and acetaldehyde (CH_3CHO) to be 26%, 2%, 7%, 20%, and 45% respectively. This method is capable of identifying the important 2nd-generation precursors (OVOCs), but does not derive a relationship to 1st-generation precursors (hydrocarbons). However, this is currently the only study that has calculated the relative contribution to PA in a forested environment. Fischer et al. [2014] employed the GEOS-CHEM global transport model to approximate a total global source attribution of PAN. According to that study, the global primary carbonyl contributors to PAN production include acetaldehyde (44%), methylglyoxal (30 %), acetone (7 %), and a sum of isoprene and terpene products (19 %). Global models such as these use highly generic mechanism details, which group classes of hydrocarbons together with similar structures and reactivity (including non-PAN precursors) due to computational restrictions. Additionally, a global source attribution is not representative of a forest environment, but a mix of various different environments with varying sources of biogenic and anthropogenic PA sources. Xue et al. [2014] employed a near explicit model based on the MCM database, such as the one used in this study. Precursors to PA were simulated in an urban plum over the city of Beijing,

showing a considerable portion of PA production from aromatics (33%), alkenes (27%), and various other sources making up less than ten percent each. However, MCM v3.2 lacks the recent updates that are included in the modified 0-D model discussed in Chapter 2. In this study we use a near-explicit model to determine important precursors of PAN by constraining the model to observed precursor data over the simulation period. This method allows us to identify specific reactions within the mechanism that are important to PA radical formation.

3.1.2 MPAN vs PAN Ratio Relationship

Methacryloyl peroxy nitrate ($CH_2C(CH_3)C(O)OONO_2$, MPAN) is an APN that has only one known chemical oxidation source through the oxidation of methacrolein (MACR, refer to Figure 1.7). Since the formation of MACR is attributed to oxidation of isoprene [Bertman and Roberts, 1991], it is reasonable to assume that all MPAN in the atmosphere is formed by oxidation of isoprene. A small MACR source exists in automobile exhaust [Biesenthal and Shepson, 1997a], but for forest influenced environments where BVOCs are dominant, this source should be very small. We hypothesize that this property can be useful in identifying the contribution of isoprene oxidation to PAN production using MPAN as an isoprene chemistry tracer. Using chamber experiment data from the previous chapter, we identified a relationship between PAN and MPAN production to approximate the contribution of isoprene to PAN production in ambient conditions. To the best of our knowledge, no other study has used chamber data in this fashion to investigate PA origins.

3.1.3 Objectives

In the previous chapter, we established a relationship between MPAN and PAN in a controlled environment where isoprene oxidation occurred in the presence of NO_x. In this chapter we aim to use this relationship for use in ambient conditions by proposing an equation to quantify PAN production due to isoprene oxidation using the observed δMPAN/δPAN from the chamber experiment. This calculation seeks to answer the question of how much isoprene contributes to PAN production within a southeast United State forest environment. Simulations of ambient conditions using a 0-D model seek to identify other important precursors to PAN within this environment. Finally, comparison between chamber and ambient data are assessed to explain discrepancies in relative PA production.

3.2 Experimental

Data for this study was obtained in Centreville, Alabama (CTR, Figure 3.2) on a rural site associated with the SouthEast Aerosol Research and Characterization (SEARCH, http://www.atmospheric-research.com/studies/SEARCH/index.html) monitoring network in conjunction with the Southern Oxidant and Aerosol Study (SOAS) field campaign. The CTR tower is located 84 km southwest of Birmingham and 55 km southeast of Tuscaloosa (32.90289 Lat, -87.24968 Long, Altidude 126 m). During the campaign, temperatures fluctuated between about 29^0C during daytime hours, and 22^0C at night. Relative humidity was high, ranging from 50% RH during the day to about 90% at night. The forest is very heterogeneous in nature with mainly loblolly pine (27%), American sweetgum (11%), and red oak (5%) as determined by a tree survey performed

by Dr. Glenn Wolfe and myself. This results in a diverse array of BVOC emissions including isoprene and several important monoterpenes (i.e., α-pinene, β-pinene, and limonene).

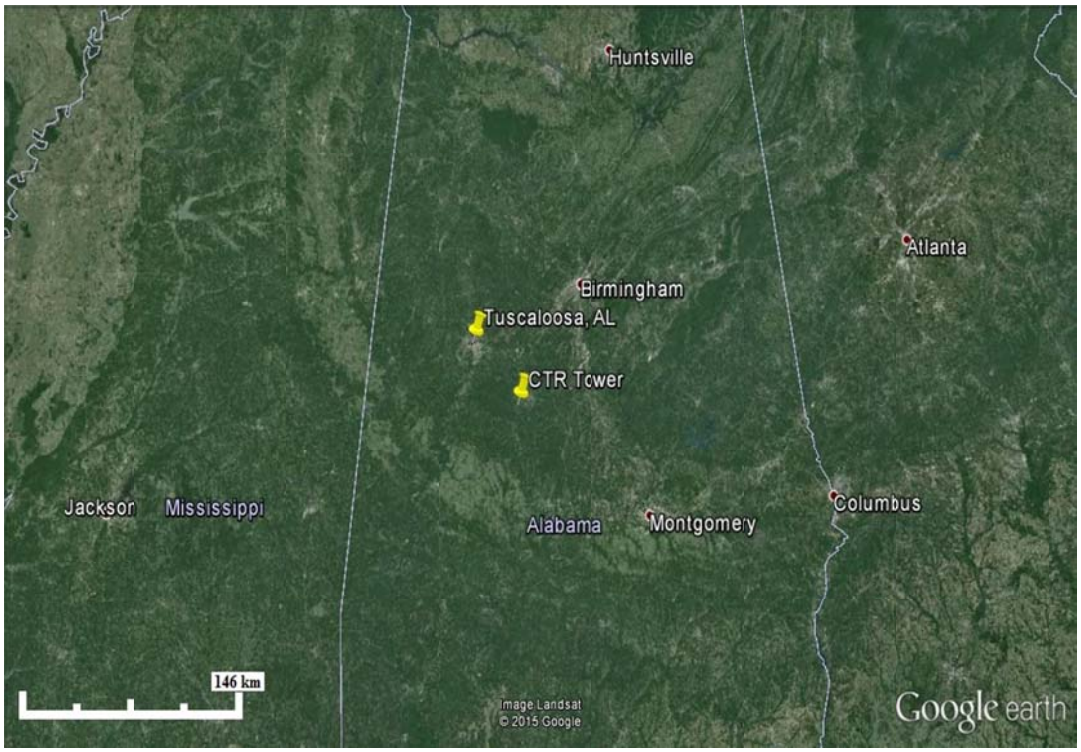

Figure 3.2 – Site map of the CTR tower.

3.2.1 Instrumentation

The measurements employed for this study were conducted during the SOAS field campaign at the CTR site. Measurements of acetaldehyde, acetone, isoprene, MVK, MACR, α-pinene, β-pinene, and limonene were obtained from the NOAA/UC Berkeley GCMS described elsewhere in detail [Gilman et al., 2010]. Measurements for OH and HO_2 were conducted by Penn State using methodology detailed in Mao et al. [2012].

Individual peroxyacyl nitrates were measured by Western Michigan University using a custom gas chromatograph equipped with a Shimadzu GC mini-2 ^{63}Ni electron capture detector (GC-ECD) maintained at 55 deg. C, described in further detail in Pippin et al. [2001].

3.3 Ambient 0-D Photochemical Model

The ambient photochemical mechanism is consistent with the isoprene mechanism described in the chamber model. In addition to the isoprene subset, the SOAS mechanism includes the α-pinene, β-pinene, and limonene subsets of the MCM v3.3 [Jenkins et al., 1997, and Saunders et al., 2003]. Terpene subsets were included due to a previous study identifying terpene oxidation products as important precursors to PAN production [Fischer et al., 2014]. Due to the interest of strictly simulating potential PAN production within ambient conditions, inorganic and organic data available from the field study were constrained over the entirety of each simulation period. The measured species to which the model was constrained (30 min resolution) were isoprene, a-pinene, b-pinene, limonene, NO_2, NO, OH, HO_2, carbon monoxide, H_2O, ozone, acetaldehyde, and acetone. Additionally, time dependent ambient temperature and the PAN deposition velocity were included.

Dry deposition of PAN has been measured in several studies due the potential of leaf uptake as a significant loss process for PAN [Sparks et al., 2003]. The flux of PAN can be expressed in Equation 3.3.

$$Flux_{(PAN)} = V_d[PAN]\ (\frac{molecules}{cm^2 s}) \qquad (3.3)$$

Here, V_d is the deposition velocity, in units of cm/s. Thus, we can derive a rate of loss for PAN for a volume above the surface shown in Equation 3.4.

$$K_{Vd} = \frac{V_d}{H}[PAN]\left(\frac{molecules}{cm^3 s}\right) \qquad (3.4)$$

Here, H is the height of the volume, in cm, in other words, the height of boundary layer. Averaged diurnal deposition velocities for PAN are employed using values obtained from measured deposition velocities in a mixed deciduous forest in North Carolina, as deposition velocities have not been measured at the CTR site [Turnipseed et al., 2006; Wu et al., 2012]. Figure 3.3 illustrates the employed PAN deposition velocities used in the ambient model.

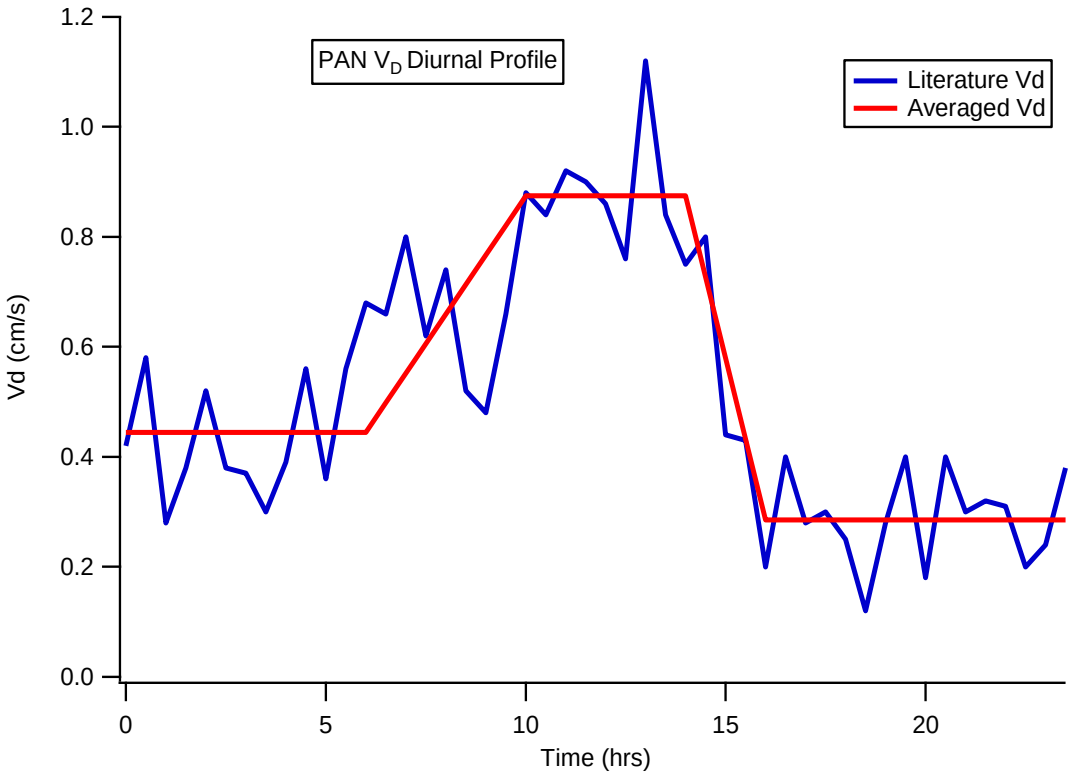

Figure 3.3 – PAN V_d diurnal profile. Average values were used for model inputs [Wu et al., 2012].

3.3.1 Terpene Oxidation Mechanism

The terpene oxidation mechanism used for this study is consistent with the MCM v3.3 subsets for α-pinene, β-pinene, and limonene. However, the lack of laboratory studies of terpene product chemistry places a limit on the certainty of the terpene oxidation mechanism. In the absence of known terpene oxidation chemistry we apply (1) similarly chemically-structured species with known chemical mechanism and (2) other theoretical studies to predict likely reaction pathways and estimate relative rate constants. Full details of the construction methodology and protocol can be found elsewhere [Jenkin et al., 1997, 2003; Saunders et al., 2003; Bloss et al., 2005].

Table 3.1 – Photolysis scaling factors used in the ambient 0-D model.

Notation	Photolysis Reaction	Ambient Scaling Factor
J1	$O_3 = O(^1D) + O_2$	$4.67 \times 10^{-8} \times SR$
J2	$O_3 = O(^3P) + O_2$	$5.34 \times 10^{-7} \times SR$
J3	$H_2O_2 = OH + OH$	$8.99 \times 10^{-9} \times SR$
J4	$NO_2 = NO + O(^3P)$	$1.10 \times 10^{-5} \times SR$
J5	$NO_3 = NO + O_2$	$2.70 \times 10^{-5} \times SR$
J6	$NO_3 = NO_2 + O(^3P)$	$2.12 \times SR$
J7	$HONO = OH + NO$	$2.42 \times 10^{-6} \times SR$
J8	$HNO_3 = OH + NO_2$	$8.59 \times 10^{-10} \times SR$
J9	$HNO_3 = HONO + O(^1D)$	$5.05 \times 10^{-5} \times J4$
J11	$HCHO = CO + HO_2$	$3.91 \times 10^{-8} \times SR$
J12	$HCHO$ = Products	$5.65 \times 10^{-5} \times SR$
J13	CH_3CHO = Products	$7.01 \times 10^{-9} \times SR$

Table 3.1, continued

Notation	Photolysis Reaction	Ambient Scaling Factor
J15	 → Products	$1.46 \times 10^{-3} \times J4$
J17	 → Products	$4.04 \times 10^{-3} \times J4$
J18	 → Products	$6.22 \times 10^{-4} \times J4$
J19	 → Products	$6.22 \times 10^{-4} \times J4$
J21	 → Products	$8.81 \times 10^{-10} \times SR$
J22	 → Products	$2.92 \times 10^{-4} \times J4$
J23	 → Products	$1 \times 10^{-3} \times J4$
J24	 → Products	$1 \times 10^{-3} \times J4$
J31	 → Products	$4.13 \times 10^{-3} \times J4$
J32	 → Products	$6.20 \times 10^{-4} \times J4$
J33	 → Products	$3.19 \times 10^{-2} \times J4$
J34	 → Products	$9.19 \times 10^{-3} \times J4$
J35	 → Products	$1.97 \times 10^{-2} \times J4$
J41	 → Products	$6.82 \times 10^{-9} \times J4$
J51	 → Products	$8.5 \times 10^{-5} \times J4$
J53	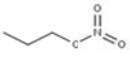 → Products	$1.32 \times 10^{-4} \times J4$
J54	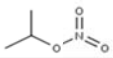 → Products	$2.20 \times 10^{-4} \times J4$
J55	 → Products	$6.13 \times 10^{-4} \times J4$
J56	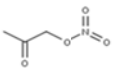 → Products	$4.02 \times 10^{-4} \times J4$
J57	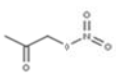 → Products	$1.8 \times 10^{-4} \times J4$
J58	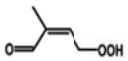 → Products	$1.08 \times 10^{-7} \times J4$

3.3.2 Photolysis Reactions

For the ambient mechanism, J values for a specific species (J_x) were obtained using the NCAR tropospheric ultraviolet and visible (TUV) radiation model during the maximum solar radiation output (SR, W/m^2) on a clear day during the field campaign. Using the ratio of J_x/SR_{max} as a scaling factor multiplied by the solar radiation vs time data from the SOAS field campaign, J values were obtained for each available chemical species during each time step of the model as seen in Equation 3.5.

$$J_x = \frac{J_{x,TUV}}{SR_{max}} \times SR_{SOAS} \qquad \text{(Eq. 3.5)}$$

J values for chemical species not available through the TUV model were calculated using a scaling factor relative to J_{NO2} by methods described in Section 2.3.3. A summary of J value scaling factors used are shown in Table 3.1.

3.4 SOAS 2013 Results and Discussion

For this study, several case study days were chosen based on criteria allowing for appropriate analysis while minimizing meteorological influences. Dates during the campaign where significant data gaps were present were not included. In addition to data availability, only days where APNs increased in concentration after the morning initial spike in APN concentrations due to downward mixing were considered, so that the ratio of chemical production was significantly greater than the rate of destruction. This enabled us to utilize the relative production rate information from the chamber study (Chapter 2). Figure 3.4 shows the case study data for PAN and MPAN. Due to 0-D model limitations, meteorological influences needed to be minimized. Changing boundary layer heights cause dilution effects to occur for each species. Therefore, the

time period during which the boundary layer remained relatively constant for case study days was established to reduce these effects.

Figure 3.5 illustrates the ceilometer data from the four case study dates that demonstrated a relatively constant boundary layer height for data analysis. A ceilometer utilizes a remote sensing technology based on LIDAR principles [NOAA, 2012] to measure distance to the cloud base (assumed in this study to be representative of BL height) by photon counting of a back-scattered pulse of near-IR light (1064 nm). In this study, we define a constant boundary layer (CBL) by analyzing the deviation from the average BL height from 11:00 CST until sunset. The criterion for a constant BL in this study was if the standard deviation was no more than (+/-) 20% from the mean BL height. In the event of a point beyond this threshold, a statistical Q-test was employed to test for outliers. A failed Q-test data point was removed and reanalyzed using the remaining data. A non-constant boundary layer height is defined as when two consecutive points fall outside of the acceptable deviation range. The four days chosen for this study were June 3rd (12:30-18:00 CDT), June 14th (11:30-18:00 CDT), June 26th (11:00-18:00 CDT) and July 12th (13:00-18:00 CDT).

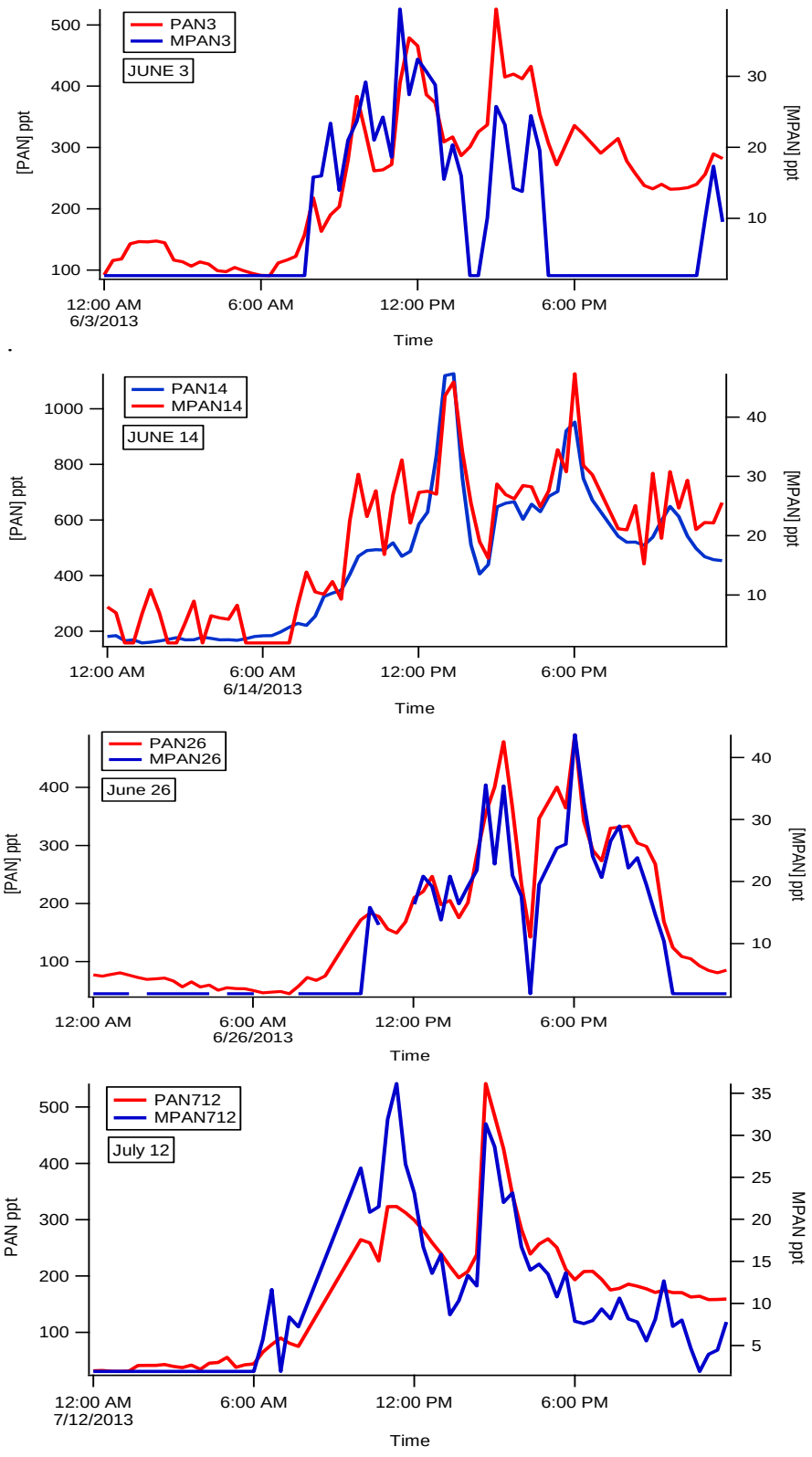

Figure 3.4 – SOAS MPAN and PAN concentration vs. time for each case study day.

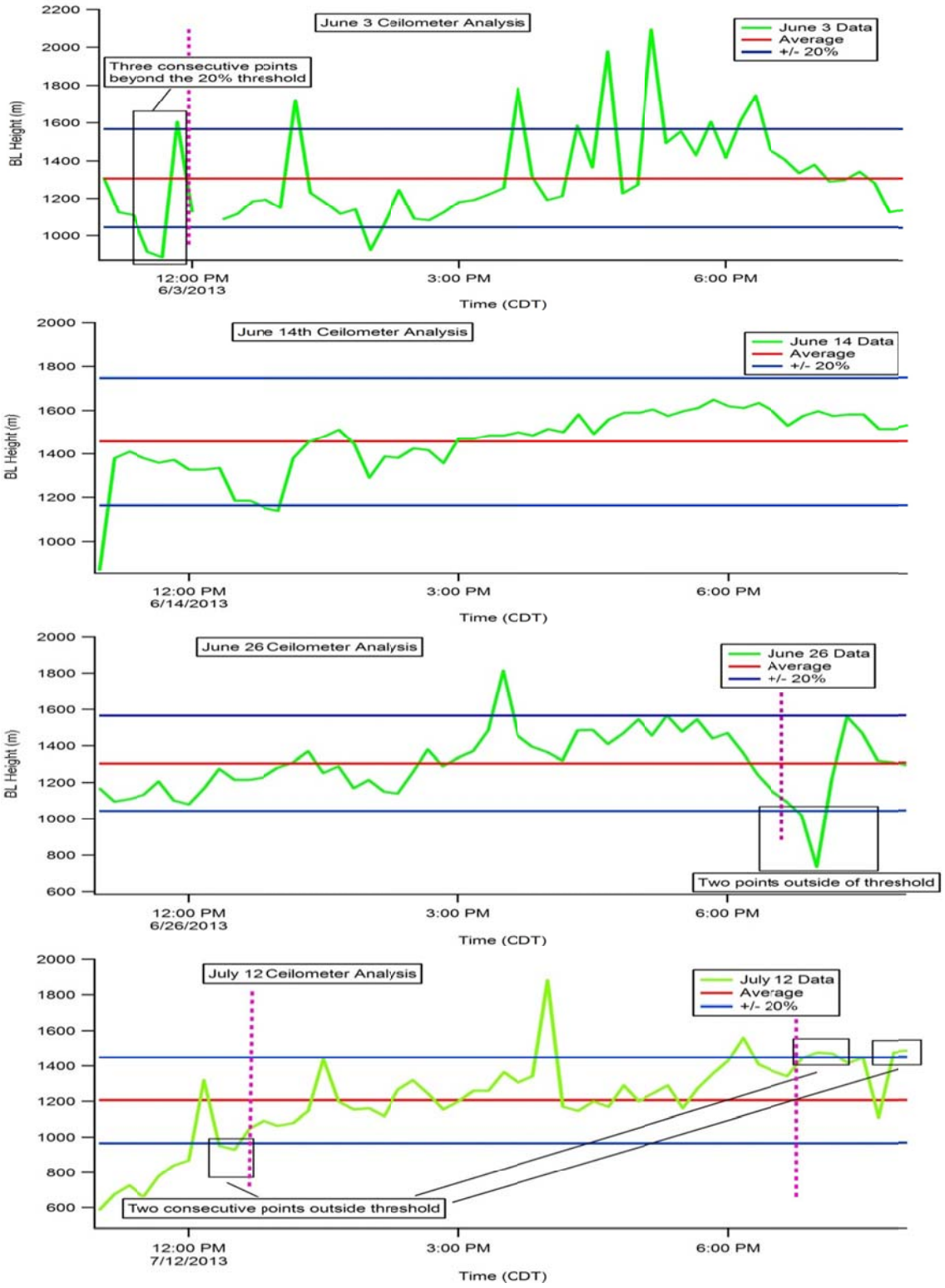

Figure 3.5 – Ceilometer data for each case study day from the SOAS campaign. The red horizontal line establishes the afternoon average, and the blue lines represent ± 20% deviations from the mean. Vertical dashed lines define time cut off points.

The May 2013 photochemical reaction chamber experiments allowed us to monitor the oxidation of isoprene in the presence of NO_x in a controlled environment, in the absence of meteorological influences. Using the assumption that MPAN production is solely formed from oxidation of MACR allows us to further accept that MPAN is derived from isoprene oxidation in ambient summer conditions [Biesenthal and Shepson, 1997a; Montzka et al., 1993]. A previous study used a similar assumption to derive ozone production from isoprene [Biesenthal et al., 1997b]. Assuming that $\delta MPAN_{SOAS}$ is strictly derived from isoprene oxidation, we ask the scientific question what percent of PAN production is formed from the oxidation of isoprene? In other words, we want to know $\frac{\delta[PAN]_{isoprene}/dt}{\delta[PAN]_{all\ sources}/dt}$. First, we established the relationship in the previous chapter that $\frac{\delta[PAN]_{isoprene}}{dt} = \frac{\delta[MPAN]/dt}{APNratio}$, where APN_{ratio} was 0.15 ± 0.03 RSD, since in the chamber $\frac{d[MPAN]/dt}{d[PAN]isoprene/dt} = 0.15$ We can use this mathematical relationship to rearrange an equation to solve for relative isoprene contribution to total PAN production as seen in equations 3.6 and 3.7.

$$\frac{\delta[PAN]_{isoprene}/dt}{\delta[PAN]_{all\ sources}/dt} = \frac{\delta[MPAN]/dt/0.151}{\delta[PAN]/dt} \qquad \text{Eq (3.6)}$$

$$\frac{\delta[PAN]_{isoprene}/dt}{\delta[PAN]_{all\ sources}/dt} = 6.6 \times \frac{\delta[MPAN]}{\delta[PAN]} \qquad \text{Eq (3.7)}$$

Using δ[MPAN]/δ[PAN] from the SOAS field campaign, we can calculate the contribution of isoprene to PAN production for ambient conditions.

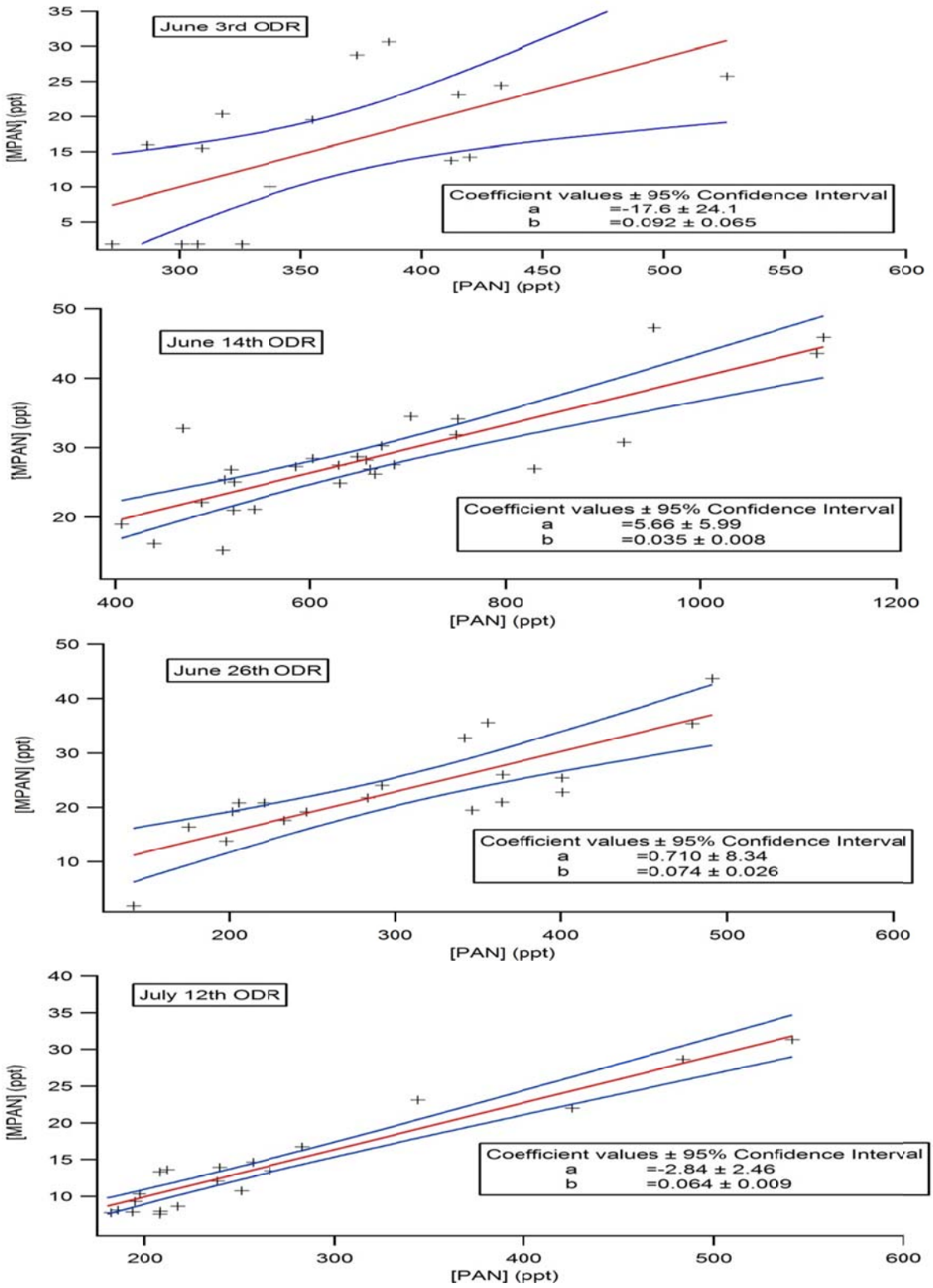

Figure 3.6 – Orthogonal Distance Regression plots for MPAN vs PAN case studies. MPAN and PAN concentrations are in units of ppt.

Figure 3.6 shows orthogonal distance regressions (ODR) for the plots of [MPAN] vs [PAN] for the case study days from the SOAS field campaign. All MPAN and PAN data from the time periods outlined in Section 3.4 were included. The slope of each ODR plot by definition is $\frac{\delta[\mathrm{MPAN}]}{\delta[\mathrm{PAN}]}$, which substitutes into equation 3.2 to solve for relative PAN contribution from isoprene. Results show isoprene oxidation accounts for 61% (June 3rd), 23% (June 14th), 49% (June 26th), and 42% (July 12th) of all PAN production. The contribution for the case study days is 44($\pm$ 16)% contribution from isoprene. This value is consistent with the value for isoprene contribution of ~55% from LaFranchi et al. [2012]. This then begs the question as to the other important contributors to PAN production within ambient air. Therefore, we employ the near-explicit constrained 0-D photochemical model described in the previous sections to determine other important chemical sources of PAN, and to examine the extent to which an explicit photochemical model yields results consistent with this analysis.

For the ambient 0-D model, a counter was employed for every reaction that produced a PA radical in order to determine the relative contribution to PA radicals from VOCs present at the CTR research cite. An example of this is shown in Reaction 3.8.

$$CH_3CHO\cdot + OH \rightarrow H_2O + PA + \text{Counter} \qquad (3.8)$$

A relative contribution to PA radicals were established over time by comparing each individual species PA radical production to the total PA production at each time step. Through this process, eleven processes were found to have significant contribution (at least ~1% of total) to PA production. The list of these reactions is shown in Table 3.2.

Table 3.2 – Important reactions producing PA radicals within 0-D ambient model.

	Species	Reaction Details
1	MGLOOA	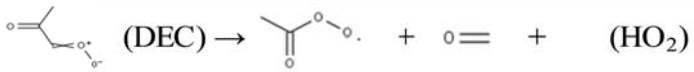
2	MACROOA	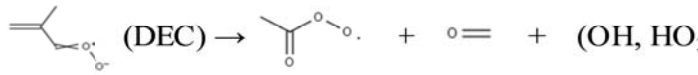
3	MGLYOX	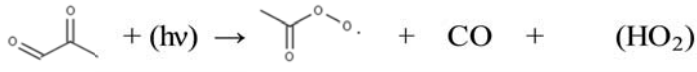
4	MGLYOX	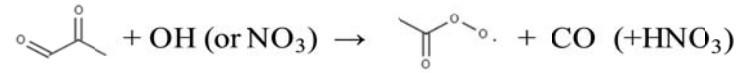
5	MACO3	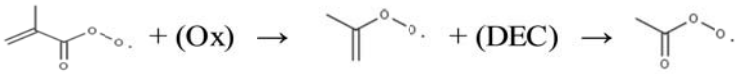
6	MVK	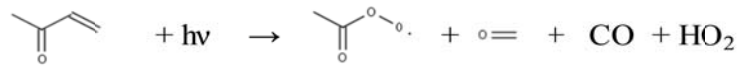
7	HMVKO2	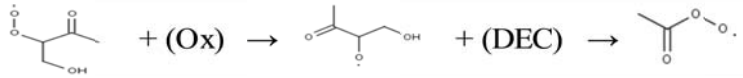
8	Acetone	
9	Acetaldehyde	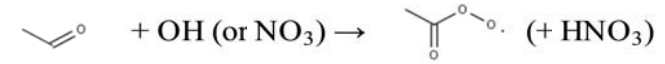
10	Terpenes	Addition of all counters leading to PA formation from Terpene chemistry
11	Other Isoprene	Addition of all other counters not listed above leading to PA formation from Isoprene chemistry

* DEC refers to a decomposition or rearrangement process
** Ox refers to various oxidants that can participate in shown reaction (OH, NO, NO_3)

Figures 3.8-3.11 show the distribution of VOCs to PA production for each of the case study days. For all case study days, acetone consists of approximately 1% of the total PA production and does not significantly change with time. The lifetime of acetone within the troposphere is expected to be ~60 hrs, and therefore it is not surprising to be a rather insignificant contributor to PAN production in the time frame of this simulation [Blitz et al., 2004]. Terpene oxidation general trends for all case studies are seen to

contribute more to PA production over time. Within MCM, there are no direct reactions that form PA radicals from α-pinene, β-pinene, and limonene. Instead, it takes several generations of oxidation products until the formation of an appropriate PA precursor. The simplest example predicted by MCM is through the oxidation of limonene initiated by ozone illustrated in the Figure 3.7. The general trend seen in all four days is consistent with the explanation that as higher generation oxidation products from terpene oxidation are formed, there is a greater potential for PA production. Combined, acetone and terpene chemistry never exceed more than 16% of the relative contribution to PA radical formation. All other production is due to isoprene related reactions and acetaldehyde oxidation.

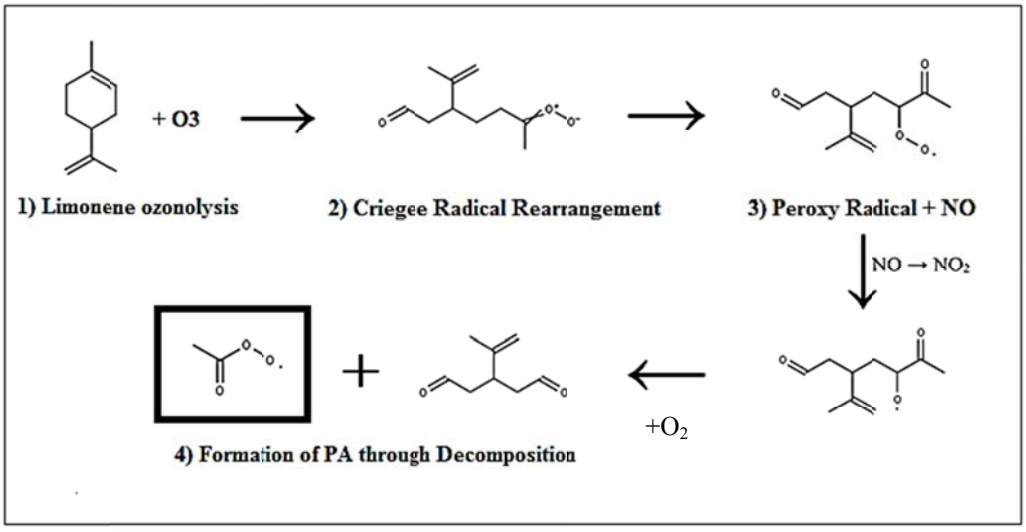

Figure 3.7 – Example of limonene oxidation leading to formation of PA radical.

Total production of PA radicals due to isoprene pathways increases with time. Figures 3.8-3.11 include isoprene derived oxidation products that form PA radicals, which are distinguished in the legend along with detailed reactions and structures listed in Table 3.2. Contributions from first generation products of MVK and MACR, as well as contributions from a MVK oxidation product, HMVKO2 (see Table 3.2), are relatively consistent over the course of the simulation. Additionally, the ozonolysis Criegee radicals MACROOA and MGLOOA (see Table 3.2) have little variability over the simulation period as they are dependent on ozone and isoprene concentration, which stay relatively constant over the simulation periods. It is the influence of second generation oxidation products that accounts for the increase in PA radical production over time. This is due to the influence of methylglyoxal and other isoprene oxidation products increasing over time, which is evident on all four case study days. On average, isoprene contributes 50% of PA radicals at the start of the simulation, but this increases to 70% at the end of the simulation. The four case study days show on average that oxidation (via OH and NO_3), ozonolysis, and photolysis pathways from isoprene account for 30%, 17%, and 20% of the total PA production respectively. The total contribution from isoprene is not statistically significantly different from the approximation from calculations based on the chamber study MPAN to PAN production ratio, which produces an estimated average PAN contribution of $44(\pm 16)\%$. Although statistically speaking 44(± 16)% and the range of 50-70% are not significantly different, it is useful to identify differences between chamber study and ambient conditions to explain differences between the mean values attained from each method.

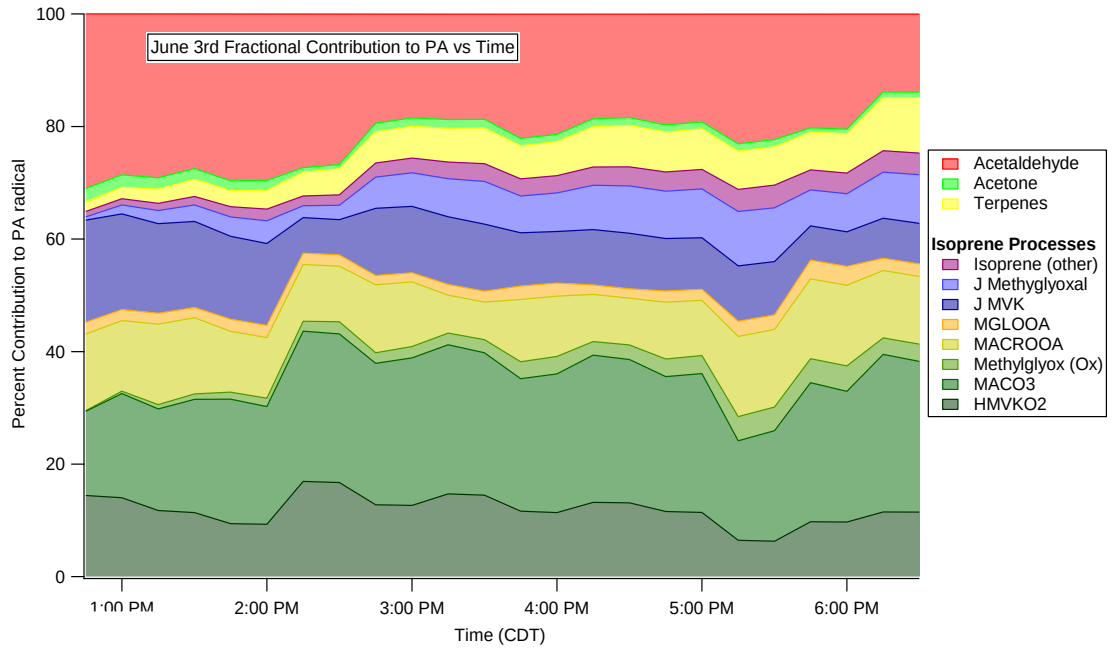

Figure 3.8 – June 3rd relative contribution to PA radicals vs. time.

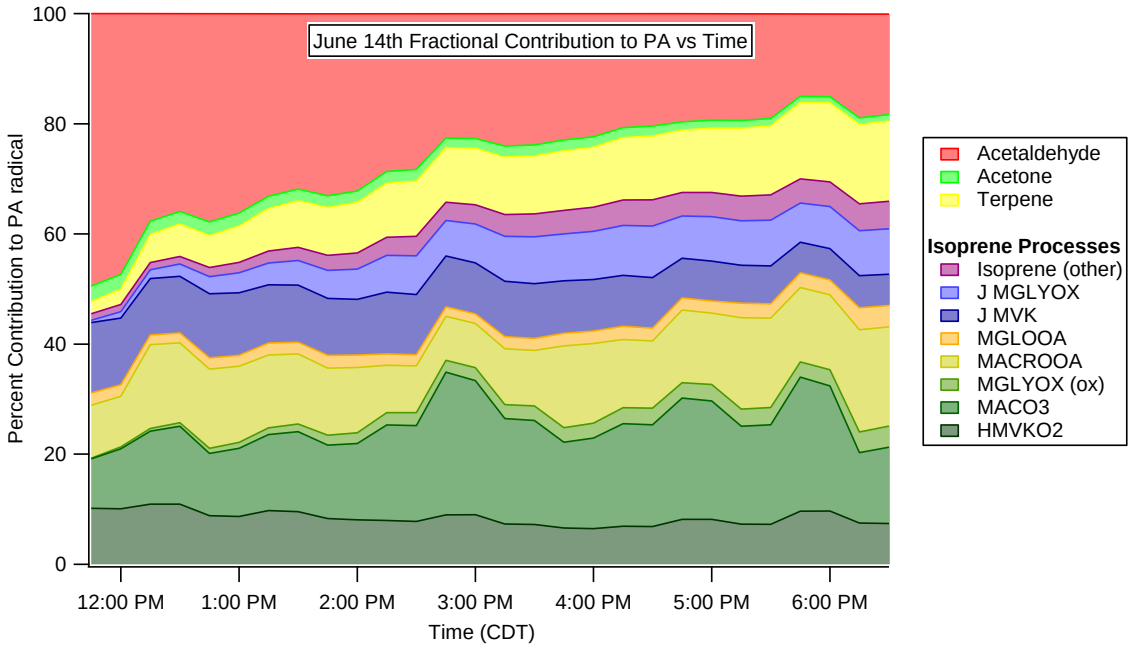

Figure 3.9 – June 14th relative contribution to PA radicals vs. time.

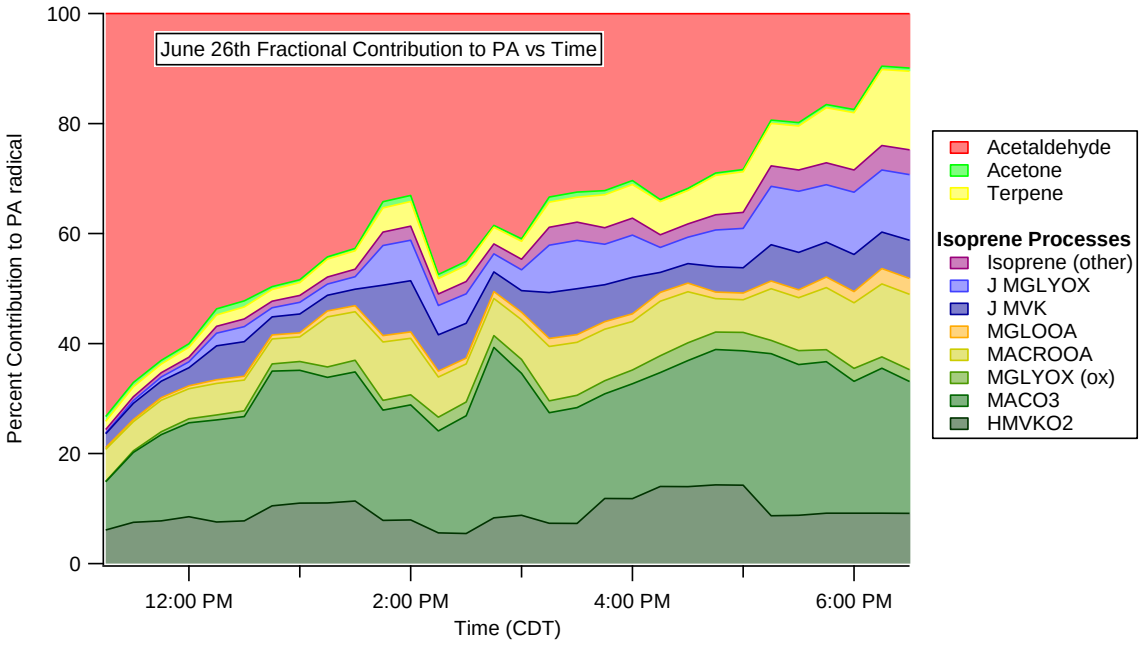

Figure 3.10 – June 26th relative contribution to PA radicals vs. time.

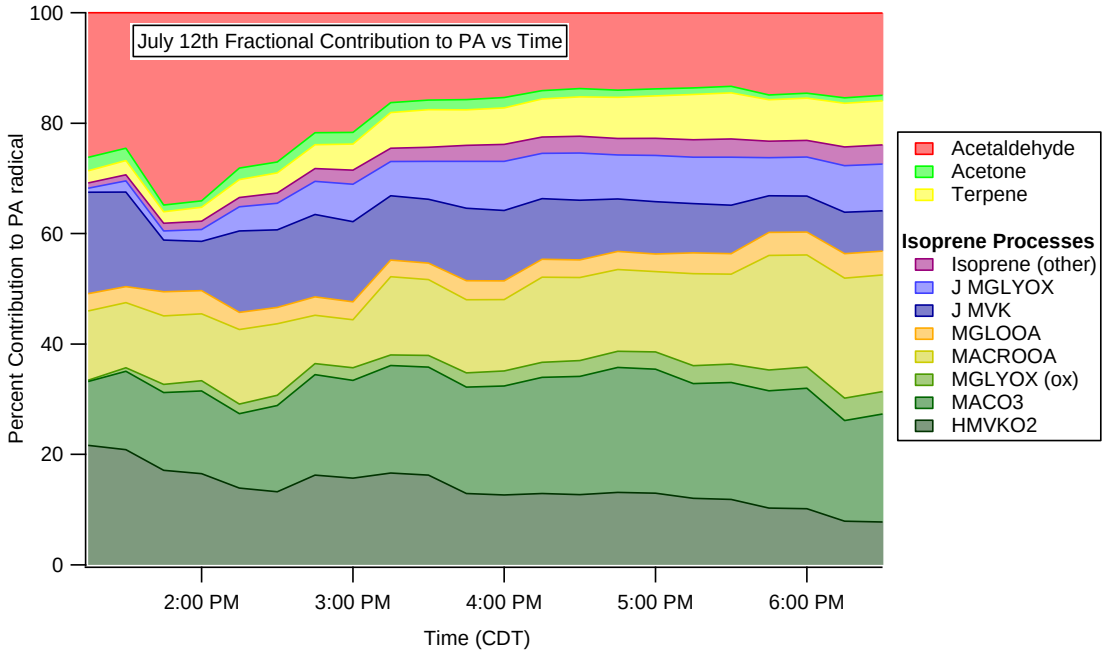

Figure 3.11 – July 12th relative contribution to PA radicals vs. time.

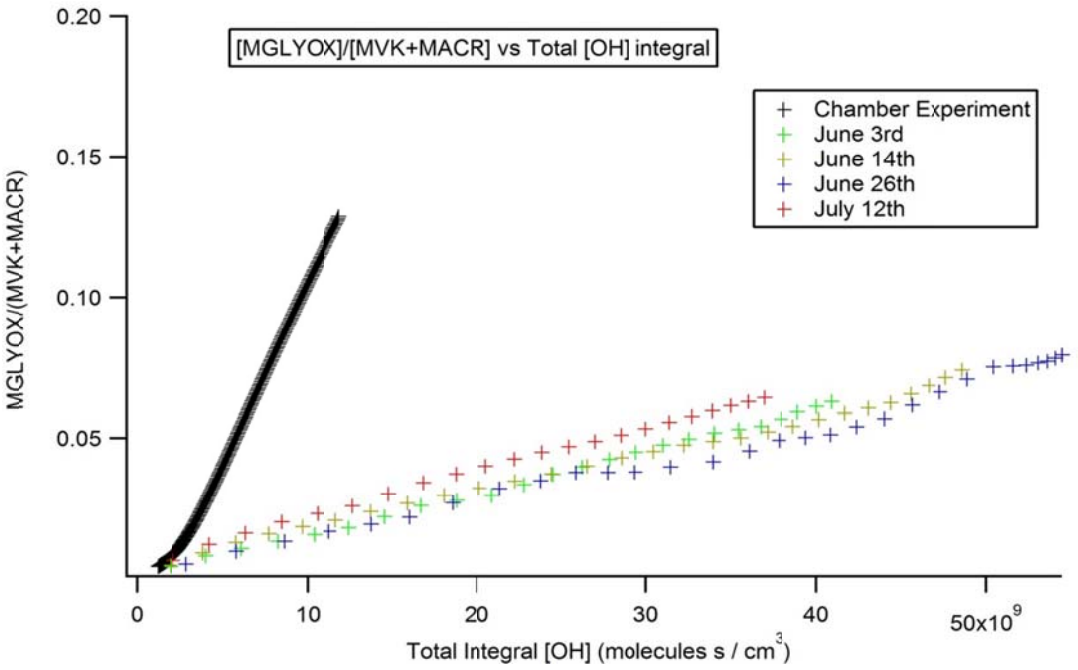

Figure 3.12 – A ratio of second generation products (MGLYOX) vs first generation products (MVK + MACR) vs total integral of [OH] at each time step.

Figure 3.12 shows a plot of MGLYOX/(MVK+MACR) vs. the total integral of [OH] at each time for the chamber experiment and the four case study days. This essentially allows us to see how the ratio of secondary generation products (represented by MGLYOX) changes with respect to first generation products. The integral of [OH] allows us to express the degree of oxidation by OH, for both the chamber and ambient conditions. In both cases, the relative amounts of secondary vs. primary oxidation products increase roughly linearly with OH oxidation, however the two data sets diverge very quickly implying more efficient production of second generation products and/or less efficient loss processes within the chamber experiment conditions. This can be explained by the fact that in the case of ambient air, there is a continuous emission of the parent VOC, isoprene, yielding a steady production of primary products MVK and

MACR. The production of first generation species is quickest during the first hour of the laboratory experiment when isoprene concentrations are large. However, as isoprene oxidation slows due to lower isoprene concentration, the production of first generation products slows down as well. In contrast, since first generation products have built up in concentration, second generation species production has increased. This causes the ratio of secondary to primary species to favor the secondary products. A similar process where higher generation products become favorable is seen in ambient conditions, demonstrated by the positive slope seen in Figure 3.12. However, emissions from vegetation maintain isoprene during the day at a relatively constant concentration. Therefore, the shift to favor secondary products will not be as fast as within the chamber experiment. This will cause the chemical system within the chamber to favor pathways, which involve more secondary production such as methylglyoxal. Perhaps the most important difference between the chamber experiment and ambient conditions is the radiation difference. Photolysis rates are significantly slower in the chamber than in ambient atmosphere by about a factor of 10. Therefore the contribution to PA radicals in the ambient air from $J_{methylglyoxal}$ and J_{MVK} is significantly larger than from the chamber experiment. As noted before, photolysis in ambient air can account for 20% of all PA radicals. These differences can help explain the discrepancies when chamber experiment data is applied to ambient conditions.

Sources of acetaldehyde are a complicated matter within the troposphere. There are many known sources of acetaldehyde, including oxidation from other VOCs [Atkinson, 1997; Seinfeld and Pandis, 1998], decomposition of biogenic organic matter (leaf litter) [Schade and Goldstein, 2001], and anthropogenic sources [Simon et al.,

2010]. Luecken et al. [2012] estimated that photochemical production accounts for the majority of the acetaldehyde concentration in the ambient atmosphere. As an example, the simple oxidation mechanism for the production of acetaldehyde from ethane is given in Equations 3.9-3.11.

$$CH_3CH_3 + \cdot OH\ (+O_2) \rightarrow CH_3CH_2\text{-}O\text{-}O + H_2O \qquad (3.9)$$

$$CH_3CH_2\text{-}O\text{-}O\cdot + NO\cdot \rightarrow CH_3CH_2O\cdot + NO_2 \qquad (3.10)$$

$$CH_3CH_2O\cdot\ (+O_2) \rightarrow CH_3CHO + HO_2 \qquad (3.11)$$

Furthermore, except in dense urban/industrial environments, they concluded reduction of emissions of acetaldehyde itself has small impact at reducing ambient concentrations. Consistent with Luecken et al., upon plotting field study measurements from the SOAS field campaign of acetaldehyde vs various VOCs (biogenic tracers), and NO_x (an anthropogenic tracer), no significant correlation with any single tracer was identified. Therefore it is likely that a complex system of several important chemical precursors and emission sources are present to explain acetaldehyde concentrations.

3.5 Conclusions

A relationship between MPAN and PAN production was employed from chamber experiment data in order to approximate isoprene contribution to PAN production in the ambient atmosphere. To date, few studies have identified key reactions and their relative production to PAN within the atmosphere. In order to identify important precursors, atmospheric case study days during the SOAS field campaign were chosen based on strict criteria to reduce meteorological effects and identify days for which PAN and MPAN concentrations both increase. Using a relationship between ambient changes in MPAN

and PAN concentration, an average of 44 (± 16)% of PAN production was determined to be explained due to isoprene oxidation during the field campaign. The need to identify other important PAN sources employed a 0-D model to simulate PAN production through the use of PA counters. This study identifies eleven important processes that dominate PAN production in ambient conditions. Simulation results show that between 50-70% of PA radicals are produced from isoprene oxidation processes. This is not significantly different from the chamber study relationship calculation and therefore is a reasonable approximation for similar conditions where MPAN and PAN production is much greater than loss. Other important sources of PAN production include acetaldehyde (14-45%), terpene oxidation (1-14%) and acetone (~1%). Furthermore, key conditions between the chamber study and ambient air, such as faster photolysis rates and secondary generational pathways favored within the chamber experiment help to explain discrepancies between the mean values attained for isoprene contribution to PA radicals.

CHAPTER 4: CONCLUSIONS

This study investigated the current understanding of VOC impact on the production of PAN in an ambient environment. Eleven important chemical processes were identified to significantly contribute to PAN production within the southeastern forest environment during the SOAS field campaign. As with all scientific studies, there is a need for further investigation to continue the natural progression of understanding the atmosphere around us. Motivated by the conclusions of this study, topics that need further examination include APN and terpene oxidation pathways, Criegee radicals, and transport model work.

In chapter 2 of this study, a clear discrepancy in the agreement between PAN and MPAN concentrations begs for a continued assessment of these chemical processes. A significant oversimulation of both species occurred. Therefore, further study of the production and loss processes of these species in the experimental conditions of this study is necessary. For example, a study in which key first generation products, such as MVK and MACR simultaneously measured along with the species observed in this study would be extremely beneficial to observe model performance for these oxidation products in attempt to identify the initial breakdown in model agreement. Terpene oxidation pathways for this study were based mostly on a general reaction scheme that MCM utilizes to predict reaction products of VOCs as they degrade via oxidation.

Although there are many first generational product studies done on terpene chemistry, much of the chemistry of higher generation (third and fourth generation) products of terpene oxidation are highly speculative, which are responsible for the production of PA radicals in this study. Terpene oxidation processes were estimated to contribute as much as 15% to PAN production. Due to its role as a significant contributor to PAN and organic aerosol production [Rindelaub 2015], understanding the terpene kinetic mechanism is vital to our complete understanding of terpene contribution to PAN within the atmosphere. Therefore additional studies in which identification of oxidation products of high generation products from terpene oxidation will be essential to assessing the explicit model details of the terpene oxidation mechanism used in this study.

This study also recognized the influence of Criegee radicals as a source of PAN production. As much as ~20% of PAN production was attributed to Criegee radical chemistry through formation of peroxyacetyl radicals. Understanding of these chemical pathways is still in their infancy stages, as it was only recently that the first direct observations of Criegee radical intermediates were detected. Much of the kinetic information included in this study is based on theoretical studies, and therefore there is still a need to verify these chemical pathways through additional direct kinetic studies. Updating this kinetic information will verify Criegee radical influence on PAN production in the atmosphere.

Future work in the field should also consider employing a detailed chemical model such as the one used in this study with chemical transport capabilities in order to analyze the full diurnal cycle of PAN production. Limitations due to lack of meteorological elements within the 0-D mechanism forced this study to focus strictly on

daytime PAN production when the boundary layer was relatively unchanging. Implementation of a transport model would be useful in assessing how much local PAN production contributes to the total observed concentration of PAN. This would also allow us to explore the nature of nighttime PAN chemistry. Although we were able to identify important precursors, uncertainties due to chemical transport make comparison of observed and simulated PAN concentrations beyond the scope of this study.

LIST OF REFERENCES

LIST OF REFERENCES

Altshuller, A.P. (1993) PANs in the atmosphere. J. Air Waste Manage Assoc., 43, 1221-1230.

Atkinson, R., and S. M. Aschmann (1984), Rate Constants for the Reaction of OH Radicals with a Series of Alkenes and Dialkenes at 295 +/- 1-K, Int. J. Chem. Kinet., 16(10), 1175-1186.

Atkinson, R., (1997), Gas-phase tropospheric chemistry of volatile organic compounds: 1. alkanes and alkenes. J. Phys. Chem. Ref., Data 26, 215-290.

Atkinson, R., D. L. Baulch, R. A. Cox, J. N. Crowley, R. F. Hampson, R. G. Hynes, M. E. Jenkin, M. J. Rossi and J. Troe (2006), Atmos. Chem. Phys., 6, 3625, IUPAC Subcommittee for Gas Kinetic Data Evaluation, (http://iupac.pole-ether.fr).

Bates, K. H., J. D. Crounse, J. M. St. Clair, N. B. Bennett, T. B. Nguyen, J. H. Seinfeld, B. M. Stoltz and P. O. Wennberg (2014), Gas Phase Production and Loss of Isoprene Epoxydiols, J. Phys. Chem. A, 118, 1237–1246.

Bertman, S. B. and J. M. Roberts (1991), A pan analog from isoprene photooxidation. Geophys. Res. Lett., 18 (8), 1461−1464.

Bell, M. L., A. McDermott, S. L. Zeger, J. M. Samet and F. Dominici (2004), Ozone and short-term mortality in 95 US urban communities, 1987-2000, J. Am. Med. Assoc. 292: 359-365.

Biesenthal, T. A. and P. B. Shepson (1997a), Observations of anthropogenic inputs of the isoprene oxidation products methyl vinyl ketone and methacrolein to the atmosphere, Geophys. Res. Lett., 24, 1375–1378.

Biesenthal, T.A., Q. Wu, P. B. Shepson, H. A. Wiebe, K. G. Anlauf and G. I. Mackay (1997b), A study of relationships between isoprene, its oxidation products, and ozone, in the Lower Fraser Valley, BC. Atmos. Environ. 31, 2049-2058.

Blitz, M.A., D. E. Heard, M. J. Pilling, S. R. Arnold and M. P. Chipperfield (2004) Pressure and temperature-dependent quantum yields for the photodissociation of acetone between 279 and 327.5nm. Geophysics Research Letters, 31, L06111

Bloss, C., V. Wagner, M. E. Jenkin, R. Volkamer, W. J. Bloss, J. D. Lee, D. E. Heard, K. Wirtz, M. Martin-Reviejo, G. Rea, J. C. Wenger and M. J. Pilling (2005), Development of a detailed chemical mechanism (MCMv3.1) for the atmospheric oxidation of aromatic hydrocarbons, Atmos. Chem. Phys., 5, 641–664.

Carter, W. P. L. and R. Atkinson (1996), Development and evaluation of a detailed mechanism for the atmospheric reactions of isoprene and NO_x, Int. J. Chem. Kinet., 28(7), 497-530.

Chen, X. H., D. Hulbert and P. B. Shepson (1998), Measurement of the organic nitrate yield from OH reaction with isoprene, J. Geophys. Res., 103(D19), 25563-25569.

Chuong, B., and P. S. Stevens (2002), Measurements of the kinetics of the OH-initiated oxidation of methyl vinyl ketone and methacrolein, Int. J. Chem. Kinet., 36(1), 12-25.

Costa, A. W. (2010), Coupling between the carbon and nitrogen cycles in a forested environment, (Doctoral dissertation), Retrieved from ProQuest Dissertations and Theses (Order No. 3507226).

DeMarini, D. M., M. L. Shelton, M. J. Kohan, E. E. Hudgens, T. E. Kleindienst, L. M. Ball, D. Walsh, J. G. de Boer, L. Lewis-Bevan, J. R. Rabinowitz, L. D. Claxton and J Lewtas (2000), Mutagenicity in lung of Big Blue® mice and induction of tandem-base substitutions in Salmonella by the air pollutant peroxyacetyl nitrate (PAN): predicted formation of intrastrand cross-links, Mutat. Res., 457, 41–55.

Espada, C., J. Grossenbacher, K. Ford, T. Couch and P. B. Shepson (2005), The Production of Organic Nitrates from Various Anthropogenic Volatile Organic Compounds, Int. J. Chem. Kinet, 37, 675–685.

Fan, J., and R. Zhang (2004), Atmospheric Oxidation Mechanism of Isoprene, Environ. Chem., 1, 140-149.

Finlayson-Pitts, B. J., and J. N. Pitts Jr. (2000), Chemistry of the Upper and Lower Atmosphere, Elsevier, New York.

Fischer, E. V., D. J. Jacob, R. M. Yantosca, M. P. Sulprizio, D. B. Millet, J. Mao, F. Paulot, H. B. Singh, A. Roiger, L. Ries, R. W. Talbot, K. Dzepina and S. Pandey Deolal (2014), Atmospheric peroxyacetyl nitrate (PAN): a global budget and source attribution, Atmos. Chem. Phys., 14, 2679–2698.

Gilman, J. B., J. F. Burkhart, B. M. Lerner, E. J. Williams, W. C. Kuster, P. D. Goldan, P. C. Murphy, C. Warneke, C. Fowler, S. A. Montzka, B. R. Miller, L. Miller, S. J. Oltmans, T. B. Ryerson, O. R. Cooper, A. Stohl and J. A. de Gouw (2010), Ozone variability and halogen oxidation within the Arctic and sub-Arctic springtime boundary layer, Atmos. Chem. Phys., 10, 10223–10236.

Goldstein, A.H., C. D. Koven, C. L. Heald, I. Y. Fung (2009), Biogenic carbon and anthropogenic pollutants combine to form a cooling haze over the southeastern United States, Proc. Natl. Acad. Sci., 106, 8835-8840.

Guenther, A., C. N. Hewitt, D. Erickson, R. Fall, C. Geron, T. Graedel, P. Harley, L. Klinger, M. Lerdau, W. A. McKay, T. Pierce, B. Scholes, R. Steinbrecher, R. Tallamraju, J. Taylor, and P. Zimmerman (1995), A Global-Model of Natural Volatile Organic-Compound Emissions, J. Geophys. Res., 100(D5), 8873-8892.

Hansen, J., R. Ruedy, R., M. Sato, and K. Lo (2010). Global surface temperature change. Rev. Geophys. 48: RG4004.

Heddle J. A., P. B. Shepson, J. D. Gingerich and K. W. So (1993), Mutagenicity of peroxyacetyl nitrate (PAN) in vivo: tests for somatic mutations and chromosomal aberrations. Environ. Mol. Mutag., 21(1): 58-66.

Hewitt, C. N. and G. L. Kok (1991), Formation and occurrence of organic hydroperoxides in the troposphere: laboratory and field observations, J. Atmos. Chem., 12, 181–194.

Holloway, A. M. and R. P. Wayne (2010), Atmospheric Chemistry, RSC Publishing, Cambridge.

Howard, J. N. (1959), The transmission of the atmosphere in the infrared, Proc. Inst. Radio Eng., 47, 1451–1457.

IPCC, 2014: Climate Change 2014: Synthesis Report. Contribution of Working Groups I, II and III to the Fifth Assessment Report of the Intergovernmental Panel on Climate Change [Core Writing Team, R.K. Pachauri and L.A. Meyer (eds.)]. IPCC, Geneva, Switzerland, 151 pp.

Jenkin, M., S. Saunders and M. Pilling (1997), The tropospheric degradation of volatile organic compounds: A protocol for mechanism development, Atmos. Environ., 31, 81-104.

Jenkin, M. E., S. M. Saunders, V. Wagner and M. J. Pilling (2003), Protocol for the development of the Master Chemical Mechanism, MCM v3 (Part B): tropospheric degradation of aromatic volatile organic compounds, Atmos. Chem. Phys., 3, 181–193.

Jones, P. D., M. New, D. E. Parker, S. Martin and I. G. Rigor (1999), Surface air temperature and its changes over the past 150 years, Rev. Geophys.1999; 37(2): 179-199.

Kleindienst, T.E., P. B. Shepson, D. F. Smith, E. E. Hudgens, C. M. Nero, L. T. Cupitt, J. J. Bufalini, L. D. Claxton and F. R. Nestman (1990) Comparison of mutagenic activities of several peroxyacyl nitrates, Environ. Mol. Mutagen, 16(2), 70–80.

Kleindienst, T. E. (1994), Recent developments in the chemistry and biology of peroxyacetyl nitrate, Res. Chem. Intermediat., 20, 335–384.

LaFranchi B. W., G. M. Wolfe, J. A. Thornton, E. C. Browne, K.-E. Min, P. J. Wooldridge, M. McKay, A. H. Goldstein, J. B. Gilman, D. Welsh-Bon, W. C. Kuster, J. A. deGouw, J. Mao, Z. Chen, X. Ren, W. H. Brune and R. C. Cohen (2009), Closing the peroxy acetyl nitrate budget: observations of acyl peroxy nitrates (PAN, PPN, and MPAN) during BEARPEX 2007, Atmos. Chem. Phys., 9, 7623-7641.

Lee, L., A. P. Teng, P. O. Wennberg, J. D. Crounse and R. C. Cohen (2014), On rates and mechanisms of OH and O3 reactions with isoprene-derived hydroxy nitrates, J. Phys. Chem. A, 118, 1622–1637.

Liao, J., H. Sihler, L. G. Huey, J. A. Neuman, D. J. Tanner, U. Friess, U. Platt, F. M. Flocke, J. J. Orlando, P. B. Shepson, H. J. Beine, A. J. Weinheimer, S. J. Sjostedt, J. B. Nowak, D. J. Knapp, R. M. Staebler, W. Zheng, R. Sander, S. R. Hall and K. Ullmann (2011), A comparison of Arctic BrO measurements by chemical ionization mass spectrometry and long path differential optical absorption spectroscopy, J. Geophys. Res., 116, D00R02.

Lightfoot, P. D., R. A. Cox, J. N. Crowley, M. Destriau, G. D. Hayman, M. E. Jenkin, G. K. Moortgat, and F. Zabel (1992), Organic peroxy radicals – kinetics, spectroscopy and tropospheric chemistry, Atmos. Environ., 26(10), 1805-1961.

Lockwood, A. L. (2008), The fate of atmospheric organic nitrates, (Doctoral dissertation), Retrieved from ProQuest Dissertations and Theses (Order No. 3373189).

Lockwood, A. L., P. B. Shepson, M. N. Fiddler, and M. Alaghmand (2010), Isoprene Nitrates: Preparation, Separation, Identification, Yields, and Atmospheric Chemistry, Atmos. Chem. Phys., 10, 6169-6178.

Lorius C., J. Jouzel and D. Raynaud (1992), The ice core record: past archive of the climate and signpost to the future. Philosophical Transactions of the Royal Society: Biological Sciences 338: 227–234.

Luecken, D. J., W. T. Hutzell, M. L. Strum and G. A. Pouliot (2012), Regional sources of atmospheric formaldehyde and acetaldehyde, and implications for atmospheric modeling, Atmos. Environ., 47, 477–490.

Mao, J., X. Ren, L. Zhang, D. M. Van Duin, R. C. Cohen, J. H. Park, A. H. Goldstein, F. Paulot, M. R. Beaver, J. D. Crounse, P. O. Wennberg, J. P. DiGangi, S. B. Henry, F. N. Keutsch, C. Park, G. W. Schade, G. M. Wolfe, J. A. Thornton and W. H. Brune (2012), Insights into hydroxyl measurements and atmospheric oxidation in a california forest, Atmos. Chem. Phys., 12, 8009–8020.

Min K.-E., S. E. Pusede, E. C. Browne, B. W. LaFranchi, P. J. Wooldridge, G. M. Wolfe, S. A. Harrold, J. A. Thornton, and R. C. Cohen (2012), Observations of atmosphere-biosphere exchange of total and speciated peroxynitrates: nitrogen fluxes and biogenic sources of peroxynitrates, Atmos. Chem. Phys., 12, 9763-9773.

Montzka, S. A., M. Trainer, P. D. Goldan, W. C. Kuster and F. C. Fehsenfeld (1993), Isoprene and its oxidation products, methylvinyl ketone and methacrolein, in the rural troposphere, J. Geophys. Res.-Atmos., 98, 1101–1111.

National Oceanic and Atmospheric Administration (NOAA) Coastal Services Center (2012), Lidar 101: An Introduction to Lidar Technology, Data, and Applications. Revised. Charleston, SC: NOAA Coastal Services Center.

Patchen, A. K., M. J. Pennino, A. C. Kiep, and M. J. Elrod (2007), Direct kinetics study of the product-forming channels of the reaction of isoprene-derived hydroxyperoxy radicals with NO, Int. J. Chem. Kinet., 39(6), 353-361.

Paulot, F., J. D. Crounse, H. G. Kjaergaard, J. H. Kroll, J. H. Seinfeld, and P. O. Wennberg (2009), Isoprene photooxidation: new insights into the production of acids and organic nitrates, Atmos. Chem. Phys., 9, 1479-1501.

Peeters, J., J. F. Müller, T. Stavrakou, and V. S. Nguyen (2014), Hydroxyl radical recycling in isoprene oxidation driven by hydrogen bonding and hydrogen tunneling: the upgraded LIM1 mechanism, J. Phys. Chem. A, 118(38), 8625–8643.

Pippin, M., S. Bertman, T. Thornberry, M. Town, M. A. Carroll, S. Sillman (2001) Seasonal variations of PAN, PPN, and O3 at the upper midwest PROPHET site. J. Geophys. Res.-Atmos., 106, 24451-24463.

Portmann, R. W., S. Solomon and G. C. Hegerl (2009), Spatial and seasonal patterns in climate change, temperatures, and precipitation across the United States. Proc. Natl. Acad. Sci. U.S.A., 106(18), 7324-7329.

Rindelaub J. D., K. M. McAvey and P. B. Shepson (2015), The photochemical production of organic nitrates from alpha-pinene and loss via acid-dependent particle phase hydrolysis, Atmos. Environ., 100, 193-201.

Roberts, J. M., M. Marchewka, S. B. Bertman, R. Sommariva, C. Warneke, J. de Gouw, W. Kuster, P. Goldan, E. Williams, B. M. Lerner, P. Murphy and F. C. Fehsenfeld (2007), Measurements of PANs during the New England air quality study 2002, J. Geophys. Res.-Atmos., 112, D20306.

Rohrer F., B. Bohn, T. Brauers, D. Bruning, F.-J. Johnen, A. Wahner, and J. Kleffmann (2005), Characterisation of the photolytic HONO-source in the atmosphere simulation chamber SAPHIR, Atmos. Chem. Phys., 5, 2189–2201.

Sakamaki, F. and H. Akimoto (1988), HONO formation as unknown radical source in photochemical smog chambers, Int. J. Chem. Kinet., 20, 111–116.

Saunders, S. M., M. E. Jenkin, R. G. Derwent and M. J. Pilling (2003) Protocol for the development of the Master Chemical Mechanism, MCM v3 (Part A): tropospheric degradation of non-aromatic volatile organic compounds, Atmos. Chem. Phys., 3, 161–180.

Schade G. and A. H. Goldstein (2001), Fluxes of oxygenated volatile organic compounds from a ponderosa pine plantation, J. Geophys. Res., 106(D3), 3111–3123.

Seinfeld, J.H. and S. N. Pandis (1998), Atmospheric Chemistry and Physics. John Wiley & Sons, Inc., New York.

Simon, H., L. Beck, P. Bhave, F. Divita, Y. Hsu, D. Luecken, D. Mobley, G. Pouliot, A. Reff, G. Sarwar and M. Strum (2010), The development and uses of EPA's SPECIATE database. Atmospheric Pollution Research 1, 196-206.

Singh, H. B. and P. L. Hanst (1981), Peroxyacetyl nitrate (PAN) in the unpolluted atmosphere: An important reservoir for nitrogen oxides, Geophys. Res. Lett., 8, 941-944.

Stephens, E.R. (1969), The formation, reactions, and properties of peroxyacyl nitrates (PANS) in photochemical air pollution, Wiley, New York.

Stephens G. L., J. Li, M. Wild, C. A. Clayson, N. Loeb, S. Kato, T. L'Ecuyer, P. W. Stackhouse Jr., M. Lebsock and T. Andrews (2012). An update on earth's energy balance in light of the latest global observations. Nat. Geosci., 5: 691-696.

Stull, R.B. (1988) An introduction to boundary layer meteorology. An introduction to boundary layer meteorology, Kluwer Acad., Norwell, Mass.

Taatjes, C. A., D. E. Shallcross and C. J. Percival (2014), Research frontiers in the chemistry of Criegee intermediates and tropospheric ozonolysis, Phys. Chem. Chem. Phys., 16(5), 1704-1718.

Tilton, B. E. (1989), Health effects of tropospheric ozone: major effects and related scientific questions. Environ. Sci.Tech. 23, 257-263.

Temple, P. and O. Taylor, (1983), World-wide ambient measurements of peroxyacetyl nitrate (PAN) and implications for plant injury. Atmos. Environ. 17 (8), 1583–1587.

Terao, Y., J. A. Logan, A. R. Douglass and R. S. Stolarski (2008), Contribution of stratospheric ozone to the interannual variability of tropospheric ozone in the northern extratropics. J. Geophys. Res., 113, D18309.

Tuazon, E. C., and R. Atkinson (1990), A product study of the gas-phase reaction of isoprene with the OH radical in the presence of NOx, Int. J. Chem. Kinet., 22(12), 1221-1236.

Turnipseed, A. A., L. G. Huey, E. Nemitz, R. Stickel, J. Higgs, D. J. Tanner, D. L. Slusher, J. P. Sparks, F. Flocke and A. Guenther (2006), Eddy covariance fluxes of peroxyacetyl nitrates (PANs) and NO(y) to a coniferous forest, J. Geophys. Res.-Atmos., 111, D09304.

Vereecken, L. and J.S. Francisco (2012), Theoretical studies of atmospheric reaction mechanisms in the troposphere, Chem. Soc. Rev., 41(19), 6259–6293.

Vonder Haar, T. H., and V. Suomi, (1971) Measurements of earth's radiation budget from satellites during a five years period. Part I: Extended time and space means, J. Atmos. Sci., 28, 305-314.

Wang, Y. H., J. A. Logan, and D. J. Jacob (1998), Global simulation of tropospheric O-3-NOx hydrocarbon chemistry 2. Model evaluation and global ozone budget, J. Geophys. Res., 103 (D9), 10727-10755.

Wu, S., L. J. Mickley, D. J. Jacob, J. A. Logan, R. M. Yantosca, and D. Rind (2007), Why are there large differences between models in global budgets of tropospheric ozone?, J. Geophys. Res., 112, D05302.

Wu, Z., X. Wang, A. A. Turnipseed, F. Chen, L. Zhang, A. B. Guenther, T. Karl, L. G. Huey, D. Niyogi, B. Xia and K. Alapaty (2012), Evaluation and improvements of two community models in simulating dry deposition velocities for peroxyacetyl nitrate (PAN) over a coniferous forest, J. Geophys. Res., 117, D04310.

Xiong et al., (2015), Isoprene nitrate production: lab experiment and field observation, manuscript in preparation.

Xue, L. K., T. Wang, X. F. Wang, D. R. Blake, J. Gao, W. Nie, R. Gao, X. M. Gao, Z. Xu, A. J. Ding, Y. Huang, S. C. Lee, Y. Z. Chen, S. L. Wang, F. H. Chai, Q. Z. Zhang and W. X. Wang (2014), On the use of an explicit chemical mechanism to dissect peroxy acetyl nitrate formation, Environ. Pollution, 195, 39–47.

Zador, J., T. Turanyi, K. Wirtz and M. J. Pilling (2006), Measurement and investigation of chamber radical sources in the European Photoreactor (EUPHORE), J. Atmos. Chem., 55, 147–166.

Zhou, X. L., Y. He, G. Huang, T. D. Thornberry, M. A. Carroll, and S. B. Bertman (2002), Photochemical production of nitrous acid on glass sample manifold surface, Geophys. Res. Lett., 29, 1681.

Ziemann, P.J. and R. Atkinson (2012), Kinetics, products, and mechanisms of secondary organic aerosol formation, Chem. Soc. Rev., 41, 6582-6605.

APPENDICES

Appendix A: 0-D Photochemical Mechanism Isoprene Reactions

Below is the FACSIMILE input script for the isoprene photo-oxidation model modified from the MCM isoprene subset. The (*) indicate comments to describe sections and are not a functioning part of the script. This was written using FACSIMILE 4.2.50, and may not be applicable to other versions of FACSIMILE. Only chemical reactions within the mechanism are listed for reasons of spatial conservation. Note that names of chemical species are consistent with the MCM website. For questions about FACSIMILE contact MCPA support (support@mcpa-software.com), and any questions about the code can be directed to me (cjgroff@att.net).

0-D Isoprene Reactions

```
COMPILE EQUATIONS;

*Inorganic Reactions and Others;

% K1f : O_3P+O2=O3;
% K2f : O_3P+O3=O2+O2;
% K3f : O_1D=O_3P;
% K4f : O_1D+H2O=OH+OH;
% K5f : O3+HO2=OH+O2+O2;
% K6f : HO2+NO=NO2+OH;
% K7f*0.70 : HO2+NO3=NO2+OH+O2;
% K7f*0.30 : HO2+NO3=HNO3+O2;
% K8f : O3+OH=HO2+O2;
% K9f : OH+HO2=HO2+H2O;
% K10f : H2O2+OH=HO2+H2O;
% K11f : HO2+HO2=H2O2+O2;
% K12f : OH+H2=H2O+HO2;
% K13f : H+O2=HO2;
% K14f : CO+OH=HO2+CO2;
% K15f : HCO+O2=CO+HO2;
% k16f : HCHO+NO3=HNO3+CO+HO2;
% K17f : HNO4=HO2+NO2;
% K18f : OH+NO3=NO2+HO2;
```

```
% k19f : CH3O+O2=HO2+HCHO;
% K20f : O_3P+NO=NO2;
% K21f : O_3P+NO2=NO+O2;
% K22f : O_3P+NO2=NO3;
% K23f : OH+NO=HONO;
% K24f : OH+NO2=HNO3;
% K25f : HO2+NO2=HNO4;
% K26f : OH+HONO=NO2+H2O;
% K27f : OH+HNO3=NO2+H2O;
% K28f : OH+HNO4=NO2+O2+H2O;
% K29f : O3+NO=NO2+O2;
% K30f : O3+NO2=NO3+O2;
% K31f : NO3+NO=NO2+NO2;
% K32f : NO3+NO2=N2O5;
% K33f : N2O5=NO2+NO3;
% K34f : NO3+NO3=NO2+NO2+O2;
% k35f : N2O5+H2O=HNO3+HNO3;
% k36f : NO2+NO2=HONO+HNO3;

* Isoprene Chemistry;

% 1.865E-11 : A2PAN + OH = HOCH2CHO + CO + NO2 ;
% 1.9D17*EXP(-14100/TEMP) : A2PAN = A2PANOO + NO2 ;
% KDEC : A2PANO = HOCH2CHO + HO2 ;
% KAPHO2*0.44 : A2PANOO + HO2 = A2PANO + OH ;
% KAPHO2*0.15 : A2PANOO + HO2 = C2OHOCO2H + O3 ;
% KAPHO2*0.41 : A2PANOO + HO2 = C2OHOCOOH ;
% KAPNO : A2PANOO + NO = A2PANO + NO2 ;
% KFPAN : A2PANOO + NO2 = A2PAN ;
% KRO2NO3*1.74 : A2PANOO + NO3 =  A2PANO + NO2 ;
% 1.00E-11*0.7*RO2 : A2PANOO = A2PANO ;
% 1.00E-11*0.3*RO2 : A2PANOO = C2OHOCO2H ;
% 5.98D-12*0.75 : OH + ACETOL = MGLYOX + HO2 + AA ;
% 5.98D-12*0.075 : OH + ACETOL = HCOOH + CO2 + CH3O2 + HO2 ;
% 5.98D-12*0.05 : OH + ACETOL = HCOOH + CH3O2 + CO ;
% 5.98D-12*0.1 : OH + ACETOL = CO2 + OH + CH3CO2H ;
% 5.98D-12*0.025 : OH + ACETOL = CO2 + CH3CO2H ;
% 1.2D-15 : ACLOO + CO = ACETOL ;
% 1.0D-14 : ACLOO + NO = ACETOL + NO2 ;
% 1.0D-15 : ACLOO + NO2 = ACETOL + NO3 ;
% 7.0D-14 : ACLOO + SO2 = ACETOL + SO3 ;
% 6.0D-18 : ACLOO + H2O = ACETOL + H2O2 ;
% KDEC*0.11 : ACLOOA = ACLOO ;
% KDEC*0.89 : ACLOOA = OH + HO2 + MGLYOX + AB ;
% 8.66D-12 : ACO2H + OH = HO2 + CO + HCHO ;
```

```
% KAPHO2*0.15 : ACO3 + HO2 = ACO2H + O3 ;
% KAPHO2*0.41 : ACO3 + HO2 = ACO3H ;
% KAPHO2*0.44 : ACO3 + HO2 = HO2 + CO + HCHO + OH ;
% KAPNO : ACO3 + NO = HO2 + CO + HCHO + NO2 ;
% KFPAN : ACO3 + NO2 = ACRPAN ;
% KRO2NO3*1.74 : ACO3 + NO3 = HO2 + CO + HCHO + NO2 ;
% 1.00D-11*0.3*RO2 : ACO3 = ACO2H ;
% 1.00D-11*0.7*RO2 : ACO3 = HO2 + CO + HCHO ;
% KRO2HO2*0.52 : ACO3B + HO2 = HOCHOCOOH ;
% KRO2NO : ACO3B + NO = CHOCOHCO + NO2 ;
% KRO2NO3 : ACO3B + NO3 = CHOCOHCO + NO2 ;
% 8.8D-13*0.6*RO2 : ACO3B = CHOCOHCO ;
% 8.8D-13*0.2*RO2 : ACO3B = HOCH2COCHO ;
% 8.8D-13*0.2*RO2 : ACO3B = OCCOHCOH ;
% 1.22D-11 : ACO3H + OH = ACO3 ;
% 3.17E-15 : ACR + NO3 = ACO3 + HNO3 ;
% 0.68*2.00E-11 : ACR + OH = ACO3 ;
% 0.255*2.00E-11 : ACR + OH = ACO3B ;
% 0.065*2.00E-11 : ACR + OH = OCCOHCO2 ;
% 0.5*2.9E-19 : ACR + O3 = CH2OOB + GLYOX ;
% 0.5*2.9E-19 : ACR + O3 = GLYOOB + HCHO ;
% 1.9D17*EXP(-14100/TEMP) : ACRPAN = ACO3 + NO2 ;
% 8.63D-12 : ACRPAN + OH = HOCH2CHO + CO + NO2 ;
% 2.59D-11 : ALLYLOH + OH  = ACR + HO2 ;
% KDEC : BIACETO = CH3CO3 + HCHO + CO + IPRENE ;
% 2.69D-12 :BIACETOH + OH = CO23C3CHO + HO2 ;
% 2.1D-16 : C2H4 + NO3 = ETHENO3O2 ;
% 1.58D-18 : C2H4 + O3 = HCHO + CH2OOA ;
% KMT15 : C2H4 + OH = HOCH2CH2O2 ;
% 1.867E-11 : C2OHOCO2H + OH = C3DIOLO2 ;
% 1.513E-11 : C2OHOCOOH + OH = A2PANOO ;
% 1.36D-10 : C32OH13CO + OH = HCOCOHCO3 ;
% KDEC : C3DIOLO = HOCH2CHO + HCHO + HO2 ;
% KRO2HO2*0.520 : C3DIOLO2 + HO2 = C3DIOLOOH ;
% KRO2NO : C3DIOLO2 + NO = C3DIOLO + NO2 ;
% KRO2NO3 : C3DIOLO2 + NO3 = C3DIOLO + NO2 ;
% 2.00D-12*RO2 : C3DIOLO2 = C3DIOLO ;
% 2.78D-11 : C3DIOLOOH + OH = C3DIOLO2 ;
% 9.54D-15*0.35 : C3H6 + NO3 = PRONO3AO2 ;
% 9.54D-15*0.65 : C3H6 + NO3 = PRONO3BO2 ;
% 1.00D-17*0.5 : C3H6 + O3 = CH2OOB + CH3CHO ;
% 1.00D-17*0.5 : C3H6 + O3 = CH3CHOOA + HCHO ;
% KMT16*0.87 : C3H6 + OH = HYPROPO2 ;
% KMT16*0.13 : C3H6 + OH = IPROPOLO2 ;
% 1.32D-10 : C3MDIALOH + OH = CHOMOHCO3 ;
```

% 2.92D-11 : C42AOH + OH = NMGLYOX + HO2 ;
% 2.53D-11*0.86 : C4M2ALOHNO3 + OH = MMALNACO3 ;
% 2.53D-11*0.14 : C4M2ALOHNO3 + OH = MMALNBCO3 ;
% 1.9D17*EXP(-14100/TEMP) : C4PAN10 = H13CO2CO3 + NO2 ;
% 5.83D-12 : C4PAN10 + OH = HOCH2COCHO + CO + NO2 ;
% 1.9D17*EXP(-14100/TEMP) : C4PAN5 = IPRHOCO3 + NO2 ;
% 4.75D-13 : C4PAN5 + OH = CH3COCH3 + CO + NO2 ;
% 1.9D17*EXP(-14100/TEMP) : C4PAN6 = CO2H3CO3 + NO2 ;
% 3.74D-12 : C4PAN6 + OH = MGLYOX + CO + NO2 + AC ;
% KDEC : C510O = NOA + GLYOX + HO2 ;
% KRO2HO2*0.706 : C510O2 + HO2 = C510OOH ;
% KRO2NO*0.919 : C510O2 + NO = C510O + NO2 ;
% KRO2NO*0.015 : C510O2 + NO = RNO3I + CO + NO2 + HO2 ;
% KRO2NO*0.066 : C510O2 + NO = RNO3I ;
% KRO2NO3 : C510O2 + NO3 = C510O + NO2 ;
% 3.50D-14*0.689*RO2 : C510O2 = C510O ;
% 3.50D-14*0.3*RO2 : C510O2 = C510OH ;
% 3.50D-14*0.011*RO2 : C510O2 = CO + RNO3I + HO2 ;
% 2.69D-11 : OH + C510OH = C510O ;
% 2.81D-11 : C510OOH + OH = C510O2 ;
% 4.21D-11 : C524CO + OH = C525O2 ;
% 2.94D-11 : C524NO3 + OH = NC524O2 ;
% KDEC : C524O = HMACR + HCHO + HO2 ;
% 7.78D-11 : C524OH + OH = C524CO + HO2 ;
% 1.18D-10*0.22 : C524OOH + OH = C524CO + OH ;
% 1.18D-10*0.03 : C524OOH + OH = C524O2 ;
% 1.18D-10*0.75 : C524OOH + OH = HIEPOXB + OH ;
% KRO2HO2*0.706 : C524O2 + HO2 = C524OOH ;
% KRO2NO*0.134 : C524O2 + NO = C524NO3 ;
% KRO2NO*0.866 : C524O2 + NO = C524O + NO2 ;
% KRO2NO3 : C524O2 + NO3 = C524O + NO2 ;
% 2.90D-12*0.1*RO2 : C524O2 = C524CO ;
% 2.90D-12*0.8*RO2 : C524O2 = C524O ;
% 2.90D-12*0.1*RO2 : C524O2 = C524OH ;
% KDEC : C525O = HOCH2CO3 + H13CO2C3 ;
% KRO2HO2*0.706 : C525O2 + HO2 = C525OOH ;
% KRO2NO : C525O2 + NO = C525O + NO2 ;
% KRO2NO3 : C525O2 + NO3 = C525O + NO2 ;
% 9.20D-14*RO2 : C525O2 = C525O ;
% 1.37D-11 : C525OOH + OH = C525O2 ;
% 9.37D-12*0.54 : C57NO3 + OH = C4M2ALOHNO3 + HO2 ;
% 9.37D-12*0.46 : C57NO3 + OH = C57NO3CO3 ;
% 6.52D-12 : C57NO3CO2H + OH = MMALNBCO2H + HO2 ;
% KAPHO2*0.15 : C57NO3CO3 + HO2 = C57NO3CO2H + O3 ;
% KAPHO2*0.41 : C57NO3CO3 + HO2 = C57NO3CO3H ;

% KAPHO2*0.44 : C57NO3CO3 + HO2 = HO12CO3C4 + NO2 + OH ;
% KAPNO : C57NO3CO3 + NO = HO12CO3C4 + NO2 + NO2 ;
% KFPAN : C57NO3CO3 + NO2 = C57NO3PAN ;
% KRO2NO3*1.74 : C57NO3CO3 + NO3 = HO12CO3C4 + NO2 + NO2 ;
% KRO2NO3*1.74 : C57NO3CO3 + NO3 = MACRNO3 + HO2 + NO2 ;
% 1.00D-11*0.3*RO2 : C57NO3CO3 = C57NO3CO2H ;
% 1.00D-11*0.7*RO2 : C57NO3CO3 = HO12CO3C4 + NO2 ;
% 6.52D-12*0.39 : C57NO3CO3H + OH = C57NO3CO3 ;
% 6.52D-12*0.61 : C57NO3CO3H + OH = MMALNBCO3H + HO2 ;
% 6.00D-12 : C57NO3PAN + OH = MMALNBPAN + HO2 ;
% 1.9D17*EXP(-14100/TEMP) : C57NO3PAN = C57NO3CO3 + NO2 ;
% KRO2HO2*0.706 : C57O2 + HO2 = C57OOH ;
% KRO2NO : C57O2 + NO = C57O + NO2 ;
% KRO2NO3 : C57O2 + NO3 = C57O + NO2 ;
% 9.20D-14*0.7*RO2 : C57O2 = C57O ;
% 9.20D-14*0.3*RO2 : C57O2 = C57OH ;
% 3.16D-11 : C57OOH + OH = C57O2 ;
% KDEC : C57O = MGLYOX + HOCH2CHO + HO2 + AD ;
% 3.04D-11 : C57OH + OH = C57O ;
% 2.32D-11 : C58NO3 + OH = C58NO3CO3 ;
% 2.49D-12 : C58NO3CO2H + OH = MMALNACO2H + HO2 ;
% KAPHO2*0.15 : C58NO3CO3 + HO2 = C58NO3CO2H + O3 ;
% KAPHO2*0.41 : C58NO3CO3 + HO2 = C58NO3CO3H ;
% KAPHO2*0.44 : C58NO3CO3 + HO2 = MACRNO3 + HO2 + OH ;
% KAPNO : C58NO3CO3 + NO = MACRNO3 + HO2 + NO2 ;
% KFPAN : C58NO3CO3 + NO2 = C58NO3PAN ;
% 1.00D-11*0.3*RO2 : C58NO3CO3 = C58NO3CO2H ;
% 1.00D-11*0.7*RO2 : C58NO3CO3 = MACRNO3 + HO2 ;
% 5.57D-12*0.68 : C58NO3CO3H + OH = C58NO3CO3 ;
% 5.57D-12*0.32 : C58NO3CO3H + OH = MMALNACO3H + HO2 ;
% 1.9D17*EXP(-14100/TEMP) : C58NO3PAN = C58NO3CO3 + NO2 ;
% 1.97D-12 : C58NO3PAN + OH = MMALNAPAN + HO2 ;
% KDEC : C58O = ACETOL + GLYOX + HO2 ;
% KRO2HO2*0.706 : C58O2 + HO2 = C58OOH ;
% KRO2NO*0.019 : C58O2 + NO = C58NO3 ;
% KRO2NO*0.981 : C58O2 + NO = C58O + NO2 ;
% KRO2NO3 : C58O2 + NO3 = C58O + NO2 ;
% 9.20D-14*0.7*RO2 : C58O2 = C58O ;
% 9.20D-14*0.3*RO2 : C58O2 = C58OH ;
% 3.04D-11 : C58OH + OH = C58O ;
% 3.16D-11 : C58OOH + OH = C58O2 ;
% KDEC : C59O = ACETOL + HOCH2CO3 ;
% KRO2HO2*0.706 : C59O2 + HO2 = C59OOH ;
% KRO2NO : C59O2 + NO = C59O + NO2 ;
% KRO2NO3 : C59O2 + NO3 = C59O + NO2 ;

```
% 9.20D-14*RO2 : C59O2 = C59O ;
% 9.70D-12 : C59OOH + OH = C59O2 ;
% 6.96D-13*0.439 : C5H8 + NO3 = NISOPAO2 ;
% 6.96D-13*0.405 : C5H8 + NO3 = NISOPBO2 ;
% 6.96D-13*0.09 : C5H8 + NO3 = NISOPCO2 ;
% 6.96D-13*0.055 : C5H8 + NO3 = NISOPDO2 ;
% 6.96D-13*0.007 : C5H8 + NO3 = NISOPEO2 ;
% 6.96D-13*0.004 : C5H8 + NO3 = NISOPFO2 ;
% 1.27D-17*0.3 : C5H8 + O3 = CH2OOE + MACR ;
% 1.27D-17*0.2 : C5H8 + O3 = CH2OOE + MVK ;
% 1.27D-17*0.3 : C5H8 + O3 = HCHO + MACROOA ;
% 1.27D-17*0.2 : C5H8 + O3 = HCHO + MVKOOA ;
% 1.0D-10*0.62*0.5 : C5H8 + OH = cisISOP2OH ;
% 1.0D-10*0.62*0.5 : C5H8 + OH = transISOP1OH ;
% 1.0D-10*0.03 : C5H8 + OH = ISOP2OH ;
% 1.0D-10*0.04 : C5H8 + OH = ISOP3OH ;
% 1.0D-10*0.31*0.7 : C5H8 + OH = cisISOP4OH ;
% 1.0D-10*0.31*0.3 : C5H8 + OH = transISOP4OH ;
% 2.5D-11*0.67 : ISOP2OH + O2 = CO51 + HO2 ;
% 2.5D-11*0.33 : ISOP2OH + O2 = ISOPFO2 ;
% 1.4D-12 : ISOP3OH + O2 = ISOPEO2 ;
% 7.0D-13 : cisISOP1OH + O2 = Z10H4OO ;
% 6.0D-13 : cisISOP1OH + O2 = ISOPBO2 ;
% 6.0D-13 : transISOP1OH + O2 = ISOPBO2 ;
% 1.0D-13 : transISOP1OH + O2 = E1OH4OO ;
% 4.0D-13 : cisISOP4OH + O2 = Z4OH1OO ;
% 7.0D-13 : cisISOP4OH + O2 = ISOPDO2 ;
% 7.0D-13 : transISOP4OH + O2 = ISOPDO2 ;
% 1.0D-13 : transISOP4OH + O2 = E4OH1OO ;
% 4.80 : Z1OH4OO = cisISOP1OH + O2 ;
% 0.054 : ISOPBO2 = cisISOP1OH + O2 ;
% 0.377 : ISOPBO2 = transISOP1OH + O2 ;
% 3.98 : E1OH4OO = transISOP1OH + O2 ;
% 0.696 : Z4OH1OO = cisISOP4OH + O2 ;
% 0.018 : ISOPDO2 = cisISOP4OH + O2 ;
% 0.029 : ISOPDO2 = transISOP4OH + O2 ;
% 0.120 : E4OH1OO = transISOP4OH + O2 ;
% 1.9D17*EXP(-14100/TEMP) : C5PAN17 = HC4ACO3 + NO2 ;
% 2.52D-11 : C5PAN17 + OH = MACROH + CO + NO2 ;
% 1.9D17*EXP(-14100/TEMP) : C5PAN18 = NC4CO3 + NO2 ;
% 2.16D-11 : OH + C5PAN18 = NOA + CO + CO + NO2 ;
% 1.9D17*EXP(-14100/TEMP) : C5PAN19 = HC4CCO3 + NO2 ;
% 2.52D-11 : C5PAN19 + OH = HO12CO3C4 + CO + NO2 ;
% 1.20D-15 : CH2OO + CO = HCHO ;
% 1.00D-14 : CH2OO + NO = HCHO + NO2 ;
```

% 1.00D-15 : CH2OO + NO2 = HCHO + NO3 ;
% 7.00D-14 : CH2OO + SO2 = HCHO + SO3 ;
% 6.00D-18*H2O : CH2OO = HCHO + H2O2 ;
% 1.00D-17*H2O : CH2OO = HCOOH ;
% KDEC*0.37 : CH2OOA = CH2OO ;
% KDEC*0.50 : CH2OOA = CO ;
% KDEC*0.13 : CH2OOA = HO2 + CO + OH ;
% KDEC*0.24 : CH2OOB = CH2OO ;
% KDEC*0.40 : CH2OOB = CO ;
% KDEC*0.36 : CH2OOB = HO2 + CO + OH ;
% KDEC*0.18 : CH2OOC = CH2OO ;
% KDEC*0.82 : CH2OOC = HO2 + CO + OH ;
% KDEC*0.22 : CH2OOE = CH2OO ;
% KDEC*0.51 : CH2OOE = CO ;
% KDEC*0.27 : CH2OOE = HO2 + CO + OH ;
% KDEC*0.37 : CH2OOG = CH2OO ;
% KDEC*0.47 : CH2OOG = CO ;
% KDEC*0.16 : CH2OOG = HO2 + CO + OH ;
% 2.73D-15 : CH3CHO + NO3 = HNO3 + CH3CO3 + ALDHYDE1 ;
% 1.50D-11*0.95 : CH3CHO + OH = CH3CO3 + ALDHYDE2 ;
% 1.50D-11*0.05 : CH3CHO + OH = HCOCH2O2 ;
% KNO3AL*2.4 : CH3CHOHCHO + NO3 = CH3CHOHCO3 + HNO3 ;
% 1.7D-11 : CH3CHOHCHO + OH = CH3CHOHCO3 ;
% KAPHO2*0.44 : CH3CHOHCO3 + HO2 = CH3CHO + HO2 + OH ;
% KAPHO2*0.56 : CH3CHOHCO3 + HO2 = IPROPOLPER ;
% KAPNO : CH3CHOHCO3 + NO = CH3CHO + HO2 + NO2 ;
% KFPAN : CH3CHOHCO3 + NO2 = IPROPOLPAN ;
% KRO2NO3*1.74 : CH3CHOHCO3 + NO3 = CH3CHO + HO2 + NO2 ;
% 1.00D-11*RO2 : CH3CHOHCO3 = CH3CHO + HO2 ;
% 1.20D-15 : CH3CHOO + CO = CH3CHO ;
% 1.00D-14 : CH3CHOO + NO = CH3CHO + NO2 ;
% 1.00D-15 : CH3CHOO + NO2 = CH3CHO + NO3 ;
% 7.00D-14 : CH3CHOO + SO2 = CH3CHO + SO3 ;
% 6.00D-18*H2O : CH3CHOO = CH3CHO + H2O2 ;
% 1.00D-17*H2O : CH3CHOO = CH3CO2H ;
% KDEC*0.24 : CH3CHOOA = CH3CHOO ;
% KDEC*0.36 : CH3CHOOA = CH3O2 + CO + OH ;
% KDEC*0.20 : CH3CHOOA = CH3O2 + HO2 ;
% KDEC*0.20 : CH3CHOOA = CH4 ;
% 8.00D-13 : CH3CO2H + OH = CH3O2 ;
% KAPHO2*0.15 : CH3CO3 + HO2 = CH3CO2H + O3 ;
% KAPHO2*0.41 : CH3CO3 + HO2 = CH3CO3H ;
% KAPHO2*0.44 : CH3CO3 + HO2 = CH3O2 + OH ;
% 1.98D-11 : CH3CO3 + NO = NO2 + CH3O2 ;
% KFPAN : CH3CO3 + NO2 = PAN ;

```
% 4.0D-12 : CH3CO3 + NO3 = NO2 + CH3O2 ;
% 4.66D-12*0.3*RO2 : CH3CO3 = CH3CO2H ;
% 4.66D-12*0.7*RO2 : CH3CO3 = CH3O2 ;
% 3.70D-12 : CH3CO3H + OH = CH3CO3 + BACK ;
% KDEC : CH3COCH2O = CH3CO3 + HCHO + IPRENE ;
% 9.02D-12*0.15 : CH3COCH2O2 + HO2 = CH3COCH2O + OH ;
% 9.02D-12*0.85 : CH3COCH2O2 + HO2 = HYPERACET ;
% KRO2NO : CH3COCH2O2 + NO = CH3COCH2O + NO2 ;
% KRO2NO3 : CH3COCH2O2 + NO3 = CH3COCH2O + NO2 ;
% 4.66D-12*0.2*RO2 : CH3COCH2O2 = ACETOL ;
% 4.66D-12*0.6*RO2 : CH3COCH2O2 = CH3COCH2O ;
% 4.66D-12*0.2*RO2 : CH3COCH2O2 = MGLYOX + AE ;
% 1.75D-13 : CH3COCH3 + OH = CH3COCH2O2 ;
% 8.0D-13 : OH + CH3COCO2H = CH3CO3 + IPRENE ;
% KAPHO2*0.44 : CH3COCO3 + HO2 = CH3CO3 + OH + IPRENE ;
% KAPHO2*0.56 : CH3COCO3 + HO2 = CH3COCO3H ;
% KAPNO : CH3COCO3 + NO = CH3CO3 + NO2 + IPRENE ;
% KFPAN : CH3COCO3 + NO2 = CH3COPAN ;
% KRO2NO3*1.74 : CH3COCO3 + NO3 = CH3CO3 + NO2 + IPRENE ;
% 1.00D-11*RO2 : CH3COCO3 = CH3CO3 + IPRENE ;
% 3.69D-12 : CH3COCO3H + OH = CH3COCO3 ;
% 1.02D-13 : CH3COPAN + OH = HCHO + CO + CO + NO2 ;
% 1.9D17*EXP(-14100/TEMP) : CH3COPAN = CH3COCO3 + NO2 ;
% 2.35D-14 : CH3NO3 + OH = HCHO + NO2 ;
% 2.35D-14*O2 : CH3O = HCHO + HO2 ;
% 5.21D-12*.09 : CH3O2 + HO2 = HCHO ;
% 5.21D-12*.91 : CH3O2 + HO2 = CH3OOH ;
% 7.70D-12*0.001 : CH3O2 + NO = CH3NO3 ;
% 7.70D-12*0.999 : CH3O2 + NO = CH3O + NO2 ;
% KMT13 : CH3O2 + NO2 = CH3O2NO2 ;
% 1.2D-12 : CH3O2 + NO3 = CH3O + NO2 ;
% 2.53D-13*RO2 : CH3O2 = CH3O ;
% 2.16D-13*RO2 : CH3O2 = CH3OH ;
% 2.16D-13*RO2 : CH3O2 = HCHO ;
% KMT14 : CH3O2NO2 = CH3O2 + NO2 ;
% 8.95D-13 : CH3OH + OH = HO2 + HCHO ;
% 1.00D-11*0.6 : CH3OOH + OH = CH3O2 ;
% 1.00D-11*0.4 : CH3OOH + OH = HCHO + OH ;
% 1.03D-13 : CH4 + CL = CH3O2 ;
% 6.37D-15 : CH4 + OH = CH3O2 ;
% KDEC : CHOCOHCO = HOCH2CHO + HO2 + CO ;
% KAPHO2*0.56 : CHOMOHCO3 + HO2 = CHOMOHCO3H ;
% KAPHO2*0.44 : CHOMOHCO3 + HO2 = MGLYOX + HO2 + OH + AF ;
% KAPNO : CHOMOHCO3 + NO = MGLYOX + NO2 + HO2 + AF ;
% KFPAN : CHOMOHCO3 + NO2 = CHOMOHPAN ;
```

% KRO2NO3*1.74 : CHOMOHCO3 + NO3 = MGLYOX + NO2 + HO2 + AF ;
% 1.00D-11*RO2 : CHOMOHCO3 = MGLYOX + HO2 + AF ;
% 6.99D-11 : CHOMOHCO3H + OH = CHOMOHCO3 ;
% 6.64D-11 : CHOMOHPAN + OH = MGLYOX + CO + NO2 + AG ;
% 1.9D17*EXP(-14100/TEMP) : CHOMOHPAN = CHOMOHCO3 + NO2 ;
% KNO3AL*2.4 : CHOPRNO3 + NO3 = PRNO3CO3 + HNO3 ;
% 3.55D-12 : CHOPRNO3 + OH = PRNO3CO3 ;
% KNO3AL*4.0 : CO23C3CHO + NO3 = CH3CO3 + CO + CO + HNO3 + IPRENE ;
% 1.23D-11 : CO23C3CHO + OH = CH3CO3 + CO + CO + IPRENE ;
% 1.30D-13 : CO23C4NO3 + OH = CO23C3CHO + NO2 ;
% KNO3AL*4.0 : CO2H3CHO + NO3 = CO2H3CO3 + HNO3 ;
% 2.45D-11 : CO2H3CHO + OH = CO2H3CO3 ;
% KAPHO2*0.56 : CO2H3CO3 + HO2 = CO2H3CO3H ;
% KAPHO2*0.44 : CO2H3CO3 + HO2 = MGLYOX + HO2 + OH + AH ;
% KAPNO : CO2H3CO3 + NO = MGLYOX + HO2 + NO2 + AH ;
% KFPAN : CO2H3CO3 + NO2 = C4PAN6 ;
% KRO2NO3*1.74 : CO2H3CO3 + NO3 = MGLYOX + HO2 + NO2 + AH ;
% 1.00D-11*RO2 : CO2H3CO3 = MGLYOX + HO2 + AH ;
% 7.34D-12 : OH + CO2H3CO3H = CO2H3CO3 ;
% 7.20D-12 : CO2N3CHO + OH = CO2N3CO3 ;
% KAPHO2*0.56 : CO2N3CO3 + HO2 = CO2N3CO3H ;
% KAPHO2*0.44 : CO2N3CO3 + HO2 = MGLYOX + NO2 + OH + AI ;
% KAPNO : CO2N3CO3 + NO = MGLYOX + NO2 + NO2 + AI ;
% KFPAN : CO2N3CO3 + NO2 = CO2N3PAN ;
% KRO2NO3*1.74 : CO2N3CO3 + NO3 = MGLYOX + NO2 + NO2 + AI ;
% 1.00D-11*RO2 : CO2N3CO3 = MGLYOX + NO2 + AI ;
% 4.11D-12 : CO2N3CO3H + OH = CO2N3CO3 ;
% 5.10D-13 : CO2N3PAN + OH = CO2N3CO3 ;
% 1.9D17*EXP(-14100/TEMP) : CO2N3PAN = CO2N3CO3 + NO2 ;
% 2.16D-11 : COHM2CO2H + OH = GLYOX + HO2 ;
% KAPHO2*0.15 : COHM2CO3 + HO2 = COHM2CO2H + O3 ;
% KAPHO2*0.41 : COHM2CO3 + HO2 = COHM2CO3H ;
% KAPHO2*0.44 : COHM2CO3 + HO2 = GLYOX + HO2 + OH ;
% KAPNO : COHM2CO3 + NO = GLYOX + HO2 + NO2 ;
% KFPAN : COHM2CO3 + NO2 = COHM2PAN ;
% KRO2NO3*1.74 : COHM2CO3 + NO3 = GLYOX + HO2 + NO2 ;
% 1.00D-11*0.3*RO2 : COHM2CO3 = COHM2CO2H ;
% 1.00D-11*0.7*RO2 : COHM2CO3 = GLYOX + HO2 ;
% 2.47D-11 : COHM2CO3H + OH = COHM2CO3 ;
% 2.11D-11 : COHM2PAN + OH = GLYOX + NO3 ;
% 1.9D17*EXP(-14100/TEMP) : COHM2PAN = COHM2CO3 + NO2 ;
% 3.70D-12 : CONM2CO2H + OH = MGLYOX + NO2 + AJ ;
% KAPHO2*0.15 : CONM2CO3 + HO2 = CONM2CO2H + O3 ;
% KAPHO2*0.41 : CONM2CO3 + HO2 = CONM2CO3H ;
% KAPHO2*0.44 : CONM2CO3 + HO2 = MGLYOX + NO2 + OH + AK ;

% KAPNO : CONM2CO3 + NO = MGLYOX + NO2 + NO2 + AK ;
% KFPAN : CONM2CO3 + NO2 = CONM2PAN ;
% KRO2NO3*1.74 : CONM2CO3 + NO3 = MGLYOX + NO2 + NO2 + AK ;
% 1.00D-11*0.3*RO2 : CONM2CO3 = CONM2CO2H ;
% 1.00D-11*0.7*RO2 : CONM2CO3 = MGLYOX + NO2 + AK ;
% 6.78D-12 : CONM2CO3H + OH = CONM2CO3 ;
% 3.18D-12 : CONM2PAN + OH = MGLYOX + NO2 + NO3 + AL ;
% 1.9D17*EXP(-14100/TEMP) : CONM2PAN = CONM2CO3 + NO2 ;
% 1.00D-11*0.5 : OH + DHMOB = ACETOL + CO + CO + HO2 ;
% 1.00D-11*0.5 : OH + DHMOB = CO + PRODUCT ;
% KDEC*0.52 : DIBO = HOCH2CHO + MGLYOX + HO2 + AM ;
% KDEC*0.48 : DIBO = ACETOL + GLYOX + HO2 ;
% 9.31D-12 : DIBOO + NO = DIBO + NO2 ;
% KRO2HO2*0.706 : DIBOO + HO2 = DIBOOH ;
% 3.50D-14*RO2 : DIBOO = PRODUCT ;
% 1.93D-11 : DNC524CO + OH = HMVKNO3 + CO + NO2 ;
% 7.00D+03 : ETHENO3O = NO2 + HCHO + HCHO ;
% KROPRIM : ETHENO3O + O2 = NO3CH2CHO + HO2 ;
% KRO2HO2*0.387 : ETHENO3O2 + HO2 = ETHO2HNO3 ;
% KRO2NO : ETHENO3O2 + NO = ETHENO3O + NO2 ;
% KRO2NO3 : ETHENO3O2 + NO3 = ETHENO3O + NO2 ;
% 6.00D-13*0.6*RO2 : ETHENO3O2 = ETHENO3O ;
% 6.00D-13*0.2*RO2 : ETHENO3O2 = ETHOHNO3 ;
% 6.00D-13*0.2*RO2 : ETHENO3O2 = NO3CH2CHO ;
% 1.45D-11 : ETHGLY + OH = HOCH2CHO + HO2 ;
% 3.60D-12 : ETHO2HNO3 + OH = ETHENO3O2 ;
% 1.62D-12 : ETHO2HNO3 + OH = NO3CH2CHO + OH ;
% 8.40D-13 : ETHOHNO3 + OH = HOCH2CHO + NO2 ;
% 1.2D-15 : GAOO + CO = HOCH2CHO ;
% 1.0D-14 : GAOO + NO = HOCH2CHO + NO2 ;
% 1.0D-15 : GAOO + NO2 = HOCH2CHO + NO3 ;
% 7.0D-14 : GAOO + SO2 = HOCH2CHO + SO3 ;
% 6.0D-18*H2O : GAOO = HOCH2CHO + H2O2 ;
% 1.0D-17*H2O : GAOO = HOCH2CO2H ;
% KDEC*0.11 : GAOOB = GAOO ;
% KDEC*0.89 : GAOOB = OH + HO2 + CO + HCHO ;
% 1.2D-15 : GLYOO + CO = GLYOX ;
% 1.0D-14 : GLYOO + NO = GLYOX + NO2 ;
% 1.0D-15 : GLYOO + NO2 = GLYOX + NO3 ;
% 7.0D-14 : GLYOO + SO2 = GLYOX + SO3 ;
% 6.0D-18*H2O : GLYOO = GLYOX + H2O2 ;
% 1.0D-17*H2O : GLYOO = HCOCO2H ;
% KDEC*0.24 : GLYOOB = GLYOO ;
% KDEC*0.20 : GLYOOB = HCHO ;
% KDEC*0.20 : GLYOOB = HO2 + HO2 + CO ;

% KDEC*0.36 : GLYOOB = OH + CO + CO + HO2 ;
% KDEC*0.11 : GLYOOC = GLYOO ;
% KDEC*0.89 : GLYOOC = OH + HO2 + CO + CO ;
% KNO3AL*0.6 : NO3 + GLYOX = CO + CO + HO2 + HNO3 ;
% KNO3AL*0.4 : NO3 + GLYOX = HCOCO3 + HNO3 ;
% 9.7D-12*0.6 : OH + GLYOX = CO + CO + HO2 ;
% 9.7D-12*0.4 : OH + GLYOX = HCOCO3 ;
% 1.9D17*EXP(-14100/TEMP) : GLYPAN = HCOCO3 + NO2 ;
% 1.22D-11 : OH + GLYPAN = CO + CO + NO2 ;
% 1.44D-11 : H1CO23CHO + OH = CO + CO + HOCH2CO3 ;
% KNO3AL*4.0 : NO3 + H13CO2CHO = H13CO2CO3 + HNO3 ;
% 2.66D-11 : OH + H13CO2CHO = H13CO2CO3 ;
% 5.25D-12 : H13CO2C3 + OH = HOCH2COCHO + HO2 ;
% KAPHO2*0.56 : H13CO2CO3 + HO2 = H13CO2CO3H ;
% KAPHO2*0.44 : H13CO2CO3 + HO2 = HOCH2COCHO + HO2 + OH ;
% KAPNO : H13CO2CO3 + NO = HOCH2COCHO + HO2 + NO2 ;
% KFPAN : H13CO2CO3 + NO2 = C4PAN10 ;
% KRO2NO3*1.74 : H13CO2CO3 + NO3 = HOCH2COCHO + HO2 + NO2 ;
% 1.00D-11*RO2 : H13CO2CO3 = HOCH2COCHO + HO2 ;
% 9.43D-12 : OH + H13CO2CO3H = H13CO2CO3 ;
% 4.44D-12 : H14CO23C4 + OH = H1CO23CHO + HO2 ;
% KNO3AL*4.25 : NO3 + HC4ACHO = HC4ACO3 + HNO3 ;
% 2.40D-17*0.5 : O3 + HC4ACHO = ACETOL + GLYOOC ;
% 2.40D-17*0.5 : O3 + HC4ACHO = ACLOOA + GLYOX ;
% 1.10D-10 : OH + HC4ACHO = HC5OO ;
% 2.52D-11 : OH + HC4ACO2H = ACETOL + CO + HO2 ;
% KAPHO2*0.44 : HC4ACO3 + HO2 = ACETOL + CO + HO2 + OH ;
% KAPHO2*0.15 : HC4ACO3 + HO2 = HC4ACO2H + O3 ;
% KAPHO2*0.41 : HC4ACO3 + HO2 = HC4ACO3H ;
% KAPNO : HC4ACO3 + NO = ACETOL + CO + HO2 + NO2 ;
% KFPAN : HC4ACO3 + NO2 = C5PAN17 ;
% KRO2NO3*1.74 : HC4ACO3 + NO3 = ACETOL + CO + HO2 + NO2 ;
% 1.00D-11*0.7*RO2 : HC4ACO3 = ACETOL + HO2 + CO ;
% 1.00D-11*0.3*RO2 : HC4ACO3 = HC4ACO2H ;
% 2.88D-11 : OH + HC4ACO3H = HC4ACO3 ;
% KNO3AL*4.25 : NO3 + HC4CCHO = HC4CCO3 + HNO3 ;
% 2.40D-17*0.5 : O3 + HC4CCHO = MGLYOOA + HOCH2CHO ;
% 2.40D-17*0.5 : O3 + HC4CCHO = MGLYOX + GAOOB + AN ;
% 1.10D-10 : OH + HC4CCHO = HC5OO ;
% 2.52D-11 : OH + HC4CCO2H = CH3CO3 + HOCH2CHO + IPRENE ;
% KAPHO2*0.44 : HC4CCO3 + HO2 = CH3CO3 + HOCH2CHO + OH + IPRENE ;
% KAPHO2*0.15 : HC4CCO3 + HO2 = HC4CCO2H + O3 ;
% KAPHO2*0.41 : HC4CCO3 + HO2 = HC4CCO3H ;
% KAPNO : HC4CCO3 + NO = CH3CO3 + HOCH2CHO + NO2 + IPRENE ;
% KFPAN : HC4CCO3 + NO2 = C5PAN19 ;

% KRO2NO3*1.74 : HC4CCO3 + NO3 = CH3CO3 + HOCH2CHO + NO2 + IPRENE ;
% 1.00D-11*0.7*RO2 : HC4CCO3 = CH3CO3 + HOCH2CHO + IPRENE ;
% 1.00D-11*0.3*RO2 : HC4CCO3 = HC4CCO2H ;
% 2.88D-11 : OH + HC4CCO3H = HC4CCO3 ;
% KDEC*0.234 : HC5O = HOCH2CHO + MGLYOX + HO2 + AO ;
% KDEC*0.216 : HC5O = GLYOX + ACETOL + HO2 ;
% KDEC*0.29 : HC5O = DHMOB + HO2;
% KDEC*0.26 : HC5O = PRODUCT + HO2;
% KRO2HO2*0.706 : HO2 + HC5OO = HC5OOH ;
% 9.31D-12 : HC5OO + NO = HC5O + NO2 ;
% 3.50D-14*0.5*RO2 : HC5OO = HC5O ;
% 3.50D-14*0.5*RO2 : HC5OO = PRODUCT ;
% 5.5D-16 : NO3 + HCHO = HNO3 + CO + HO2 ;
% 8.49D-12 : OH + HCHO = HO2 + CO ;
% 3.81D-11 : OH + HCOC5 = C59O2 ;
% KDEC : HCOCH2O = HCHO + CO + HO2 ;
% KRO2HO2*0.387 : HCOCH2O2 + HO2 = HCOCH2OOH ;
% KRO2NO : HCOCH2O2 + NO = NO2 + HCOCH2O ;
% KRO2NO3 : HCOCH2O2 + NO3 = HCOCH2O + NO2 ;
% 2.00D-12*0.2*RO2 : HCOCH2O2 = GLYOX ;
% 2.00D-12*0.6*RO2 : HCOCH2O2 = HCOCH2O ;
% 2.00D-12*0.2*RO2 : HCOCH2O2 = HOCH2CHO ;
% 2.91D-11 : HCOCH2OOH + OH = GLYOX + OH ;
% 3.60D-12 : HCOCH2OOH + OH = HCOCH2O2 ;
% 1.23D-11 : OH + HCOCO2H = CO + HO2 ;
% KAPHO2*0.15 : HCOCO3 + HO2 = HCOCO2H + O3 ;
% KAPHO2*0.41 : HCOCO3 + HO2 = HCOCO3H ;
% KAPHO2*0.44 : HCOCO3 + HO2 = HO2 + CO + OH ;
% KAPNO : HCOCO3 + NO = HO2 + CO + NO2 ;
% KFPAN : HCOCO3 + NO2 = GLYPAN ;
% KRO2NO3*1.74 : HCOCO3 + NO3 = HO2 + CO + NO2 ;
% 1.00D-11*0.7*RO2 : HCOCO3 = CO + HO2 ;
% 1.00D-11*0.3*RO2 : HCOCO3 = HCOCO2H ;
% 1.58D-11 : OH + HCOCO3H = HCOCO3 ;
% KAPHO2*0.44 : HCOCOHCO3 + HO2 = GLYOX + HO2 + OH ;
% KAPHO2*0.56 : HCOCOHCO3 + HO2 = HCOCOHCO3H ;
% KAPNO : HCOCOHCO3 + NO = GLYOX + HO2 + NO2 ;
% KFPAN : HCOCOHCO3 + NO2 = HCOCOHPAN ;
% KRO2NO3*1.74 : HCOCOHCO3 + NO3 = GLYOX + HO2 + NO2 ;
% 1.00D-11*RO2 : HCOCOHCO3 = GLYOX + HO2 ;
% 7.33D-11 : HCOCOHCO3H + OH = HCOCOHCO3 ;
% 6.97D-11 : HCOCOHPAN + OH = GLYOX + CO + NO2 ;
% 1.9D17*EXP(-14100/TEMP) : HCOCOHPAN = HCOCOHCO3 + NO2 ;
% 4.5D-13 : HCOOH + OH = HO2 ;
% KDEC : HIEB1O = HOCH2COCHO + HOCH2CHO + HO2 ;

% KRO2HO2*0.706 : HIEB1O2 + HO2 = HIEB1OOH ;
% KRO2NO : HIEB1O2 + NO = HIEB1O + NO2 ;
% KRO2NO3 : HIEB1O2 + NO3 = HIEB1O + NO2 ;
% 9.20D-14*RO2 : HIEB1O2 = HIEB1O ;
% 4.30D-11 : HIEB1OOH + OH = MVKOHAOH + CO + OH ;
% KDEC : HIEB2O = H13CO2C3 + GLYOX + HO2 ;
% KRO2HO2*0.706 : HIEB2O2 + HO2 = HIEB2OOH ;
% KRO2NO : HIEB2O2 + NO = HIEB2O + NO2 ;
% KRO2NO3 : HIEB2O2 + NO3 = HIEB2O + NO2 ;
% 8.80D-13*RO2 : HIEB2O2 = HIEB2O ;
% 5.74D-11 : HIEB2OOH + OH = HMACROH + CO + OH ;
% 1.31D-11*0.667 : HIEPOXB + OH = HIEB1O2 ;
% 1.31D-11*0.333 : HIEPOXB + OH = HIEB2O2 ;
% 1.84D-11 : HMACO2H + OH = HOCH2CO3 + HCHO ;
% KAPHO2*0.15 : HMACO3 + HO2 = HMACO2H + O3 ;
% KAPHO2*0.41 : HMACO3 + HO2 = HMACO3H ;
% KAPHO2*0.44 : HMACO3 + HO2 = HOCH2CO3 + HCHO + OH ;
% KAPNO : HMACO3 + NO = HOCH2CO3 + HCHO + NO2 ;
% KFPAN : HMACO3 + NO2 = HMPAN ;
% KRO2NO3*1.74 : HMACO3 + NO3 = HOCH2CO3 + HCHO + NO2 ;
% 1.00D-11*0.3*RO2 : HMACO3 = HMACO2H ;
% 1.00D-11*0.7*RO2 : HMACO3 = HOCH2CO3 + HCHO ;
% 1.99D-11 : HMACO3H + OH = HMACO3 ;
% 3.40D-15 : HMACR + NO3 = HMACO3 + HNO3 ;
% 7.80D-19*0.5 : HMACR + O3 = CH2OOA + HOCH2COCHO ;
% 7.80D-19*0.5 : HMACR + O3 = HCHO + HMGLYOOA ;
% 4.83D-11*0.376 : HMACR + OH = HMACO3 ;
% 4.83D-11*0.624 : HMACR + OH = HMACRO2 ;
% KDEC : HMACRO = H13CO2C3 + CO + HO2 ;
% KRO2HO2*0.625 : HMACRO2 + HO2 = HMACROOH ;
% KRO2NO : HMACRO2 + NO = HMACRO + NO2 ;
% KRO2NO3 : HMACRO2 + NO3 = HMACRO + NO2 ;
% 9.20D-14*0.7*RO2 : HMACRO2 = HMACRO ;
% 9.20D-14*0.3*RO2 : HMACRO2 = HMACROH ;
% 3.82D-11 : HMACROH + OH = HMACRO ;
% 4.17D-11 : HMACROOH + OH = HMACRO2 ;
% 1.20D-15 : HMGLOO + CO = HOCH2COCHO ;
% 1.00D-14 : HMGLOO + NO = HOCH2COCHO + NO2 ;
% 1.00D-15 : HMGLOO + NO2 = HOCH2COCHO + NO3 ;
% 7.00D-14 : HMGLOO + SO2 = HOCH2COCHO + SO3 ;
% 6.00D-18*H2O : HMGLOO = HOCH2COCHO + H2O2 ;
% 1.00D-17*H2O : HMGLOO = HOCH2COCO2H ;
% KDEC*0.24 : HMGLOOA = HMGLOO ;
% KDEC*0.20 : HMGLOOA = HOCH2CHO ;
% KDEC*0.20 : HMGLOOA = HOCH2CO3 + HO2 ;

% KDEC*0.36 : HMGLOOA = OH + CO + HOCH2CO3 ;
% 1.20D-15 : HMGLYOO + CO = HOCH2COCHO ;
% 1.00D-14 : HMGLYOO + NO = HOCH2COCHO + NO2 ;
% 1.00D-15 : HMGLYOO + NO2 = HOCH2COCHO + NO3 ;
% 7.00D-14 : HMGLYOO + SO2 = HOCH2COCHO + SO3 ;
% 6.00D-18*H2O : HMGLYOO = HOCH2COCHO + H2O2 ;
% KDEC*0.18 : HMGLYOOA = HMGLYOO ;
% KDEC*0.82 : HMGLYOOA = HOCH2CO3 + CO + HO2 ;
% 2.90D-11 : HMPAN + OH = H13CO2C3 + HCHO + CO + NO2 ;
% 1.9D17*EXP(-14100/TEMP) : HMPAN = HMACO3 + NO2 ;
% 1.36D-11 : HMVKNGLYOX + OH = CO + CO + HOCH2CHO + NO2 ;
% 3.85D-12 : HMVKNO3 + OH = HMVKNGLYOX + HO2 ;
% KRO2NO*0.625 : HMVKO2 + NO = NO2 + HOCH2CHO + CH3CO3 + COW ;
% KRO2NO*0.265 : HMVKO2 + NO = MGLYOX + HCHO + NO2 + HO2 + AQ ;
% KRO2NO*0.11 : HMVKO2 + NO = MVKNO3 ;
% KRO2HO2*0.625 : HMVKO2 + HO2 = HMVKOOH ;
% 3.50D-14*0.35*RO2 : HMVKO2 = HOCH2CHO + COW + IPRENE ;
% 3.50D-14*0.15*RO2 : HMVKO2 = MGLYOX + HCHO + HO2 + AQ ;
% 3.50D-14*0.5*RO2 : HMVKO2 = MEK ;
% 2.67D-11 : HNC524CO + OH = HMVKNO3 + CO + HO2 ;
% 1.88D-11 : OH + HO12CO3C4 = BIACETOH + HO2 ;
% 1.78D+5 : HOCH2CH2O = HO2 + HCHO + HCHO ;
% KROPRIM : HOCH2CH2O + O2 = HO2 + HOCH2CHO ;
% KNO3AL : HOCH2CHO + NO3 = HOCH2CO3 + HNO3 ;
% 1.00D-11*0.200 : HOCH2CHO + OH = GLYOX + HO2 ;
% 1.00D-11*0.800 : HOCH2CHO + OH = HOCH2CO3 ;
% 1.20D-11 : HOCH2CH2O2 + HO2 = HYETHO2H ;
% KRO2NO*0.005 : HOCH2CH2O2 + NO = ETHOHNO3 ;
% KRO2NO*0.995 : HOCH2CH2O2 + NO = HOCH2CH2O + NO2 ;
% KRO2NO3 : HOCH2CH2O2 + NO3 = HOCH2CH2O + NO2 ;
% 1.75D-12*0.2*RO2 : HOCH2CH2O2 = ETHGLY ;
% 1.75D-12*0.6*RO2 : HOCH2CH2O2 = HOCH2CH2O ;
% 1.75D-12*0.2*RO2 : HOCH2CH2O2 = HOCH2CHO ;
% 2.73D-12 : HOCH2CO2H + OH = HCHO + HO2 ;
% KAPHO2*0.44 : HOCH2CO3 + HO2 = HO2 + HCHO + OH ;
% KAPHO2*0.15 : HOCH2CO3 + HO2 = HOCH2CO2H + O3 ;
% KAPHO2*0.41 : HOCH2CO3 + HO2 = HOCH2CO3H ;
% KAPNO : HOCH2CO3 + NO = NO2 + HO2 + HCHO ;
% KFPAN : HOCH2CO3 + NO2 = PHAN ;
% KRO2NO3*1.74 : HOCH2CO3 + NO3 = NO2 + HO2 + HCHO ;
% 1.00D-11*0.7*RO2 : HOCH2CO3 = HCHO + HO2 ;
% 1.00D-11*0.3*RO2 : HOCH2CO3 = HOCH2CO2H ;
% 6.19D-12 : HOCH2CO3H + OH = HOCH2CO3 ;
% KNO3AL*2.4 : NO3 + HOCH2COCHO = HOCH2CO3 + CO + HNO3 ;
% 1.44D-11 : OH + HOCH2COCHO = HOCH2CO3 + CO ;

% 2.89D-12 : HOCH2COCO2H + OH = HOCH2CO3 ;
% 4.77D-11 : HOCHOCOOH + OH = HOCH2COCHO + OH ;
% 5.1D-11 : HPALD + OH = OH ;
% 2.98D-11 : HPNC524CO + OH = HMVKNO3 + CO + OH ;
% 3.60D-12 : HYETHO2H + OH = HOCH2CH2O2 ;
% 1.38D-11 : HYETHO2H + OH = HOCH2CHO + OH ;
% 3.60D-12 : HYPERACET + OH = CH3COCH2O2 ;
% 8.39D-12 : HYPERACET + OH = MGLYOX + OH + AR ;
% 9.11D+4 : HYPROPO = CH3CHO + HCHO + HO2 ;
% KRO2HO2*0.520 : HYPROPO2 + HO2 = HYPROPO2H ;
% KRO2NO3 : HYPROPO2 + NO3 = HYPROPO + NO2 ;
% 8.80D-13*0.2*RO2 : HYPROPO2 = ACETOL ;
% 8.80D-13*0.6*RO2 : HYPROPO2 = HYPROPO ;
% 8.80D-13*0.2*RO2 : HYPROPO2 = PROPGLY ;
% KRO2NO*0.977 : NO + HYPROPO2 = HYPROPO + NO2 ;
% KRO2NO*0.023 : NO + HYPROPO2 = PROPOLNO3 ;
% 2.44D-11 : HYPROPO2H + OH = ACETOL + OH ;
% 3.60D-12 : HYPROPO2H + OH = HYPROPO2 ;
% 1.4D-11 : IBUTALOH + OH = IPRHOCO3 ;
% 2.87D-13 : OH + IC3H7NO3 = CH3COCH3 + NO2 ;
% 6.93D-15 : IC3H7O + O2 = CH3COCH3 + HO2 ;
% KRO2HO2*0.520 : IC3H7O2 + HO2 = IC3H7OOH ;
% 9.04D-12*0.042 : IC3H7O2 + NO = IC3H7NO3 ;
% 9.04D-12*0.958 : IC3H7O2 + NO = IC3H7O + NO2 ;
% KRO2NO3 : IC3H7O2 + NO3 = IC3H7O + NO2 ;
% 3.70D-14*0.2*RO2 : IC3H7O2 = CH3COCH3 ;
% 3.70D-14*0.6*RO2 : IC3H7O2 = IC3H7O ;
% 3.70D-14*0.2*RO2 : IC3H7O2 = IPROPOL ;
% 1.66D-11 : OH + IC3H7OOH = CH3COCH3 + OH ;
% 3.60D-12 : OH + IC3H7OOH = IC3H7O2 ;
% KAPHO2*0.44 : IEACO3 + HO2 = HMVKO2 + OH ;
% KAPHO2*0.56 : IEACO3 + HO2 = IEACO3H ;
% KAPNO : IEACO3 + NO = HMVKO2 + NO2 ;
% KFPAN : IEACO3 + NO2 = IEAPAN ;
% KRO2NO3*1.74 : IEACO3 + NO3 = HMVKO2 + NO2 ;
% 1.00D-11*RO2 : IEACO3 = HMVKO2 ;
% 4.81D-12 : OH + IEACO3H = IEACO3 ;
% 1.9D17*EXP(-14100/TEMP) : IEAPAN = IEACO3 + NO2 ;
% 1.21D-12 : OH + IEAPAN = HMVKO2 + CO + NO2 ;
% KDEC : IEB1O = MGLYOX + HOCH2CHO + HO2 + AS ;
% KRO2HO2*0.706 : IEB1O2 + HO2 = IEB1OOH ;
% KRO2NO : IEB1O2 + NO = IEB1O + NO2 ;
% KRO2NO3 : IEB1O2 + NO3 = IEB1O + NO2 ;
% 9.20D-14*RO2 : IEB1O2 = IEB1O ;
% 3.90D-11 : OH + IEB1OOH = HO12CO3C4 + OH + CO ;

% KDEC : IEB2O = GLYOX + ACETOL + HO2 ;
% KRO2HO2*0.706 : IEB2O2 + HO2 = IEB2OOH ;
% KRO2NO : IEB2O2 + NO = IEB2O + NO2 ;
% KRO2NO3 : IEB2O2 + NO3 = IEB2O + NO2 ;
% 8.80D-13*RO2 : IEB2O2 = IEB2O ;
% 5.34D-11 : OH + IEB2OOH = MACROH + OH + CO ;
% KDEC : IEC1O = BIACETOH + HCHO + HO2 ;
% KRO2HO2*0.706 : IEC1O2 + HO2 = IEC1OOH ;
% KRO2NO : IEC1O2 + NO = IEC1O + NO2 ;
% KRO2NO3 : IEC1O2 + NO3 = IEC1O + NO2 ;
% 9.20D-14*RO2 : IEC1O2 = IEC1O ;
% 3.60D-12 : OH + IEC1OOH = IEC1O2 ;
% 1.57D-11 : OH + IEC1OOH = IEC2OOH + HO2 ;
% 2.73D-11 : OH + IEC2OOH = BIACETOH + OH + CO ;
% KNO3AL*7.5 : NO3 + IECCHO = IECCO3 + HNO3 ;
% 2.76D-11 : OH + IECCHO = IECCO3 ;
% KAPHO2*0.56 : IECCO3 + HO2 = IECCO3H ;
% KAPHO2*0.44 : IECCO3 + HO2 = MACRO2 + OH ;
% KAPNO : IECCO3 + NO = MACRO2 + NO2 ;
% KFPAN : IECCO3 + NO2 = IECPAN ;
% KRO2NO3*1.74 : IECCO3 + NO3 = MACRO2 + NO2 ;
% 1.00D-11*RO2 : IECCO3 = MACRO2 ;
% 1.04D-11 : OH + IECCO3H = IECCO3 ;
% 1.9D17*EXP(-14100/TEMP) : IECPAN = IECCO3 + NO2 ;
% 6.80D-12 : OH + IECPAN = MACRO2 + CO + NO2 ;
% 2.29D-11 : OH + INAHCHO = INAHCO3 ;
% 3.04D-12 : OH + INAHCO2H = MVKNO3 + HO2 ;
% KAPHO2*0.44 : INAHCO3 + HO2 = MVKNO3 + HO2 + OH ;
% KAPHO2*0.15 : INAHCO3 + HO2 = INAHCO2H + O3 ;
% KAPHO2*0.41 : INAHCO3 + HO2 = INAHCO3H ;
% KAPNO : INAHCO3 + NO = MVKNO3 + HO2 + NO2 ;
% KFPAN : INAHCO3 + NO2 = INAHPAN ;
% KRO2NO3*1.74 : INAHCO3 + NO3 = MVKNO3 + HO2 + NO2 ;
% 1.00D-11*0.7*RO2 : INAHCO3 = MVKNO3 + HO2 ;
% 1.00D-11*0.3*RO2 : INAHCO3 = INAHCO2H ;
% 6.12D-12 : OH + INAHCO3H = INAHCO3 ;
% 1.9D17*EXP(-14100/TEMP) : INAHPAN = INAHPCO3 + NO2 ;
% 2.52D-12 : OH + INAHPAN = MVKNO3 + HO2 + CO + NO2 ;
% 2.67D-11 : OH + INAHPCHO = INAHPCO3 ;
% 4.22D-12 : OH + INANCHO = INANCO3 ;
% 6.50D-12 : OH + INAHPCO2H = MVKNO3 + OH ;
% KAPHO2*0.44 : INAHPCO3 + HO2 = MVKNO3 + OH + OH ;
% KAPHO2*0.15 : INAHPCO3 + HO2 = INAHPCO2H + O3 ;
% KAPHO2*0.41 : INAHPCO3 + HO2 = INAHPCO3H ;
% KAPNO : INAHPCO3 + NO = MVKNO3 + OH + NO2 ;

% KFPAN : INAHPCO3 + NO2 = INAHPPAN ;
% KRO2NO3*1.74 : INAHPCO3 + NO3 = MVKNO3 + OH + NO2 ;
% 1.00D-11*0.7*RO2 : INAHPCO3 = MVKNO3 + OH ;
% 1.00D-11*0.3*RO2 : INAHPCO3 = INAHPCO2H ;
% 9.58D-12 : OH + INAHPCO3H = INAHPCO3 ;
% 1.9D17*EXP(-14100/TEMP) : INAHPPAN = INAHPCO3 + NO2 ;
% 5.98D-12 : OH + INAHPPAN = MVKNO3 + OH + CO + NO2 ;
% 1.21D-12*0.56 : OH + INANCO = INANCOCHO + HO2 ;
% 1.21D-12*0.44 : OH + INANCO = INB1GLYOX + NO2 ;
% 1.36D-12 : OH + INANCO2H = MVKNO3 + NO2 ;
% KAPHO2*0.44 : INANCO3 + HO2 = MVKNO3 + NO2 + OH ;
% KAPHO2*0.15 : INANCO3 + HO2 = INANCO2H + O3 ;
% KAPHO2*0.41 : INANCO3 + HO2 = INANCO3H ;
% KAPNO : INANCO3 + NO = MVKNO3 + NO2 + NO2 ;
% KFPAN : INANCO3 + NO2 = INANPAN ;
% KRO2NO3*1.74 : INANCO3 + NO3 = MVKNO3 + NO2 + NO2 ;
% 1.00D-11*0.7*RO2 : INANCO3 = MVKNO3 + NO2 ;
% 1.00D-11*0.3*RO2 : INANCO3 = INANCO2H ;
% 4.08D-12 : OH + INANCO3H = INANCO3 ;
% 3.79D-12 : OH + INANCOCHO = INANCOCO3 ;
% 9.35D-13 : OH + INANCOCO2H = NO2 + CO23C4NO3 ;
% KAPHO2*0.15 : INANCOCO3 + HO2 = INANCOCO2H + O3 ;
% KAPHO2*0.41 : INANCOCO3 + HO2 = INANCOCO3H ;
% KAPHO2*0.44 : INANCOCO3 + HO2 = NO2 + CO23C4NO3 + OH ;
% KAPNO : INANCOCO3 + NO = NO2 + CO23C4NO3 + NO2 ;
% KFPAN : INANCOCO3 + NO2 = INANCOPAN ;
% KRO2NO3*1.74 : INANCOCO3 + NO3 = NO2 + CO23C4NO3 + NO2 ;
% 1.00D-11*0.3*RO2 : INANCOCO3 = INANCOCO2H ;
% 1.00D-11*0.7*RO2 : INANCOCO3 = NO2 + CO23C4NO3 ;
% 4.02D-12 : OH + INANCOCO3H = INANCOCO3 ;
% 1.9D17*EXP(-14100/TEMP) : INANCOPAN = INANCOCO3 + NO2 ;
% 4.15D-13 : OH + INANCOPAN = NO3 + CO23C4NO3 ;
% 2.00D-12*0.07 : OH + INANO3 = ACETOL + NO2 + NO3CH2CHO ;
% 2.00D-12*0.39 : OH + INANO3 = C58NO3 + NO2 ;
% 2.00D-12*0.07 : OH + INANO3 = HCHO + NO2 + MVKNO3;
% 2.00D-12*0.33 : OH + INANO3 = INANCHO + HO2 ;
% 2.00D-12*0.14 : OH + INANO3 = INANCO + HO2 ;
% 1.9D17*EXP(-14100/TEMP) : INANPAN = INANCO3 + NO2 ;
% 4.85D-13 : OH + INANPAN = MVKNO3 + NO2 + CO + NO2 ;
% KDEC*0.15 : INAO = NOA + OHCH2CHO + HO2 ;
% KDEC*0.13 : INAO = ACETOL + NO3CH2CHO + HO2 ;
% KDEC*0.07 : INAO = MVKNO3 + HCHO + HO2 ;
% KDEC*0.34 : INAO = DHBN + HCHO + NO2 ;
% KDEC*0.31 : INAO = ACETOL + NO3 + HCHO + HCOOH ;
% KRO2HO2*0.706 : INAO2 + HO2 = INAOOH ;

```
% KRO2NO3 : INAO2 + NO3 = INAO + NO2 ;
% KRO2NO : INAO2 + NO = INAO + NO2 ;
% 8.00D-13*0.5*RO2 : INAO2 = INAO ;
% 8.00D-13*0.5*RO2 : INAO2 = INAOH ;
% 6.68D-12 : OH + INAOH = INAHCHO + HO2 ;
% 1.01D-11*0.65 : OH + INAOOH = INAHPCHO + HO2 ;
% 1.01D-11*0.35 : OH + INAOOH = INAO2 ;
% 3.27D-12 : INB1CO + OH = INB1GLYOX + HO2 ;
% 1.35D-11 : INB1GLYOX + OH = MACRNCO3 + CO ;
% 2.41D-11 : OH + INB1HPCHO = INB1HPCO3 ;
% 1.85D-11 : OH + INB1NACHO = INB1NACO3 ;
% 1.85D-11 : OH + INB1NBCHO = INB1NBCO3 ;
% 7.40D-12 : INB1HPCO2H + OH = MACRNO3 + OH ;
% KAPHO2*0.15 : INB1HPCO3 + HO2 = INB1HPCO2H + O3 ;
% KAPHO2*0.41 : INB1HPCO3 + HO2 = INB1HPCO3H ;
% KAPHO2*0.44 : INB1HPCO3 + HO2 = MACRNO3 + OH + OH ;
% KAPNO : INB1HPCO3 + NO = MACRNO3 + OH + NO2 ;
% KFPAN : INB1HPCO3 + NO2 = INB1HPPAN ;
% KRO2NO3*1.74 : INB1HPCO3 + NO3 = MACRNO3 + OH + NO2 ;
% 1.00D-11*0.3*RO2 : INB1HPCO3 = INB1HPCO2H ;
% 1.00D-11*0.7*RO2 : INB1HPCO3 = MACRNO3 + OH ;
% 1.09D-11 : INB1HPCO3H + OH = INB1HPCO3 ;
% 7.26D-12 : INB1HPPAN + OH = MACRNO3 + CO + OH + NO2 ;
% 1.9D17*EXP(-14100/TEMP) : INB1HPPAN = INB1HPCO3 + NO2 ;
% 1.72D-12 : INB1NACO2H + OH = MACRNO3 + NO2 ;
% KAPHO2*0.15 : INB1NACO3 + HO2 = INB1NACO2H + O3 ;
% KAPHO2*0.41 : INB1NACO3 + HO2 = INB1NACO3H ;
% KAPHO2*0.44 : INB1NACO3 + HO2 = MACRNO3 + NO2 + OH ;
% KAPNO : INB1NACO3 + NO = MACRNO3 + NO2 + NO2 ;
% KFPAN : INB1NACO3 + NO2 = INB1NAPAN ;
% KRO2NO3*1.74 : INB1NACO3 + NO3 = MACRNO3 + NO2 + NO2 ;
% 1.00D-11*0.3*RO2 : INB1NACO3 = INB1NACO2H ;
% 1.00D-11*0.7*RO2 : INB1NACO3 = MACRNO3 + NO2 ;
% 5.18D-12 : INB1NACO3H + OH = INB1NACO3 ;
% 1.58D-12 : INB1NAPAN + OH = MACRNO3 + CO + NO2 + NO2 ;
% 1.9D17*EXP(-14100/TEMP) : INB1NAPAN = INB1NACO3 + NO2 ;
% 1.73D-12 : INB1NBCO2H + OH = MVKNO3 + NO2 ;
% KAPHO2*0.15 : INB1NBCO3 + HO2 = INB1NBCO2H + O3 ;
% KAPHO2*0.41 : INB1NBCO3 + HO2 = INB1NBCO3H ;
% KAPHO2*0.44 : INB1NBCO3 + HO2 = MVKNO3 + NO2 + OH ;
% KAPNO : INB1NBCO3 + NO = MVKNO3 + NO2 + NO2 ;
% KFPAN : INB1NBCO3 + NO2 = INB1NBPAN ;
% KRO2NO3*1.74 : INB1NBCO3 + NO3 = MVKNO3 + NO2 + NO2 ;
% 1.00D-11*0.3*RO2 : INB1NBCO3 = INB1NBCO2H ;
% 1.00D-11*0.7*RO2 : INB1NBCO3 = MVKNO3 + NO2 ;
```

% 5.19D-12 : INB1NBCO3H + OH = INB1NBCO3 ;
% 1.59D-12 : INB1NBPAN + OH = MVKNO3 + CO + NO2 + NO2 ;
% 1.9D17*EXP(-14100/TEMP) : INB1NBPAN = INB1NBCO3 + NO2 ;
% 1.63D-12*0.50 : INB1NO3 + OH = INB1NACHO + HO2 ;
% 1.63D-12*0.50 : INB1NO3 + OH = INB1NBCHO + HO2 ;
% 6.65D-12*0.71 : INB1OH + OH = C58NO3 + HO2 ;
% 6.65D-12*0.29 : INB1OH + OH = INB1CO + HO2 ;
% 1.27D-11*0.35 : INBOOH + OH = INB1CO + OH ;
% 1.27D-11*0.34 : INBOOH + OH = INB1HPCHO ;
% 1.27D-11*0.31 : INBOOH + OH = INBO2 ;
% KDEC*0.14 : INBO = MVKNO3 + HCHO + HO2 ;
% KDEC*0.26 : INBO = MACRNO3 + HCHO + HO2 ;
% KDEC*0.6 : INBO = ACETOL + HOCH2CHO + NO2 ;
% 1.59D-11*0.73 : INBOOH + OH = C58NO3 + OH ;
% 1.59D-11*0.27 : INBOOH + OH = INBO2 ;
% KRO2HO2*0.706 : INBO2 + HO2 = INBOOH ;
% KRO2NO : INBO2 + NO = INBO + NO2 ;
% KRO2NO3 : INBO2 + NO3 = INBO + NO2 ;
% 2.90D-12*0.5*RO2 : INBO2 = INBO ;
% 2.90D-12*0.5*RO2 : INBO2 = INBOH ;
% 3.30D-12 : OH + INCCO = INCGLYOX + HO2 ;
% 1.34D-11 : OH + INCGLYOX = MACRNBCO3 + CO ;
% 4.52D-12*0.19 : INCNCHO + OH = INCGLYOX + NO2 ;
% 4.52D-12*0.81 : INCNCHO + OH = INCNCO3 ;
% 1.66D-12 : OH + INCNCO2H = MACRNO3 + NO2 ;
% KAPHO2*0.15 : INCNCO3 + HO2 = INCNCO2H + O3 ;
% KAPHO2*0.41 : INCNCO3 + HO2 = INCNCO3H ;
% KAPHO2*0.44 : INCNCO3 + HO2 = MACRNO3 + NO2 + OH ;
% KAPNO : INCNCO3 + NO = MACRNO3 + NO2 + NO2 ;
% KFPAN : INCNCO3 + NO2 = INCNPAN ;
% KRO2NO3*1.74 : INCNCO3 + NO3 = MACRNO3 + NO2 + NO2 ;
% 1.00D-11*0.3*RO2 : INCNCO3 = INCNCO2H ;
% 1.00D-11*0.7*RO2 : INCNCO3 = MACRNO3 + NO2 ;
% 4.74D-12 : OH + INCNCO3H = INCNCO3 ;
% 1.98D-12*0.445 : OH + INCNO3 = INCCO + NO2 ;
% 1.98D-12*0.414 : OH + INCNO3 = INCNCHO + HO2 ;
% 1.98D-12*0.141 : OH + INCNO3 = NOA + HOCH2CHO + NO2 ;
% 1.9D17*EXP(-14100/TEMP) : INCNPAN = INCNCO3 + NO2 ;
% 1.14D-12 : OH + INCNPAN = MACRNO3 + NO2 + NO3 ;
% KDEC*0.15 : INCO = NOA + OHCH2CHO + HO2 ;
% KDEC*0.13 : INCO = ACETOL + NO3CH2CHO + HO2 ;
% KDEC*0.07 : INCO = MVKNO3 + HCHO + HO2 ;
% KDEC*0.34 : INCO = DHBN + HCHO + NO2 ;
% KDEC*0.31 : INCO = ACETOL + NO3 + HCHO + HCOOH ;
% KRO2HO2*0.706 : INCO2 + HO2 = INCOOH ;

% KRO2NO : INCO2 + NO = INCO + NO2 ;
% KRO2NO3 : INCO2 + NO3 = INCO + NO2 ;
% 2.90D-12*0.5*RO2 : INCO2 = INCO ;
% 2.90D-12*0.5*RO2 : INCO2 = INCOH ;
% 1.53D-11 : OH + INCOH = INCCO + HO2 ;
% 3.31D-11*0.89 : OH + INCOOH = INCCO + OH ;
% 3.31D-11*0.11 : OH + INCOOH = INCO2 ;
% 2.27D-11 : INDHCHO + OH = INDHCO3 ;
% KAPHO2*0.56 : INDHCO3 + HO2 = INDHCO3H ;
% KAPHO2*0.44 : INDHCO3 + HO2 = MVKNO3 + HO2 + OH ;
% KAPNO : INDHCO3 + NO = MVKNO3 + HO2 + NO2 ;
% KFPAN : INDHCO3 + NO2 = INDHPAN ;
% KRO2NO3*1.74 : INDHCO3 + NO3 = MVKNO3 + HO2 + NO2 ;
% 1.00D-11*RO2 : INDHCO3 = MVKNO3 + HO2 ;
% 5.66D-12 : INDHCO3H + OH = INDHCO3 ;
% 1.96D-12 : INDHPAN + OH = MVKNO3 + NO3 ;
% 1.9D17*EXP(-14100/TEMP) : INDHPAN = INDHCO3 + NO2 ;
% 2.58D-11 : INDHPCHO + OH = INDHPCO3 ;
% KAPHO2*0.56 : INDHPCO3 + HO2 = INDHPCO3H ;
% KAPHO2*0.44 : INDHPCO3 + HO2 = MVKNO3 + OH + OH ;
% KAPNO : INDHPCO3 + NO = MVKNO3 + OH + NO2 ;
% KFPAN : INDHPCO3 + NO2 = INDHPPAN ;
% KRO2NO3*1.74 : INDHPCO3 + NO3 = MVKNO3 + OH + NO2 ;
% 1.00D-11*RO2 : INDHPCO3 = MVKNO3 + OH ;
% 8.64D-12 : INDHPCO3H + OH = INDHPCO3 ;
% 5.04D-12 : INDHPPAN + OH = MVKNO3 + NO3 ;
% 1.9D17*EXP(-14100/TEMP) : INDHPPAN = INDHPCO3 + NO2 ;
% KDEC*0.14 : INDO = MVKNO3 + HCHO + HO2 ;
% KDEC*0.26 : INDO = MACRNO3 + HCHO + HO2 ;
% KDEC*0.6 : INDO = ACETOL + HOCH2CHO + NO2 ;
% KRO2HO2*0.706 : INDO2 + HO2 = INDOOH ;
% KRO2NO : INDO2 + NO = INDO + NO2 ;
% KRO2NO3 : INDO2 + NO3 = INDO + NO2 ;
% 8.00D-13*0.5*RO2 : INDO2 = INDO ;
% 8.00D-13*0.5*RO2 : INDO2 = INDOH ;
% 5.60D-12 : INDOH + OH = INDHCHO + HO2 ;
% 9.20D-12*0.61 : INDOOH + OH = INDHPCHO + HO2 ;
% 9.20D-12*0.39 : INDOOH + OH = INDO2 ;
% 1.72D-12 : IPRHOCO2H + OH = CH3COCH3 + HO2 ;
% KAPHO2*0.44 : IPRHOCO3 + HO2 = CH3COCH3 + HO2 + OH ;
% KAPHO2*0.15 : IPRHOCO3 + HO2 = IPRHOCO2H + O3 ;
% KAPHO2*0.41 : IPRHOCO3 + HO2 = IPRHOCO3H ;
% KAPNO : IPRHOCO3 + NO = CH3COCH3 + HO2 + NO2 ;
% KFPAN : IPRHOCO3 + NO2 = C4PAN5 ;
% KRO2NO3*1.74 : IPRHOCO3 + NO3 = CH3COCH3 + HO2 + NO2 ;

```
% 1.00D-11*0.7*RO2 : IPRHOCO3 = CH3COCH3 + HO2 ;
% 1.00D-11*0.3*RO2 : IPRHOCO3 = IPRHOCO2H ;
% 4.80D-12 : OH + IPRHOCO3H = IPRHOCO3 ;
% 5.09D-12*0.861 : IPROPOL + OH = CH3COCH3 + HO2 ;
% 5.09D-12*0.139 : IPROPOL + OH = IPROPOLO2 ;
% 1.90D+6 : IPROPOLO = CH3CHO + HCHO + HO2 ;
% KRO2HO2*0.520 : IPROPOLO2 + HO2 = IPROPOLO2H ;
% KRO2NO*0.991 : IPROPOLO2 + NO = IPROPOLO + NO2 ;
% KRO2NO*0.009 : IPROPOLO2 + NO = PROLNO3 ;
% KRO2NO3 : IPROPOLO2 + NO3 = IPROPOLO + NO2 ;
% 2.00D-12*0.2*RO2 : IPROPOLO2 = CH3CHOHCHO ;
% 2.00D-12*0.6*RO2 : IPROPOLO2 = IPROPOLO ;
% 2.00D-12*0.2*RO2 : IPROPOLO2 = PROPGLY ;
% 1.83D-11 : IPROPOLO2H + OH = CH3CHOHCHO + OH ;
% 3.59D-12 : IPROPOLO2H + OH = IPROPOLO2 ;
% 2.34D-12 : IPROPOLPAN + OH = CH3CHO + CO + NO2 ;
% 1.9D17*EXP(-14100/TEMP) : IPROPOLPAN = CH3CHOHCO3 + NO2 ;
% 9.34D-12 : IPROPOLPER + OH = CH3CHOHCO3 ;
% 2.8D-17*0.69 : O3 + ISOPANO3 = NO3CH2CHO + OH + MGLYOX + HO2 + AU ;
% 2.8D-17*0.31 : O3 + ISOPANO3 = ACETOL + OH + GLYOX + NO2 ;
% 4.2D-11 : OH + ISOPANO3 = INAO2 ;
% 7.01D-14 : NO3 + ISOPANO3 = NISOPANO3OO ;
% KDEC*0.3 : ISOPAO = DIBOO ;
% KDEC*0.55 : ISOPAO = HC4CCHO + HO2 ;
% KDEC*0.15 : ISOPAO = MF ;
% KRO2HO2*0.706 : E1OH4OO + HO2 = ISOPAOOH ;
% KRO2NO*0.07 : E1OH4OO + NO = ISOPANO3 ;
% KRO2NO*0.93 : E1OH4OO + NO = ISOPAO + NO2 ;
% KRO2NO3 : E1OH4OO + NO3 = ISOPAO + NO2 ;
% 2.4D-12*0.1*RO2 : E1OH4OO = HC4ACHO ;
% 2.4D-13*0.8*RO2 : E1OH4OO = ISOPAO ;
% 2.4D-13*0.1*RO2 : E1OH4OO = ISOPAOH ;
% KRO2HO2*0.706 : Z1OH4OO + HO2 = ISOPAOOH ;
% KRO2NO*0.07 : Z1OH4OO + NO = ISOPANO3 ;
% KRO2NO*0.93 : Z1OH4OO + NO = ISOPAO + NO2 ;
% KRO2NO3 : Z1OH4OO + NO3 = ISOPAO + NO2 ;
% 2.4D-12*0.1*RO2 : Z1OH4OO = HC4ACHO ;
% 2.4D-12*0.8*RO2 : Z1OH4OO = ISOPAO ;
% 2.4D-12*0.1*RO2 : Z1OH4OO = ISOPAOH ;
% 0.52 : Z1OH4OO = HO2 + HPALD ;
% 5.72 : Z4OH1OO = HO2 + HPALD ;
% 9.30D-11*0.5 : OH + ISOPAOH = HC4ACHO + HO2 ;
% 9.30D-11*0.5 : OH + ISOPAOH = HC4CCHO + HO2 ;
% 1.54D-10*0.93 : OH + ISOPAOOH = IEPOXA + OH ;
% 1.54D-10*0.01 : OH + ISOPAOOH = Z1OH4OO ;
```

```
% 1.54D-10*0.01 : OH + ISOPAOOH = E1OH4OO ;
% 1.54D-10*0.05 : OH + ISOPAOOH = HC4ACHO + OH ;
% 8.4D-12 : OH + IEPOXA = IEACHO + HO2 ;
% KNO3AL*7.5 : NO3 + IEACHO = IEACO3 + HNO3 ;
% 2.20D-11 : OH + IEACHO = IEACO3 ;
% 2.5D-19*0.53 : O3 + ISOPBNO3 = MACRNO3 + HCOOH ;
% 2.5D-19*0.47 : O3 + ISOPBNO3 = RNO3I + HCHO + OH ;
% 2.9D-11 : OH + ISOPBNO3 = INBO2 ;
% 7.01D-14 : NO3 + ISOPBNO3 = NISOPBNO3OO ;
% KDEC : ISOPBO = MVK + HCHO + HO2 ;
% 6.49D-4 : ISOPBO2 = MVK + HCHO + OH ;
% KRO2HO2*0.706*0.83 : ISOPBO2 + HO2 = ISOPBOOH ;
% KRO2HO2*0.706*0.17 : ISOPBO2 + HO2 = ISOPBO + OH ;
% KRO2NO*0.07 : ISOPBO2 + NO = ISOPBNO3 ;
% KRO2NO*0.93 : ISOPBO2 + NO = ISOPBO + NO2 ;
% KRO2NO3 : ISOPBO2 + NO3 = ISOPBO + NO2 ;
% 8D-13*0.8*RO2 : ISOPBO2 = ISOPBO ;
% 8D-13*0.2*RO2 : ISOPBO2 = ISOPBOH ;
% 3.85D-11 : OH + ISOPBOH = ISOPBO ;
% 5.0D-11*0.92 : OH + ISOPBOOH = IEPOXB + OH ;
% 5.0D-11*0.08 : OH + ISOPBOOH = ISOPBO2 ;
% 2.8D-17*0.6 : O3 + ISOPCNO3 = NOA + OH + GLYOX + HO2 ;
% 2.8D-17*0.4 : O3 + ISOPCNO3 = HOCH2CHO + OH + MGLYOX + NO2 + AV ;
% 1.1D-10 : OH + ISOPCNO3 = INCO2 ;
% 7E-14 : NO3 + ISOPCNO3 = NISOPCNO3OO ;
% KDEC*0.55 : ISOPCO = HC4ACHO + HO2 ;
% KDEC*0.3 : ISOPCO = DIBOO ;
% KDEC*0.15 : ISOPCO = MF ;
% KRO2HO2*0.706 : E4OH1OO + HO2 = ISOPCOOH ;
% KRO2NO*0.07 : E4OH1OO + NO = ISOPCNO3 ;
% KRO2NO*0.93 : E4OH1OO + NO = ISOPCO + NO2 ;
% KRO2NO3 : E4OH1OO + NO3 = ISOPCO + NO2 ;
% 2.00D-12*0.1*RO2 : E4OH1OO = HC4CCHO ;
% 2.00D-12*0.1*RO2 : E4OH1OO = ISOPAOH ;
% 2.00D-12*0.8*RO2 : E4OH1OO = ISOPCO ;
% KRO2HO2*0.706 : Z4OH1OO + HO2 = ISOPCOOH ;
% KRO2NO*0.07 : Z4OH1OO + NO = ISOPCNO3 ;
% KRO2NO*0.93 : Z4OH1OO + NO = ISOPCO + NO2 ;
% KRO2NO3 : Z4OH1OO + NO3 = ISOPCO + NO2 ;
% 2.00D-12*0.1*RO2 : Z4OH1OO = HC4CCHO ;
% 2.00D-12*0.1*RO2 : Z4OH1OO = ISOPAOH ;
% 2.00D-12*0.8*RO2 : Z4OH1OO = ISOPCO ;
% 1.54D-10*0.93 : OH + ISOPCOOH = IEPOXC + OH ;
% 1.54D-10*0.01 : OH + ISOPCOOH = Z4OH1OO ;
% 1.54D-10*0.01 : OH + ISOPCOOH = E4OH1OO ;
```

```
% 1.54D-10*0.05 : OH + ISOPCOOH = HC4CCHO + OH ;
% 8.4D-12*0.719 : OH + IEPOXC = IEC1O2 ;
% 8.4D-11*0.281 : OH + IEPOXC = IECCHO + HO2 ;
% 2.5D-19*0.33 : O3 + ISOPDNO3 = MVKNO3 + HCOOH ;
% 2.5D-19*0.67 : O3 + ISOPDNO3 = BACL + OH + NO2 ;
% 2.9D-11 : OH + ISOPDNO3 = INDO2 ;
% 7.01D-14 : NO3 + ISOPDNO3 = NISOPDNO3OO ;
% KDEC : ISOPDO = MACR + HCHO + HO2 ;
% KRO2HO2*0.706*0.83 : ISOPDO2 + HO2 = ISOPDOOH ;
% KRO2HO2*0.706*0.17 : ISOPDO2 + HO2 = ISOPDO + OH ;
% KRO2NO*0.07 : ISOPDO2 + NO = ISOPDNO3 ;
% KRO2NO*0.93 : ISOPDO2 + NO = ISOPDO + NO2 ;
% KRO2NO3 : ISOPDO2 + NO3 = ISOPDO + NO2 ;
% 1.15D-3 : ISOPDO2 = MACR + HCHO + OH ;
% 2.90D-12*0.1*RO2 : ISOPDO2 = HCOC5 ;
% 2.90D-12*0.8*RO2 : ISOPDO2 = ISOPDO ;
% 2.90D-12*0.1*RO2 : ISOPDO2 = ISOPDOH ;
% 7.38D-11 : OH + ISOPDOH = HCOC5 + HO2 ;
% 1.15D-10*0.75 : OH + ISOPDOOH = IEPOXB + OH ;
% 1.15D-10*0.015 : OH + ISOPDOOH = Z4OH1OO ;
% 1.15D-10*0.015 : OH + ISOPDOOH = E4OH1OO ;
% 1.15D-10*0.22 : OH + ISOPDOOH = HCOC5 + OH ;
% KRO2HO2*0.706*0.83 : ISOPEO2 + HO2 = ISOPEOOH ;
% KRO2HO2*0.706*0.17 : ISOPEO2 + HO2 = ISOPEO + OH ;
% KRO2NO*0.07 : ISOPEO2 + NO = ISOPENO3 ;
% KRO2NO*0.93 : ISOPEO2 + NO = ISOPEO + NO2 ;
% KRO2NO3 : ISOPEO2 + NO3 = ISOPEO + NO2 ;
% 2.9D-11 : OH + ISOPENO3 = INEO2 ;
% KRO2NO : INEO2 + NO = NO2 + NO3CH2CHO + ACETOL ;
% KDEC : ISOPEO = HCHO + HO2 + MACR ;
% KRO2HO2*0.706*0.83 : ISOPFO2 + HO2 = ISOPFOOH ;
% KRO2HO2*0.706*0.17 : ISOPFO2 + HO2 = ISOPFO + OH ;
% KRO2NO*0.07 : ISOPFO2 + NO = ISOPFNO3 ;
% KRO2NO*0.93 : ISOPFO2 + NO = ISOPFO + NO2 ;
% KRO2NO3 : ISOPFO2 + NO3 = ISOPFO + NO2 ;
% 2.9D-11 : OH + ISOPFNO3 = INFO2 ;
% KRO2NO : INFO2 + NO = NO2 + NOA + OHCH2CHO ;
% KDEC : ISOPFO = HCHO + HO2 + MVK ;
% 1.51D-11 : OH + MACO2H = CH3C2H2O2 ;
% 1.661D-11 : OH + MACO3H = MACO3 ;
% KAPHO2*0.25 : MACO3 + HO2 = MACO2H + O3 ;
% KAPHO2*0.75 : MACO3 + HO2 = MACO3H ;
% 2.30E-11 : MACO3 + NO = CH3CO3 + HCHO + NO2 + B ;
% KFPAN : MACO3 + NO2 = MPAN ;
% KRO2NO3*1.74 : MACO3 + NO3 = CH3CO3 + HCHO + NO2 + B ;
```

% 1.60D-11*RO2 : MACO3 = CH3CO3 + HCHO + B ;
% 3.4D-15 : NO3 + MACR = MACO3 + HNO3 ;
% 1.22D-18*0.12 : O3 + MACR = HCHO + MGLYOOB ;
% 1.22D-18*0.88 : O3 + MACR = MGLYOX + CH2OOG + AW ;
% 2.86D-11*0.45 : OH + MACR = MACO3 ;
% 2.86D-11*0.47 : OH + MACR = MACRO2 ;
% 2.86D-11*0.08 : OH + MACR = MACROHO2 ;
% 1.23D-12*0.32 : MACRNBCO2H + OH = COHM2CO2H + NO2 ;
% 1.23D-12*0.68 : MACRNBCO2H + OH = NOA + HO2 ;
% KAPHO2*0.15 : MACRNBCO3 + HO2 = MACRNBCO2H + O3 ;
% KAPHO2*0.41 : MACRNBCO3 + HO2 = MACRNBCO3H ;
% KAPHO2*0.44 : MACRNBCO3 + HO2 = NOA + HO2 + OH ;
% KAPNO : MACRNBCO3 + NO = NOA + HO2 + NO2 ;
% KFPAN : MACRNBCO3 + NO2 = MACRNBPAN ;
% KRO2NO3*1.74 : MACRNBCO3 + NO3 = NOA + HO2 + NO2 ;
% 1.00D-11*0.3*RO2 : MACRNBCO3 = MACRNBCO2H ;
% 1.00D-11*0.7*RO2 : MACRNBCO3 = NOA + HO2 ;
% 4.31D-12*0.09 : MACRNBCO3H + OH = COHM2CO3H + NO2 ;
% 4.31D-12*0.91 : MACRNBCO3H + OH = MACRNBCO3 ;
% 7.10D-13 : MACRNBPAN + OH = COHM2PAN + NO2 ;
% 1.9D17*EXP(-14100/TEMP) : MACRNBPAN = MACRNBCO3 + NO2 ;
% 1.34D-12*0.44 : MACRNCO2H + OH = ACETOL + NO2 ;
% 1.34D-12*0.15 : MACRNCO2H + OH = CONM2CO2H + HO2 ;
% KAPHO2*0.44 : MACRNCO3 + HO2 = ACETOL + NO2 + OH ;
% KAPHO2*0.15 : MACRNCO3 + HO2 = MACRNCO2H + O3 ;
% KAPHO2*0.41 : MACRNCO3 + HO2 = MACRNCO3H ;
% KAPNO : MACRNCO3 + NO = ACETOL + NO2 + NO2 ;
% KFPAN : MACRNCO3 + NO2 = MACRNPAN ;
% KRO2NO3*1.74 : MACRNCO3 + NO3 = ACETOL + NO2 + NO2 ;
% 1.00D-11*0.7*RO2 : MACRNCO3 = ACETOL + NO2 ;
% 1.00D-11*0.3*RO2 : MACRNCO3 = MACRNCO2H ;
% 4.42D-12*0.15 : MACRNCO3H + OH = CONM2CO3H + HO2 ;
% 4.42D-12*0.85 : MACRNCO3H + OH = MACRNCO3 ;
% 2.15D-11 : OH + MACRNO3 = MACRNBCO3 ;
% 4.98D-11*0.85 : OH + MACRNO3 = ACETOL + NO2 + CO2 ;
% 4.98D-11*0.08 : OH + MACRNO3 = CH3CO2H + HCHO + NO3 + CO2 ;
% 4.98D-11*0.07 : OH + MACRNO3 = HCOOH + NO3 + MGLYOX + AX ;
% 1.2D-15 : MACRNOO + CO = MACRNO3 ;
% 1.0D-14 : MACRNOO + NO = MACRNO3 + NO2 ;
% 1.0D-15 : MACRNOO + NO2 = MACRNO3 + NO3 ;
% 7.0D-14 : MACRNOO + SO2 = MACRNO3 + SO3 ;
% 1.0D-17*H2O : MACRNOO = MACRNCO2H ;
% 6.0D-18*H2O : MACRNOO = MACRNO3 + H2O2 ;
% KDEC*0.36 : MACRNOOA = ACETOL + NO2 + CO + OH ;
% KDEC*0.20 : MACRNOOA = ACETOL + NO2 + HO2 ;

% KDEC*0.24 : MACRNOOA = MACRNOO ;
% KDEC*0.20 : MACRNOOA = PROPOLNO3 ;
% 8.21D-13 : MACRNPAN + OH = CONM2PAN + HO2 ;
% 1.9D17*EXP(-14100/TEMP) : MACRNPAN = MACRNCO3 + NO2 ;
% KDEC*0.847 : MACRO = ACETOL + CO + HO2 ;
% KDEC*0.153 : MACRO = MGLYOX + HCHO + HO2 + AY ;
% KRO2HO2*0.625 : MACRO2 + HO2 = MACROOH ;
% KRO2NO*0.85 : MACRO2 + NO = MACRO + NO2 ;
% KRO2NO*0.15 : MACRO2 + NO = MACRNO3 ;
% KRO2NO3 : MACRO2 + NO3 = MACRO + NO2 ;
% 3.50D-14*0.5*RO2 : MACRO2 = MACRO ;
% 3.50D-14*0.5*RO2 : MACRO2 = MACROH ;
% 3.42D-11 : OH + MACROH = C3MDIALOH + HO2 ;
% 2.18D-11 : MACROHNO3 + OH = NOA + CO + HO2 ;
% KDEC : MACROHO = MGLYOX + HCHO + HO2 + AZ ;
% 5.55D-11 : MACROHOOH + OH = C3MDIALOH + OH ;
% 1.2D-15 : MACROO + CO = MACR ;
% 1.0D-14 : MACROO + NO = MACR + NO2 ;
% 1.0D-15 : MACROO + NO2 = MACR + NO3 ;
% 7.0D-14 : MACROO + SO2 = MACR + SO3 ;
% 1.0D-17*H2O : MACROO = MACO2H ;
% 6.0D-18*H2O : MACROO = MACR + H2O2 ;
% KDEC*0.255 : MACROOA = C3H6 ;
% KDEC*0.255 : MACROOA = CH3CO3 + HCHO + HO2 + A ;
% KDEC*0.22 : MACROOA = MACROO ;
% KDEC*0.27 : MACROOA = OH + CO + CH3CO3 + HCHO + A ;
% 3.77D-11 : OH + MACROOH = ACETOL + CO + OH ;
% 1.2D-15 : MGLOO + CO = MGLYOX + BA ;
% 1.0D-14 : MGLOO + NO = MGLYOX + NO2 + BA ;
% 1.0D-15 : MGLOO + NO2 = MGLYOX + NO3 + BA ;
% 7.0D-14 : MGLOO + SO2 = MGLYOX + SO3 + BA ;
% 1.0D-17*H2O : MGLOO = CH3COCO2H ;
% 6.0D-18*H2O : MGLOO = MGLYOX + H2O2 + BA ;
% KDEC*0.20 : MGLOOA = CH3CHO ;
% KDEC*0.20 : MGLOOA = CH3CO3 + HCHO + HO2 + G ;
% KDEC*0.24 : MGLOOA = MGLOO ;
% KDEC*0.36 : MGLOOA = OH + CO + CH3CO3 + G ;
% 1.2D-15 : MGLYOO + CO = MGLYOX + BB ;
% 1.0D-14 : MGLYOO + NO = MGLYOX + NO2 + BB ;
% 1.0D-15 : MGLYOO + NO2 = MGLYOX + NO3 + BB ;
% 7.0D-14 : MGLYOO + SO2 = MGLYOX + SO3 + BB ;
% 6.0D-18*H2O : MGLYOO = MGLYOX + H2O2 + BB ;
% KDEC*0.11 : MGLYOOA = MGLYOO ;
% KDEC*0.89 : MGLYOOA = OH + CO + CH3CO3 + HOW ;
% KDEC*0.18 : MGLYOOB = MGLYOO ;

% KDEC*0.82 : MGLYOOB = OH + CO + CH3CO3 + IPRENE ;
% KNO3AL*2.4 : NO3 + MGLYOX = CH3CO3 + CO + HNO3 + F ;
% 1.31D-11 : OH + MGLYOX = CH3CO3 + CO + F ;
% 4.93D-12 : MMALNACO2H + OH = CONM2CHO + HO2 ;
% KAPHO2*0.44 : MMALNACO3 + HO2 = CONM2CHO + HO2 + OH ;
% KAPHO2*0.15 : MMALNACO3 + HO2 = MMALNACO2H + O3 ;
% KAPHO2*0.41 : MMALNACO3 + HO2 = MMALNACO3H ;
% KAPNO : MMALNACO3 + NO = CONM2CHO + HO2 + NO2 ;
% KFPAN : MMALNACO3 + NO2 = MMALNAPAN ;
% KRO2NO3*1.74 : MMALNACO3 + NO3 = CONM2CHO + HO2 + NO2 ;
% 1.00D-11*0.7*RO2 : MMALNACO3 = CONM2CHO + HO2 ;
% 1.00D-11*0.3*RO2 : MMALNACO3 = MMALNACO2H ;
% 8.01D-12 : MMALNACO3H + OH = MMALNACO3 ;
% 4.41D-12 : MMALNAPAN + OH = CONM2CHO + HO2 + NO3 ;
% 1.9D17*EXP(-14100/TEMP) : MMALNAPAN = MMALNACO3 + NO2 ;
% 2.23D-11 : MMALNBCO2H + OH = CO2H3CHO + NO2 ;
% KAPHO2*0.44 : MMALNBCO3 + HO2 = CO2H3CHO + NO2 + OH ;
% KAPHO2*0.15 : MMALNBCO3 + HO2 = MMALNBCO2H + O3 ;
% KAPHO2*0.41 : MMALNBCO3 + HO2 = MMALNBCO3H ;
% KAPNO : MMALNBCO3 + NO = CO2H3CHO + NO2 + NO2 ;
% KFPAN : MMALNBCO3 + NO2 = MMALNBPAN ;
% KRO2NO3*1.74 : MMALNBCO3 + NO3 = CO2H3CHO + NO2 + NO2 ;
% 1.00D-11*0.7*RO2 : MMALNBCO3 = CO2H3CHO + NO2 ;
% 1.00D-11*0.3*RO2 : MMALNBCO3 = MMALNBCO2H ;
% 2.59D-11 : MMALNBCO3H + OH = MMALNBCO3 ;
% 2.18D-11 : MMALNBPAN + OH = CO2H3CHO + NO2 + NO3 ;
% 1.9D17*EXP(-14100/TEMP) : MMALNBPAN = MMALNBCO3 + NO2 ;
% 1.9D17*EXP(-14100/TEMP) : MPAN = MACO3 + NO2 ;
% 8.2D-18 : O3 + MPAN = HCHO + CH3CO3 + NO3 + IPRENE ;
% 2.9D-11 : OH + MPAN = ACETOL + CO + NO2 ;
% 5.18D-18*0.5 : O3 + MVK = MGLOOA + HCHO ;
% 5.18D-18*0.5 : O3 + MVK = MGLYOX + CH2OOB + BC ;
% 2.01D-11 : OH + MVK = HMVKO2 ;
% 1.33D-12*0.65 : OH + MVKNO3 = HCOOH + MGLYOX + NO3 + BD ;
% 1.33D-12*0.35 : OH + MVKNO3 = HCHO + CH3COCOOH + NO3 ;
% KDEC : MVKO = HCHO + ACO3 ;
% KRO2HO2*0.625 : MVKO2 + HO2 = MVKOOH ;
% KRO2NO : MVKO2 + NO = MVKO + NO2 ;
% KRO2NO3 : MVKO2 + NO3 = MVKO + NO2 ;
% 2.00D-12*0.6*RO2 : MVKO2 = MVKO ;
% 2.00D-12*0.2*RO2 : MVKO2 = MVKOH ;
% 2.00D-12*0.2*RO2 : MVKO2 = VGLYOX ;
% 4.56D-18*0.5 : MVKOH + O3 = HMGLOOA + HCHO ;
% 4.56D-18*0.5 : MVKOH + O3 = HOCH2COCHO + CH2OOB ;
% 2.09D-11*0.3 : MVKOH + OH = MVKOHAO2 ;

% 2.09D-11*0.7 : MVKOH + OH = MVKOHBO2 ;
% 4.37D-12 : MVKOHANO3 + OH = H13CO2CHO + NO2 ;
% KDEC : MVKOHAO = HOCH2COCHO + HCHO + HO2 ;
% KRO2HO2*0.625 : MVKOHAO2 + HO2 = MVKOHAOOH ;
% KRO2NO*0.017 : MVKOHAO2 + NO = MVKOHANO3 ;
% KRO2NO*0.983 : MVKOHAO2 + NO = MVKOHAO + NO2 ;
% KRO2NO3 : MVKOHAO2 + NO3 = MVKOHAO + NO2 ;
% 2.00D-12*0.2*RO2 : MVKOHAO2 = H13CO2CHO ;
% 2.00D-12*0.6*RO2 : MVKOHAO2 = MVKOHAO ;
% 2.00D-12*0.2 : MVKOHAO2 = MVKOHAOH ;
% 2.10D-11 : MVKOHAOH + OH = H13CO2CHO + HO2 ;
% 5.98D-11 : MVKOHAOOH + OH = H13CO2CHO + OH ;
% KDEC : MVKOHBO = HOCH2CHO + HOCH2CO3 ;
% KRO2HO2*0.625 : MVKOHBO2 + HO2 = MVKOHBOOH ;
% KRO2NO : MVKOHBO2 + NO = MVKOHBO + NO2 ;
% KRO2NO3 : MVKOHBO2 + NO3 = MVKOHBO + NO2 ;
% 8.80D-13*0.2*RO2 : MVKOHBO2 = H14CO23C4 ;
% 8.80D-13*0.2*RO2 : MVKOHBO2 = MVKOHAOH ;
% 8.80D-13*0.6*RO2 : MVKOHBO2 = MVKOHBO ;
% 4.39D-12 : MVKOHBOOH + OH = H14CO23C4 + OH ;
% 1.2D-15 : MVKOO + CO = MVK ;
% 1.0D-14 : MVKOO + NO = MVK + NO2 ;
% 1.0D-15 : MVKOO + NO2 = MVK + NO3 ;
% 7.0D-14 : MVKOO + SO2 = MVK + SO3 ;
% 6.0D-18*H2O : MVKOO = MVK + H2O2 ;
% KDEC*0.255 : MVKOOA = C3H6 ;
% KDEC*0.255 : MVKOOA = CH3O2 + HCHO + CO + HO2 ;
% KDEC*0.22 : MVKOOA = MVKOO ;
% KDEC*0.27 : MVKOOA = OH + MVKO2 ;
% 3.59D-12 : OH + MVKOOH = MVKO2 ;
% 2.55D-11 : OH + MVKOOH = VGLYOX + OH ;
% 1.2D-15 : NC2OO + CO = NO3CH2CHO ;
% 1.0D-14 : NC2OO + NO = NO3CH2CHO + NO2 ;
% 1.0D-15 : NC2OO + NO2 = NO3CH2CHO + NO3 ;
% 7.0D-14 : NC2OO + SO2 = NO3CH2CHO + SO3 ;
% 6.0D-18*H2O : NC2OO = NO3CH2CHO + H2O2 ;
% 1.0D-17*H2O : NC2OO = NO3CH2CO2H ;
% KDEC*0.11 : NC2OOA = NC2OO ;
% KDEC*0.89 : NC2OOA = OH + NO2 + GLYOX ;
% 1.2D-15 : NC3OO + CO = NOA ;
% 1.0D-14 : NC3OO + NO = NOA + NO2 ;
% 1.0D-15 : NC3OO + NO2 = NOA + NO3 ;
% 7.0D-14 : NC3OO + SO2 = NOA + SO3 ;
% 6.0D-18*H2O : NC3OO = NOA + H2O2 ;
% KDEC*0.11 : NC3OOA = NC3OO ;

% KDEC*0.89 : NC3OOA = OH + NO2 + MGLYOX + BE ;
% KNO3AL*4.25*0.6 : NO3 + NC4CHO = NC4CO3 + HNO3 ;
% KNO3AL*4.25*0.4 : NO3 + NC4CHO = NNC4CHOO2 ;
% 2.52D-17*0.15 : O3 + NC4CHO = OH + CO2 + HO2 + CO + NO2 + MGLYOX + GLYOX;
% 2.52D-17*0.3 : O3 + NC4CHO = NOA + HO2 + CO ;
% 2.52D-17*0.55 : O3 + NC4CHO = NO2 + MGLYOX + GLYOX + OH + BG ;
% 4.16D-11*0.655 : OH + NC4CHO = C510O2 ;
% 4.16D-11*0.345 : OH + NC4CHO = NC4CO3 ;
% 2.16D-11 : OH + NC4CO2H = NOA + CO + HO2 ;
% 4D-12 : NC4CO3 + NO3 = NO2 + NOA + CO + CO2 + HO2 ;
% KAPHO2*0.15 : NC4CO3 + HO2 = NC4CO2H + O3 ;
% KAPHO2*0.41 : NC4CO3 + HO2 = NC4CO3H ;
% KAPHO2*0.44 : NC4CO3 + HO2 = NOA + CO + HO2 + OH ;
% KAPNO : NC4CO3 + NO = NOA + CO + HO2 + NO2 ;
% KFPAN : NC4CO3 + NO2 = C5PAN18 ;
% KRO2NO3*1.74 : NC4CO3 + NO3 = NOA + CO + HO2 + NO2 ;
% 1.00D-11*0.3*RO2 : NC4CO3 = NC4CO2H ;
% 1.00D-11*0.7*RO2 : NC4CO3 = NOA + HO2 + CO ;
% 2.52D-11 : OH + NC4CO3H = NC4CO3 ;
% 1.2D-15 : NC4OO + CO = MVKNO3 ;
% 1.0D-14 : NC4OO + NO = MVKNO3 + NO2 ;
% 1.0D-15 : NC4OO + NO2 = MVKNO3 + NO3 ;
% 7.0D-14 : NC4OO + SO2 = MVKNO3 + SO3 ;
% 6.0D-18*H2O : NC4OO = MVKNO3 + H2O2 ;
% 2.43D-12 : NC524NO3 + OH = DNC524CO + HO2 ;
% 2.04D+7 : NC524O = HMVKNO3 + HCHO + HO2 ;
% 2.27D+6 : NC524O = HOCH2CHO + NO2 + H13CO2C3 ;
% KRO2HO2*0.706 : NC524O2 + HO2 = NC524OOH ;
% KRO2NO*0.072 : NC524O2 + NO = NC524NO3 ;
% KRO2NO*0.928 : NC524O2 + NO = NC524O + NO2 ;
% KRO2NO3 : NC524O2 + NO3 = NC524O + NO2 ;
% 8.00D-13*0.8*RO2 : NC524O2 = NC524O ;
% 8.00D-13*0.2*RO2 : NC524O2 = NC524OH ;
% 9.60D-12 : NC524OH + OH = HNC524CO + HO2 ;
% 1.32D-11*0.728 : NC524OOH + OH = HPNC524CO + HO2 ;
% 1.32D-11*0.272 : NC524OOH + OH = NC524O2 ;
% 9.31D-12 : NISOPANO3OO + NO = NO2 + ACETOL + NO3CH2CHO + NO2 ;
% 2.3D-12 : NISOPANO3OO + NO3 = NO2 + ACETOL + NO3CH2CHO + NO2 ;
% KRO2HO2*0.706 : NISOPANO3OO + HO2 = NISOPANO3OOH ;
% 2D-13*0.7*RO2 : NISOPANO3OO = NO2 + ACETOL + NO3CH2CHO ;
% 2D-13*0.3*RO2 : NISOPANO3OO = RNO3I ;
% 9.31D-12 : NISOPBNO3OO + NO = NO2 + ACETOL + NO3CH2CHO + NO2 ;
% 2.3D-12 : NISOPBNO3OO + NO3 = NO2 + ACETOL + NO3CH2CHO + NO2 ;
% KRO2HO2*0.706 : NISOPBNO3OO + HO2 = NISOPBNO3OOH ;

% 2D-13*0.7*RO2 : NISOPBNO3OO = NO2 + ACETOL + NO3CH2CHO ;
% 2D-13*0.3*RO2 : NISOPBNO3OO = RNO3I ;
% 9.31D-12 : NISOPCNO3OO + NO = NO2 + NOA + HOCH2CHO + NO2 ;
% 2.3D-12 : NISOPCNO3OO + NO3 = NO2 + NOA + HOCH2CHO + NO2 ;
% KRO2HO2*0.706 : NISOPCNO3OO + HO2 = NISOPCNO3OOH ;
% 3.50D-14*0.7*RO2 : NISOPCNO3OO = NO2 + NOA + HOCH2CHO ;
% 3.50D-14*0.3*RO2 : NISOPCNO3OO = RNO3I ;
% 9.31D-12 : NISOPDNO3OO + NO = NO2 + NOA + HOCH2CHO + NO2 ;
% 2.3D-12 : NISOPDNO3OO + NO3 = NO2 + NOA + HOCH2CHO + NO2 ;
% KRO2HO2*0.706 : NISOPDNO3OO + HO2 = NISOPDNO3OOH ;
% 2D-13*0.7*RO2 : NISOPDNO3OO = NO2 + NOA + HOCH2CHO ;
% 2D-13*0.3*RO2 : NISOPDNO3OO = RNO3I ;
% 8.55D-11 : OH + NISOPNO3 = NC4CHO + NO2 ;
% KROPRIM*O2 : NISOPO = NC4CHO + HO2 ;
% KRO2HO2*0.706 : NISOPAO2 + HO2 = NISOPOOH ;
% KRO2HO2*0.706 : NISOPBO2 + HO2 = NISOPOOH ;
% KRO2HO2*0.706 : NISOPCO2 + HO2 = NISOPOOH ;
% KRO2HO2*0.706 : NISOPDO2 + HO2 = NISOPOOH ;
% KRO2HO2*0.706 : NISOPEO2 + HO2 = NISOPOOH ;
% KRO2HO2*0.706 : NISOPFO2 + HO2 = NISOPOOH ;
% KRO2NO*0.07 : NISOPAO2 + NO = NISOPNO3 ;
% KRO2NO*0.07 : NISOPBO2 + NO = NISOPNO3 ;
% KRO2NO*0.07 : NISOPCO2 + NO = NISOPNO3 ;
% KRO2NO*0.07 : NISOPDO2 + NO = NISOPNO3 ;
% KRO2NO*0.07 : NISOPEO2 + NO = NISOPNO3 ;
% KRO2NO*0.07 : NISOPFO2 + NO = NISOPNO3 ;
% KRO2NO*0.93 : NISOPAO2 + NO = NO2 + HO2 + NC4CHO ;
% KRO2NO*0.93 : NISOPBO2 + NO = NO2 + HCHO + MVK ;
% KRO2NO*0.93 : NISOPCO2 + NO = NO2 + HO2 + NC4CHO ;
% KRO2NO*0.93 : NISOPDO2 + NO = NO2 + HCHO + MACR ;
% KRO2NO*0.93 : NISOPEO2 + NO = NO2 + HCHO + MACR ;
% KRO2NO*0.93 : NISOPFO2 + NO = NO2 + HCHO + MVK ;
% KRO2NO3 : NISOPAO2 + NO3 = NO2 + HO2 + NC4CHO ;
% KRO2NO3 : NISOPBO2 + NO3 = NO2 + HCHO + MVK ;
% KRO2NO3 : NISOPCO2 + NO3 = NO2 + HO2 + NC4CHO ;
% KRO2NO3 : NISOPDO2 + NO3 = NO2 + HCHO + MACR ;
% KRO2NO3 : NISOPEO2 + NO3 = NO2 + HCHO + MACR ;
% KRO2NO3 : NISOPFO2 + NO3 = NO2 + HCHO + MVK ;
% 2.0D-12*0.2*RO2 : NISOPAO2 = ISOPCNO3 ;
% 2.0D-12*0.2*RO2 : NISOPAO2 = NC4CHO ;
% 2.0D-12*0.6*RO2 : NISOPAO2 = HO2 + NC4CHO ;
% 1.59D-13*0.3*RO2 : NISOPBO2 = ISOPFNO3 ;
% 1.59D-13*0.7*RO2 : NISOPBO2 = NO2 + HCHO + MVK ;
% 2.0D-12*0.2*RO2 : NISOPCO2 = ISOPANO3 ;
% 2.0D-12*0.2*RO2 : NISOPCO2 = NC4CHO ;

% 2.0D-12*0.6*RO2 : NISOPCO2 = HO2 + NC4CHO ;
% 1.44D-12*0.2*RO2 : NISOPDO2 = ISOPENO3 ;
% 1.44D-12*0.2*RO2 : NISOPDO2 = NC4CHO ;
% 1.44D-12*0.6*RO2 : NISOPDO2 = NO2 + HCHO + MACR ;
% 2.0D-12*0.2*RO2 : NISOPEO2 = ISOPDNO3 ;
% 2.0D-12*0.2*RO2 : NISOPEO2 = NC4CHO ;
% 2.0D-12*0.6*RO2 : NISOPEO2 = NO2 + HCHO + MACR ;
% 2.0D-12*0.2*RO2 : NISOPFO2 = ISOPBNO3 ;
% 2.0D-12*0.2*RO2 : NISOPFO2 = NC4CHO ;
% 2.0D-12*0.6*RO2 : NISOPFO2 = NO2 + HCHO + MVK ;
% 1.03D-10 : OH + NISOPOOH = OH + NC4CHO ;
% 7.01D-14 : NISOPOOH + NO3 = NNISOPOOHOO ;
% KNO3AL*2.4 : NO3 + NMGLYOX = NO3CH2CO3 + CO + HNO3 ;
% 1.24D-11 : OH + NMGLYOX = NO3CH2CO3 + CO ;
% 2.3D-12 : NNC4CHOO2 + NO3 = NOA + HOCH2CHO + NO2 + NO2 ;
% 9.31D-12 : NNC4CHOO2 + NO = NOA + HOCH2CHO + NO2 + NO2 ;
% 1.615E-11 : NNC4CHOO2 + HO2 = RNO3I ;
% 3.5D-14*0.7*RO2 : NNC4CHOO2 = NOA + HOCH2CHO + NO2 ;
% 3.5D-14*0.3*RO2 : NNC4CHOO2 = RNO3I ;
% KRO2HO2*0.706 : NNISOPOOHOO + HO2 = RNO3I ;
% 9.31D-12 : NNISOPOOHOO + NO = RNO3I ;
% 2.3D-12 : NNISOPOOHOO + NO3 = RNO3I ;
% 2D-13*RO2 : NNISOPOOHOO = RNO3I ;
% KNO3AL : NO3CH2CHO + NO3 = NO3CH2CO3 + HNO3 ;
% 1.00D-11 : NO3CH2CHO + OH = NO3CH2CO3 ;
% 1.68D-13 : NO3CH2CO2H + OH = HCHO + NO2 ;
% KAPHO2*0.44 : NO3CH2CO3 + HO2 = HCHO + NO2 + OH ;
% KAPHO2*0.15 : NO3CH2CO3 + HO2 = NO3CH2CO2H + O3 ;
% KAPHO2*0.41 : NO3CH2CO3 + HO2 = NO3CH2CO3H ;
% KAPNO : NO3CH2CO3 + NO = HCHO + NO2 + NO2 ;
% KFPAN : NO3CH2CO3 + NO2 = NO3CH2PAN ;
% KRO2NO3*1.74 : NO3CH2CO3 + NO3 = HCHO + NO2 + NO2 ;
% 1.00D-11*0.7*RO2 : NO3CH2CO3 = HCHO + NO2 ;
% 1.00D-11*0.3*RO2 : NO3CH2CO3 = NO3CH2CO2H ;
% 3.63D-12 : NO3CH2CO3H + OH = NO3CH2CO3 ;
% 1.12D-14 : NO3CH2PAN + OH = HCHO + CO + NO2 + NO2 ;
% 1.9D17*EXP(-14100/TEMP) : NO3CH2PAN = NO3CH2CO3 + NO2 ;
% 4.00D-13 : NOA + OH = MGLYOX + NO2 + BH ;
% 1.2D-15 : NOAOO + CO = NOA ;
% 1.0D-14 : NOAOO + NO = NOA + NO2 ;
% 1.0D-15 : NOAOO + NO2 = NOA + NO3 ;
% 7.0D-14 : NOAOO + SO2 = NOA + SO3 ;
% 6.0D-18*H2O : NOAOO = NOA + H2O2 ;
% KDEC*0.11 : NOAOOA = NOAOO ;
% KDEC*0.89 : NOAOOA = OH + NO2 + MGLYOX + BI ;

```
% KDEC : OCCOHCO = HCHO + GLYOX + HO2 ;
% 0.4*0.52*KRO2HO2 : OCCOHCO2 + HO2 = C32OH13CO + O3 ;
% 0.6*0.52*KRO2HO2 : OCCOHCO2 + HO2 = OCCOHCOOH ;
% 0.05*KRO2NO : OCCOHCO2 + NO = C42AOH ;
% 0.95*KRO2NO : OCCOHCO2 + NO = OCCOHCO + NO2 ;
% KRO2NO3 : OCCOHCO2 + NO3 = C42AOH + NO2 ;
% 2.0D-12*0.2*RO2 : OCCOHCO2 = C32OH13CO ;
% 2.0D-12*0.6*RO2 : OCCOHCO2 = OCCOHCO ;
% 2.0D-12*0.2*RO2 : OCCOHCO2 = OCCOHCOH ;
% 6.22D-11 : OCCOHCOH + OH = A2PANOO ;
% 9.258E-11 : OCCOHCOOH + OH = OCCOHCO2 ;
% 3D-14 : PAN + OH = HCHO + CO + NO2 ;
% 1.9D17*EXP(-14100/TEMP) : PAN = CH3CO3 + NO2 + BACK ;
% KVDPAN : PAN = product ;
% 1.12D-12 : PHAN + OH = HCHO + CO + NO2 ;
% 1.9D17*EXP(-14100/TEMP) : PHAN = HOCH2CO3 + NO2 ;
% 1.69D-12 : PR1O2HNO3 + OH = CHOPRNO3 + OH ;
% 3.60D-12 : PR1O2HNO3 + OH = PRONO3AO2 ;
% 3.47D-12 : PR2O2HNO3 + OH = NOA + OH ;
% 3.60D-12 : PR2O2HNO3 + OH = PRONO3BO2 ;
% 3.14D-13 : PRNO3CO2H + OH = CH3CHO + NO2 ;
% KAPHO2*0.44 : PRNO3CO3 + HO2 = CH3CHO + NO2 + OH ;
% KAPHO2*0.15 : PRNO3CO3 + HO2 = PRNO3CO2H + O3 ;
% KAPHO2*0.41 : PRNO3CO3 + HO2 = PRNO3CO3H ;
% KAPNO : PRNO3CO3 + NO = CH3CHO + NO2 + NO2 ;
% KFPAN : PRNO3CO3 + NO2 = PRNO3PAN ;
% KRO2NO3*1.74 : PRNO3CO3 + NO3 = CH3CHO + NO2 + NO2 ;
% 1.00D-11*0.7*RO2 : PRNO3CO3 = CH3CHO + NO2 ;
% 1.00D-11*0.3*RO2 : PRNO3CO3 = PRNO3CO2H ;
% 3.77D-12 : PRNO3CO3H + OH = PRNO3CO3 ;
% 1.43D-13 : PRNO3PAN + OH = CH3CHO + CO + NO2 + NO2 ;
% 1.9D17*EXP(-14100/TEMP) : PRNO3PAN = PRNO3CO3 + NO2 ;
% 1.71D-12 : PROLNO3 + OH = CH3CHOHCHO + NO2 ;
% KROPRIM : PRONO3AO + O2 = CHOPRNO3 + HO2 ;
% 7.00D+03 : PRONO3AO = HCHO + CH3CHO + NO2 ;
% KRO2HO2*0.520 : PRONO3AO2 + HO2 = PR1O2HNO3 ;
% KRO2NO : PRONO3AO2 + NO = PRONO3AO + NO2 ;
% KRO2NO3 : PRONO3AO2 + NO3 = PRONO3AO + NO2 ;
% 6.00D-13*0.2*RO2 : PRONO3AO2 = CHOPRNO3 ;
% 6.00D-13*0.6*RO2 : PRONO3AO2 = PRONO3AO ;
% 6.00D-13*0.2*RO2 : PRONO3AO2 = PROPOLNO3 ;
% 7.00D+03 : PRONO3BO = CH3CHO + HCHO + NO2 ;
% KROSEC : PRONO3BO + O2 = NOA + HO2 ;
% KRO2HO2*0.520 : PRONO3BO2 + HO2 = PR2O2HNO3 ;
% KRO2NO : PRONO3BO2 + NO = PRONO3BO + NO2 ;
```

```
% KRO2NO3 : PRONO3BO2 + NO3 = PRONO3BO + NO2 ;
% 4.00D-14*0.2*RO2 : PRONO3BO2 = NOA ;
% 4.00D-14*0.2*RO2 : PRONO3BO2 = PROLNO3 ;
% 4.00D-14*0.6*RO2 : PRONO3BO2 = PRONO3BO ;
% KDEC : PROPALO = CH3CHO + HO2 + CO ;
% 1.20D-11*0.613 : PROPGLY + OH = ACETOL + HO2 ;
% 1.20D-11*0.387 : PROPGLY + OH = CH3CHOHCHO + HO2 ;
% 9.16D-13 : PROPOLNO3 + OH = ACETOL + NO2 ;
% 8D-12 : RNO3I + OH = NO2 + HO2 + DHBN ;
% KNO3AL*2.0 : NO3 + VGLYOX = CO + ACO3 + HNO3 ;
% 2.95D-11 : OH + VGLYOX = CO + ACO3 ;
```

Appendix B: 0-D Photochemical Mechanism Terpene Reactions

Below is a list of reactions from the MCM terpene subset used in all simulations of this study. Note that names of chemical species are consistent with the MCM website.

0-D Terpene Reactions

*Terpene Chemistry;

% 2.41D-11 : ALCOCH2OOH + OH = CHOCOCH2O2 ;
% 5.50D-12 : APINANO3 + OH = PINAL + NO2 ;
% KDEC : APINAO = PINAL + HO2 ;
% KRO2HO2*0.914 : APINAO2 + HO2 = APINAOOH ;
% KRO2NO*0.230 : APINAO2 + NO = APINANO3 ;
% KRO2NO*0.770 : APINAO2 + NO = APINAO + NO2 ;
% KRO2NO3 : APINAO2 + NO3 = APINAO + NO2 ;
% 9.20D-14*0.7*RO2 : APINAO2 = APINAO ;
% 9.20D-14*0.3*RO2 : APINAO2 = APINBOH ;
% 1.83D-11 : APINAOOH + OH = APINAO2 ;
% 8.18D-12 : APINBCO + OH = C96CO3 ;
% 3.64D-12 : APINBNO3 + OH = APINBCO + NO2 ;
% KDEC : APINBO = PINAL + HO2 ;
% KRO2HO2*0.914 : APINBO2 + HO2 = APINBOOH ;
% KRO2NO*0.230 : APINBO2 + NO = APINBNO3 ;
% KRO2NO*0.770 : APINBO2 + NO = APINBO + NO2 ;
% KRO2NO3 : APINBO2 + NO3 = APINBO + NO2 ;
% 8.80D-13*0.2*RO2 : APINBO2 = APINBCO ;
% 8.80D-13*0.6*RO2 : APINBO2 = APINBO ;
% 8.80D-13*0.2*RO2 : APINBO2 = APINBOH ;
% 1.49D-11 : APINBOH + OH = APINBCO + HO2 ;
% 1.20D-15 : APINBOO + CO = PINAL ;
% 1.00D-14 : APINBOO + NO = PINAL + NO2 ;
% 1.00D-15 : APINBOO + NO2 = PINAL + NO3 ;
% 7.00D-14 : APINBOO + SO2 = PINAL + SO3 ;
% 1.40D-17*H2O : APINBOO = PINAL + H2O2 ;
% 2.00D-18*H2O : APINBOO = PINONIC ;
% 3.28D-11 : APINBOOH + OH = APINBCO + OH ;
% 9.87D-11 : APINCNO3 + OH = CH3COCH3 + HCC7CO + NO2 ;
% KDEC : APINCO = CH3COCH3 + C720O2 ;
% KRO2HO2*0.914 : APINCO2 + HO2 = APINCOOH ;
% KRO2NO*0.125 : APINCO2 + NO = APINCNO3 ;
% KRO2NO*0.875 : APINCO2 + NO = APINCO + NO2 ;

% KRO2NO3 : APINCO2 + NO3 = APINCO + NO2 ;
% 6.70D-15*0.7*RO2 : APINCO2 = APINCO ;
% 6.70D-15*0.3*RO2 : APINCO2 = APINCOH ;
% 9.91D-11 : APINCOH + OH = APINCO ;
% 1.03D-10 : APINCOOH + OH = APINCO2 ;
% 6.21D-12*0.65 : APINENE + NO3 = NAPINAO2 ;
% 6.21D-12*0.35 : APINENE + NO3 = NAPINBO2 ;
% 9.00D-17*0.6 : APINENE + O3 = APINOOA ;
% 9.00D-17*0.4 : APINENE + O3 = APINOOB ;
% 5.25D-11*0.572 : APINENE + OH = APINAO2 ;
% 5.25D-11*0.353 : APINENE + OH = APINBO2 ;
% 5.25D-11*0.075 : APINENE + OH = APINCO2 ;
% KDEC*0.55 : APINOOA = C107O2 + OH ;
% KDEC*0.45 : APINOOA = C109O2 + OH ;
% KDEC*0.50 : APINOOB = APINBOO ;
% KDEC*0.50 : APINOOB = C96O2 + OH + CO ;
% KRO2HO2*0.625 : BIACETO2 + HO2 = BIACETOOH ;
% KRO2NO : BIACETO2 + NO = BIACETO + NO2 ;
% KRO2NO3 : BIACETO2 + NO3 = BIACETO + NO2 ;
% 2.00D-12*0.6*RO2 : BIACETO2 = BIACETO ;
% 2.00D-12*0.2*RO2 : BIACETO2 = BIACETOH ;
% 2.00D-12*0.2*RO2 : BIACETO2 = CO23C3CHO ;
% 2.69D-12 : OH + BIACETOH = CO23C3CHO + HO2 ;
% 3.59D-12 : OH + BIACETOOH = BIACETO2 ;
% 5.99D-12 : OH + BIACETOOH = CO23C3CHO + OH ;
% 4.70D-12 : BPINANO3 + OH = NOPINONE + HCHO + NO2 ;
% KDEC : BPINAO = NOPINONE + HCHO + HO2 ;
% KRO2HO2*0.914 : BPINAO2 + HO2 = BPINAOOH ;
% KRO2NO*0.240 : BPINAO2 + NO = BPINANO3 ;
% KRO2NO*0.760 : BPINAO2 + NO = BPINAO + NO2 ;
% KRO2NO3 : BPINAO2 + NO3 = BPINAO + NO2 ;
% 9.20D-14*0.7*RO2 : BPINAO2 = BPINAO ;
% 9.20D-14*0.3*RO2 : BPINAO2 = BPINAOH ;
% 9.88D-12 : BPINAOH + OH = C918CHO + HO2 ;
% 1.33D-11 : BPINAOOH + OH = BPINAO2 ;
% 6.12D-12 : BPINBNO3 + OH = C918CHO + NO2 ;
% KDEC : BPINBO = NOPINONE + HCHO + HO2 ;
% KRO2HO2*0.914 : BPINBO2 + HO2 = BPINBOOH ;
% KRO2NO*0.240 : BPINBO2 + NO = BPINBNO3 ;
% KRO2NO*0.760 : BPINBO2 + NO = BPINBO + NO2 ;
% KRO2NO3 : BPINBO2 + NO3 = BPINBO + NO2 ;
% 2.00D-12*0.2*RO2 : BPINBO2 = BPINAOH ;
% 2.00D-12*0.6*RO2 : BPINBO2 = BPINBO ;
% 2.00D-12*0.2*RO2 : BPINBO2 = C918CHO ;
% 1.90D-11 : BPINBOOH + OH = C918CHO + OH ;

% 9.38D-11 : BPINCNO3 + OH = HCC7CO + CH3COCH3 + NO2 ;
% KDEC : BPINCO = C720O2 + CH3COCH3 ;
% KRO2HO2*0.914 : BPINCO2 + HO2 = BPINCOOH ;
% KRO2NO*0.125 : BPINCO2 + NO = BPINCNO3 ;
% KRO2NO*0.875 : BPINCO2 + NO = BPINCO + NO2 ;
% KRO2NO3 : BPINCO2 + NO3 = BPINCO + NO2 ;
% 6.70D-15*0.7*RO2 : BPINCO2 = BPINCO ;
% 6.70D-15*0.3*RO2 : BPINCO2 = BPINCOH ;
% 9.37D-11 : BPINCOH + OH = BPINCO ;
% 9.72D-11 : BPINCOOH + OH = BPINCO2 ;
% 2.51D-12*0.8 : BPINENE + NO3 = NBPINAO2 ;
% 2.51D-12*0.2 : BPINENE + NO3 = NBPINBO2 ;
% 1.50D-17*0.4 : BPINENE + O3 = NOPINONE + CH2OOF ;
% 1.50D-17*0.6 : BPINENE + O3 = NOPINOOA + HCHO ;
% 7.89D-11*0.849 : BPINENE + OH = BPINAO2 ;
% 7.89D-11*0.076 : BPINENE + OH = BPINBO2 ;
% 7.89D-11*0.075 : BPINENE + OH = BPINCO2 ;
% 7.03D-11 : C106NO3 + OH = CO235C6CHO + CH3COCH3 + NO2 ;
% KDEC : C106O = C716O2 + CH3COCH3 ;
% KRO2HO2*0.914 : C106O2 + HO2 = C106OOH ;
% KRO2NO*0.125 : C106O2 + NO = C106NO3 ;
% KRO2NO*0.875 : C106O2 + NO = C106O + NO2 ;
% KRO2NO3 : C106O2 + NO3 = C106O + NO2 ;
% 6.70D-15*0.7*RO2 : C106O2 = C106O ;
% 6.70D-15*0.3*RO2 : C106O2 = C106OH ;
% 7.66D-11 : C106OH + OH = C106O ;
% 8.01D-11 : C106OOH + OH = C106O2 ;
% KDEC : C107O = C108O2 ;
% KRO2HO2*0.914 : C107O2 + HO2 = C107OOH ;
% KRO2NO : C107O2 + NO = C107O + NO2 ;
% KRO2NO3 : C107O2 + NO3 = C107O + NO2 ;
% 9.20D-14*0.7*RO2 : C107O2 = C107O ;
% 9.20D-14*0.3*RO2 : C107O2 = C107OH ;
% 2.66D-11 : C107OH + OH = C107O ;
% 3.01D-11 : C107OOH + OH = C107O2 ;
% 2.85D-11 : C108NO3 + OH = CO235C6CHO + CH3COCH3 + NO2 ;
% KDEC : C108O = C717O2 + CH3COCH3 ;
% KRO2HO2*0.914 : C108O2 + HO2 = C108OOH ;
% KRO2NO*0.125 : C108O2 + NO = C108NO3 ;
% KRO2NO*0.875 : C108O2 + NO = C108O + NO2 ;
% KRO2NO3 : C108O2 + NO3 = C108O + NO2 ;
% 6.70D-15*0.7*RO2 : C108O2 = C108O ;
% 6.70D-15*0.3*RO2 : C108O2 = C108OH ;
% 5.93D-11 : C108OH + OH = C108O ;
% 6.28D-11 : C108OOH + OH = C108O2 ;

% 5.47D-11 : C109CO + OH = C89CO3 + CO ;
% KDEC*0.80 : C109O = C89CO3 + HCHO ;
% KDEC*0.20 : C109O = C920CO3 ;
% KRO2HO2*0.914 : C109O2 + HO2 = C109OOH ;
% KRO2NO : C109O2 + NO = C109O + NO2 ;
% KRO2NO3 : C109O2 + NO3 = C109O + NO2 ;
% 2.00D-12*0.05*RO2 : C109O2 = C109CO ;
% 2.00D-12*0.90*RO2 : C109O2 = C109O ;
% 2.00D-12*0.05*RO2 : C109O2 = C109OH ;
% 4.45D-11 : C109OH + OH = C109CO + HO2 ;
% 5.47D-11 : C109OOH + OH = C109CO + OH ;
% 3.66D-12 : C10PAN2 + OH = NORPINAL + CO + NO2 ;
% 1.9D17*EXP(-14100/TEMP) : C10PAN2 = C96CO3 + NO2 ;
% 4.75D-12 : C235C6CO3H + OH = CO235C6CO3 ;
% KAPHO2*0.56 : C312COCO3 + HO2 = C312COCO3H ;
% KAPHO2*0.44 : C312COCO3 + HO2 = CHOCOCH2O2 + OH ;
% KAPNO : C312COCO3 + NO = CHOCOCH2O2 + NO2;
% KFPAN : C312COCO3 + NO2 = C312COPAN ;
% KRO2NO3*1.74 : C312COCO3 + NO3 = CHOCOCH2O2 + NO2 ;
% 1.00D-11*RO2 : C312COCO3 = CHOCOCH2O2 ;
% 1.63D-11 : C312COCO3H + OH = C312COCO3 ;
% 1.27D-11 : C312COPAN + OH = C33CO + CO + NO2 ;
% 1.9D17*EXP(-14100/TEMP) : C312COPAN = C312COCO3 + NO2 ;
% 5.77D-11 : C33CO + OH = CO + CO + CO + HO2 ;
% 1.9D17*EXP(-14100/TEMP) : C3PAN1 = HOC2H4CO3 + NO2 ;
% 4.51D-12 : OH + C3PAN1 = HOCH2CHO + CO + NO2 ;
% 1.9D17*EXP(-14100/TEMP) : C3PAN2 = HCOCH2CO3 + NO2 ;
% 2.10D-11 : OH + C3PAN2 = GLYOX + CO + NO2 ;
% 8.33D-11 : C413COOOH + OH = CHOC3COO2 ;
% KDEC : C44O = HCOCH2CHO + HO2 ;
% KRO2HO2*0.625 : C44O2 + HO2 = C44OOH ;
% KRO2NO : C44O2 + NO = C44O + NO2 ;
% KRO2NO3 : C44O2 + NO3 = C44O + NO2 ;
% 8.80D-13*RO2 : C44O2 = C44O ;
% 7.46D-11 : C44OOH + OH = C44O2 ;
% 2*KNO3AL*4.0 : C4CODIAL + NO3 = C312COCO3 + HNO3 ;
% 3.39D-11 : C4CODIAL + OH = C312COCO3 ;
% 5.13D-11 : C511CHO + OH = C511CO3 ;
% KAPHO2*0.56 : C511CO3 + HO2 = C511CO3H ;
% KAPHO2*0.44 : C511CO3 + HO2 = C511O2 + OH ;
% KAPNO : C511CO3 + NO = C511O2 + NO2 ;
% KFPAN : C511CO3 + NO2 = C511PAN ;
% KRO2NO3*1.74 : C511CO3 + NO3 = C511O2 + NO2 ;
% 1.00D-11*RO2 : C511CO3 = C511O2 ;
% 3.14D-11 : C511CO3H + OH = C511CO3 ;

% KDEC : C511O = CH3CO3 + HCOCH2CHO + TPENE ;
% KRO2HO2*0.706 : C511O2 + HO2 = C511OOH ;
% KRO2NO :C511O2 + NO = C511O + NO2 ;
% KRO2NO3 : C511O2 + NO3 = C511O + NO2 ;
% 8.80D-13*RO2 : C511O2 = C511O ;
% 7.49D-11 : C511OOH + OH = C511O2 ;
% 2.78D-11 : C511PAN + OH = CO23C4CHO + CO + NO2 ;
% 1.9D17*EXP(-14100/TEMP) : C511PAN = C511CO3 + NO2 ;
% 7.23D-11 : C512CO2H + OH = C512O2 ;
% KAPHO2*0.15 : C512CO3 + HO2 = C512CO2H + O3 ;
% KAPHO2*0.41 : C512CO3 + HO2 = C512CO3H ;
% KAPHO2*0.44 : C512CO3 + HO2 = C512O2 + OH ;
% KAPNO : C512CO3 + NO = C512O2 + NO2 ;
% KFPAN : C512CO3 + NO2 = C512PAN ;
% KRO2NO3*1.74 : C512CO3 + NO3 = C512O2 + NO2 ;
% 1.00D-11*0.3*RO2 : C512CO3 = C512CO2H ;
% 1.00D-11*0.7*RO2 : C512CO3 = C512O2 ;
% 7.54D-11 : C512CO3H + OH = C512CO3 ;
% 1.52D+7 : C512O = C513O2 ;
% KDEC : C512O = CO13C3CO2H + HCHO + HO2 ;
% KRO2HO2*0.706 : C512O2 + HO2 = C512OOH ;
% KRO2NO*0.052 : C512O2 + NO = C512NO3 ;
% KRO2NO*0.948 : C512O2 + NO = C512O + NO2 ;
% KRO2NO3 : C512O2 + NO3 = C512O + NO2 ;
% 1.30D-12*0.6*RO2 : C512O2 = C512O ;
% 1.30D-12*0.2*RO2 : C512O2 = C512OH ;
% 1.30D-12*0.2*RO2 : C512O2 = CO13C4CHO ;
% 7.96D-11 : C512OH + OH = CO13C4CHO + HO2 ;
% 1.01D-10 : C512OOH + OH = CO13C4CHO + OH ;
% 6.76D-11 : C512PAN + OH = CO13C4CHO + CO + NO2 ;
% 1.9D17*EXP(-14100/TEMP) : C512PAN = C512CO3 + NO2 ;
% 2.64D-11 : C513CO + OH = HOC2H4CO3 + CO + CO ;
% KDEC : C513O = GLYOX + HOC2H4CO3 ;
% KRO2HO2*0.706 : C513O2 + HO2 = C513OOH ;
% KRO2NO : C513O2 + NO = C513O + NO2 ;
% KRO2NO3 : C513O2 + NO3 = C513O + NO2 ;
% 8.80D-13*0.2*RO2 : C513O2 = C513CO ;
% 8.80D-13*0.6*RO2 : C513O2 = C513O ;
% 8.80D-13*0.2*RO2 : C513O2 = C513OH ;
% 8.35D-11 : C513OH + OH = C513CO + HO2 ;
% 9.23D-11 : C513OOH + OH = C513CO + OH ;
% 4.33D-11 : C514NO3 + OH = CO13C4CHO + NO2 ;
% 7.52D-15 : C514O + O2 = CO13C4CHO + HO2 ;
% KRO2HO2*0.706 : C514O2 + HO2 = C514OOH ;
% KRO2NO*0.129 : C514O2 + NO = C514NO3 ;

% KRO2NO*0.871 : C514O2 + NO = C514O + NO2 ;
% KRO2NO3 : C514O2 + NO3 = C514O + NO2 ;
% 2.50D-13*0.6*RO2 : C514O2 = C514O ;
% 2.50D-13*0.2*RO2 : C514O2 = C514OH ;
% 2.50D-13*0.2*RO2 : C514O2 = CO13C4CHO ;
% 6.99D-11 : C514OH + OH = CO13C4CHO + HO2 ;
% 1.10D-10 : C514OOH + OH = CO13C4CHO + OH ;
% 1.33D-10 : C515CHO + OH = C515CO3 ;
% 7.90D-11 : C515CO + OH = CO + CO + HCOCH2CO3 ;
% KAPHO2*0.56 : C515CO3 + HO2 = C515CO3H ;
% KAPHO2*0.44 : C515CO3 + HO2 = C515O2 + OH ;
% KAPNO : C515CO3 + NO = C515O2 + NO2 ;
% KFPAN : C515CO3 + NO2 = C515PAN ;
% KRO2NO3*1.74 : C515CO3 + NO3 = C515O2 + NO2 ;
% 1.00D-11*RO2 : C515CO3 = C515O2 ;
% 7.05D-11 : C515CO3H + OH = C515CO3 ;
% KDEC : C515O = HCHO + CO + HCOCH2CO3 ;
% KRO2HO2*0.706 : C515O2 + HO2 = C515OOH ;
% KRO2NO : C515O2 + NO = C515O + NO2 ;
% KRO2NO3 : C515O2 + NO3 = C515O + NO2 ;
% 2.00D-12*RO2 : C515O2 = C515O ;
% 7.91D-11 : C515OOH + OH = C515CO + OH ;
% 6.69D-11 : C515PAN + OH = C515CO + CO + NO2 ;
% 1.9D17*EXP(-14100/TEMP) : C515PAN = C515CO3 + NO2 ;
% KDEC : C516O = CO13C3CO2H + HCHO + HO2 ;
% KRO2HO2*0.706 : C516O2 + HO2 = C516OOH ;
% KRO2NO : C516O2 + NO = C516O + NO2 ;
% KRO2NO3 : C516O2 + NO3 = C516O + NO2 ;
% 8.8D-13*RO2 : C516O2 = C516O ;
% 3.38D-11 : OH + C516OOH = C516O2 + OH ;
% KNO3AL*8.5 : C517CHO + NO3 = C517CO3 + HNO3 ;
% 4.35D-11 : C517CHO + OH = C517CO3 ;
% 1.84D-11 : C517CO2H + OH = C517O2 ;
% KAPHO2*0.15 : C517CO3 + HO2 = C517CO2H + O3 ;
% KAPHO2*0.41 : C517CO3 + HO2 = C517CO3H ;
% KAPHO2*0.44 : C517CO3 + HO2 = C517O2 + OH;
% KAPNO : C517CO3 + NO = C517O2 + NO2 ;
% KFPAN : C517CO3 + NO2 = C517PAN ;
% KRO2NO3*1.74 : C517CO3 + NO3 = C517O2 + NO2 ;
% 1.00D-11*0.3*RO2 : C517CO3 = C517CO2H ;
% 1.00D-11*0.7*RO2 : C517CO3 = C517O2 ;
% 2.15D-11 : C517CO3H + OH = C517CO3 ;
% 1.38D-11 : C517NO3 + OH = HMVKBCHO + NO2 ;
% KROPRIM*O2 : C517O = HMVKBCHO + HO2 ;
% KRO2HO2*0.706 : C517O2 + HO2 = C517OOH ;

% KRO2NO*0.052 : C517O2 + NO = C517NO3 ;
% KRO2NO*0.948 : C517O2 + NO = C517O + NO2 ;
% KRO2NO3 : C517O2 + NO3 = C517O + NO2 ;
% 1.30D-12*0.6*RO2 : C517O2 = C517O ;
% 1.30D-12*0.2*RO2 : C517O2 = C517OH ;
% 1.30D-12*0.2*RO2 : C517O2 = HMVKBCHO ;
% 2.81D-11 : C517OH + OH = HMVKBCHO + HO2 ;
% 4.93D-11 : C517OOH + OH = HMVKBCHO + OH ;
% 1.79D-11 : C517PAN + OH = HMVKBCHO + CO + NO2 ;
% 1.9D17*EXP(-14100/TEMP) : C517PAN = C517CO3 + NO2 ;
% KNO3AL*8.5 : C518CHO + NO3 = C518CO3 + HNO3 ;
% 3.30D-13 : C518CHO + NO3 = NC623O2 ;
% 1.30D-17*0.670 : C518CHO + O3 = C520OOA + HCHO ;
% 1.30D-17*0.330 : C518CHO + O3 = HMVKBCHO + CH2OOF ;
% 8.70D-11*0.288 : C518CHO + OH = C518CO3 ;
% 8.70D-11*0.712 : C518CHO + OH = C623O2 ;
% 5.80D-11 : C518CO2H + OH = ISOPDO2 ;
% KAPHO2*0.15 : C518CO3 + HO2 = C518CO2H + O3 ;
% KAPHO2*0.41 : C518CO3 + HO2 = C518CO3H ;
% KAPHO2*0.44 : C518CO3 + HO2 = ISOPDO2 + OH ;
% KAPNO : C518CO3 + NO = ISOPDO2 + NO2 ;
% KFPAN : C518CO3 + NO2 = C518PAN ;
% KRO2NO3*1.74 : C518CO3 + NO3 = ISOPDO2 + NO2 ;
% 1.00D-11*0.3*RO2 : C518CO3 = C518CO2H ;
% 1.00D-11*0.7*RO2 : C518CO3 = ISOPDO2 ;
% 6.11D-11 : C518CO3H + OH = C518CO3 ;
% 5.75D-11 : C518PAN + OH = HCOC5 + CO + NO2 ;
% 1.9D17*EXP(-14100/TEMP) : C518PAN = C518CO3 + NO2 ;
% KNO3AL*8.5 : C519CHO + NO3 = C519CO3 + HNO3 ;
% 3.50D-11 : C519CHO + OH = C519CO3 ;
% 1.06D-11 : C519CO2H + OH = C519O2 ;
% KAPHO2*0.15 : C519CO3 + HO2 = C519CO2H + O3 ;
% KAPHO2*0.41 : C519CO3 + HO2 = C519CO3H ;
% KAPHO2*0.44 : C519CO3 + HO2 = C519O2 + OH ;
% KAPNO : C519CO3 + NO = C519O2 + NO2 ;
% KFPAN : C519CO3 + NO2 = C519PAN ;
% KRO2NO3*1.74 : C519CO3 + NO3 = C519O2 + NO2 ;
% 1.00D-11*0.3*RO2 : C519CO3 = C519CO2H ;
% 1.00D-11*0.7*RO2 : C519CO3 = C519O2 ;
% 1.37D-11 : C519CO3H + OH = C519CO3 ;
% KDEC : C519O = CH3CO3 + HOC2H4CHO + TPENE ;
% KRO2HO2*0.706 : C519O2 + HO2 = C519OOH ;
% KRO2NO : C519O2 + NO = C519O + NO2 ;
% KRO2NO3 : C519O2 + NO3 = C519O + NO2 ;
% 8.80D-13*0.6*RO2 : C519O2 = C519O ;

% 8.80D-13*0.2*RO2 : C519O2 = HO13CO4C5 ;
% 8.80D-13*0.2*RO2 : C519O2 = HO1CO34C5 ;
% 2.74D-11 : C519OOH + OH = HO1CO34C5 + OH ;
% 1.01D-11 : C519PAN + OH = HO1CO34C5 + CO + NO2 ;
% 1.9D17*EXP(-14100/TEMP) : C519PAN = C519CO3 + NO2 ;
% KDEC*0.5 : C520O = BIACETOH + CO + HO2 ;
% KDEC*0.5 : C520O = HOCH2COCHO + CH3CO3 + TPENE ;
% KRO2HO2*0.706 : C520O2 + HO2 = C520OOH ;
% KRO2NO : C520O2 + NO = C520O + NO2 ;
% KRO2NO3 : C520O2 + NO3 = C520O + NO2 ;
% 9.20D-14*0.7*RO2 : C520O2 = C520O ;
% 9.20D-14*0.3*RO2 : C520O2 = C520OH ;
% 3.40D-11 : C520OH + OH = C520O ;
% KDEC : C520OOA = C520O2 + OH ;
% 3.74D-11 : C520OOH + OH = C520O2 ;
% KDEC : C55O = HCHO + IPRHOCO3 ;
% KRO2HO2*0.706 : C55O2 + HO2 = C55OOH ;
% KRO2NO : C55O2 + NO = C55O + NO2 ;
% KRO2NO3 : C55O2 + NO3 = C55O + NO2 ;
% 2.00D-12*RO2 : C55O2 = C55O ;
% 1.32D-11 : OH + C55OOH = C55O2 ;
% KDEC : C59O = ACETOL + HOCH2CO3 ;
% KRO2HO2*0.706 : C59O2 + HO2 = C59OOH ;
% KRO2NO : C59O2 + NO = C59O + NO2 ;
% KRO2NO3 : C59O2 + NO3 = C59O + NO2 ;
% 9.20D-14*RO2 : C59O2 = C59O ;
% 9.70D-12 : OH + C59OOH = C59O2 ;
% 1.9D17*EXP(-14100/TEMP) : C5PAN11 = H2M2C3CO3 + NO2 ;
% 1.23D-12 : OH + C5PAN11 = IBUTALOH + CO + NO2 ;
% 1.9D17*EXP(-14100/TEMP) : C5PAN2 = CO2C4CO3 + NO2 ;
% 1.90D-12 : OH + C5PAN2 = CO2C3CHO + CO + NO2 ;
% 1.9D17*EXP(-14100/TEMP) : C5PAN9 = CO23C4CO3 + NO2 ;
% 3.12D-13 : OH + C5PAN9 = CO23C3CHO + CO + NO2 ;
% 3.22D-12 : C614CO + OH = CO235C5CHO + HO2 ;
% 71.11D-12 : C614NO3 + OH = C614CO + NO2 ;
% KDEC : C614O = CO23C4CHO + HCHO + HO2 ;
% KRO2HO2*0.770 : C614O2 + HO2 = C614OOH ;
% KRO2NO*0.098 : C614O2 + NO = C614NO3 ;
% KRO2NO*0.902 : C614O2 + NO = C614O + NO2 ;
% KRO2NO3 : C614O2 + NO3 = C614O + NO2 ;
% 8.80D-13*0.2*RO2 : C614O2 = C614CO ;
% 8.80D-13*0.6*RO2 : C614O2 = C614O ;
% 8.80D-13*0.2*RO2 : C614O2 = C614OH ;
% 3.78D-11 : C614OH + OH = C614CO + HO2 ;
% 8.69D-11 : C614OOH + OH = C614CO + OH ;

% 7.88D-11 : C615CO + OH = CO1M22CO3 + CO ;
% 9.13D-11 : C615CO2H + OH = C615O2 ;
% KAPHO2*0.15 : C615CO3 + HO2 = C615CO2H + O3 ;
% KAPHO2*0.41 : C615CO3 + HO2 = C615CO3H ;
% KAPHO2*0.44 : C615CO3 + HO2 = C615O2 + OH ;
% KAPNO : C615CO3 + NO = C615O2 + NO2 ;
% KFPAN : C615CO3 + NO2 = C615PAN ;
% KRO2NO3*1.74 : C615CO3 + NO3 = C615O2 + NO2 ;
% 1.00D-11*0.3*RO2 : C615CO3 = C615CO2H ;
% 1.00D-11*0.7*RO2 : C615CO3 = C615O2 ;
% 9.44D-11 : C615CO3H + OH = C615CO3 ;
% KDEC : C615O = CO1M22CHO + HO2 + CO ;
% KRO2HO2*0.770 : C615O2 + HO2 = C615OOH ;
% KRO2NO : C615O2 + NO = C615O + NO2 ;
% KRO2NO3 : C615O2 + NO3 = C615O + NO2 ;
% 8.80D-13*0.2*RO2 : C615O2 = C615CO ;
% 8.80D-13*0.6*RO2 : C615O2 = C615O ;
% 8.80D-13*0.2*RO2 : C615O2 = C615OH ;
% 6.15D-11 : C615OH + OH = C615CO + HO2 ;
% 9.31D-11 : C615OOH + OH = C615CO + OH ;
% 8.47D-11 : C615PAN + OH = C615CO + CO + NO2 ;
% 1.9D17*EXP(-14100/TEMP) : C615PAN = C615CO3 + NO2 ;
% KDEC*0.5 : C616O = CHOC2CO3 + GLYOX ;
% KDEC*0.5 : C616O = CO12C4CHO + HO2 + CO ;
% KRO2HO2*0.770 : C616O2 + HO2 = C616OOH ;
% KRO2NO : C616O2 + NO = C616O + NO2 ;
% KRO2NO3 : C616O2 + NO3 = C616O + NO2 ;
% 8.80D-13*0.6*RO2 : C616O2 = C616O ;
% 8.80D-13*0.2*RO2 : C616O2 = C616OH ;
% 8.80D-13*0.2*RO2 : C616O2 = CO123C5CHO ;
% 9.27D-11 : C616OH + OH = CO123C5CHO + HO2 ;
% 1.02D-10 : C616OOH + OH = CO123C5CHO + OH ;
% KNO3AL*8.5 : C617CHO + NO3 = C617CO3 + HNO3 ;
% KNO3AL*8.5 : C617CHO + NO3 = C618CO3 + HNO3 ;
% 1.33D-10*0.5 : C617CHO + OH = C617CO3 ;
% 1.33D-10*0.5 : C617CHO + OH = C618CO3 ;
% 6.72D-11 : C617CO2H + OH = C617O2 ;
% KAPHO2*0.15 : C617CO3 + HO2 = C617CO2H + O3 ;
% KAPHO2*0.41 : C617CO3 + HO2 = C617CO3H ;
% KAPHO2*0.44 : C617CO3 + HO2 = C617O2 + OH ;
% KAPNO : C617CO3 + NO = C617O2 + NO2 ;
% KFPAN : C617CO3 + NO2 = C617PAN ;
% KRO2NO3*1.74 : C617CO3 + NO3 = C617O2 + NO2 ;
% 1.00D-11*0.3*RO2 : C617CO3 = C617CO2H ;
% 1.00D-11*0.7*RO2 : C617CO3 = C617O2 ;

% 7.03D-11 : C617CO3H + OH = C617CO3 ;
% KDEC : C617O = CO1M22CO3 + HCHO ;
% KRO2HO2*0.770 : C617O2 + HO2 = C617OOH ;
% KRO2NO : C617O2 + NO = C617O + NO2 ;
% KRO2NO3 : C617O2 + NO3 = C617O + NO2 ;
% 2.00D-12*0.2*RO2 : C617O2 = C615CO ;
% 2.00D-12*0.6*RO2 : C617O2 = C617O ;
% 2.00D-12*0.2*RO2 : C617O2 = C617OH ;
% 6.89D-11 : C617OH + OH = C615CO + HO2 ;
% 7.56D-11 : C617OOH + OH = C615CO + OH ;
% 6.74D-11 : C617PAN + OH = C615CO + CO + NO2 ;
% 1.9D17*EXP(-14100/TEMP) : C617PAN = C617CO3 + NO2 ;
% 6.72D-11 : C618CO2H + OH = C618O2 ;
% KAPHO2*0.15 : C618CO3 + HO2 = C618CO2H + O3 ;
% KAPHO2*0.41 : C618CO3 + HO2 = C618CO3H ;
% KAPHO2*0.44 : C618CO3 + HO2 = C618O2 + OH ;
% KAPNO : C618CO3 + NO = C618O2 + NO2 ;
% KFPAN : C618CO3 + NO2 = C618PAN ;
% KRO2NO3*1.74 : C618CO3 + NO3 = C618O2 + NO2 ;
% 1.00D-11*0.3*RO2 : C618CO3 = C618CO2H ;
% 1.00D-11*0.7*RO2 : C618CO3 = C618O2 ;
% 7.03D-11 : C618CO3H + OH = C618CO3 ;
% KDEC : C618O = HCOCH2CO3 + CH3COCH3 ;
% KRO2HO2*0.770 : C618O2 + HO2 = C618OOH ;
% KRO2NO : C618O2 + NO = C618O + NO2 ;
% KRO2NO3 : C618O2 + NO3 = C618O + NO2 ;
% 9.20D-14*0.7*RO2 : C618O2 = C618O ;
% 9.20D-14*0.3*RO2 : C618O2 = C67CHO ;
% 7.03D-11 : C618OOH + OH = C618O2 ;
% 6.67D-11 : C618PAN + OH = CH3COCH3 + HCOCH2CHO + CO + NO2 ;
% 1.9D17*EXP(-14100/TEMP) : C618PAN = C618CO3 + NO2 ;
% 5.99D-12 : C619CO + OH = C512CO3 ;
% KDEC : C619O = C512CO3 ;
% KRO2HO2*0.770 : C619O2 + HO2 = C619OOH ;
% KRO2NO : C619O2 + NO = C619O + NO2 ;
% KRO2NO3 : C619O2 + NO3 = C619O + NO2 ;
% 8.80D-13*0.2*RO2 : C619O2 = C619CO ;
% 8.80D-13*0.6*RO2 : C619O2 = C619O ;
% 8.80D-13*0.2*RO2 : C619O2 = C619OH ;
% 2.82D-11 : C619OH + OH = C619CO + HO2 ;
% 5.95D-11 : C619OOH + OH = C619CO + OH ;
% KDEC : C620O = HCOCH2CHO + HCOCH2CO3 ;
% KRO2HO2*0.770 : C620O2 + HO2 = C620OOH ;
% KRO2NO : C620O2 + NO = C620O + NO2 ;
% KRO2NO3 : C620O2 + NO3 = C620O + NO2 ;

% 8.80D-13*0.2*RO2 : C620O2 = C515CHO ;
% 8.80D-13*0.6*RO2 : C620O2 = C620O ;
% 8.80D-13*0.2*RO2 : C620O2 = C620OH ;
% 9.44D-11 : C620OH + OH = C515CHO + HO2 ;
% 1.15D-10 : C620OOH + OH = C515CHO + OH ;
% KDEC : C621O = HCHO + H1C23C4CHO + HO2 ;
% KRO2HO2*0.770 : C621O2 + HO2 = C621OOH ;
% KRO2NO : C621O2 + NO = C621O + NO2 ;
% KRO2NO3 : C621O2 + NO3 = C621O + NO2 ;
% 8.80D-13*RO2 : C621O2 = C621O ;
% 1.00D-10 : C621OOH + OH = C621O2 ;
% KNO3AL*8.5 : C622CHO + NO3 = C622CO3 + HNO3 ;
% 3.30D-13 : C622CHO + NO3 = NC728O2 ;
% 1.30D-17*0.330 : C622CHO + O3 = C517CHO + CH2OOF ;
% 1.30D-17*0.670 : C622CHO + O3 = C628OOA + HCHO ;
% 8.67D-11*0.288 : C622CHO + OH = C622CO3 ;
% 8.67D-11*0.712 : C622CHO + OH = C728O2 ;
% 6.00D-11 : C622CO2H + OH = C622O2 ;
% KAPHO2*0.15 : C622CO3 + HO2 = C622CO2H + O3 ;
% KAPHO2*0.41 : C622CO3 + HO2 = C622CO3H ;
% KAPHO2*0.44 : C622CO3 + HO2 = C622O2 + OH ;
% KAPNO : C622CO3 + NO = C622O2 + NO2 ;
% KFPAN : C622CO3 + NO2 = C622PAN ;
% KRO2NO3*1.74 : C622CO3 + NO3 = C622O2 + NO2 ;
% 1.00D-11*0.3*RO2 : C622CO3 = C622CO2H ;
% 1.00D-11*0.7*RO2 : C622CO3 = C622O2 ;
% 6.31D-11 : C622CO3H + OH = C622CO3 ;
% 5.64D-11 : C622NO3 + OH = C518CHO + NO2 ;
% KROPRIM*O2 : C622O = C518CHO + HO2 ;
% KRO2HO2*0.770 : C622O2 + HO2 = C622OOH ;
% KRO2NO*0.078 : C622O2 + NO = C622NO3 ;
% KRO2NO*0.922 : C622O2 + NO = C622O + NO2 ;
% KRO2NO3 : C622O2 + NO3 = C622O + NO2 ;
% 1.30D-12*0.2*RO2 : C622O2 = C518CHO ;
% 1.30D-12*0.6*RO2 : C622O2 = C622O ;
% 1.30D-12*0.2*RO2 : C622O2 = C622OH ;
% 6.29D-11 : C622OH + OH = C518CHO + HO2 ;
% 7.17D-11 : C622OOH + OH = C518CHO + OH ;
% 5.95D-11 : C622PAN + OH = C518CHO + CO + NO2 ;
% 1.9D17*EXP(-14100/TEMP) : C622PAN = C622CO3 + NO2 ;
% 3.51D-11 : C623NO3 + OH = HMVKBCHO + HCHO + NO2 ;
% KDEC : C623O = HMVKBCHO + HCHO + HO2 ;
% KRO2HO2*0.770 : C623O2 + HO2 = C623OOH ;
% KRO2NO*0.030 : C623O2 + NO = C623NO3 ;
% KRO2NO*0.970 : C623O2 + NO = C623O + NO2 ;

% KRO2NO3 : C623O2 + NO3 = C623O + NO2 ;
% 8.00D-13*0.7*RO2 : C623O2 = C623O ;
% 8.00D-13*0.3*RO2 : C623O2 = C623OH ;
% 4.91D-11 : C623OH + OH = HMVKBCHO + HCHO + HO2 ;
% 5.26D-11 : C623OOH + OH = C623O2 ;
% KNO3AL*8.5 : C624CHO + NO3 = C624CO3 + HNO3 ;
% 3.30D-13 : C624CHO + NO3 = NC730O2 ;
% 1.30D-17*0.330 : C624CHO + O3 = C519CHO + CH2OOF ;
% 1.30D-17*0.670 : C624CHO + O3 = C629OOA + HCHO ;
% 8.26D-11*0.288 : C624CHO + OH = C624CO3 ;
% 8.26D-11*0.712 : C624CHO + OH = C730O2 ;
% 6.04D-11 : C624CO + OH = C625O2 ;
% 5.94D-11 : C624CO2H + OH = C624O2 ;
% KAPHO2*0.15 : C624CO3 + HO2 = C624CO2H + O3 ;
% KAPHO2*0.41 : C624CO3 + HO2 = C624CO3H ;
% KAPHO2*0.44 : C624CO3 + HO2 = C624O2 + OH ;
% KAPNO : C624CO3 + NO = C624O2 + NO2 ;
% KFPAN : C624CO3 + NO2 = C624PAN ;
% KRO2NO3*1.74 : C624CO3 + NO3 = C624O2 + NO2 ;
% 1.00D-11*0.3*RO2 : C624CO3 = C624CO2H ;
% 1.00D-11*0.7*RO2 : C624CO3 = C624O2 ;
% 6.25D-11 : C624CO3H + OH = C624CO3 ;
% 2.92D-11 : C624NO3 + OH = C624CO + NO2 ;
% KROSEC*O2 : C624O = C624CO + HO2 ;
% 2.60D+4 : C624O = MACR + HOCH2CH2O2 ;
% KRO2HO2*0.770 : C624O2 + HO2 = C624OOH ;
% KRO2NO*0.209 : C624O2 + NO = C624NO3 ;
% KRO2NO*0.791 : C624O2 + NO = C624O + NO2 ;
% KRO2NO3 : C624O2 + NO3 = C624O + NO2 ;
% 2.50D-13*0.2*RO2 : C624O2 = C624CO ;
% 2.50D-13*0.6*RO2 : C624O2 = C624O ;
% 2.50D-13*0.2*RO2 : C624O2 = C624OH ;
% 9.53D-11 : C624OH + OH = C624CO + HO2 ;
% 1.10D-10 : C624OOH + OH = C624CO + OH ;
% 5.89D-11 : C624PAN + OH = C624CO + CO + NO2 ;
% 1.9D17*EXP(-14100/TEMP) : C624PAN = C624CO3 + NO2 ;
% KDEC : C625O = ACETOL + HOC2H4CO3 ;
% KRO2HO2*0.770 : C625O2 + HO2 = C625OOH ;
% KRO2NO : C625O2 + NO = C625O + NO2 ;
% KRO2NO3 : C625O2 + NO3 = C625O + NO2 ;
% 9.20D-14*0.7*RO2 : C625O2 = C625O ;
% 9.20D-14*0.3*RO2 : C625O2 = C625OH ;
% 2.70D-11 : C625OH + OH = HOC2H4CO3 + ACETOL ;
% 3.04D-11 : C625OOH + OH = C625O2 ;
% KNO3AL*8.5 : C626CHO + NO3 = C626CO3 + HNO3 ;

% 5.41D-11 : C626CHO + OH = C626CO3 ;
% 3.19D-11 : C626CO2H + OH = C626O2 ;
% KAPHO2*0.15 : C626CO3 + HO2 = C626CO2H + O3 ;
% KAPHO2*0.41 : C626CO3 + HO2 = C626CO3H ;
% KAPHO2*0.44 : C626CO3 + HO2 = C626O2 + OH ;
% KAPNO : C626CO3 + NO = C626O2 + NO2 ;
% KFPAN : C626CO3 + NO2 = C626PAN ;
% KRO2NO3*1.74 : C626CO3 + NO3 = C626O2 + NO2 ;
% 1.00D-11*0.3*RO2 : C626CO3 = C626CO2H ;
% 1.00D-11*0.7*RO2 : C626CO3 = C626O2 ;
% 3.50D-11 : C626CO3H + OH = C626CO3 ;
% 2.84D-11 : C626NO3 + OH = C517CHO + NO2 ;
% KDEC : C626O = C622CO3 ;
% KRO2HO2*0.770 : C626O2 + HO2 = C626OOH ;
% KRO2NO*0.078 : C626O2 + NO = C626NO3 ;
% KRO2NO*0.922 : C626O2 + NO = C626O + NO2 ;
% KRO2NO3 : C626O2 + NO3 = C626O + NO2 ;
% 1.30D-12*0.2*RO2 : C626O2 = C511CHO ;
% 1.30D-12*0.2*RO2 : C626O2 = C517CHO ;
% 1.30D-12*0.6*RO2 : C626O2 = C626O ;
% 4.38D-11 : C626OOH + OH = C517CHO + OH ;
% 3.14D-11 : C626PAN + OH = C517CHO + CO + NO2 ;
% 1.9D17*EXP(-14100/TEMP) : C626PAN = C626CO3 + NO2 ;
% KDEC : C627O = CO2C4CO3 + HCHO ;
% KRO2HO2*0.770 : C627O2 + HO2 = C627OOH ;
% KRO2NO : C627O2 + NO = C627O + NO2 ;
% KRO2NO3 : C627O2 + NO3 = C627O + NO2 ;
% 2.50D-12*0.6*RO2 : C627O2 = C627O ;
% 2.50D-12*0.2*RO2 : C627O2 = C627OH ;
% 2.50D-12*0.2*RO2 : C627O2 = CO2C4GLYOX ;
% 8.25D-12 : C627OH + OH = CO2C4GLYOX + HO2 ;
% 1.51D-11 : C627OOH + OH = CO2C4GLYOX + OH ;
% 6.15D-12 : C627PAN + OH = CO2C4GLYOX + CO + NO2 ;
% 1.9D17*EXP(-14100/TEMP) : C627PAN = CO25C6CO3 + NO2 ;
% KDEC : C628O = CO13C4OH + CH3CO3 + TPENE ;
% KRO2HO2*0.770 : C628O2 + HO2 = C628OOH ;
% KRO2NO : C628O2 + NO = C628O + NO2 ;
% KRO2NO3 : C628O2 + NO3 = C628O + NO2 ;
% 9.20D-14*0.7*RO2 : C628O2 = C628O ;
% 9.20D-14*0.3*RO2 : C628O2 = C628OH ;
% 2.80D-11 : C628OH + OH = C628O ;
% KDEC : C628OOA = C628O2 + OH ;
% 3.14D-11 : C628OOH + OH = C628O2;
% KDEC*0.5 : C629O = HO1CO34C5 + CO + HO2 ;
% KDEC*0.5 : C629O = HO1CO3CHO + CH3CO3 + TPENE ;

% KRO2HO2*0.770 : C629O2 + HO2 = C629OOH ;
% KRO2NO : C629O2 + NO = C629O + NO2 ;
% KRO2NO3 : C629O2 + NO3 = C629O + NO2 ;
% 9.20D-14*0.7*RO2 : C629O2 = C629O ;
% 9.20D-14*0.3*RO2 : C629O2 = C629OH ;
% 2.97D-11 : C629OH + OH = C629O ;
% KDEC : C629OOA = C629O2 + OH ;
% 3.31D-11 : C629OOH + OH = C629O2 ;
% KNO3AL*8.5 : NO3 + C67CHO = C67CO3 + HNO3 ;
% 6.76D-11 : OH + C67CHO = C67CO3 ;
% KAPHO2*0.44 : C67CO3 + HO2 = C55O2 + OH ;
% KAPHO2*0.56 : C67CO3 + HO2 = C67CO3H ;
% KAPNO : C67CO3 + NO = C55O2 + NO2 ;
% KFPAN : C67CO3 + NO2 = C6PAN9 ;
% KRO2NO3*1.74 : C67CO3 + NO3 = C55O2 + NO2 ;
% 1.00D-11*RO2 : C67CO3 = C55O2 ;
% 5.33D-12 : OH + C67CO3H = C67CO3 ;
% 1.9D17*EXP(-14100/TEMP) : C6PAN9 = C67CO3 + NO2 ;
% 1.41D-12 : OH + C6PAN9 = MIBKHO4CHO + CO + NO2 ;
% KDEC : C716O = CO13C4CHO + CH3CO3 + TPENE ;
% KRO2HO2*0.820 : C716O2 + HO2 = C716OOH ;
% KRO2NO : C716O2 + NO = C716O + NO2 ;
% KRO2NO3 : C716O2 + NO3 = C716O + NO2 ;
% 8.80D-13*0.6*RO2 : C716O2 = C716O ;
% 8.80D-13*0.2*RO2 : C716O2 = C716OH ;
% 8.80D-13*0.2*RO2 : C716O2 = CO235C6CHO ;
% KNO3AL*5.5 : C716OH + NO3 = H3C25C6CO3 + HNO3 ;
% 8.92D-11*0.232 : C716OH + OH = CO235C6CHO + HO2 ;
% 8.92D-11*0.768 : C716OH + OH = H3C25C6CO3 ;
% 1.20D-10 : C716OOH + OH = CO235C6CHO + OH ;
% 2.23D-11 : C717NO3 + OH = CO235C6CHO + NO2 ;
% KROSEC : C717O + O2 = CO235C6CHO + HO2 ;
% KRO2HO2*0.820 : C717O2 + HO2 = C717OOH ;
% KRO2NO*0.278 : C717O2 + NO = C717NO3 ;
% KRO2NO*0.722 : C717O2 + NO = C717O + NO2 ;
% KRO2NO3 : C717O2 + NO3 = C717O + NO2 ;
% 2.50D-13*0.6*RO2 : C717O2 = C717O ;
% 2.50D-13*0.2*RO2 : C717O2 = C717OH ;
% 2.50D-13*0.2*RO2 : C717O2 = CO235C6CHO ;
% 1.26D-10 : C717OH + OH = CO235C6CHO + HO2 ;
% 2.00D-10 : C717OOH + OH = CO235C6CHO + OH ;
% 7.21D-11 : C718CO2H + OH = C718O2 ;
% KAPHO2*0.15 : C718CO3 + HO2 = C718CO2H + O3 ;
% KAPHO2*0.41 : C718CO3 + HO2 = C718CO3H ;
% KAPHO2*0.44 : C718CO3 + HO2 = C718O2 + OH ;

% KAPNO : C718CO3 + NO = C718O2 + NO2 ;
% KFPAN : C718CO3 + NO2 = C718PAN ;
% KRO2NO3*1.74 : C718CO3 + NO3 = C718O2 + NO2 ;
% 1.00D-11*0.3*RO2 : C718CO3 = C718CO2H ;
% 1.00D-11*0.7*RO2 : C718CO3 = C718O2 ;
% 7.52D-11 : C718CO3H + OH = C718CO3 ;
% 6.65D-11 : C718NO3 + OH = C617CHO + NO2 ;
% KDEC : C718O = C617CHO + HO2 ;
% KRO2HO2*0.820 : C718O2 + HO2 = C718OOH ;
% KRO2NO*0.138 : C718O2 + NO = C718NO3 ;
% KRO2NO*0.862 : C718O2 + NO = C718O + NO2 ;
% KRO2NO3 : C718O2 + NO3 = C718O + NO2 ;
% 1.30D-12*0.2*RO2 : C718O2 = C617CHO ;
% 1.30D-12*0.6*RO2 : C718O2 = C718O ;
% 1.30D-12*0.2*RO2 : C718O2 = C718OH ;
% 7.96D-11 : C718OH + OH = C617CHO + HO2 ;
% 1.01D-10 : C718OOH + OH = C617CHO + OH ;
% 6.81D-11 : C718PAN + OH = C617CHO + CO + NO2 ;
% 1.9D17*EXP(-14100/TEMP) : C718PAN = C718CO3 + NO2 ;
% 1.26D-11 : C719NO3 + OH = C716OH + NO2 ;
% KDEC : C719O = C716OH + HO2 ;
% KRO2HO2*0.820 : C719O2 + HO2 = C719OOH ;
% KRO2NO*0.042 : C719O2 + NO = C719NO3 ;
% KRO2NO*0.958 : C719O2 + NO = C719O + NO2 ;
% KRO2NO3 : C719O2 + NO3 = C719O + NO2 ;
% 9.20D-14*0.7*RO2 : C719O2 = C719O ;
% 9.20D-14*0.3*RO2 : C719O2 = C719OH ;
% 6.72D-11 : C719OH + OH = C719O ;
% 7.06D-11 : C719OOH + OH = C719O2 ;
% 9.60D-11 : C720NO3 + OH = HCC7CO + NO2 ;
% KROSEC*O2 : C720O = HCC7CO + HO2 ;
% KRO2HO2*0.820 : C720O2 + HO2 = C720OOH ;
% KRO2NO*0.278 : C720O2 + NO = C720NO3 ;
% KRO2NO*0.722 : C720O2 + NO = C720O + NO2 ;
% KRO2NO3 : C720O2 + NO3 = C720O + NO2 ;
% 2.50D-13*0.6*RO2 : C720O2 = C720O ;
% 2.50D-13*0.2*RO2 : C720O2 = C720OH ;
% 2.50D-13*0.2*RO2 : C720O2 = HCC7CO ;
% 1.09D-10 : C720OH + OH = HCC7CO + HO2 ;
% 1.27D-10 : C720OOH + OH = HCC7CO + OH ;
% KNO3AL*8.5 : C721CHO + NO3 = C721CO3 + HNO3 ;
% 2.63D-11 : C721CHO + OH = C721CO3 ;
% KAPHO2*0.41 : C721CO3 + HO2 = C721CO3H ;
% KAPHO2*0.44 : C721CO3 + HO2 = C721O2 + OH ;
% KAPHO2*0.15 : C721CO3 + HO2 = NORPINIC + O3 ;

```
% KAPNO : C721CO3 + NO = C721O2 + NO2 ;
% KFPAN : C721CO3 + NO2 = C721PAN ;
% KRO2NO3*1.74 : C721CO3 + NO3 = C721O2 + NO2 ;
% 1.00D-11*0.7*RO2 : C721CO3 = C721O2 ;
% 1.00D-11*0.3*RO2 : C721CO3 = NORPINIC ;
% 9.65D-12 : C721CO3H + OH = C721CO3 ;
% KDEC : C721O = C722O2 ;
% KRO2HO2*0.820 : C721O2 + HO2 = C721OOH ;
% KRO2NO : C721O2 + NO = C721O + NO2 ;
% KRO2NO3 : C721O2 + NO3 = C721O + NO2 ;
% 1.30D-12*RO2 : C721O2 = C721O ;
% 1.27D-11 : C721OOH + OH = C721O2 ;
% 2.96D-12 : C721PAN + OH = C721OOH + CO + NO2 ;
% 1.9D17*EXP(-14100/TEMP) : C721PAN = C721CO3 + NO2 ;
% KDEC : C722O = CH3COCH3 + C44O2 ;
% KRO2HO2*0.820 : C722O2 + HO2 = C722OOH ;
% KRO2NO : C722O2 + NO = C722O + NO2 ;
% KRO2NO3 : C722O2 + NO3 = C722O + NO2 ;
% 6.70D-15*RO2 : C722O2 = C722O ;
% 3.31D-11 : C722OOH + OH = C722O2 ;
% 5.67D-12 : C727CO + OH = C821O2 ;
% KAPHO2*0.56 : C727CO3 + HO2 = C727CO3H ;
% KAPHO2*0.44 : C727CO3 + HO2 = C727O2 + OH ;
% KAPNO : C727CO3 + NO = C727O2 + NO2 ;
% KFPAN : C727CO3 + NO2 = C727PAN ;
% KRO2NO3*1.74 : C727CO3 + NO3 = C727O2 + NO2;
% 1.00D-11*RO2 : C727CO3 = C727O2;
% 1.05D-11 : C727CO3H + OH = C727CO3 ;
% KDEC : C727O = CH3CO3 + CO2C4CHO + TPENE ;
% KRO2HO2*0.820 : C727O2 + HO2 = C727OOH ;
% KRO2NO : C727O2 + NO = C727O + NO2 ;
% KRO2NO3 : C727O2 + NO3 = C727O + NO2 ;
% 8.80D-13*RO2 : C727O2 = C727O ;
% 2.42D-11 : C727OOH + OH = C727CO + OH ;
% 6.89D-12 : C727PAN + OH = C727CO + CO + NO2 ;
% 1.9D17*EXP(-14100/TEMP) : C727PAN = C727CO3 + NO2 ;
% 3.28D-11 : C728NO3 + OH = C517CHO + HCHO + NO2 ;
% KDEC : C728O = C517CHO + HCHO + HO2 ;
% KRO2HO2*0.770 : C728O2 + HO2 = C728OOH ;
% KRO2NO*0.031 : C728O2 + NO = C728NO3 ;
% KRO2NO*0.969 : C728O2 + NO = C728O + NO2 ;
% KRO2NO3 : C728O2 + NO3 = C728O + NO2 ;
% 9.20D-14*RO2*0.7 : C728O2 = C728O ;
% 9.20D-14*RO2*0.3 : C728O2 = C728OH ;
% 4.18D-11 : C728OH + OH = C517CHO + HCHO + HO2 ;
```

% 4.52D-11 : C728OOH + OH = C728O2 ;
% KNO3AL*17.0 : C729CHO + NO3 = C729CO3 + HNO3 ;
% 3.30D-13 : C729CHO + NO3 = NC826O2 ;
% 1.30D-17*0.330 : C729CHO + O3 = C626CHO + CH2OOF ;
% 1.30D-17*0.670 : C729CHO + O3 = C735OOA + HCHO ;
% 1.06D-10*0.447 : C729CHO + OH = C729CO3 ;
% 1.06D-10*0.553 : C729CHO + OH = C826O2 ;
% 8.38D-11 : C729CO2H + OH = C729O2 ;
% KAPHO2*0.15 : C729CO3 + HO2 = C729CO2H + O3 ;
% KAPHO2*0.41 : C729CO3 + HO2 = C729CO3H ;
% KAPHO2*0.44 : C729CO3 + HO2 = C729O2 + OH ;
% KAPNO : C729CO3 + NO = C729O2 + NO2 ;
% KFPAN : C729CO3 + NO2 = C729PAN ;
% KRO2NO3*1.74 : C729CO3 + NO3 = C729O2 + NO2 ;
% 1.00D-11*0.3*RO2 : C729CO3 = C729CO2H ;
% 1.00D-11*0.7*RO2 : C729CO3 = C729O2 ;
% 8.69D-11 : C729CO3H + OH = C729CO3 ;
% 7.51D-11 : C729NO3 + OH = C622CHO + NO2 ;
% KDEC : C729O = C622CO3 ;
% KRO2HO2*0.820 : C729O2 + HO2 = C729OOH ;
% KRO2NO*0.111 : C729O2 + NO = C729NO3 ;
% KRO2NO*0.889 : C729O2 + NO = C729O + NO2 ;
% KRO2NO3 : C729O2 + NO3 = C729O + NO2 ;
% 1.30D-12*0.4*RO2 : C729O2 = C622CHO ;
% 1.30D-12*0.6*RO2 : C729O2 = C729O ;
% 9.57D-11 : C729OOH + OH = C622CHO + OH ;
% 8.33D-11 : C729PAN + OH = C622CHO + CO + NO2 ;
% 1.9D17*EXP(-14100/TEMP) : C729PAN = C729CO3 + NO2 ;
% 3.09D-11 : C730NO3 + OH = C519CHO + HCHO + NO2 ;
% KDEC : C730O = C519CHO + HCHO + HO2 ;
% KRO2HO2*0.820 : C730O2 + HO2 = C730OOH ;
% KRO2NO*0.056 : C730O2 + NO = C730NO3 ;
% KRO2NO*0.944 : C730O2 + NO = C730O + NO2 ;
% KRO2NO3 : C730O2 + NO3 = C730O + NO2 ;
% 9.20D-14*0.7*RO2 : C730O2 = C730O ;
% 9.20D-14*0.3*RO2 : C730O2 = C730OH ;
% 3.66D-11 : C730OH + OH = C519CHO + HCHO + HO2 ;
% 4.00D-11 : C730OOH + OH = C730O2 ;
% KDEC*0.2 : C731CO2 = C731O2 ;
% KDEC*0.8 : C731CO2 = C732CO3 ;
% 3.88D-11 : C731CO2H + OH = C731CO2 ;
% KAPHO2*0.44 : C731CO3 + HO2 = C731CO2 + OH ;
% KAPHO2*0.15 : C731CO3 + HO2 = C731CO2H + O3 ;
% KAPHO2*0.41 : C731CO3 + HO2 = C731CO3H ;
% KAPNO : C731CO3 + NO = C731CO2 + NO2 ;

% KFPAN : C731CO3 + NO2 = C731PAN ;
% KRO2NO3*1.74 : C731CO3 + NO3 = C731CO2 + NO2 ;
% 1.00D-11*0.7*RO2 : C731CO3 = C731CO2 ;
% 1.00D-11*0.3*RO2 : C731CO3 = C731CO2H ;
% 4.18D-11 : C731CO3H + OH = C731CO3 ;
% 3.17D-11 : C731NO3 + OH = C626CHO + NO2 ;
% KDEC : C731O = C733O2 ;
% KRO2HO2*0.859 : C731O2 + HO2 = C731OOH ;
% KRO2NO*0.138 : C731O2 + NO = C731NO3 ;
% KRO2NO*0.862 : C731O2 + NO = C731O + NO2 ;
% KRO2NO3 : C731O2 + NO3 = C731O + NO2 ;
% 1.30D-12*0.2*RO2 : C731O2 = C626CHO ;
% 1.30D-12*0.6*RO2 : C731O2 = C731O ;
% 1.30D-12*0.2*RO2 : C731O2 = C731OH ;
% 3.92D-11 : C731OH + OH = C626CHO + HO2 ;
% 4.83D-11 : C731OOH + OH = C626CHO + OH ;
% 3.82D-11 : C731PAN + OH = C626CHO + CO + NO2 ;
% 1.9D17*EXP(-14100/TEMP) : C731PAN = C731CO3 + NO2 ;
% 2.81D-11 : C732CO + OH = C734O2 ;
% KAPHO2*0.41 : C732CO3 + HO2 = C732CO3H ;
% KAPHO2*0.44 : C732CO3 + HO2 = C732O2 + OH ;
% KAPHO2*0.15 : C732CO3 + HO2 = KLIMONIC + O3 ;
% KAPNO : C732CO3 + NO = C732O2 + NO2 ;
% KFPAN : C732CO3 + NO2 = C732PAN ;
% KRO2NO3*1.74 : C732CO3 + NO3 = C732O2 + NO2 ;
% 1.00D-11*0.7*RO2 : C732CO3 = C732O2 ;
% 1.00D-11*0.3*RO2 : C732CO3 = KLIMONIC ;
% 2.16D-11 : C732CO3H + OH = C732CO3 ;
% 7.97D-12 : C732NO3 + OH = C732CO + NO2 ;
% KDEC : C732O = C734O2 ;
% KRO2HO2*0.859 : C732O2 + HO2 = C732OOH ;
% KRO2NO*0.138 : C732O2 + NO = C732NO3 ;
% KRO2NO*0.862 : C732O2 + NO = C732O + NO2 ;
% KRO2NO3 : C732O2 + NO3 = C732O + NO2 ;
% 1.30D-12*0.2*RO2 : C732O2 = C732CO ;
% 1.30D-12*0.6*RO2 : C732O2 = C732O ;
% 1.30D-12*0.2*RO2 : C732O2 = C732OH ;
% 2.82D-11 : C732OH + OH = C732CO + HO2 ;
% 4.95D-11 : C732OOH + OH = C732CO + OH ;
% 1.80D-11 : C732PAN + OH = C732CO + CO + NO2 ;
% 1.9D17*EXP(-14100/TEMP) : C732PAN = C732CO3 + NO2 ;
% 2.28D-11 : C733CO + OH = C519CO3 + CO ;
% KDEC : C733O = C519CHO + CO + HO2 ;
% KRO2HO2*0.859 : C733O2 + HO2 = C733OOH ;
% KRO2NO : C733O2 + NO = C733O + NO2 ;

% KRO2NO3 : C733O2 + NO3 = C733O + NO2 ;
% 8.80D-12*0.2*RO2 : C733O2 = C733CO ;
% 8.80D-12*0.6*RO2 : C733O2 = C733O ;
% 8.80D-12*0.2*RO2 : C733O2 = C733OH ;
% 4.30D-11 : C733OH + OH = C733CO + HO2 ;
% 5.51D-11 : C733OOH + OH = C733CO + OH ;
% 2.43D-11 : C734CO + OH = C517CO3 ;
% KDEC : C734O = C517CHO + HO2 ;
% KRO2HO2*0.859 : C734O2 + HO2 = C734OOH ;
% KRO2NO : C734O2 + NO = C734O + NO2 ;
% KRO2NO3 : C734O2 + NO3 = C734O + NO2 ;
% 8.80D-12*0.2*RO2 : C734O2 = C734CO ;
% 8.80D-12*0.6*RO2 : C734O2 = C734O ;
% 8.80D-12*0.2*RO2 : C734O2 = C734OH ;
% 2.95D-11 : C734OH + OH = C734CO + HO2 ;
% 4.16D-11 : C734OOH + OH = C734CO + OH ;
% KDEC : C735O = CO13C4CHO + CH3CO3 + TPENE ;
% KRO2HO2*0.820 : C735O2 + HO2 = C735OOH ;
% KRO2NO : C735O2 + NO = C735O + NO2 ;
% KRO2NO3 : C735O2 + NO3 = C735O + NO2 ;
% 9.20D-14*0.7*RO2 : C735O2 = C735O ;
% 9.20D-14*0.3*RO2 : C735O2 = C735OH ;
% 4.73D-11 : C735OH + OH = C735O ;
% KDEC : C735OOA = C735O2 + OH ;
% 5.07D-11 : C735OOH + OH = C735O2 ;
% 8.83D-13 : C7PAN3 + OH = CO235C5CHO + CO + NO2 ;
% 1.9D17*EXP(-14100/TEMP) : C7PAN3 = CO235C6CO3 + NO2 ;
% 4.96D-11 : C810NO3 + OH = CH3COCH3 + CO13C4CHO + NO2 ;
% 5.62D+4 : C810O = CH3COCH3 + C514O2 ;
% KRO2HO2*0.914 : C810O2 + HO2 = C810OOH ;
% KRO2NO*0.104 : C810O2 + NO = C810NO3 ;
% KRO2NO*0.896 : C810O2 + NO = C810O + NO2 ;
% KRO2NO3 : C810O2 + NO3 = C810O + NO2 ;
% 6.70D-15*0.7*RO2 : C810O2 = C810O ;
% 6.70D-15*0.3*RO2 : C810O2 = C810OH ;
% 8.00D-11 : C810OH + OH = C810O ;
% 8.35D-11 : C810OOH + OH = C810O2 ;
% KAPHO2*0.41 : C811CO3 + HO2 = C811CO3H ;
% KAPHO2*0.44 : C811CO3 + HO2 = C811O2 + OH ;
% KAPHO2*0.15 : C811CO3 + HO2 = PINIC + O3 ;
% KAPNO : C811CO3 + NO = C811O2 + NO2 ;
% KFPAN : C811CO3 + NO2 = C811PAN ;
% KRO2NO3*1.74 : C811CO3 + NO3 = C811O2 + NO2 ;
% 1.00D-11*0.7*RO2 : C811CO3 = C811O2 ;
% 1.00D-11*0.3*RO2 : C811CO3 = PINIC ;

```
% 1.04D-11 : C811CO3H + OH = C811CO3 ;
% 3.29D-12 : C811NO3 + OH = C721CHO + NO2 ;
% KDEC : C811O = C812O2 ;
% KRO2HO2*0.859 : C811O2 + HO2 = C811OOH ;
% KRO2NO*0.138 : C811O2 + NO = C811NO3 ;
% KRO2NO*0.862 : C811O2 + NO = C811O + NO2 ;
% KRO2NO3 : C811O2 + NO3 = C811O + NO2 ;
% 1.30D-12*0.2*RO2 : C811O2 = C721CHO ;
% 1.30D-12*0.6*RO2 : C811O2 = C811O ;
% 1.30D-12*0.2*RO2 : C811O2 = C811OH ;
% 7.89D-12 : C811OH + OH = C721CHO + HO2 ;
% 1.70D-11 : C811OOH + OH = C721CHO + OH ;
% 6.77D-12 : C811PAN + OH = C721CHO + CO + NO2 ;
% 1.9D17*EXP(-14100/TEMP) : C811PAN = C811CO3 + NO2 ;
% KDEC : C812O = C813O2 ;
% KRO2HO2*0.859 : C812O2 + HO2 = C812OOH ;
% KRO2NO : C812O2 + NO = C812O + NO2 ;
% KRO2NO3 : C812O2 + NO3 = C812O + NO2 ;
% 9.20D-14*0.7*RO2 : C812O2 = C812O ;
% 9.20D-14*0.3*RO2 : C812O2 = C812OH ;
% 7.42D-12 : C812OH + OH = C812O ;
% 1.09D-11 : C812OOH + OH = C812O2 ;
% 7.82D-12 : C813NO3 + OH = CH3COCH3 + CO13C3CO2H + HCHO + NO2 ;
% KDEC : C813O = CH3COCH3 + C516O2 ;
% KRO2HO2*0.859 : C813O2 + HO2 = C813OOH ;
% KRO2NO*0.104 : C813O2 + NO = C813NO3 ;
% KRO2NO*0.896 : C813O2 + NO = C813O + NO2 ;
% KRO2NO3 : C813O2 + NO3 = C813O + NO2 ;
% 6.70D-15*0.7*RO2 : C813O2 = C813O ;
% 6.70D-15*0.3*RO2 : C813O2 = C813OH ;
% 1.75D-11 : C813OH + OH = C813O ;
% 1.86D-11 : C813OOH + OH = C813O2;
% 5.20D-11 : C816CO + OH = C819O2;
% KAPHO2*0.56 : C816CO3 + HO2 = C816CO3H ;
% KAPHO2*0.44 : C816CO3 + HO2 = C816O2 + OH ;
% KAPNO : C816CO3 + NO = C816O2 + NO2 ;
% KFPAN : C816CO3 + NO2 = C816PAN ;
% KRO2NO3*1.74 : C816CO3 + NO3 = C816O2 + NO2 ;
% 1.00D-11*RO2 : C816CO3 = C816O2 ;
% 6.28D-11 : C816CO3H + OH = C816CO3 ;
% KROSEC : C816O + O2 =  C816CO + HO2 ;
% 2.27D+4 : C816O = MACR + MEKAO2 ;
% KRO2HO2*0.859 : C816O2 + HO2 = C816OOH ;
% KRO2NO : C816O2 + NO = C816O + NO2 ;
% KRO2NO3 : C816O2 + NO3 = C816O + NO2 ;
```

% 2.50D-13*RO2 : C816O2 = C816O ;
% 8.06D-11 : C816OOH + OH = C816CO + OH ;
% 5.92D-11 : C816PAN + OH = C816CO + CO + NO2 ;
% 1.9D17*EXP(-14100/TEMP) : C816PAN = C816CO3 + NO2 ;
% 2.72D-11 : C817CO + OH = C727CO3 ;
% KAPHO2*0.41 : C817CO3 + HO2 = C817CO3H ;
% KAPHO2*0.44 : C817CO3 + HO2 = C817O2 + OH ;
% KAPHO2*0.15 : C817CO3 + HO2 = KLIMONONIC + O3 ;
% KAPNO : C817CO3 + NO = C817O2 + NO2 ;
% KFPAN : C817CO3 + NO2 = C817PAN ;
% KRO2NO3*1.74 : C817CO3 + NO3 = C817O2 + NO2 ;
% 1.00D-11*0.7*RO2 : C817CO3 = C817O2 ;
% 1.00D-11*0.3*RO2 : C817CO3 = KLIMONONIC ;
% 2.28D-11 : C817CO3H + OH = C817CO3 ;
% 1.62D-11 : C817NO3 + OH = C817CO + NO2 ;
% KDEC : C817O = C818O2 ;
% KRO2HO2*0.859 : C817O2 + HO2 = C817OOH ;
% KRO2NO*0.138 : C817O2 + NO = C817NO3 ;
% KRO2NO*0.862 : C817O2 + NO = C817O + NO2 ;
% KRO2NO3 : C817O2 + NO3 = C817O + NO2 ;
% 1.30D-12*0.2*RO2 : C817O2 = C817CO ;
% 1.30D-12*0.6*RO2 : C817O2 = C817O ;
% 1.30D-12*0.2*RO2 : C817O2 = C817OH ;
% 2.31D-11 : C817OH + OH = C817CO + HO2 ;
% 3.21D-11 : C817OOH + OH = C817CO + OH ;
% 1.92D-11 : C817PAN + OH = C817CO + CO + NO2 ;
% 1.9D17*EXP(-14100/TEMP) : C817PAN = C817CO3 + NO2 ;
% 1.41D-11 : C818CO + OH = C820O2 ;
% KDEC : C818O = C517CHO + CH3CO3 + TPENE ;
% KRO2HO2*0.859 : C818O2 + HO2 = C818OOH ;
% KRO2NO : C818O2 + NO = C818O + NO2 ;
% KRO2NO3 : C818O2 + NO3 = C818O + NO2 ;
% 1.30D-12*0.2*RO2 : C818O2 = C818CO ;
% 1.30D-12*0.6*RO2 : C818O2 = C818O ;
% 1.30D-12*0.2*RO2 : C818O2 = C818OH ;
% 2.72D-11 : C818OH + OH = C818CO + HO2 ;
% 3.94D-11 : C818OOH + OH = C818CO + OH ;
% KDEC : C819O = ACETOL + CO2C4CO3 ;
% KRO2HO2 : C819O2 + HO2 = C819OOH ;
% KRO2NO : C819O2 + NO = C819O + NO2 ;
% KRO2NO3 : C819O2 + NO3 = C819O + NO2 ;
% 9.20D-14*RO2 : C819O2 = C819O ;
% 1.35D-11 : C819OOH + OH = C819O2 ;
% KDEC : C820O = CH3CO3 + C614CO + TPENE ;
% KRO2HO2*0.859 : C820O2 + HO2 = C820OOH ;

% KRO2NO : C820O2 + NO = C820O + NO2 ;
% KRO2NO3 : C820O2 + NO3 = C820O + NO2 ;
% 9.20D-14*RO2 : C820O2 = C820O ;
% 1.76D-11 : C820OOH + OH = C820O2 ;
% KDEC : C821O = CH3CO3 + CO + CO2C3CHO + TPENE ;
% KRO2HO2*0.859 : C821O2 + HO2 = C821OOH ;
% KRO2NO : C821O2 + NO = C821O + NO2 ;
% KRO2NO3 : C821O2 + NO3 = C821O + NO2 ;
% 8.80D-13*RO2 : C821O2 = C821O ;
% 5.42D-11 : C821OOH + OH = C821O2 ;
% KDEC*0.2 : C822CO2 = C822O2 ;
% KDEC*0.8 : C822CO2 = C823CO3 ;
% 8.47D-11 : C822CO2H + OH = C822CO2 ;
% KAPHO2*0.44 : C822CO3 + HO2 = C822CO2 + OH ;
% KAPHO2*0.15 : C822CO3 + HO2 = C822CO2H + O3 ;
% KAPHO2*0.41 : C822CO3 + HO2 = C822CO3H ;
% KAPNO : C822CO3 + NO = C822CO2 + NO2 ;
% KFPAN : C822CO3 + NO2 = C822PAN ;
% KRO2NO3*1.74 : C822CO3 + NO3 = C822CO2 + NO2 ;
% 1.00D-11*0.7*RO2 : C822CO3 = C822CO2 ;
% 1.00D-11*0.3*RO2 : C822CO3 = C822CO2H ;
% 8.82D-11 : C822CO3H + OH = C822CO3 ;
% 8.31D-11 : C822NO3 + OH = C729CHO + NO2 ;
% KDEC : C822O = C824O2 ;
% KRO2HO2*0.859 : C822O2 + HO2 = C822OOH ;
% KRO2NO*0.138 : C822O2 + NO = C822NO3 ;
% KRO2NO*0.862 : C822O2 + NO = C822O + NO2 ;
% KRO2NO3 : C822O2 + NO3 = C822O + NO2 ;
% 1.30D-12*0.2*RO2 : C822O2 = C729CHO ;
% 1.30D-12*0.6*RO2 : C822O2 = C822O ;
% 1.30D-12*0.2*RO2 : C822O2 = C822OH ;
% 8.80D-11 : C822OH + OH = C729CHO + HO2 ;
% 9.71D-11 : C822OOH + OH = C729CHO + OH ;
% 8.46D-11 : C822PAN + OH = C729CHO + CO + NO2 ;
% 1.9D17*EXP(-14100/TEMP) : C822PAN = C822CO3 + NO2 ;
% 7.70D-11 : C823CO + OH = C825O2 ;
% KAPHO2*0.41 : C823CO3 + HO2 = C823CO3H ;
% KAPHO2*0.44 : C823CO3 + HO2 = C823O2 + OH ;
% KAPHO2*0.15 : C823CO3 + HO2 = LIMONIC + O3 ;
% KAPNO : C823CO3 + NO = C823O2 + NO2 ;
% KFPAN : C823CO3 + NO2 = C823PAN ;
% KRO2NO3*1.74 : C823CO3 + NO3 = C823O2 + NO2 ;
% 1.00D-11*0.7*RO2 : C823CO3 = C823O2 ;
% 1.00D-11*0.3*RO2 : C823CO3 = LIMONIC ;
% 6.18D-11 : C823CO3H + OH = C823CO3 ;

% 5.53D-11 : C823NO3 + OH = C823CO + NO2 ;
% KDEC : C823O = C825O2 ;
% KRO2HO2*0.859 : C823O2 + HO2 = C823OOH ;
% KRO2NO*0.138 : C823O2 + NO = C823NO3 ;
% KRO2NO*0.862 : C823O2 + NO = C823O + NO2 ;
% KRO2NO3 : C823O2 + NO3 = C823O + NO2 ;
% 1.30D-12*0.2*RO2 : C823O2 = C823CO ;
% 1.30D-12*0.6*RO2 : C823O2 = C823O ;
% 1.30D-12*0.2*RO2 : C823O2 = C823OH ;
% 6.16D-11 : C823OH + OH = C823CO + HO2 ;
% 7.06D-11 : C823OOH + OH = C823CO + OH ;
% 5.82D-11 : C823PAN + OH = C823CO + CO + NO2 ;
% 1.9D17*EXP(-14100/TEMP) : C823PAN = C823CO3 + NO2 ;
% 7.46D-11 : C824CO + OH = C624CO3 + CO ;
% KDEC : C824O = C624CHO + CO + HO2 ;
% KRO2HO2*0.859 : C824O2 + HO2 = C824OOH ;
% KRO2NO : C824O2 + NO = C824O + NO2 ;
% KRO2NO3 : C824O2 + NO3 = C824O + NO2 ;
% 8.80D-12*0.2*RO2 : C824O2 = C824CO ;
% 8.80D-12*0.6*RO2 : C824O2 = C824O ;
% 8.80D-12*0.2*RO2 : C824O2 = C824OH ;
% 9.34D-11 : C824OH + OH = C824CO + HO2 ;
% 1.02D-10 : C824OOH + OH = C824CO + OH ;
% 6.64D-11 : C825CO + OH = C622CO3 ;
% KDEC : C825O = C622CHO + HO2 ;
% KRO2HO2*0.859 : C825O2 + HO2 = C825OOH ;
% KRO2NO : C825O2 + NO = C825O + NO2 ;
% KRO2NO3 : C825O2 + NO3 = C825O + NO2 ;
% 8.80D-12*0.2*RO2 : C825O2 = C825CO ;
% 8.80D-12*0.6*RO2 : C825O2 = C825O ;
% 8.80D-12*0.2*RO2 : C825O2 = C825OH ;
% 6.69D-11 : C825OH + OH = C825CO + HO2 ;
% 7.90D-11 : C825OOH + OH = C825CO + OH ;
% 4.59D-11 : C826NO3 + OH = C626CHO + HCHO + NO2 ;
% KDEC : C826O = C626CHO + HCHO + HO2 ;
% KRO2HO2*0.859 : C826O2 + HO2 = C826OOH ;
% KRO2NO*0.069 : C826O2 + NO = C826NO3 ;
% KRO2NO*0.931 : C826O2 + NO = C826O + NO2 ;
% KRO2NO3 : C826O2 + NO3 = C826O + NO2 ;
% 9.20D-14*0.7*RO2 : C826O2 = C826O ;
% 9.20D-14*0.3*RO2 : C826O2 = C826OH ;
% 5.70D-11 : C826OH + OH = C826O ;
% 6.05D-11 : C826OOH + OH = C826O2 ;
% KAPHO2*0.56 : C85CO3 + HO2 = C85CO3H ;
% KAPHO2*0.44 : C85CO3 + HO2 = C85O2 + OH ;

% KAPNO : C85CO3 + NO = C85O2 + NO2 ;
% KFPAN : C85CO3 + NO2 = C9PAN2 ;
% KRO2NO3*1.74 : C85CO3 + NO3 = C85O2 + NO2 ;
% 1.00D-11*RO2 : C85CO3 = C85O2 ;
% 1.02D-11 : C85CO3H + OH = C85CO3 ;
% KDEC : C85O = C86O2 ;
% KRO2HO2*0.859 : C85O2 + HO2 = C85OOH ;
% KRO2NO : C85O2 + NO = C85O + NO2 ;
% KRO2NO3 : C85O2 + NO3 = C85O + NO2 ;
% 6.70D-15*RO2 : C85O2 = C85O ;
% 1.29D-11 : C85OOH + OH = C85O2 ;
% KDEC : C86O = C511O2 + CH3COCH3 ;
% KRO2HO2*0.859 : C86O2 + HO2 = C86OOH ;
% KRO2NO : C86O2 + NO = C86O + NO2 ;
% KRO2NO3 : C86O2 + NO3 = C86O + NO2 ;
% 6.70D-15*RO2 : C86O2 = C86O ;
% 3.45D-11 : C86OOH + OH = C86O2 ;
% 1.03D-10 : C87CO + OH = C615CO3 + CO ;
% 9.19D-11 : C87CO2H + OH = C87O2 ;
% KAPHO2*0.15 : C87CO3 + HO2 = C87CO2H + O3 ;
% KAPHO2*0.41 : C87CO3 + HO2 = C87CO3H ;
% KAPHO2*0.44 : C87CO3 + HO2 = C87O2 + OH ;
% KAPNO : C87CO3 + NO = C87O2 + NO2 ;
% KFPAN : C87CO3 + NO2 = C87PAN ;
% KRO2NO3*1.74 : C87CO3 + NO3 = C87O2 + NO2 ;
% 1.00D-11*0.3*RO2 : C87CO3 = C87CO2H ;
% 1.00D-11*0.7*RO2 : C87CO3 = C87O2 ;
% 9.50D-11 : C87CO3H + OH = C87CO3 ;
% KDEC : C87O = C615CO3 + HCHO ;
% KRO2HO2*0.859 : C87O2 + HO2 = C87OOH ;
% KRO2NO : C87O2 + NO = C87O + NO2 ;
% KRO2NO3 : C87O2 + NO3 = C87O + NO2 ;
% 2.00D-12*0.2*RO2 : C87O2 = C87CO ;
% 2.00D-12*0.6*RO2 : C87O2 = C87O ;
% 2.00D-12*0.2*RO2 : C87O2 = C87OH ;
% 9.34D-11 : C87OH + OH = C87CO + HO2 ;
% 1.00D-10 : C87OOH + OH = C87CO + OH ;
% 9.11D-11 : C87PAN + OH = C87CO + CO + NO2 ;
% 1.9D17*EXP(-14100/TEMP) : C87PAN = C87CO3 + NO2 ;
% KNO3AL*8.5 : C88CHO + NO3 = C88CO3 + HNO3 ;
% 7.30D-11 : C88CHO + OH = C88CO3 ;
% 5.80D-12 : C88CO + OH = C718CO3 ;
% 1.02D-11 : C88CO2H + OH = C88O2 ;
% KAPHO2*0.15 : C88CO3 + HO2 = C88CO2H + O3 ;
% KAPHO2*0.41 : C88CO3 + HO2 = C88CO3H ;

% KAPHO2*0.44 : C88CO3 + HO2 = C88O2 + OH ;
% KAPNO : C88CO3 + NO = C88O2 + NO2 ;
% KFPAN : C88CO3 + NO2 = C88PAN ;
% KRO2NO3*1.74 : C88CO3 + NO3 = C88O2 + NO2 ;
% 1.00D-11*0.3*RO2 : C88CO3 = C88CO2H ;
% 1.00D-11*0.7*RO2 : C88CO3 = C88O2 ;
% 1.37D-11 : C88CO3H + OH = C88CO3 ;
% KDEC : C88O = C718CO3 ;
% KRO2HO2*0.859 : C88O2 + HO2 = C88OOH ;
% KRO2NO : C88O2 + NO = C88O + NO2 ;
% KRO2NO3 : C88O2 + NO3 = C88O + NO2 ;
% 8.80D-13*0.2*RO2 : C88O2 = C88CO ;
% 8.80D-13*0.6*RO2 : C88O2 = C88O ;
% 8.80D-13*0.2*RO2 : C88O2 = C88OH ;
% 2.58D-11 : C88OH + OH = C88CO + HO2 ;
% 5.71D-11 : C88OOH + OH = C88CO + OH ;
% 7.50D-12 : C88PAN + OH = C88CO + CO + NO2 ;
% 1.9D17*EXP(-14100/TEMP) : C88PAN = C88CO3 + NO2 ;
% KDEC*0.80 : C89CO2 = C811CO3 ;
% KDEC*0.20 : C89CO2 = C89O2 ;
% 2.69D-11 : C89CO2H + OH = C89CO2 ;
% KAPHO2*0.44 : C89CO3 + HO2 = C89CO2 + OH ;
% KAPHO2*0.15 : C89CO3 + HO2 = C89CO2H + O3 ;
% KAPHO2*0.41 : C89CO3 + HO2 = C89CO3H ;
% KAPNO : C89CO3 + NO = C89CO2 + NO2 ;
% KFPAN : C89CO3 + NO2 = C89PAN ;
% KRO2NO3*1.74 : C89CO3 + NO3 = C89CO2 + NO2 ;
% 1.00D-11*0.7*RO2 : C89CO3 = C89CO2 ;
% 1.00D-11*0.3*RO2 : C89CO3 = C89CO2H ;
% 3.00D-11 : C89CO3H + OH = C89CO3 ;
% 2.56D-11 : C89NO3 + OH = CH3COCH3 + CO13C4CHO + NO2 ;
% 5.62D+4 : C89O = C810O2 ;
% KRO2HO2*0.859 : C89O2 + HO2 = C89OOH ;
% KRO2NO*0.104 : C89O2 + NO = C89NO3 ;
% KRO2NO*0.896 : C89O2 + NO = C89O + NO2 ;
% KRO2NO3 : C89O2 + NO3 = C89O + NO2 ;
% 6.70D-15*0.7*RO2 : C89O2 = C89O ;
% 6.70D-15*0.3*RO2 : C89O2 = C89OH ;
% 2.86D-11 : C89OH + OH = C89O ;
% 3.61D-11 : C89OOH + OH = C89O2 ;
% 2.52D-11 : C89PAN + OH = CH3COCH3 + CO13C4CHO + CO + NO2 ;
% 1.9D17*EXP(-14100/TEMP) : C89PAN = C89CO3 + NO2 ;
% 3.04D-12 : C8BC + OH = C8BCO2 ;
% 3.94D-12 : C8BCCO + OH = C89O2 ;
% 1.84D-12 : C8BCNO3 + OH = C8BCCO + NO2 ;

% KDEC : C8BCO = C89O2 ;
% KRO2HO2*0.859 : C8BCO2 + HO2 = C8BCOOH ;
% KRO2NO*0.138 : C8BCO2 + NO = C8BCNO3 ;
% KRO2NO*0.862 : C8BCO2 + NO = C8BCO + NO2 ;
% KRO2NO3 : C8BCO2 + NO3 = C8BCO + NO2 ;
% 2.50D-13*0.2*RO2 : C8BCO2 = C8BCCO ;
% 2.50D-13*0.6*RO2 : C8BCO2 = C8BCO ;
% 2.50D-13*0.2*RO2 : C8BCO2 = C8BCOH ;
% 6.81D-12 : C8BCOH + OH = C8BCCO + HO2 ;
% 1.62D-11 : C8BCOOH + OH = C8BCCO + OH ;
% 7.09D-11 : C914CO + OH = C87CO3 ;
% KDEC : C914O = C87CO3 ;
% KRO2HO2*0.890 : C914O2 + HO2 = C914OOH ;
% KRO2NO : C914O2 + NO = C914O + NO2 ;
% KRO2NO3 : C914O2 + NO3 = C914O + NO2 ;
% 8.80D-13*0.2*RO2 : C914O2 = C914CO ;
% 8.80D-13*0.6*RO2 : C914O2 = C914O ;
% 8.80D-13*0.2*RO2 : C914O2 = C914OH ;
% 7.44D-11 : C914OH + OH = C914CO + HO2 ;
% 8.67D-11 : C914OOH + OH = C914CO + OH ;
% 6.96D-11 : C915NO3 + OH = C88CHO + NO2 ;
% KROSEC : C915O + O2 = C88CHO + HO2 ;
% 5.62D+4 : C915O = C916O2 ;
% KRO2HO2*0.890 : C915O2 + HO2 = C915OOH ;
% KRO2NO*0.157 : C915O2 + NO = C915NO3 ;
% KRO2NO*0.843 : C915O2 + NO = C915O + NO2 ;
% KRO2NO3 : C915O2 + NO3 = C915O + NO2 ;
% 8.80D-13*0.2*RO2 : C915O2 = C88CHO ;
% 8.80D-13*0.6*RO2 : C915O2 = C915O ;
% 8.80D-13*0.2*RO2 : C915O2 = C915OH ;
% 8.33D-11 : C915OH + OH = C88CHO + HO2 ;
% 1.01D-10 : C915OOH + OH = C88CHO + OH ;
% 9.23D-11 : C916NO3 + OH = CH3COCH3 + CO123C5CHO + NO2 ;
% KDEC : C916O = CH3COCH3 + C616O2 ;
% KRO2HO2*0.890 : C916O2 + HO2 = C916OOH ;
% KRO2NO*0.118 : C916O2 + NO = C916NO3 ;
% KRO2NO*0.882 : C916O2 + NO = C916O + NO2 ;
% KRO2NO3 : C916O2 + NO3 = C916O + NO2 ;
% 6.70D-15*0.7*RO2 : C916O2 = C916O ;
% 6.70D-15*0.3*RO2 : C916O2 = C916OH ;
% 9.03D-11 : C916OH + OH = C916O ;
% 9.73D-11 : C916OOH + OH = C916O2 ;
% 9.97D-12 : C917NO3 + OH = CH3COCH3 + C619CO + NO2 ;
% KDEC : C917O = C619O2 + CH3COCH3 ;
% KRO2HO2*0.890 : C917O2 + HO2 = C917OOH ;

% KRO2NO*0.118 : C917O2 + NO = C917NO3 ;
% KRO2NO*0.882 : C917O2 + NO = C917O + NO2 ;
% KRO2NO3 : C917O2 + NO3 = C917O + NO2 ;
% 6.70D-15*0.7*RO2 : C917O2 = C917O ;
% 6.70D-15*0.3*RO2 : C917O2 = C917OH ;
% 1.56D-11 : C917OH + OH = C917O ;
% 1.91D-11 : C917OOH + OH = C917O2 ;
% KNO3AL*8.5 : C918CHO + NO3 = C918CO3 + HNO3 ;
% 3.17D-11 : C918CHO + OH = C918CO3 ;
% KAPHO2*0.56 : C918CO3 + HO2 = C918CO3H ;
% KAPHO2*0.44 : C918CO3 + HO2 = NOPINONE + HO2 + OH ;
% KAPNO : C918CO3 + NO = NOPINONE + HO2 + NO2 ;
% KFPAN : C918CO3 + NO2 = C918PAN ;
% KRO2NO3*1.74 : C918CO3 + NO3 = NOPINONE + HO2 + NO2 ;
% 1.00D-11*RO2 : C918CO3 = NOPINONE + HO2 ;
% 1.46D-11 : C918CO3H + OH = C918CO3 ;
% 6.79D-11 : C918NO3+OH = HCOCH2CHO+HCOCH2CHO+CH3COCH3 + NO2;
% KDEC : C918O = C919O2 ;
% KRO2HO2*0.890 : C918O2 + HO2 = C918OOH ;
% KRO2NO*0.047 : C918O2 + NO = C918NO3 ;
% KRO2NO*0.953 : C918O2 + NO = C918O + NO2 ;
% KRO2NO3 : C918O2 + NO3 = C918O + NO2 ;
% 6.70D-15*0.7*RO2 : C918O2 = C918O ;
% 6.70D-15*0.3*RO2 : C918O2 = C918OH ;
% 7.16D-11 : C918OH + OH = C918O ;
% 7.91D-11 : C918OOH + OH = C918O2 ;
% 5.71D-12 : C918PAN + OH = NOPINONE + CO + NO2 ;
% 1.9D17*EXP(-14100/TEMP) : C918PAN = C918CO3 + NO2 ;
% 9.14D-11 : C919NO3+OH = HCOCH2CHO+HCOCH2CHO+CH3COCH3 + NO2;
% KDEC : C919O = C620O2 + CH3COCH3 ;
% KRO2HO2*0.890 : C919O2 + HO2 = C919OOH ;
% KRO2NO*0.118 : C919O2 + NO = C919NO3 ;
% KRO2NO*0.882 : C919O2 + NO = C919O + NO2 ;
% KRO2NO3 : C919O2 + NO3 = C919O + NO2 ;
% 6.70D-15*0.7*RO2 : C919O2 = C919O ;
% 6.70D-15*0.3*RO2 : C919O2 = C919OH ;
% 9.73D-11 : C919OH + OH = C919O ;
% 1.01D-10 : C919OOH + OH = C919O2 ;
% KAPHO2*0.41 : C920CO3 + HO2 = C920CO3H ;
% KAPHO2*0.44 : C920CO3 + HO2 = C920O2 + OH;
% KAPHO2*0.15 : C920CO3 + HO2 = HOPINONIC + O3 ;
% KAPNO : C920CO3 + NO = C920O2 + NO2 ;
% KFPAN : C920CO3 + NO2 = C920PAN ;
% KRO2NO3*1.74 : C920CO3 + NO3 = C920O2 + NO2 ;
% 1.00D-11*0.7*RO2 : C920CO3 = C920O2 ;

% 1.00D-11*0.3*RO2 : C920CO3 = HOPINONIC ;
% 9.16D-12 : C920CO3H + OH = C920CO3 ;
% 3.08D+5 : C920O = C921O2 ;
% KRO2HO2*0.890 : C920O2 + HO2 = C920OOH ;
% KRO2NO : C920O2 + NO = C920O + NO2 ;
% KRO2NO3 : C920O2 + NO3 = C920O + NO2 ;
% 1.30D-12*RO2 : C920O2 = C920O ;
% 2.36D-11 : C920OOH + OH = C920O2 ;
% 5.56D-12 : C920PAN + OH = C109OH + CO + NO2 ;
% 1.9D17*EXP(-14100/TEMP) : C920PAN = C920CO3 + NO2 ;
% KDEC : C921O = C922O2 ;
% KRO2HO2*0.890 : C921O2 + HO2 = C921OOH ;
% KRO2NO : C921O2 + NO = C921O + NO2 ;
% KRO2NO3 : C921O2 + NO3 = C921O + NO2 ;
% 6.70D-15*RO2 : C921O2 = C921O ;
% 1.29D-11 : C921OOH + OH = C921O2 ;
% KDEC : C922O = CH3COCH3 + C621O2 ;
% KRO2HO2*0.890 : C922O2 + HO2 = C922OOH ;
% KRO2NO : C922O2 + NO = C922O + NO2 ;
% KRO2NO3 : C922O2 + NO3 = C922O + NO2 ;
% 6.70D-15*RO2 : C922O2 = C922O ;
% 1.51D-11 : C922OOH + OH = C922O2 ;
% KAPHO2*0.41 : C923CO3 + HO2 = C923CO3H ;
% KAPHO2*0.44 : C923CO3 + HO2 = C923O2 + OH ;
% KAPHO2*0.15 : C923CO3 + HO2 = LIMONONIC + O3 ;
% KAPNO : C923CO3 + NO = C923O2 + NO2 ;
% KFPAN : C923CO3 + NO2 = C923PAN ;
% KRO2NO3*1.74 : C923CO3 + NO3 = C923O2 + NO2 ;
% 1.00D-11*0.7*RO2 : C923CO3 = C923O2 ;
% 1.00D-11*0.3*RO2 : C923CO3 = LIMONONIC ;
% 7.29D-11 : C923CO3H + OH = C923CO3 ;
% 5.82D-11 : C923NO3 + OH = NORLIMAL + NO2 ;
% KDEC : C923O = C924O2 ;
% KRO2HO2*0.890 : C923O2 + HO2 = C923OOH ;
% KRO2NO*0.157 : C923O2 + NO = C923NO3 ;
% KRO2NO*0.843 : C923O2 + NO = C923O + NO2 ;
% KRO2NO3 : C923O2 + NO3 = C923O + NO2 ;
% 1.32D-12*0.6*RO2 : C923O2 = C923O ;
% 1.32D-12*0.2*RO2 : C923O2 = C923OH ;
% 1.32D-12*0.2*RO2 : C923O2 = NORLIMAL ;
% 6.91D-11 : C923OH + OH = NORLIMAL + HO2 ;
% 7.39D-11 : C923OOH + OH = NORLIMAL + OH ;
% 6.93D-11 : C923PAN + OH = NORLIMAL + CO + NO2 ;
% 1.9D17*EXP(-14100/TEMP) : C923PAN = C923CO3 + NO2 ;
% 6.67D-11 : C924CO + OH = C925O2 ;

% KDEC : C924O = CH3CO3 + C622CHO + TPENE ;
% KRO2HO2*0.890 : C924O2 + HO2 = C924OOH ;
% KRO2NO : C924O2 + NO = C924O + NO2 ;
% KRO2NO3 : C924O2 + NO3 = C924O + NO2 ;
% 8.80D-13*0.2*RO2 : C924O2 = C924CO ;
% 8.80D-13*0.6*RO2 : C924O2 = C924O ;
% 8.80D-13*0.2*RO2 : C924O2 = C924OH ;
% 7.47D-11 : C924OH + OH = C924CO + HO2 ;
% 8.69D-11 : C924OOH + OH = C924CO + OH ;
% KDEC : C925O = C818CO + HCHO + HO2 ;
% KRO2HO2*0.890 : C925O2 + HO2 = C925OOH ;
% KRO2NO : C925O2 + NO = C925O + NO2 ;
% KRO2NO3 : C925O2 + NO3 = C925O + NO2 ;
% 9.20D-14*RO2 : C925O2 = C925O ;
% 2.45D-11 : C925OOH + OH = C925O2 ;
% KDEC : C926O = CH3CO3 + CO25C6CHO + TPENE ;
% KRO2HO2*0.890 : C926O2 + HO2 = C926OOH ;
% KRO2NO : C926O2 + NO = C926O + NO2 ;
% KRO2NO3 : C926O2 + NO3 = C926O + NO2 ;
% 9.20D-14*0.7*RO2 : C926O2 = C926O ;
% 9.20D-14*0.3*RO2 : C926O2 = C926OH ;
% 2.73D-11 : C926OH + OH = CH3CO3 + CO25C6CHO + TPENE ;
% 3.08D-11 : C926OOH + OH = C926O2 ;
% KAPHO2*0.44 : C96CO3 + HO2 = C96O2 + OH;
% KAPHO2*0.41 : C96CO3 + HO2 = PERPINONIC ;
% KAPHO2*0.15 : C96CO3 + HO2 = PINONIC + O3 ;
% KAPNO : C96CO3 + NO = C96O2 + NO2 ;
% KFPAN : C96CO3 + NO2 = C10PAN2 ;
% KRO2NO3*1.74 : C96CO3 + NO3 = C96O2 + NO2 ;
% 1.00D-11*0.7*RO2 : C96CO3 = C96O2 ;
% 1.00D-11*0.3*RO2 : C96CO3 = PINONIC ;
% 2.88D-12 : C96NO3 + OH = NORPINAL + NO2 ;
% 3.08D+5 : C96O = C97O2 ;
% KRO2HO2*0.890 : C96O2 + HO2 = C96OOH ;
% KRO2NO*0.157 : C96O2 + NO = C96NO3 ;
% KRO2NO*0.843 : C96O2 + NO = C96O + NO2 ;
% KRO2NO3 : C96O2 + NO3 = C96O + NO2 ;
% 1.30D-12*0.6*RO2 : C96O2 = C96O ;
% 1.30D-12*0.2*RO2 : C96O2 = C96OH ;
% 1.30D-12*0.2*RO2 : C96O2 = NORPINAL ;
% 7.67D-12 : C96OH + OH = NORPINAL + HO2 ;
% 3.60D-12 : C96OOH + OH = C96O2 ;
% 1.30D-11 : C96OOH + OH = NORPINAL + OH ;
% KDEC : C97O = C98O2 ;
% KRO2HO2*0.890 : C97O2 + HO2 = C97OOH ;

% KRO2NO : C97O2 + NO = C97O + NO2 ;
% KRO2NO3 : C97O2 + NO3 = C97O + NO2 ;
% 6.70D-15*0.7*RO2 : C97O2 = C97O ;
% 6.70D-15*0.3*RO2 : C97O2 = C97OH ;
% 7.20D-12 : C97OH + OH = C97O ;
% 1.05D-11 : C97OOH + OH = C97O2 ;
% 5.37D-12 : C98NO3 + OH = CH3COCH3 + C614CO + NO2 ;
% KDEC : C98O = C614O2 + CH3COCH3 ;
% KRO2HO2*0.890 : C98O2 + HO2 = C98OOH ;
% KRO2NO*0.118 : C98O2 + NO = C98NO3 ;
% KRO2NO*0.882 : C98O2 + NO = C98O + NO2 ;
% KRO2NO3 : C98O2 + NO3 = C98O + NO2 ;
% 6.70D-15*0.7*RO2 : C98O2 = C98O ;
% 6.70D-15*0.3*RO2 : C98O2 = C98OH ;
% 1.69D-11 : C98OH + OH = C98O ;
% 2.05D-11 : C98OOH + OH = C98O2 ;
% 6.07D-12 : C9DC + OH = C9DCO2 ;
% 1.32D-12 : C9DCCO + OH = C914O2 ;
% 1.58D-12 : C9DCNO3 + OH = C9DCCO + NO2 ;
% KDEC : C9DCO = C914O2 ;
% KRO2HO2*0.890 : C9DCO2 + HO2 = C9DCOOH ;
% KRO2NO*0.157 : C9DCO2 + NO = C9DCNO3 ;
% KRO2NO*0.843 : C9DCO2 + NO = C9DCO + NO2 ;
% KRO2NO3 : C9DCO2 + NO3 = C9DCO + NO2 ;
% 2.50D-13*0.2*RO2 : C9DCO2 = C9DCCO ;
% 2.50D-13*0.6*RO2 : C9DCO2 = C9DCO ;
% 2.50D-13*0.2*RO2 : C9DCO2 = C9DCOH ;
% 3.11D-11 : C9DCOH + OH = C9DCCO + HO2 ;
% 7.50D-11 : C9DCOOH + OH = C9DCCO + OH ;
% 6.60D-12 : C9PAN2 + OH = C85OOH + CO + NO2 ;
% 1.9D17*EXP(-14100/TEMP) : C9PAN2 = C85CO3 + NO2 ;
% KDEC*0.370 : CH2OOF = CH2OO ;
% KDEC*0.500 : CH2OOF = CO ;
% KDEC*0.130 : CH2OOF = HO2 + CO + OH ;
% 2.64D-11 : CHOC2CO2H + OH = CHOC2H4O2 ;
% KAPHO2*0.15 : CHOC2CO3 + HO2 = CHOC2CO2H + O3 ;
% KAPHO2*0.41 : CHOC2CO3 + HO2 = CHOC2CO3H ;
% KAPHO2*0.44 : CHOC2CO3 + HO2 = CHOC2H4O2 + OH ;
% KAPNO : CHOC2CO3 + NO = CHOC2H4O2 + NO2 ;
% KFPAN : CHOC2CO3 + NO2 = CHOC2PAN ;
% KRO2NO3*1.74 : CHOC2CO3 + NO3 = CHOC2H4O2 + NO2 ;
% 1.00D-11*0.3*RO2 : CHOC2CO3 = CHOC2CO2H ;
% 1.00D-11*0.7*RO2 : CHOC2CO3 = CHOC2H4O2 ;
% 3.00D-11 : CHOC2CO3H + OH = CHOC2CO3 ;
% KROPRIM*O2 : CHOC2H4O = HCOCH2CHO + HO2 ;

% KRO2HO2*0.520 : CHOC2H4O2 + HO2 = CHOC2H4OOH ;
% KRO2NO : CHOC2H4O2 + NO = CHOC2H4O + NO2 ;
% KRO2NO3 : CHOC2H4O2 + NO3 = CHOC2H4O + NO2 ;
% 6.00D-13*RO2 : CHOC2H4O2 = CHOC2H4O ;
% 7.31D-11 : CHOC2H4OOH + OH = CHOC2H4O2 ;
% 2.64D-11 : CHOC2PAN + OH = HCOCH2CHO + CO + NO2 ;
% 1.9D17*EXP(-14100/TEMP) : CHOC2PAN = CHOC2CO3 + NO2 ;
% KAPHO2*0.44 : CHOC3COCO3 + HO2 = CHOC3COO2 + OH ;
% KAPHO2*0.56 : CHOC3COCO3 + HO2 = CHOC3COOOH ;
% KAPNO : CHOC3COCO3 + NO = CHOC3COO2 + NO2 ;
% KFPAN : CHOC3COCO3 + NO2 = CHOC3COPAN ;
% KRO2NO3*1.74 : CHOC3COCO3 + NO3 = CHOC3COO2 + NO2 ;
% 1.00D-11*RO2 : CHOC3COCO3 = CHOC3COO2 ;
% KDEC : CHOC3COO = HCOCH2CO3 + HCHO ;
% KRO2HO2*0.625 : CHOC3COO2 + HO2 = C413COOOH ;
% KRO2NO : CHOC3COO2 + NO = CHOC3COO + NO2 ;
% KRO2NO3 : CHOC3COO2 + NO3 = CHOC3COO + NO2 ;
% 2.00D-12*RO2 : CHOC3COO2 = CHOC3COO ;
% 7.55D-11 : CHOC3COOOH + OH = CHOC3COCO3 ;
% 7.19D-11 : CHOC3COPAN + OH = C4CODIAL + CO + NO2 ;
% 1.9D17*EXP(-14100/TEMP) : CHOC3COPAN = CHOC3COCO3 + NO2 ;
% KDEC*0.6 : CHOCOCH2O = HCHO + HO2 + CO + CO ;
% KDEC*0.4 : CHOCOCH2O = HCOCO3 + HCHO ;
% 2*KNO3AL*5.5 : CO123C5CHO + NO3 = CHOC2CO3 + CO + CO + HNO3 ;
% 3.89D-11 : CO123C5CHO + OH = CHOC2CO3 + CO + CO ;
% 2*KNO3AL*5.5 : CO12C4CHO + NO3 = CHOC2CO3 + CO + HNO3 ;
% 3.89D-11 : CO12C4CHO + OH = CHOC2CO3 + CO ;
% 6.69D-11 : CO13C3CO2H + OH = HCOCH2CO3 ;
% 2*KNO3AL*5.5 : CO13C4CHO + NO3 = CHOC3COCO3 + HNO3 ;
% 1.33D-10 : CO13C4CHO + OH = CHOC3COCO3 ;
% 2.39D-11 : CO13C4OH + OH = C4CODIAL + HO2 ;
% 2*KNO3AL*8.5 : CO1M22CHO + NO3 = CO1M22CO3 + HNO3 ;
% 1.32D-10 : CO1M22CHO + OH = CO1M22CO3 ;
% 6.67D-11 : CO1M22CO2H + OH = IBUTALCO2 ;
% KAPHO2*0.15 : CO1M22CO3 + HO2 = CO1M22CO2H + O3 ;
% KAPHO2*0.41 : CO1M22CO3 + HO2 = CO1M22CO3H ;
% KAPHO2*0.44 : CO1M22CO3 + HO2 = IBUTALCO2 + OH ;
% KAPNO : CO1M22CO3 + NO = IBUTALCO2 + NO2 ;
% KFPAN : CO1M22CO3 + NO2 = CO1M22PAN ;
% KRO2NO3*1.74 : CO1M22CO3 + NO3 = IBUTALCO2 + NO2 ;
% 1.00D-11*0.3*RO2 : CO1M22CO3 = CO1M22CO2H ;
% 1.00D-11*0.7*RO2 : CO1M22CO3 = IBUTALCO2 ;
% 6.98D-11 : CO1M22CO3H + OH = CO1M22CO3 ;
% 2.11D-11 : CO1M22PAN + OH = CH3COCH3 + CO + NO2 ;
% 1.9D17*EXP(-14100/TEMP) : CO1M22PAN = CO1M22CO3 + NO2 ;

% KNO3AL*5.5 : CO235C5CHO + NO3 = CO23C4CO3 + CO + HNO3 ;
% 1.33D-11 : CO235C5CHO + OH = CO23C4CO3 + CO ;
% KNO3AL*5.5 : CO235C6CHO + NO3 = CO235C6CO3 + HNO3 ;
% 6.70D-11 : CO235C6CHO + OH = CO235C6CO3 ;
% KAPHO2*0.56 : CO235C6CO3 + HO2 = C235C6CO3H ;
% KAPHO2*0.44 : CO235C6CO3 + HO2 = CO235C6O2 + OH ;
% KAPNO : CO235C6CO3 + NO = CO235C6O2 + NO2 ;
% KFPAN : CO235C6CO3 + NO2 = C7PAN3 ;
% KRO2NO3*1.74 : CO235C6CO3 + NO3 = CO235C6O2 + NO2 ;
% 1.00D-11*RO2 : CO235C6CO3 = CO235C6O2 ;
% KDEC : CO235C6O = CO23C4CO3 + HCHO ;
% KRO2HO2*0.770 : CO235C6O2 + HO2 = CO235C6OOH ;
% KRO2NO : CO235C6O2 + NO = CO235C6O + NO2 ;
% KRO2NO3 : CO235C6O2 + NO3 = CO235C6O + NO2 ;
% 2.00D-12*RO2 : CO235C6O2 = CO235C6O ;
% 1.01D-11 : CO235C6OOH + OH = CO235C6O2 ;
% KNO3AL*5.5 : NO3 + CO23C4CHO = CO23C4CO3 + HNO3 ;
% 6.65D-11 : OH + CO23C4CHO = CO23C4CO3 ;
% KAPHO2*0.44 : CO23C4CO3 + HO2 = BIACETO2 + OH ;
% KAPHO2*0.56 : CO23C4CO3 + HO2 = CO23C4CO3H ;
% KAPNO : CO23C4CO3 + NO = BIACETO2 + NO2 ;
% KFPAN : CO23C4CO3 + NO2 = C5PAN9 ;
% KRO2NO3*1.74 : CO23C4CO3 + NO3 = BIACETO2 + NO2 ;
% 1.00D-11*RO2 : CO23C4CO3 = BIACETO2 ;
% 4.23D-12 : OH + CO23C4CO3H = CO23C4CO3 ;
% KNO3AL*5.5 : CO25C6CHO + NO3 = CO25C6CO3 + HNO3 ;
% 2.69D-11 : CO25C6CHO + OH = CO25C6CO3 ;
% 6.67D-12 : CO25C6CO2H + OH = C627O2 ;
% KAPHO2*0.44 : CO25C6CO3 + HO2 = C627O2 + OH ;
% KAPHO2*0.15 : CO25C6CO3 + HO2 = CO25C6CO2H + O3 ;
% KAPHO2*0.41 : CO25C6CO3 + HO2 = CO25C6CO3H ;
% KAPNO : CO25C6CO3 + NO = C627O2 + NO2 ;
% KFPAN : CO25C6CO3 + NO2 = C627PAN ;
% KRO2NO3*1.74 : CO25C6CO3 + NO3 = C627O2 + NO2 ;
% 1.00D-11*0.7*RO2 : CO25C6CO3 = C627O2 ;
% 9.75D-11 : CO25C6CO3H + OH = CO25C6CO3 ;
% KNO3AL*4.0 : CO2C3CHO + NO3 = CO2C3CO3 + HNO3 ;
% 7.15D-11 : CO2C3CHO + OH = CO2C3CO3 ;
% KAPHO2*0.44 : CO2C3CO3 + HO2 = CH3COCH2O2 + OH ;
% KAPHO2*0.56 : CO2C3CO3 + HO2 = CO2C3CO3H ;
% KAPNO : CO2C3CO3 + NO = CH3COCH2O2 + NO2 ;
% KFPAN : CO2C3CO3 + NO2 = CO2C3PAN ;
% KRO2NO3*1.74 : CO2C3CO3 + NO3 = CH3COCH2O2 + NO2 ;
% 1.00D-11*RO2 : CO2C3CO3 = CH3COCH2O2 ;
% 4.18D-12 : CO2C3CO3H + OH = CO2C3CO3 ;

% 5.93D-13 : CO2C3PAN + OH = MGLYOX + CO + NO2 + BJ ;
% 1.9D17*EXP(-14100/TEMP) : CO2C3PAN = CO2C3CO3 + NO2 ;
% KNO3AL*5.5 : NO3 + CO2C4CHO = CO2C4CO3 + HNO3 ;
% 2.63D-11 : OH + CO2C4CHO = CO2C4CO3 ;
% 5.71D-12 : OH + CO2C4CO2H = MEKAO2 ;
% KAPHO2*0.15 : CO2C4CO3 + HO2 = CO2C4CO2H + O3 ;
% KAPHO2*0.41 : CO2C4CO3 + HO2 = CO2C4CO3H ;
% KAPHO2*0.44 : CO2C4CO3 + HO2 = MEKAO2 + OH ;
% KAPNO : CO2C4CO3 + NO = MEKAO2 + NO2 ;
% KFPAN : CO2C4CO3 + NO2 = C5PAN2 ;
% KRO2NO3*1.74 : CO2C4CO3 + NO3 = MEKAO2 + NO2 ;
% 1.00D-11*0.3*RO2 : CO2C4CO3 = CO2C4CO2H ;
% 1.00D-11*0.7*RO2 : CO2C4CO3 = MEKAO2 ;
% 9.17D-12 : OH + CO2C4CO3H = CO2C4CO3 ;
% 1.83D-11 : CO2C4GLYOX + OH = CO2C4CO3 + CO ;
% KNO3AL*5.5 : H1C23C4CHO + NO3 = H1C23C4CO3 + HNO3 ;
% 2.37D-11 : H1C23C4CHO + OH = H1C23C4CO3 ;
% KAPHO2*0.44 : H1C23C4CO3 + HO2 = H1C23C4O2 + OH ;
% KAPHO2*0.56 : H1C23C4CO3 + HO2 = HC23C4CO3H ;
% KAPNO : H1C23C4CO3 + NO = H1C23C4O2 + NO2 ;
% KFPAN : H1C23C4CO3 + NO2 = H1C23C4PAN ;
% KRO2NO3*1.74 : H1C23C4CO3 + NO3 = H1C23C4O2 + NO2 ;
% 1.00D-11*RO2 : H1C23C4CO3 = H1C23C4O2 ;
% KDEC : H1C23C4O = HCHO + CO + HOCH2CO3 ;
% KRO2HO2*0.625 : H1C23C4O2 + HO2 = H1C23C4OOH ;
% KRO2NO : H1C23C4O2 + NO = H1C23C4O + NO2 ;
% KRO2NO3 : H1C23C4O2 + NO3 = H1C23C4O + NO2 ;
% 2.00D-12*RO2 : H1C23C4O2 = H1C23C4O ;
% 9.61D-12 : H1C23C4OOH + OH = H1C23C4O2 ;
% 2.92D-12 : H1C23C4PAN + OH = H1CO23CHO + CO + NO2 ;
% 1.9D17*EXP(-14100/TEMP) : H1C23C4PAN = H1C23C4CO3 + NO2 ;
% 1.44D-11 : H1CO23CHO + OH = CO + CO + HOCH2CO3 ;
% KAPHO2*0.56 : H2M2C3CO3 + HO2 = H2M2C3CO3H ;
% KAPHO2*0.44 : H2M2C3CO3 + HO2 = TBUTOLO2 + OH;
% KAPNO : H2M2C3CO3 + NO = TBUTOLO2 + NO2;
% KFPAN : H2M2C3CO3 + NO2 = C5PAN11 ;
% KRO2NO3*1.74 : H2M2C3CO3 + NO3 = TBUTOLO2 + NO2;
% 1.00D-11*RO2 : H2M2C3CO3 = TBUTOLO2 ;
% 4.83D-12 : OH + H2M2C3CO3H = H2M2C3CO3 ;
% 3.55D-11 : H3C25C5CHO + OH = H3C2C4CO3 + CO ;
% KAPHO2*0.44 : H3C25C6CO3 + HO2 = H3C25C6O2 + OH ;
% KAPHO2*0.15 : H3C25C6CO3 + HO2 = H3C25CCO2H + O3 ;
% KAPHO2*0.41 : H3C25C6CO3 + HO2 = H3C25CCO3H ;
% KAPNO : H3C25C6CO3 + NO = H3C25C6O2 + NO2 ;
% KFPAN : H3C25C6CO3 + NO2 = H3C25C6PAN ;

```
% KRO2NO3*1.74 : H3C25C6CO3 + NO3 = H3C25C6O2 + NO2 ;
% 1.00D-11*0.7*RO2 : H3C25C6CO3 = H3C25C6O2 ;
% 1.00D-11*0.3*RO2 : H3C25C6CO3 = H3C25CCO2H ;
% KDEC : H3C25C6O = H3C2C4CO3 + HCHO ;
% KRO2HO2*0.770 : H3C25C6O2 + HO2 = H3C25C6OOH ;
% KRO2NO : H3C25C6O2 + NO = H3C25C6O + NO2 ;
% KRO2NO3 : H3C25C6O2 + NO3 = H3C25C6O + NO2 ;
% 2.00D-12*0.2*RO2 : H3C25C6O2 = H3C25C5CHO ;
% 2.00D-12*0.6*RO2 : H3C25C6O2 = H3C25C6O ;
% 2.00D-12*0.2*RO2 : H3C25C6O2 = H3C25C6OH ;

% 2.54D-11*0.890 : H3C25C6OH + OH = C614CO + HO2 ;
% 2.54D-11*0.110 : H3C25C6OH + OH = H3C25C5CHO + HO2 ;

% 3.23D-11 : H3C25C6OOH + OH = H3C25C5CHO + OH ;

% 2.29D-11 : H3C25C6PAN + OH = H3C25C5CHO + CO + NO2 ;
% 1.9D17*EXP(-14100/TEMP) : H3C25C6PAN = H3C25C6CO3 + NO2 ;

% 2.39D-11 : H3C25CCO2H + OH = H3C25C6O2 ;
% 2.70D-11 : H3C25CCO3H + OH = H3C25C6CO3 ;

% 2.34D-11 : H3C2C4CO2H + OH = HMVKO2 ;

% KAPHO2*0.15 : H3C2C4CO3 + HO2 = H3C2C4CO2H + O3 ;
% KAPHO2*0.41 : H3C2C4CO3 + HO2 = H3C2C4CO3H ;
% KAPHO2*0.44 : H3C2C4CO3 + HO2 = HMVKO2 + OH ;
% KAPNO : H3C2C4CO3 + NO = HMVKO2 + NO2 ;
% KFPAN : H3C2C4CO3 + NO2 = H3C2C4PAN ;
% KRO2NO3*1.74 : H3C2C4CO3 + NO3 = HMVKO2 + NO2 ;
% 1.00D-11*0.3*RO2 : H3C2C4CO3 = H3C2C4CO2H ;
% 1.00D-11*0.7*RO2 : H3C2C4CO3 = HMVKO2 ;
% 2.65D-11 : H3C2C4CO3H + OH = H3C2C4CO3 ;
% 7.60D-12 : H3C2C4PAN + OH = CO2H3CHO + CO + NO2 ;
% 1.9D17*EXP(-14100/TEMP) : H3C2C4PAN = H3C2C4CO3 + NO2 ;
% 6.55D-12 : HC23C4CO3H + OH = H1C23C4CO3 ;
% 1.19D-10 : HCC7CO + OH = C719O2 ;
% 2*KNO3AL*2.4 : NO3 + HCOCH2CHO = HCOCH2CO3 + HNO3 ;
% 4.29D-11 : OH + HCOCH2CHO = HCOCH2CO3 ;
% 2.14D-11 : OH + HCOCH2CO2H = HCOCH2O2 ;
% KAPHO2*0.15 : HCOCH2CO3 + HO2 = HCOCH2CO2H + O3 ;
% KAPHO2*0.41 : HCOCH2CO3 + HO2 = HCOCH2CO3H ;
% KAPHO2*0.44 : HCOCH2CO3 + HO2 = HCOCH2O2 + OH ;
% KAPNO : HCOCH2CO3 + NO = HCOCH2O2 + NO2 ;
% KFPAN : HCOCH2CO3 + NO2 = C3PAN2 ;
```

% KRO2NO3*1.74 : HCOCH2CO3 + NO3 = HCOCH2O2 + NO2 ;
% 1.00D-11*0.3*RO2 : HCOCH2CO3 = HCOCH2CO2H ;
% 1.00D-11*0.7*RO2 : HCOCH2CO3 = HCOCH2O2 ;
% 2.49D-11 : OH + HCOCH2CO3H = HCOCH2CO3 ;
% KDEC : HCOCH2O = HCHO + CO + HO2 ;
% KNO3AL*8.5 : HMVKBCHO + NO3 = HMVKBCO3 + HNO3 ;
% 3.51D-11 : HMVKBCHO + OH = HMVKBCO3 ;
% 1.48D-11 : HMVKBCO2H + OH = HMVKO2 ;
% KAPHO2*0.15 : HMVKBCO3 + HO2 = HMVKBCO2H + O3 ;
% KAPHO2*0.41 : HMVKBCO3 + HO2 = HMVKBCO3H ;
% KAPHO2*0.44 : HMVKBCO3 + HO2 = HMVKO2 + OH ;
% KAPNO : HMVKBCO3 + NO = HMVKO2 + NO2 ;
% KFPAN : HMVKBCO3 + NO2 = HMVKBPAN ;
% KRO2NO3*1.74 : HMVKBCO3 + NO3 = HMVKO2 + NO2 ;
% 1.00D-11*0.3*RO2 : HMVKBCO3 = HMVKBCO2H ;
% 1.00D-11*0.7*RO2 : HMVKBCO3 = HMVKO2 ;
% 1.79D-11 : HMVKBCO3H + OH = HMVKBCO3 ;
% 1.43D-11 : HMVKBPAN + OH = BIACETOH + CO + NO2;
% 1.9D17*EXP(-14100/TEMP) : HMVKBPAN = HMVKBCO3 + NO2 ;
% 1.51D-11 : OH + HO13CO4C5 = HO1CO34C5 + HO2 ;
% 1.57D-11 : HO14CO2C4 + OH = HO1CO3CHO + HO2 ;
% 1.39D-11 : OH + HO1CO34C5 = CO23C4CHO + HO2 ;
% KDEC : HO1CO3C4O = HOC2H4CO3 + HCHO ;
% KRO2HO2*0.625 : HO1CO3C4O2 + HO2 = HOCO3C4OOH ;
% KRO2NO : HO1CO3C4O2 + NO = HO1CO3C4O + NO2 ;
% KRO2NO3 : HO1CO3C4O2 + NO3 = HO1CO3C4O + NO2 ;
% 2.00D-12*0.2*RO2 : HO1CO3C4O2 = HO14CO2C4 ;
% 2.00D-12*0.6*RO2 : HO1CO3C4O2 = HO1CO3C4O ;
% 2.00D-12*0.2*RO2 : HO1CO3C4O2 = HO1CO3CHO ;
% KNO3AL*4.0 : HO1CO3CHO + NO3 = HOC2H4CO3 + CO + HNO3 ;
% 2.56D-11 : HO1CO3CHO + OH = HOC2H4CO3 + CO ;
% KNO3AL*2.4 : NO3 + HOC2H4CHO = HOC2H4CO3 + HNO3 ;
% 3.06D-11 : OH + HOC2H4CHO = HOC2H4CO3 ;
% 1.39D-11 : OH + HOC2H4CO2H = HOCH2CH2O2 ;
% KAPHO2*0.15 : HOC2H4CO3 + HO2 = HOC2H4CO2H + O3 ;
% KAPHO2*0.41 : HOC2H4CO3 + HO2 = HOC2H4CO3H ;
% KAPHO2*0.44 : HOC2H4CO3 + HO2 = HOCH2CH2O2 + OH ;
% KAPNO : HOC2H4CO3 + NO = HOCH2CH2O2 + NO2 ;
% KFPAN : HOC2H4CO3 + NO2 = C3PAN1 ;
% KRO2NO3*1.74 : HOC2H4CO3 + NO3 = HOCH2CH2O2 + NO2 ;
% 1.00D-11*0.3*RO2 : HOC2H4CO3 = HOC2H4CO2H ;
% 1.00D-11*0.7*RO2 : HOC2H4CO3 = HOCH2CH2O2 ;
% 1.73D-11 : OH + HOC2H4CO3H = HOC2H4CO3 ;
% 3.59D-12 : HOCO3C4OOH + OH = HO1CO3C4O2 ;
% 2.16D-11 : HOCO3C4OOH + OH = HO1CO3CHO + OH ;

% 5.70D-12 : HOPINONIC + OH = C920O2 ;
% KRO2HO2*0.625 : IBUTALCO2 + HO2 = IBUTALO2H ;
% KRO2NO : IBUTALCO2 + NO = M2PROPAL2O + NO2 ;
% KRO2NO3 : IBUTALCO2 + NO3 = M2PROPAL2O + NO2 ;
% 9.20D-14*0.3*RO2 : IBUTALCO2 = IBUTALOH ;
% 9.20D-14*0.7*RO2 : IBUTALCO2 = M2PROPAL2O ;
% 2.57D-11 : IBUTALO2H + OH = IBUTALCO2 ;
% 4.64D-12 : IBUTOLOHB + OH = IBUTALOH + HO2 ;
% 9.05D-12*0.5 : OH + IEPOXB = IEB1O2 ;
% 9.05D-12*0.5 : OH + IEPOXB = IEB2O2 ;
% 1.85D-11 : KLIMONIC + OH = C732O2 ;
% 1.97D-11 : KLIMONONIC + OH = C817O2 ;
% 2.60D-13*0.092 : LIMAL + NO3 = C923CO3 + HNO3 ;
% 2.60D-13*0.988 : LIMAL + NO3 = NLIMALO2 ;
% 8.30D-18*0.670 : LIMAL + O3 = LIMALOOA + HCHO ;
% 8.30D-18*0.330 : LIMAL + O3 = LMLKET + CH2OOF ;
% 1.10D-10*0.288 : LIMAL + OH = C923CO3 ;
% 1.10D-10*0.712 : LIMAL + OH = LIMALO2 ;
% 8.34D-11 : LIMALACO + OH = C729CHO + CH3CO3 + TPENE ;
% KDEC : LIMALAO = C729CHO + CH3CO3 + TPENE ;
% KRO2HO2*0.914 : LIMALAO2 + HO2 = LIMALAOOH ;
% KRO2NO : LIMALAO2 + NO = LIMALAO + NO2 ;
% KRO2NO3 : LIMALAO2 + NO3 = LIMALAO + NO2 ;
% 8.80D-13*0.2*RO2 : LIMALAO2 = LIMALACO ;
% 8.80D-13*0.6*RO2 : LIMALAO2 = LIMALAO ;
% 8.80D-13*0.2*RO2 : LIMALAO2 = LIMALAOH ;
% 9.34D-11 : LIMALAOH + OH = LIMALACO + HO2 ;
% 1.06D-10 : LIMALAOOH + OH = LIMALACO + OH ;
% 1.01D-10 : LIMALBCO + OH = C822CO3 + CO ;
% KDEC : LIMALBO = C822CO3 + HCHO ;
% KRO2HO2*0.914 : LIMALBO2 + HO2 = LIMALBOOH ;
% KRO2NO : LIMALBO2 + NO = LIMALBO + NO2 ;
% KRO2NO3 : LIMALBO2 + NO3 = LIMALBO + NO2 ;
% 8.80D-13*0.05*RO2 : LIMALBO2 = LIMALBCO ;
% 8.80D-13*0.9*RO2 : LIMALBO2 = LIMALBO ;
% 8.80D-13*0.05*RO2 : LIMALBO2 = LIMALBOH ;
% 9.04D-11 : LIMALBOH + OH = LIMALBCO + HO2 ;
% 9.73D-11 : LIMALBOOH + OH = LIMALBCO + OH ;
% 3.01D-11 : LIMALNO3 + OH = LMLKET + HCHO + NO2 ;
% KDEC : LIMALO = LMLKET + HCHO + HO2 ;
% KRO2HO2*0.914 : LIMALO2 + HO2 = LIMALOOH ;
% KRO2NO*0.059 : LIMALO2 + NO = LIMALNO3 ;
% KRO2NO*0.941 : LIMALO2 + NO = LIMALO + NO2 ;
% KRO2NO3 : LIMALO2 + NO3 = LIMALO + NO2 ;
% 9.20D-14*0.7*RO2 : LIMALO2 = LIMALO ;

% 9.20D-14*0.3*RO2 : LIMALO2 = LIMALOH ;
% 4.31D-11 : LIMALOH + OH = LMLKET + HCHO + HO2 ;
% KDEC : LIMALOOA = C926O2 + OH ;
% 4.65D-11 : LIMALOOH + OH = LIMALO2 ;
% 6.20D-11 : LIMANO3 + OH = LIMAL + NO2 ;
% KDEC : LIMAO = LIMAL + HO2 ;
% KRO2HO2*0.914 : LIMAO2 + HO2 = LIMAOOH ;
% KRO2NO*0.228 : LIMAO2 + NO = LIMANO3 ;
% KRO2NO*0.772 : LIMAO2 + NO = LIMAO + NO2 ;
% KRO2NO3 : LIMAO2 + NO3 = LIMAO + NO2 ;
% 9.20D-14*0.7*RO2 : LIMAO2 = LIMAO ;
% 9.20D-14*0.3*RO2 : LIMAO2 = LIMAOH ;
% 7.02D-11 : LIMAOH + OH = LIMBCO + HO2 ;
% 7.36D-11 : LIMAOOH + OH = LIMAO2 ;
% 6.70D-11 : LIMBCO + OH = C923CO3 ;
% 5.91D-11 : LIMBNO3 + OH = LIMBCO + NO2 ;
% KDEC : LIMBO = LIMAL + HO2 ;
% KRO2HO2*0.914 : LIMBO2 + HO2 = LIMBOOH ;
% KRO2NO*0.228 : LIMBO2 + NO = LIMBNO3 ;
% KRO2NO*0.772 : LIMBO2 + NO = LIMBO + NO2 ;
% KRO2NO3 : LIMBO2 + NO3 = LIMBO + NO2 ;
% 8.80D-13*0.2*RO2 : LIMBO2 = LIMAOH ;
% 8.80D-13*0.2*RO2 : LIMBO2 = LIMBCO ;
% 8.80D-13*0.6*RO2 : LIMBO2 = LIMBO ;
% 1.20D-15 : LIMBOO + CO = LIMAL ;
% 1.00D-14 : LIMBOO + NO = LIMAL + NO2 ;
% 1.00D-15 : LIMBOO + NO2 = LIMAL + NO3 ;
% 7.00D-14 : LIMBOO + SO2 = LIMAL + SO3 ;
% 1.40D-17*H2O : LIMBOO = LIMAL + H2O2 ;
% 2.00D-18*H2O : LIMBOO = LIMONONIC ;
% 1.04D-10 : LIMBOOH + OH = LIMBCO + OH ;
% 9.31D-11 : LIMCNO3 + OH = LIMKET + HCHO + NO2 ;
% KDEC : LIMCO = LIMKET + HCHO + HO2 ;
% KRO2HO2*0.914 : LIMCO2 + HO2 = LIMCOOH ;
% KRO2NO*0.228 : LIMCO2 + NO = LIMCNO3 ;
% KRO2NO*0.772 : LIMCO2 + NO = LIMCO + NO2 ;
% KRO2NO3 : LIMCO2 + NO3 = LIMCO + NO2 ;
% 9.20D-14*0.7*RO2 : LIMCO2 = LIMCO ;
% 9.20D-14*0.3*RO2 : LIMCO2 = LIMCOH ;
% 9.94D-11 : LIMCOH + OH = LIMKET + HCHO + HO2 ;
% 1.03D-10 : LIMCOOH + OH = LIMCO2 ;
% 9.40D-12 : LIMKET + NO3 = NLMKAO2 ;
% 1.50D-16*0.730 : LIMKET + O3 = LMKOOA ;
% 1.50D-16*0.270 : LIMKET + O3 = LMKOOB ;
% 9.97D-11*0.647 : LIMKET + OH = LMKAO2 ;

% 9.97D-11*0.353 : LIMKET + OH = LMKBO2 ;
% 1.22D-11 : LIMONENE + NO3 = NLIMO2 ;
% 2.13D-16*0.730 : LIMONENE + O3 = LIMOOA ;
% 2.13D-16*0.270 : LIMONENE + O3 = LIMOOB ;
% 1.64D-10*0.408 : LIMONENE + OH = LIMAO2 ;
% 1.64D-10*0.222 : LIMONENE + OH = LIMBO2 ;
% 1.64D-10*0.370 : LIMONENE + OH = LIMCO2 ;
% 5.89D-11 : LIMONIC + OH = C823O2 ;
% 6.98D-11 : LIMONONIC + OH = C923O2 ;
% KDEC*0.5 : LIMOOA = LIMALAO2 + OH ;
% KDEC*0.5 : LIMOOA = LIMALBO2 + OH ;
% KDEC*0.5 : LIMOOB = C923O2 + CO + OH ;
% KDEC*0.5 : LIMOOB = LIMBOO ;
% 9.20D-12 : LMKANO3 + OH = LMLKET + NO2 ;
% KDEC : LMKAO = LMLKET + HO2 ;
% KRO2HO2*0.914 : LMKAO2 + HO2 = LMKAOOH ;
% KRO2NO*0.240 : LMKAO2 + NO = LMKANO3 ;
% KRO2NO*0.760 : LMKAO2 + NO = LMKAO + NO2 ;
% KRO2NO3 : LMKAO2 + NO3 = LMKAO + NO2 ;
% 9.20D-14*0.7*RO2 : LMKAO2 = LMKAO ;
% 9.20D-14*0.3*RO2 : LMKAO2 = LMKAOH ;
% 1.74D-11 : LMKAOH + OH = LMKBCO + HO2 ;
% 2.08D-11 : LMKAOOH + OH = LMKAO2 ;
% 1.60D-11 : LMKBCO + OH = C817CO3 ;
% 6.30D-12 : LMKBNO3 + OH = LMKBCO + NO2 ;
% KDEC : LMKBO = LMLKET + HO2 ;
% KRO2HO2*0.914 : LMKBO2 + HO2 = LMKBOOH ;
% KRO2NO*0.240 : LMKBO2 + NO = LMKBNO3 ;
% KRO2NO*0.760 : LMKBO2 + NO = LMKBO + NO2 ;
% KRO2NO3 : LMKBO2 + NO3 = LMKBO + NO2 ;
% 8.80D-13*0.2*RO2 : LMKBO2 = LMKAOH ;
% 8.80D-13*0.2*RO2 : LMKBO2 = LMKBCO ;
% 8.80D-13*0.6*RO2 : LMKBO2 = LMKBO ;
% 1.20D-15 : LMKBOO + CO = LMLKET ;
% 1.00D-14 : LMKBOO + NO = LMLKET + NO2 ;
% 1.00D-15 : LMKBOO + NO2 = LMLKET + NO3 ;
% 7.00D-14 : LMKBOO + SO2 = LMLKET + SO3 ;
% 2.00D-18*H2O : LMKBOO = KLIMONONIC ;
% 1.40D-17*H2O : LMKBOO = LMLKET + H2O2 ;
% 4.76D-11 : LMKBOOH + OH = LMKBCO + OH ;
% KDEC*0.5 : LMKOOA = LMLKAO2 + OH ;
% KDEC*0.5 : LMKOOA = LMLKBO2 + OH ;
% KDEC*0.5 : LMKOOB = C817O2 + CO + OH ;
% KDEC*0.5 : LMKOOB = LMKBOO ;
% 3.58D-11 : LMLKACO + OH = C626CHO + CH3CO3 + TPENE ;

% KDEC : LMLKAO = C626CHO + CH3CO3 + TPENE ;
% KRO2HO2*0.914 : LMLKAO2 + HO2 = LMLKAOOH ;
% KRO2NO : LMLKAO2 + NO = LMLKAO + NO2 ;
% KRO2NO3 : LMLKAO2 + NO3 = LMLKAO + NO2 ;
% 8.80D-13*0.2*RO2 : LMLKAO2 = LMLKACO ;
% 8.80D-13*0.6*RO2 : LMLKAO2 = LMLKAO2 ;
% 8.80D-13*0.2*RO2 : LMLKAO2 = LMLKAOH ;
% 4.57D-11 : LMLKAOH + OH = LMLKACO + HO2 ;
% 5.79D-11 : LMLKAOOH + OH = LMLKACO + OH ;
% 5.09D-11 : LMLKBCO + OH = C731CO3 + CO ;
% KDEC : LMLKBO = C731CO3 + HCHO ;
% KRO2HO2*0.914 : LMLKBO2 + HO2 = LMLKBOOH ;
% KRO2NO : LMLKBO2 + NO = LMLKBO + NO2 ;
% KRO2NO3 : LMLKBO2 + NO3 = LMLKBO + NO2 ;
% 8.80D-13*0.05*RO2 : LMLKBO2 = LMLKBCO ;
% 8.80D-13*0.9*RO2 : LMLKBO2 = LMLKBO ;
% 8.80D-13*0.05*RO2 : LMLKBO2 = LMLKBOH ;
% 4.09D-11 : LMLKBOH + OH = LMLKBCO + HO2 ;
% 4.77D-11 : LMLKBOOH + OH = LMLKBCO + OH ;
% KNO3AL*8.5 : LMLKET + NO3 = C817CO3 + HNO3 ;
% 3.60D-11*0.748 : LMLKET + OH = C817CO3 ;
% 3.60D-11*0.252 : LMLKET + OH = C926O2 ;
% KDEC : M2PROPAL2O = CH3COCH3 + HO2 + CO ;
% 9.64D-13 : MEKANO3 + OH = CO2C3CHO + NO2 ;
% KROPRIM : MEKAO + O2 = CO2C3CHO + HO2 ;
% 1.26D+5 : MEKAO = HO1CO3C4O2 ;
% KRO2HO2*0.625 : MEKAO2 + HO2 = MEKAOOH ;
% KRO2NO*0.033 : MEKAO2 + NO = MEKANO3 ;
% KRO2NO*0.967 : MEKAO2 + NO = MEKAO + NO2 ;
% KRO2NO3 : MEKAO2 + NO3 = MEKAO + NO2 ;
% 2.00D-12*0.2*RO2 : MEKAO2 = CO2C3CHO ;
% 2.00D-12*0.6*RO2 : MEKAO2 = MEKAO ;
% 2.00D-12*0.2*RO2 : MEKAO2 = MEKAOH ;
% 1.35D-11 : MEKAOH + OH = CO2C3CHO + HO2 ;
% 4.88D-11 : MEKAOOH + OH = CO2C3CHO + OH ;
% 3.59D-12 : MEKAOOH + OH = MEKAO2 ;
% KNO3AL*8.5 : MIBKHO4CHO + NO3 = TBUTOLO2 + CO + CO + HNO3 ;
% 1.34D-11 : MIBKHO4CHO + OH = TBUTOLO2 + CO + CO ;
% KDEC : NAPINAO = PINAL + NO2 ;
% KRO2HO2*0.914 : NAPINAO2 + HO2 = NAPINAOOH ;
% KRO2NO : NAPINAO2 + NO = NAPINAO + NO2 ;
% KRO2NO3 : NAPINAO2 + NO3 = NAPINAO + NO2 ;
% 6.70D-15*0.1*RO2 : NAPINAO2 = APINBNO3 ;
% 6.70D-15*0.9*RO2 : NAPINAO2 = NAPINAO ;
% 6.87D-12 : NAPINAOOH + OH = NAPINAO2 ;

% KROSEC*O2 : NAPINBO = NC101CO + HO2 ;
% 4.00D+05 : NAPINBO = PINAL + NO2 ;
% KRO2HO2*0.914 : NAPINBO2 + HO2 = NAPINBOOH ;
% KRO2NO : NAPINBO2 + NO = NAPINBO + NO2 ;
% KRO2NO3 : NAPINBO2 + NO3 = NAPINBO + NO2 ;
% 2.50D-13*0.1*RO2 : NAPINBO2 = APINANO3 ;
% 2.50D-13*0.8*RO2 : NAPINBO2 = NAPINBO ;
% 2.50D-13*0.1*RO2 : NAPINBO2 = NC101CO ;
% 3.59D-12 : NAPINBOOH + OH = NAPINBO2 ;
% 1.23D-11 : NAPINBOOH + OH = NC101CO + OH ;
% KDEC : NBPINAO = NOPINONE + HCHO + NO2 ;
% KRO2HO2*0.914 : NBPINAO2 + HO2 = NBPINAOOH ;
% KRO2NO : NBPINAO2 + NO = NBPINAO + NO2 ;
% KRO2NO3 : NBPINAO2 + NO3 = NBPINAO + NO2 ;
% 9.20D-14*0.3*RO2 : NBPINAO2 = BPINBNO3 ;
% 9.20D-14*0.7*RO2 : NBPINAO2 = NBPINAO ;
% 9.58D-12 : NBPINAOOH + OH = NBPINAO2 ;
% 7.00D+03 : NBPINBO = NOPINONE + HCHO + NO2 ;
% KRO2HO2*0.914 : NBPINBO2 + HO2 = NBPINBOOH ;
% KRO2NO : NBPINBO2 + NO = NBPINBO + NO2 ;
% KRO2NO3 : NBPINBO2 + NO3 = NBPINBO + NO2 ;
% 2.00D-12*0.2*RO2 : NBPINBO2 = BPINANO3 ;
% 2.00D-12*0.6*RO2 : NBPINBO2 = NBPINBO ;
% 2.00D-12*0.6*RO2 : NBPINBO2 = NC91CHO ;
% 9.08D-12 : NBPINBOOH + OH = NC91CHO + OH ;
% 5.55D-12 : NC101CO + OH = NC101O2 ;
% KDEC : NC101O = NC102O2 ;
% KRO2HO2*0.914 : NC101O2 + HO2 = NC101OOH ;
% KRO2NO : NC101O2 + NO = NC101O + NO2 ;
% KRO2NO3 : NC101O2 + NO3 = NC101O + NO2 ;
% 6.70D-15*RO2 : NC101O2 = NC101O ;
% 5.94D-12 : NC101OOH + OH = NC101O2 ;
% KDEC : NC102O = NC71O2 + CH3COCH3 ;
% KRO2HO2*0.914 : NC102O2 + HO2 = NC102OOH ;
% KRO2NO : NC102O2 + NO = NC102O + NO2 ;
% KRO2NO3 : NC102O2 + NO3 = NC102O + NO2 ;
% 6.70D-15*RO2 : NC102O2 = NC102O ;
% 8.03D-12 : NC102OOH + OH = NC102O2 ;
% KAPHO2*0.44 : NC61CO3 + HO2 = CO235C5CHO + NO2 + OH ;
% KAPHO2*0.56 : NC61CO3 + HO2 = NC61CO3H ;
% KAPNO : NC61CO3 + NO = CO235C5CHO + NO2 + NO2 ;
% KFPAN : NC61CO3 + NO2 = NC6PAN1 ;
% KRO2NO3*1.74 : NC61CO3 + NO3 = CO235C5CHO + NO2 + NO2 ;
% 1.00D-11*RO2 : NC61CO3 = CO235C5CHO + NO2 ;
% 1.68D-11 : NC61CO3H + OH = NC61CO3 ;

% KDEC : NC623O = HMVKBCHO + HCHO + NO2 ;
% KRO2HO2*0.770 : NC623O2 + HO2 = NC623OOH ;
% KRO2NO : NC623O2 + NO = NC623O + NO2 ;
% KRO2NO3 : NC623O2 + NO3 = NC623O + NO2 ;
% 8.00D-13*0.7*RO2 : NC623O2 = NC623O ;
% 8.00D-13*0.3*RO2 : NC623O2 = NC623OH ;
% 3.62D-11 : NC623OH + OH = HMVKBCHO + HCHO + NO2 ;
% 3.96D-11 : NC623OOH + OH = NC623O2 ;
% 1.32D-11 : NC6PAN1 + OH = CO235C5CHO + CO + NO2 + NO2 ;
% 1.9D17*EXP(-14100/TEMP) : NC6PAN1 = NC61CO3 + NO2 ;
% 1.25D-12 : NC71CO + OH = NC72O2 ;
% 4.00D+04 : NC71O = CO235C6CHO + NO2 ;
% KROSEC*O2 : NC71O = NC71CO + HO2 ;
% KRO2HO2*0.820 : NC71O2 + HO2 = NC71OOH ;
% KRO2NO : NC71O2 + NO = NC71O + NO2 ;
% KRO2NO3 : NC71O2 + NO3 = NC71O + NO2 ;
% 2.50D-13*RO2 : NC71O2 = NC71O ;
% 3.25D-11 : NC71OOH + OH = NC71O2 ;
% KDEC : NC728O = C517CHO + HCHO + NO2 ;
% KRO2HO2*0.770 : NC728O2 + HO2 = NC728OOH ;
% KRO2NO : NC728O2 + NO = NC728O + NO2 ;
% KRO2NO3 : NC728O2 + NO3 = NC728O + NO2 ;
% 9.20D-14*0.7*RO2 : NC728O2 = NC728O ;
% 9.20D-14*0.3*RO2 : NC728O2 = NC728OH ;
% 3.59D-11 : NC728OH + OH = C517CHO + HCHO + NO2 ;
% 3.94D-11 : NC728OOH + OH = NC728O2 ;
% KDEC : NC72O = NC61CO3 ;
% KRO2HO2*0.820 : NC72O2 + HO2 = NC72OOH ;
% KRO2NO : NC72O2 + NO = NC72O + NO2 ;
% KRO2NO3 : NC72O2 + NO3 = NC72O + NO2 ;
% 8.80D-13*RO2 : NC72O2 = NC72O ;
% 1.85D-11 : NC72OOH + OH = NC72O2 ;
% KDEC : NC730O = C519CHO + HCHO + NO2 ;
% KRO2HO2*0.820 : NC730O2 + HO2 = NC730OOH ;
% KRO2NO : NC730O2 + NO = NC730O + NO2 ;
% KRO2NO3 : NC730O2 + NO3 = NC730O + NO2 ;
% 9.20D-14*0.7*RO2 : NC730O2 = NC730O ;
% 9.20D-14*0.3*RO2 : NC730O2 = NC730OH ;
% 3.34D-11 : NC730OH + OH = C519CHO + HCHO + NO2 ;
% 3.58D-11 : NC730OOH + OH = NC730O2 ;
% KDEC : NC826O = C626CHO + HCHO + NO2 ;
% KRO2HO2*0.859 : NC826O2 + HO2 = NC826OOH ;
% KRO2NO : NC826O2 + NO = NC826O + NO2 ;
% KRO2NO3 : NC826O2 + NO3 = NC826O + NO2 ;
% 9.20D-14*0.7*RO2 : NC826O2 = NC826O ;

% 9.20D-14*0.3*RO2 : NC826O2 = NC826OH ;
% 5.54D-11 : NC826OH + OH = NC826O ;
% 5.89D-11 : NC826OOH + OH = NC826O2 ;
% KNO3AL*8.5 : NC91CHO + NO3 = NC91CO3 + HNO3 ;
% 8.63D-12 : NC91CHO + OH = NC91CO3 ;
% KAPHO2*0.56 : NC91CO3 + HO2 = NC91CO3H ;
% KAPHO2*0.44 : NC91CO3 + HO2 = NOPINONE + NO2 + OH ;
% KAPNO : NC91CO3 + NO = NOPINONE + NO2 + NO2 ;
% KFPAN : NC91CO3 + NO2 = NC91PAN ;
% KRO2NO3*1.74 : NC91CO3 + NO3 = NOPINONE + NO2 + NO2 ;
% 1.00D-11*RO2 : NC91CO3 = NOPINONE + NO2 ;
% 8.85D-12 : NC91CO3H + OH = NC91CO3 ;
% 4.90D-12 : NC91PAN + OH = NOPINONE + CO + NO2 + NO2 ;
% 1.9D17*EXP(-14100/TEMP) : NC91PAN = NC91CO3 + NO2 ;
% KDEC : NLIMALO = LMLKET + HCHO + NO2 ;
% KRO2HO2*0.914 : NLIMALO2 + HO2 = NLIMALOOH ;
% KRO2NO : NLIMALO2 + NO = NLIMALO + NO2 ;
% KRO2NO3 : NLIMALO2 + NO3 = NLIMALO + NO2 ;
% 9.20D-14*0.7*RO2 : NLIMALO2 = NLIMALO ;
% 9.20D-14*0.3*RO2 : NLIMALO2 = NLIMALOH ;
% 3.93D-11 : NLIMALOH + OH = LMLKET + HCHO + NO2 ;
% 4.28D-11 : NLIMALOOH + OH = NLIMALO2 ;
% KDEC : NLIMO = LIMAL + NO2 ;
% KRO2HO2*0.914 : NLIMO2 + HO2 = NLIMOOH ;
% KRO2NO : NLIMO2 + NO = NLIMO + NO2 ;
% KRO2NO3 : NLIMO2 + NO3 = NLIMO + NO2 ;
% 9.20D-14*0.3*RO2 : NLIMO2 = LIMBNO3 ;
% 9.20D-14*0.7*RO2 : NLIMO2 = NLIMO ;
% 4.28D-11 : NLIMOOH + OH = NLIMO2 ;
% KDEC : NLMKAO = LMLKET + NO2 ;
% KRO2HO2*0.914 : NLMKAO2 + HO2 = NLMKAOOH ;
% KRO2NO*0.760 : NLMKAO2 + NO = NLMKAO + NO2 ;
% KRO2NO3 : NLMKAO2 + NO3 = NLMKAO + NO2 ;
% 9.20D-14*0.3*RO2 : NLMKAO2 = LMKBNO3 ;
% 9.20D-14*0.7*RO2 : NLMKAO2 = NLMKAO ;
% 1.01D-11 : NLMKAOOH + OH = NLMKAO2 ;
% 3.24D-12 : NOPINANO3 + OH = C9DC + NO2 ;
% 5.62D+4 : NOPINAO = C918O2 ;
% KROSEC*O2 : NOPINAO = C9DC + HO2 ;
% KRO2HO2*0.890 : NOPINAO2 + HO2 = NOPINAOOH ;
% KRO2NO*0.157 : NOPINAO2 + NO = NOPINANO3 ;
% KRO2NO*0.843 : NOPINAO2 + NO = NOPINAO + NO2 ;
% KRO2NO3 : NOPINAO2 + NO3 = NOPINAO + NO2 ;
% 2.50D-13*0.2*RO2 : NOPINAO2 = C9DC ;
% 2.50D-13*0.6*RO2 : NOPINAO2 = NOPINAO ;

% 2.50D-13*0.2*RO2 : NOPINAO2 = NOPINAOH ;
% 3.68D-11 : NOPINAOH + OH = C9DC + HO2 ;
% 8.59D-11 : NOPINAOOH + OH = C9DC + OH ;
% 1.64D-11 : NOPINBCO + OH = C915O2 ;
% 6.05D-12 : NOPINBNO3 + OH = NOPINBCO + NO2 ;
% KDEC : NOPINBO = C915O2 ;
% KRO2HO2*0.890 : NOPINBO2 + HO2 = NOPINBOOH ;
% KRO2NO*0.157 : NOPINBO2 + NO = NOPINBNO3 ;
% KRO2NO*0.843 : NOPINBO2 + NO = NOPINBO + NO2 ;
% KRO2NO3 : NOPINBO2 + NO3 = NOPINBO + NO2 ;
% 2.50D-13*0.2*RO2 : NOPINBO2 = NOPINBCO ;
% 2.50D-13*0.6*RO2 : NOPINBO2 = NOPINBO ;
% 2.50D-13*0.2*RO2 : NOPINBO2 = NOPINBOH ;
% 1.81D-11 : NOPINBOH + OH = NOPINBCO + HO2 ;
% 3.44D-11 : NOPINBOOH + OH = NOPINBCO + OH ;
% 6.37D-12 : NOPINCNO3 + OH = CH3COCH3 + C619CO + NO2 ;
% KDEC : NOPINCO = C917O2 ;
% KRO2HO2*0.890 : NOPINCO2 + HO2 = NOPINCOOH ;
% KRO2NO*0.118 : NOPINCO2 + NO = NOPINCNO3 ;
% KRO2NO*0.882 : NOPINCO2 + NO = NOPINCO + NO2 ;
% KRO2NO3 : NOPINCO2 + NO3 = NOPINCO + NO2 ;
% 6.70D-15*0.7*RO2 : NOPINCO2 = NOPINCO ;
% 6.70D-15*0.3*RO2 : NOPINCO2 = NOPINCOH ;
% 7.69D-12 : NOPINCOH + OH = NOPINCO ;
% 1.11D-11 : NOPINCOOH + OH = NOPINCO2 ;
% 3.07D-12 : NOPINDCO + OH = C89CO3 ;
% KDEC : NOPINDO = C89CO3 ;
% KRO2HO2*0.890 : NOPINDO2 + HO2 = NOPINDOOH ;
% KRO2NO : NOPINDO2 + NO = NOPINDO + NO2 ;
% KRO2NO3 : NOPINDO2 + NO3 = NOPINDO + NO2 ;
% 2.00D-12*0.05*RO2 : NOPINDO2 = NOPINDCO ;
% 2.00D-12*0.9*RO2 : NOPINDO2 = NOPINDO ;
% 2.00D-12*0.05*RO2 : NOPINDO2 = NOPINDOH ;
% 1.41D-11 : NOPINDOH + OH = NOPINDCO + HO2 ;
% 2.63D-11 : NOPINDOOH + OH = NOPINDCO + OH ;
% 1.55D-11*0.535 : NOPINONE + OH = NOPINAO2 ;
% 1.55D-11*0.199 : NOPINONE + OH = NOPINBO2 ;
% 1.55D-11*0.130 : NOPINONE + OH = NOPINCO2 ;
% 1.55D-11*0.136 : NOPINONE + OH = NOPINDO2 ;
% 1.20D-15 : NOPINOO + CO = NOPINONE ;
% 1.00D-14 : NOPINOO + NO = NOPINONE + NO2 ;
% 1.00D-15 : NOPINOO + NO2 = NOPINONE + NO3 ;
% 7.00D-14 : NOPINOO + SO2 = NOPINONE + SO3 ;
% 6.00D-18*H2O : NOPINOO = NOPINONE + H2O2 ;
% KDEC*0.330 : NOPINOOA = C8BC ;

% KDEC*0.500 : NOPINOOA = NOPINDO2 + OH ;
% KDEC*0.170 : NOPINOOA = NOPINOO ;
% 8.00D-11*0.288 : NORLIMAL + OH = C816CO3 ;
% 8.00D-11*0.712 : NORLIMAL + OH = NORLIMO2 ;
% KDEC : NORLIMO = C817CO + HCHO + HO2 ;
% KRO2HO2*0.890 : NORLIMO2 + HO2 = NORLIMOOH ;
% KRO2NO : NORLIMO2 + NO = NORLIMO + NO2 ;
% KRO2NO3 : NORLIMO2 + NO3 = NORLIMO + NO2 ;
% 9.20D-14*RO2 : NORLIMO2 = NORLIMO ;
% 3.64D-11 : NORLIMOOH + OH = NORLIMO2 ;
% KNO3AL*8.5 : NORPINAL + NO3 = C85CO3 + HNO3 ;
% 2.64D-11 : NORPINAL + OH = C85CO3 ;
% 6.57D-12 : NORPINIC + OH = C721O2 ;
% 9.73D-12 : PERPINONIC + OH = C96CO3 ;
% 2.0D-14 : PINAL + NO3 = C96CO3 + HNO3 ;
% 3.89D-11*0.772 : PINAL + OH = C96CO3 ;
% 3.89D-11*0.228 : PINAL + OH = PINALO2 ;
% 2.25D-11 : PINALNO3 + OH = CO235C6CHO + CH3COCH3 + NO2 ;
% KDEC : PINALO = C106O2 ;
% KRO2HO2*0.914 : PINALO2 + HO2 = PINALOOH ;
% KRO2NO*0.050 : PINALO2 + NO = PINALNO3 ;
% KRO2NO*0.950 : PINALO2 + NO = PINALO + NO2 ;
% KRO2NO3 : PINALO2 + NO3 = PINALO + NO2 ;
% 6.70D-15*0.7*RO2 : PINALO2 = PINALO ;
% 6.70D-15*0.3*RO2 : PINALO2 = PINALOH ;
% 2.41D-11 : PINALOH + OH = PINALO ;
% 2.75D-11 : PINALOOH + OH = PINALO2 ;
% 7.29D-12 : PINIC + OH = C811O2 ;
% 6.65D-12 : PINONIC + OH = C96O2 ;
% 5.21D-13 : TBUTOLNO3 + OH = IBUTALOH + NO2 ;
% 1.40D+7 : TBUTOLO = CH3COCH3 + HCHO + HO2 ;
% 1.42D-11 : TBUTOLO2 + HO2 = TBUTOLOOH ;
% KRO2NO*0.017 : TBUTOLO2 + NO = TBUTOLNO3 ;
% KRO2NO*0.983 : TBUTOLO2 + NO = TBUTOLO + NO2 ;
% KRO2NO3 : TBUTOLO2 + NO3 = NO2 + TBUTOLO ;
% 2.00D-13*0.2*RO2 : TBUTOLO2 = IBUTALOH ;
% 2.00D-13*0.2*RO2 : TBUTOLO2 = IBUTOLOHB ;
% 2.00D-13*0.6*RO2 : TBUTOLO2 = TBUTOLO ;
% 9.98D-12 : TBUTOLOOH + OH = IBUTALOH + OH ;
% 3.60D-12 : TBUTOLOOH + OH = TBUTOLO2 ;

Appendix C: 0-D Photochemical Mechanism Photolysis Reactions

Below is a list of photolysis reactions (isoprene and terpene subsets) used in all simulations of this study. Note that names of chemical species are consistent with the MCM website.

0-D Photolysis Reactions

*All Photolysis Reactions;

% J1 : O3 = O2 + O_1D ;
% J2 : O3 = O2 + O_3P ;
% J3 : H2O2 = OH + OH ;
% J4 : NO2 = NO + O_3P ;
% J5 : NO3 = NO ;
% J6 : NO3 = NO2 + O_3P ;
% J7 : HONO = OH + NO ;
% J8 : HNO3 = OH + NO2;
% J9 : HNO3 = HONO + O_1D;
% J11 : HCHO = CO + HO2 + HO2 ;
% J12 : HCHO = H2 + CO ;
% J13 : CH3CHO = CH3O2 + HO2 + CO ;
% J13 : HPALD = products + OH + OH ;
% J15*2 : C32OH13CO = GLYOX + HO2 + HO2 + CO ;
% J15 : C42AOH = HO2 + CO + HO2 + NO3CH2CHO ;
% J15 : C4M2ALOHNO3 = CONM2CHO + HO2 + CO + HO2 ;
% J15 : C58NO3 = HO2 + CO + MACRNO3 + HO2 ;
% J15 : CO2H3CHO = MGLYOX + CO + HO2 + HO2 + BL ;
% J15 : CO2N3CHO = CO + HO2 + MGLYOX + NO2 + BM ;
% J15 : H13CO2CHO = HOCH2CHO + CO + HO2 + HO2 ;
% J15 : HCOCH2OOH = HO2 + CO + HCHO + OH ;
% J15 : HCOCO3H = HO2 + CO + OH ;
% J15 : HIEB2OOH = HMACROH + CO + OH + HO2 ;
% J15 : HOCH2CHO = HO2 + HCHO + HO2 + CO ;
% J15 : IECCHO = MACRO2 + HO2 + CO ;
% J15 : IEB2OOH = MACROH + OH + CO + HO2 ;
% J15 : INB1NACHO = MACRNO3 + NO2 + CO + HO2 ;
% J15 : INB1HPCHO = MACRNO3 + OH + CO + HO2 ;
% J15 : INCNCHO = MACRNO3 + CO + NO2 + HO2 ;
% J15 : MMALNBPAN = CONM2PAN + HO2 + CO + HO2 ;
% J15 : MMALNBCO3H = CONM2CO3H + HO2 + CO + HO2 ;

% J15 : MMALNBCO2H = CONM2CO2H + HO2 + CO + HO2 ;
% J15 : C107OOH = C107O + OH ;
% J15 : C107OH = C107O + HO2 ;
% J15 : C109OOH = C109O + OH ;
% J15 : C109CO = C89CO3 + CO + HO2 ;
% J15 : C109OH = C920O2 + CO + HO2 ;
% J15 : C89CO2H = C89CO2 + HO2 ;
% J15 : C89CO3H = C89CO2 + OH ;
% J15 : C918OOH = C918O + OH ;
% J15 : C918NO3 = C918O + NO2 ;
% J15 : C918OH = C918O + HO2 ;
% J15 : C915OOH = C915O + OH ;
% J15 : C915NO3 = C915O + NO2 ;
% J15 : C88CHO = C88O2 + HO2 + CO ;
% J15*2 : C626CHO = C626O2 + CO + HO2 ;
% J15 : C729CO2H = C729O2 + HO2 ;
% J15 : C729CO3H = C729O2 + OH ;
% J15 : C716OH = H3C25C6O2 + CO + HO2 ;
% J15 : C512CO2H = C512O2 + HO2 ;
% J15 : C512CO3H = C512O2 + OH ;
% J15 : C89OOH = C89O + OH ;
% J15 : C89NO3 = C89O + NO2 ;
% J15 : C89OH = C89O + HO2 ;
% J15*2 : C926OOH = C926O + OH ;
% J15*2 : C926OH = C926O + HO2 ;
% J15*2 : C826OOH = C826O + OH ;
% J15*2 : C826OH = C826O + HO2 ;
% J15 : C729OOH = C729O + OH ;
% J15 : C622CHO = C622O2 + CO + HO2 ;
% J15 : C106OOH = C106O + OH ;
% J15 : C106NO3 = C106O + NO2 ;
% J15 : C106OH = C106O + HO2 ;
% J15 : C86OOH = C86O + OH ;
% J15*2 : C919OOH = C919O + OH ;
% J15*2 : C919NO3 = C919O + NO2 ;
% J15 : C919OH = C919O + HO2 ;
% J15 : C914OOH = C914O + OH ;
% J15 : C914CO = C87CO3 ;
% J15*2 : C916OOH = C916O + OH ;
% J15*2 : C916NO3 = C916O + NO2 ;
% J15*2 : C916OH = C916O + HO2 ;
% J15 : C512OOH = C512O + OH ;
% J15 : C512NO3 = C512O + NO2 ;
% J15 : C512OH = C512O + HO2 ;
% J15 : CO25C6CHO = C627O2 + CO + HO2 ;

% J15 : C626CO2H = C626O2 + HO2 ;
% J15 : C626CO3H = C626O2 + OH ;
% J15 : C626OOH = C626O + OH ;
% J15 : C517CHO = C517O2 + CO + HO2 ;
% J15*2 : C735OOH = CO13C4CHO + CH3CO3 + OH + TPENE ;
% J15*2 : C735OH = CO13C4CHO + CH3CO3 + HO2 + TPENE ;
% J15 : C721CHO = C721O2 + CO + HO2 ;
% J15 : C413COOOH = CHOC3COO + OH ;
% J15*2 : C729CHO = C729O2 + CO + HO2 ;
% J15 : C810OOH = C810O + OH ;
% J15 : C810NO3 = C810O + NO2 ;
% J15 : C810OH = C810O + HO2 ;
% J15 : C518CHO = ISOPDO2 + CO + HO2 ;
% J15 : C823CO = C825O2 + HO2 ;
% J15 : C4CODIAL = CHOCOCH2O2 + HO2 + CO ;
% J15 : C716OOH = C716O + OH ;
% J15 : C511OOH = C511O + OH ;
% J15*2 : C620OOH = C620O + OH ;
% J15*2 : C515CHO = C515O2 + HO2 + CO ;
% J15*2 : C620OH = C620O + HO2 ;
% J15*2 : C87CO2H = C87O2 + HO2 ;
% J15*2 : C87CO3H = C87O2 + OH ;
% J15*2 : C616OOH = C616O + OH ;
% J15*2 : C616OH = C616O + HO2 ;
% J15 : C718CO2H = C718O2 + HO2 ;
% J15 : C718CO3H = C718O2 + OH ;
% J15 : C513OOH = C513O + OH ;
% J15 : C513OH = C513O + HO2 ;
% J15 : C511CO3H = C511O2 + OH ;
% J15 : C628OOH = CO13C4OH + CH3CO3 + OH + TPENE ;
% J15 : C628OH = CO13C4OH + CH3CO3 + HO2 + TPENE ;
% J15*2 : C87CO = C615CO3 + CO + HO2 ;
% J15 : C718OOH = C718O + OH ;
% J15 : C718NO3 = C718O + NO2 ;
% J15 : C617CHO = C617O2 + HO2 + CO ;
% J15 : C617CHO = C618O2 + HO2 + CO ;
% J15 : C718OH = C718O + HO2 ;
% J15*2 : C514OOH = C514O + OH ;
% J15*2 : C514NO3 = C514O + NO2 ;
% J15*2 : C514OH = C514O + HO2 ;
% J15 : C520OOH = BIACETOH + CO + HO2 + OH ;
% J15 : C520OH = BIACETOH + CO + HO2 + HO2 ;
% J15 : C732CO = C734O2 + HO2 ;
% J15*2 : C33CO = CO + HO2 + CO + CO + HO2 ;
% J15*2 : C615CO2H = C615O2 + HO2 ;

% J15*2 : C615CO3H = C615O2 + OH ;
% J15 : C617CO2H = C617O2 + HO2 ;
% J15 : C617CO3H = C617O2 + OH ;
% J15 : C618CO2H = C618O2 + HO2 ;
% J15 : C618CO3H = C618O2 + OH ;
% J15 : C617OOH = C617O + OH ;
% J15 : C615CO = CO1M22CO3 + CO + HO2 ;
% J15 : C617OH = C617O + HO2 ;
% J15 : C618OOH = C618O + OH ;
% J15 : C67CHO = C55O2 + HO2 + CO ;
% J15*2 : C615OOH = C615O + OH ;
% J15*2 : C615OH = C615O + HO2 ;
% J15 : C629OOH = HO1CO34C5 + CO + HO2 + OH ;
% J15 : C629OH = HO1CO34C5 + CO + HO2 + HO2 ;
% J15*2 : CO1M22CHO = IBUTALCO2 + CO + HO2 ;
% J15 : CO1M22CO2H = IBUTALCO2 + HO2 ;
% J15 : CO1M22CO3H = IBUTALCO2 + OH ;
% J15 : CO2C4CHO = MEKAO2 + HO2 + CO ;
% J15 : CO13C4OH = MGLYOX + HO2 + HO2 + CO + BM ;
% J15 : CO23C4CO3H = BIACETO2 + OH ;
% J15 : CO23C4CHO = BIACETO2 + HO2 + CO ;
% J15 : CO12C4CHO = CHOC2CO3 + HO2 + CO ;
% J15 : CO123C5CHO = CHOC2CO3 + HO2 + CO + CO ;
% J15 : CO13C3CO2H = HCOCH2CO3 + HO2 ;
% J15 : CO2C3CHO = CH3COCH2O2 + HCHO ;
% J15*2 : CO13C4CHO = CHOC3COO2 + CO + HO2 ;
% J15 : CHOC3COOOH = CHOC3COO2 + OH ;
% J15 : CHOC2H4OOH = CHOC2H4O + OH ;
% J15 : CHOC2CO3H = CHOC2H4O2 + OH ;
% J15*2 : HCOCH2CHO = HCOCH2O2 + HO2 + CO ;
% J15 : HCOCH2CO2H = HCOCH2O2 + HO2 ;
% J15 : HCOCH2CO3H = HCOCH2O2 + OH ;
% J15 : HMVKBCHO = HMVKO2 + CO + HO2 ;
% J15 : H1C23C4CHO = H1C23C4O2 + CO + HO2 ;
% J15 : HOC2H4CHO = HOCH2CH2O2 + HO2 + CO ;
% J15 : LIMAL = C923O2 + CO + HO2 ;
% J15 : LMLKET = C817O2 + CO + HO2 ;
% J15 : NC91CHO = NOPINONE + CO + HO2 + NO2 ;
% J15*2 : NC826OOH = NC826O + OH ;
% J15*2 : NC826OH = NC826O + HO2 ;
% J15 : NORLIMAL = C816O2 + CO + HO2 ;
% J15 : NORPINAL = C85O2 + CO + HO2 ;
% J15 : PINAL = C96O2 + CO + HO2 ;
% J15 : PINALOOH = PINALO + OH ;
% J15 : PINALNO3 = PINALO + NO2 ;

% J17*2 : C3MDIALOH = MGLYOX + HO2 + CO + HO2 + BN ;
% J17 : C4M2ALOHNO3 = CO2H3CHO + NO2 + CO + HO2 ;
% J17 : C57NO3 = HO2 + CO + HO12CO3C4 + NO2 ;
% J17 : CH3CHOHCHO = CH3CHO + HO2 + CO + HO2 ;
% J17 : CHOMOHCO3H = MGLYOX + OH + HO2 + BO ;
% J17 : COHM2PAN = GLYPAN + CO + HO2 ;
% J17 : COHM2CO3H = HCOCO3H + CO + HO2 ;
% J17 : COHM2CO2H = HCOCO2H + CO + HO2 ;
% J17 : DNC524CO = HMVKNO3 + CO + HO2 + NO2 ;
% J17 : HIEB1OOH = MVKOHAOH + CO + OH + HO2 ;
% J17 : HMACROH = H13CO2C3 + CO + HO2 + HO2 ;
% J17 : HMACROOH = H13CO2C3 + CO + HO2 + OH ;
% J17 : HNC524CO = HMVKNO3 + CO + HO2 + HO2 ;
% J17 : HPNC524CO = HMVKNO3 + CO + HO2 + OH ;
% J17 : IBUTALOH = CH3COCH3 + HO2 + HO2 + CO ;
% J17 : IEB1OOH = HO12CO3C4 + OH + CO + HO2 ;
% J17 : IEC2OOH = BIACETOH + OH + CO + HO2 ;
% J17 : INAHCHO = MVKNO3 + HO2 + CO + HO2 ;
% J17 : INAHPCHO = MVKNO3+ OH + CO + HO2 ;
% J17 : INANCHO = MVKNO3 + NO2 + CO + HO2 ;
% J17 : INB1NBCHO = MVKNO3 + NO2 + CO + HO2 ;
% J17 : INDHCHO = CO + HO2 + MVKNO3 + HO2 ;
% J17 : INDHPCHO = CO + HO2 + MVKNO3 + OH ;
% J17 : MACROH = ACETOL + CO + HO2 + HO2 ;
% J17 : MACROHOOH = IBUTALOH + CO + HO2 + OH ;
% J17 : MACROOH = ACETOL + CO + HO2 + OH ;
% J17 : MACRNO3 = ACETOL + NO2 + CO + HO2 ;
% J17 : MACROHNO3 = NOA + HO2 + CO + HO2 ;
% J17 : C918CHO = NOPINONE + CO + HO2 + HO2 ;
% J17 : IBUTALO2H = CH3COCH3 + OH + HO2 + CO ;
% 0.3*J18 : ACR = ACO3 ;
% 0.4*J18 : ACR = C2H4 + CO ;
% 0.3*J18 : ACR = HCHO + HO2 + CO ;
% J18 : HC4CCHO = CH3CO3 + HO2 + CO + HOCH2CHO + IPRENE ;
% J18 : HC4ACHO = ACETOL + HO2 + HO2 + CO + CO ;
% J18 : NC4CHO = NOA + CO + CO + HO2 + HO2 ;
% J18 : MACR = CH3C2H2O2 + CO + HO2 ;
% J18 : C816CO = MACO3 + MEKAO2 ;
% J19 : HC4ACHO = HC4ACO3 + HO2 ;
% J19 : HC4CCHO = HC4CCO3 + HO2 ;
% J19 : MACR = MACO3 + HO2 ;
% J19 : C816CO = MACO3 + MEKAO2 ;
% J21 : CH3COCH3 = CH3CO3 + CH3O2 + ATONE ;
% J22*0.175 : ACETOL = CH3CO3 + HCHO + HO2 + IPRENE ;
% J22 : C59OOH = HOCH2CO3 + ACETOL + OH ;

% J22 : CO2H3CO3H = CH3CO3 + HO2 + HCOCO3H + IPRENE ;
% J22 : H13CO2C3 = HOCH2CO3 + HCHO + HO2 ;
% J22 : HYPERACET = CH3CO3 + HCHO + OH + IPRENE ;
% J22 : HO12CO3C4 = CH3CO3 + HOCH2CHO + HO2 + IPRENE ;
% J22 : IEC2OOH = MGLYOX + OH + HOCH2CO3 + BP ;
% J22 : IEC1OOH = ACETOL + OH + HOCH2CO3 ;
% J22 : MVKOHBOOH = HOCH2CHO + HOCH2CO3 + OH ;
% J22 : MVKOHAOH = HOCH2CO3 + HOCH2CHO + HO2 ;
% J22 : MVKOHAOOH = MVKOHAO + OH ;
% J22 : C109OOH = C89CO3 + HCHO + OH ;
% J22 : C109OH = C89CO3 + HCHO + HO2 ;
% J22 : PINONIC = C96O2 + HO2 ;
% J22 : C96OOH = C96O + OH ;
% J22 : C96NO3 = C96O + NO2 ;
% J22 : C96OH = C96O + HO2 ;
% J22 : LIMALAOOH = C729CHO + OH + CH3CO3 + TPENE ;
% J22 : LIMALAOH = C729CHO + HO2 + CH3CO3 + TPENE ;
% J22 : LIMALBOOH = C822CO3 + HCHO + OH ;
% J22 : LIMALBOH = C822CO3 + HCHO + HO2 ;
% J22 : PERPINONIC = C96O2 + OH ;
% J22 : PINALOH = PINALO + HO2 ;
% J22 : C920CO3H = C920O2 + OH ;
% J22 : HOPINONIC = C920O2 + HO2 ;
% J22 : C920OOH = C920O + OH ;
% J22 : C97OOH = C97O + OH ;
% J22 : C97OH = C97O + HO2 ;
% J22 : C85CO3H = C85O2 + OH ;
% J22 : C85OOH = C85O + OH ;
% J22*2 : C817CO3H = C817O2 + OH ;
% J22*2 : KLIMONONIC = C817O2 + HO2 ;
% J22*2 : C817OOH = C817O + OH ;
% J22*2 : C817NO3 = C817O + NO2 ;
% J22*2 : C817OH = C818O2 + HO2 ;
% J22 : LMLKAOOH = C626CHO + OH + CH3CO3 + TPENE ;
% J22 : LMLKAOH = C626CHO + HO2 + CH3CO3 + TPENE ;
% J22 : LMLKBOOH = C731CO3 + HCHO + OH ;
% J22 : LMLKBOH = C731CO3 + HCHO + HO2 ;
% J22 : C921OOH = C921O + OH ;
% J22 : C735OOH = CO13C4CHO + CH3CO3 + OH + TPENE ;
% J22 : C735OH = CO13C4CHO + CH3CO3 + HO2 + TPENE ;
% J22 : MEKAOOH = MEKAO + OH ;
% J22 : MEKANO3 = MEKAO + NO2 ;
% J22 : MEKAOH = HOCH2CH2O2 + CH3CO3 + TPENE ;
% J22 : CHOC3COOOH = CHOC3COO2 + OH ;
% J22 : C413COOOH = CHOC3COO + OH ;

% J22 : C614CO = BIACETO2 + HOCH2CO3 ;
% J22*2 : H3C25CCO2H = H3C25C6O2 + HO2 ;
% J22 : C816OOH = C816O + OH ;
% J22*2 : H3C25CCO3H = H3C25C6O2 + OH ;
% J22*2 : H3C25C6OOH = H3C25C6O + OH ;
% J22*2 : H3C25C6OH = HMVKO2 + HOCH2CO3 ;
% J22*2 : C818OOH = C517CHO + CH3CO3 + OH + TPENE ;
% J22*2 : C818OH = C517CHO + CH3CO3 + HO2 + TPENE;
% J22*2 : C727CO3H = C727O2 + OH ;
% J22*2 : C819OOH = C819O + OH ;
% J22 : C922OOH = C922O + OH ;
% J22*2 : CO25C6CO2H = C627O2 + HO2 ;
% J22*2 : CO25C6CO3H = C627O2 + OH ;
% J22*2 : C627OOH = CO2C4CO3 + HCHO + OH ;
% J22*2 : C627OH = CO2C4CO3 + HCHO + HO2 ;
% J22 : C628OOH = CO13C4OH + CH3CO3 + OH + TPENE ;
% J22 : C628OH = CO13C4OH + CH3CO3 + HO2 + TPENE ;
% J22 : HOCO3C4OOH = HO1CO3C4O + OH ;
% J22 : HO14CO2C4 = HOCH2CO3 + HOCH2CH2O2 ;
% J22 : CO2C3CO3H = CH3COCH2O2 + OH ;
% J22 : H3C2C4CO2H = HMVKO2 + HO2 ;
% J22 : H3C2C4CO3H = HMVKO2 + OH ;
% J22 : C820OOH = C820O + OH ;
% J22 : CO13C4OH = HCOCH2O2 + HOCH2CO3 ;
% J22 : C825CO = C622CO3 + HO2 ;
% J22 : CO2C4CO3H = MEKAO2 + OH ;
% J22 : C621OOH = C621O + OH ;
% J22 : C520OOH = HOCH2COCHO + CH3CO3 + OH + TPENE ;
% J22 : C520OH = HOCH2COCHO + CH3CO3 + HO2 + TPENE ;
% J22 : C624CO = MACO3 + HOCH2CH2O2 ;
% J22 : C519CO3H = C519O2 + OH ;
% J22 : C629OOH = HO1CO3CHO + CH3CO3 + OH + TPENE ;
% J22 : C629OH = HO1CO3CHO + CH3CO3 + HO2 + TPENE ;
% J22 : C734CO = C517CO3 + HO2 ;
% J22 : C516OOH = C516O + OH ;
% J22 : C55OOH = C55O + OH ;
% J22 : C67CO3H = C55O2 + OH ;
% J22 : C519OOH = CH3CO3 + HOC2H4CHO + OH + TPENE ;
% J22 : HO13CO4C5 = CH3CO3 + HOC2H4CHO + HO2 + TPENE ;
% J22 : C625OOH = HOC2H4CO3 + ACETOL + OH ;
% J22 : C625OH = HOC2H4CO3 + ACETOL + HO2 ;
% J23 : MVK = C3H6 + CO ;
% J23 : MVKOH = ALLYLOH + CO ;
% J24 : C524CO = HOCH2CO3 + HOCH2CO3 + HCHO ;
% J24 : HCOC5 = CH3CO3 + HCHO + HOCH2CO3 + IPRENE ;

% J24 : MVK = CH3CO3 + HCHO + CO + HO2 + E ;
% J24 : MVKOH = HCHO + HO2 + HOCH2CO3 ;
% J24 : MVKOOH = HCHO + OH + ACO3 ;
% J31 : GLYOX = CO + CO + H2 ;
% J32 : GLYOX = HCHO + CO ;
% J33 : GLYOX = CO + CO + HO2 + HO2 ;
% J34 : CH3COCO2H = CH3CO3 + HO2 + IPRENE ;
% J34 : CH3COCOOH = CH3CO3 + HO2 + IPRENE ;
% J34 : VGLYOX = HO2 + CO + ACO3 ;
% J34 : HOCH2COCHO = HOCH2CO3 + CO + HO2 ;
% J34 : CO23C3CHO = CH3CO3 + CO + CO + HO2 + IPRENE ;
% J34 : MGLYOX = CH3CO3 + CO + HO2 + D ;
% J34 : HCOCO2H = HO2 + HO2 + CO ;
% J34 : INCGLYOX = MACRNBCO3 + CO + HO2 ;
% J34 : NMGLYOX = NO3CH2CO3 + CO + HO2 ;
% J34 : H1CO23CHO = CO + CO + HOCH2CO3 + HO2 ;
% J34 : HOCH2COCO2H = HOCH2CO3 + HO2 ;
% J34 : INB1GLYOX = MACRNCO3 + CO + HO2 ;
% J34 : HMVKNGLYOX = CO + CO + HOCH2CHO + NO2 + HO2 ;
% J34 : C109CO = C89CO3 + CO + HO2 ;
% J34 : LIMALBCO = C822CO3 + CO + HO2 ;
% J34 : LMLKBCO = C731CO3 + CO + HO2 ;
% J34 : H3C25C5CHO = H3C2C4CO3 + CO + HO2 ;
% J34 : CO123C5CHO = CHOC2CO3 + HO2 + CO + CO ;
% J34 : CO13C3CO2H = HCOCH2CO3 + HO2 ;
% J34 : CO235C5CHO = CO23C4CO3 + CO + HO2 ;
% J34 : C4CODIAL = HCOCH2CO3 + HO2 + CO ;
% J34 : C513CO = HOC2H4CO3 + HO2 + CO + CO ;
% J34 : CO2C4GLYOX = CO2C4CO3 + CO + HO2 ;
% J34 : C824CO = C624CO3 + CO + HO2 ;
% J34 : HO1CO3CHO = HOC2H4CO3 + HO2 + CO ;
% J34 : C87CO = C615CO3 + CO + HO2 ;
% J34 : CO12C4CHO = CHOC2CO3 + HO2 + CO ;
% J34 : C312COCO3H = CHOCOCH2O2 + OH ;
% J34 : ALCOCH2OOH = CHOCOCH2O + OH ;
% J34 : C813OOH = C813O + OH ;
% J34 : C813NO3 = C813O + NO2 ;
% J34 : C813OH = C813O + HO2 ;
% J34 : C515CO = HO2 + CO + CO + HCOCH2CO3 ;
% J34 : C615CO = CO1M22CO3 + CO + HO2 ;
% J34 : C733CO = C519CO3 + CO + HO2 ;
% J34 : MIBKHO4CHO = H2M2C3CO3 + HO2 + CO ;
% J35 : BIACETOH = CH3CO3 + HOCH2CO3 + IPRENE ;
% J35 : CH3COCO3H = CH3CO3 + OH + IPRENE ;
% J35 : CO23C3CHO = CH3CO3 + HCOCO3 + IPRENE ;

% J35 : CO23C4NO3 = NO3CH2CO3 + CH3CO3 + IPRENE ;
% J35 : H1CO23CHO = CO + CO + HOCH2CO3 + HO2 ;
% J35 : H14CO23C4 = HOCH2CO3 + HOCH2CO3 ;
% J35 : H1C23C4CHO = HCOCH2CO3 + HOCH2CO3 ;
% J35 : C820OOH = C820O + OH ;
% J35 : BIACETOOH = BIACETO + OH ;
% J35 : CO123C5CHO = CHOC2CO3 + HO2 + CO + CO ;
% J35 : C235C6CO3H = CO235C6O2 + OH ;
% J35 : C108OOH = C108O + OH ;
% J35 : LIMALACO = C729CO3 + CH3CO3 + TPENE ;
% J35 : C108NO3 = C108O + NO2 ;
% J35 : C108OH = C108O + HO2 ;
% J35 : C924CO = C622CO3 + CH3CO3 + TPENE ;
% J35 : CO235C6CHO = CHOC3COCO3 + CH3CO3 + TPENE ;
% J35 : LMLKACO = C626CO3 + CH3CO3 + TPENE ;
% J35 : C717OOH = C717O + OH ;
% J35 : C717NO3 = C717O + NO2 ;
% J35 : C717OH = C717O + HO2 ;
% J35 : C98OOH = C98O + OH ;
% J35 : C98NO3 = C98O + NO2 ;
% J35 : C98OH = C98O + HO2 ;
% J35 : CO235C6OOH = CO235C6O + OH ;
% J35 : C614OOH = C614O + OH ;
% J35 : C614NO3 = C614O + NO2 ;
% J35 : C614OH = C614O + HO2 ;
% J35 : C515CHO = HCOCH2CO3 + HCOCH2CO3 ;
% J35 : C513CO = HOC2H4CO3 + HO2 + CO + CO ;
% J35 : C727CO = CH3CO3 + CO2C4CO3 + TPENE ;
% J35 : CO23C4CHO = CH3CO3 + HCOCH2CO3 + TPENE ;
% J35 : C515CO3H = C515O2 + OH ;
% J35 : C515OOH = C515O + OH ;
% J35 : C821OOH = C821O + OH ;
% J35 : C515CO = HO2 + CO + CO + HCOCH2CO3 ;
% J35 : HC23C4CO3H = H1C23C4O2 + OH ;
% J35 : H1C23C4OOH = H1C23C4O + OH ;
% J35 : HO1CO34C5 = CH3CO3 + HOC2H4CO3 + TPENE ;
% J41 : ACO3H = HO2 + CO + HCHO + OH ;
% J41 : C2OHOCOOH = C3DIOLO2 ;
% J41 : C3DIOLOOH = C3DIOLO + OH ;
% J41 : C510OOH = C510O + OH ;
% J41 : C524OOH = C524O + OH ;
% J41 : C525OOH = C525O + OH ;
% J41 : C57NO3CO3H = HO12CO3C4 + NO2 + OH ;
% J41 : C57OOH = C57O + OH ;
% J41 : C58NO3CO3H = MACRNO3 + HO2 + OH ;

% J41 : C58OOH = C58O + OH ;
% J41 : C59OOH = C59O + OH ;
% J41 : CH3COCO3H = CH3CO3 + OH + IPRENE ;
% J41 : CH3CO3H = CH3O2 + OH ;
% J41 : CH3OOH = CH3O + OH ;
% J41 : CHOMOHCO3H = MGLYOX + OH + HO2 + BQ ;
% J41 : CO2N3PAN = MGLYOX + NO2 + NO3 + BR ;
% J41 : CO2N3CO3H = MGLYOX + NO2 + OH + BS ;
% J41 : CO2H3CO3H = MGLYOX + HO2 + OH + BT ;
% J41 : COHM2CO3H = GLYOX + HO2 + OH ;
% J41 : CONM2CO3H = MGLYOX + NO2 + OH + BU ;
% J41 : ETHO2HNO3 = ETHENO3O + OH ;
% J41 : H13CO2CO3H = HOCH2COCHO + HO2 + OH ;
% J41 : HC4ACO3H = ACETOL + CO + HO2 + OH ;
% J41 : HC4CCO3H = HOCH2CHO + CH3CO3 + OH + IPRENE ;
% J41 : HCOCH2OOH = HCOCH2O + OH ;
% J41 : HCOCO3H = HO2 + CO + OH ;
% J41 : HCOCOHCO3H = GLYOX + HO2 + OH ;
% J41 : HIEB1OOH = HIEB1O + OH ;
% J41 : HIEB2OOH = HIEB2O + OH ;
% J41 : HMACROOH = HMACRO + OH ;
% J41 : HMACO3H = HOCH2CO3 + HCHO + OH ;
% J41 : HOCH2CO3H = HCHO + HO2 + OH ;
% J41 : HOCHOCOOH = CHOCOHCO + OH ;
% J41 : HYETHO2H = HOCH2CH2O + OH ;
% J41 : HYPERACET = CH3COCH2O + OH ;
% J41 : HYPROPO2H = HYPROPO + OH ;
% J41 : IC3H7OOH = IC3H7O + OH ;
% J41 : IEACO3H = HMVKO2 + OH ;
% J41 : IEB1OOH = IEB1O + OH ;
% J41 : IEB2OOH = IEB2O + OH ;
% J41 : IEC1OOH = IEC1O + OH ;
% J41 : IECCO3H = MACRO2 + OH ;
% J41 : INAHCO3H = MVKNO3 + HO2 + OH ;
% J41 : INAHPCHO = MVKNO3 + OH + CO + HO2 ;
% J41 : INAHPCO2H = MVKNO3 + OH + HO2 ;
% J41*2 : INAHPCO3H = MVKNO3 + OH + OH ;
% J41 : INAHPPAN = MVKNO3 + OH + NO3 ;
% J41 : INANCO3H = MVKNO3 + NO2 + OH ;
% J41 : INANCOCO3H = NO2 + CO23C4NO3 + OH ;
% J41 : INAOOH = INAO + OH ;
% J41 : INB1HPCO3H = MACRNO3 + OH + OH ;
% J41 : INB1NACO3H = MACRNO3 + NO2 + OH ;
% J41 : INB1NBCO3H = MVKNO3 + NO2 + OH ;
% J41 : INB1OOH = INB1O + OH ;

% J41 : INB2OOH = INB2O + OH ;
% J41 : INCOOH = INCO + OH ;
% J41 : INCNCO3H = MACRNO3 + NO2 + OH ;
% J41 : INDHCO3H = MVKNO3 + OH + HO2 ;
% J41 : INDOOH = INDO + OH ;
% J41 : INDHPCHO = CO + HO2 + MVKNO3 + OH ;
% J41*2 : INDHPCO3H = MVKNO3 + OH + OH ;
% J41 : INDHPPAN = MVKNO3 + OH + NO3 ;
% J41 : IPRHOCO3H = CH3COCH3 + HO2 + OH ;
% J41 : IPROPOLO2H = IPROPOLO + OH ;
% J41 : IPROPOLPER = CH3CHO + HO2 + OH ;
% J41 : ISOPAOOH = ISOPAO + OH ;
% J41 : ISOPBOOH = ISOPBO + OH ;
% J41 : ISOPCOOH = ISOPCO + OH ;
% J41 : ISOPDOOH = ISOPDO + OH ;
% J41 : MACO3H = CH3C2H2O2 + OH ;
% J41 : MACROHOOH = MACROHO + OH ;
% J41 : MACROOH = MACRO + OH ;
% J41 : MACRNBCO3H = NOA + HO2 + OH ;
% J41 : MACRNCO3H = ACETOL + NO2 + OH ;
% J41 : MMALNACO3H = CONM2CHO + HO2 + OH ;
% J41 : MMALNBCO3H = CO2H3CHO + NO2 + OH ;
% J41 : MVKOHBOOH = MVKOHBO + OH ;
% J41 : MVKOHAOOH = MVKOHAO + OH ;
% J41 : MVKOOH = MVKO + OH ;
% J41 : NC4CO3H = NOA + CO + HO2 + OH ;
% J41 : NC524OOH = NC524O + OH ;
% J41 : NISOPOOH = NISOPO + OH ;
% J41 : NO3CH2CO3H = HCHO + NO2 + OH ;
% J41 : OCCOHCOOH = OCCOHCO + OH ;
% J41 : PR1O2HNO3 = PRONO3AO + OH ;
% J41 : PR2O2HNO3 = PRONO3BO + OH ;
% J41 : PRNO3CO3H = CH3CHO + NO2 + OH ;
% J41 : ALCOCH2OOH = CHOCOCH2O + OH ;
% J41 : APINAOOH = APINAO + OH ;
% J41 : APINBOOH = APINBO + OH ;
% J41 : APINCOOH = APINCO + OH ;
% J41 : BPINAOOH = BPINAO + OH ;
% J41 : BPINBOOH = BPINBO + OH ;
% J41 : BPINCOOH = BPINCO + OH ;
% J41 : BIACETOOH = BIACETO + OH ;
% J41 : C106OOH = C106O + OH ;
% J41 : C107OOH = C107O + OH ;
% J41 : C108OOH = C108O + OH ;
% J41 : C109OOH = C109O + OH ;

% J41 : C235C6CO3H = CO235C6O2 + OH ;
% J41 : C312COCO3H = CHOCOCH2O2 + OH ;
% J41 : C413COOOH = CHOC3COO + OH ;
% J41 : C44OOH = C44O + OH ;
% J41 : C511CO3H = C511O2 + OH ;
% J41 : C511OOH = C511O + OH ;
% J41 : C512CO3H = C512O2 + OH ;
% J41 : C512OOH = C512O + OH ;
% J41 : C513OOH = C513O + OH ;
% J41 : C514OOH = C514O + OH ;
% J41 : C515CO3H = C515O2 + OH ;
% J41 : C515OOH = C515O + OH ;
% J41 : C516OOH = C516O + OH ;
% J41 : C517CO3H = C517O2 + OH ;
% J41 : C517OOH = C517O + OH ;
% J41 : C518CO3H = ISOPDO2 + OH ;
% J41 : C519CO3H = C519O2 + OH ;
% J41 : C519OOH = C519O + OH ;
% J41 : C520OOH = C520O + OH ;
% J41 : C55OOH = C55O + OH ;
% J41 : C614OOH = C614O + OH ;
% J41 : C615CO3H = C615O2 + OH ;
% J41 : C615OOH = C615O + OH ;
% J41 : C616OOH = C616O + OH ;
% J41 : C617CO3H = C617O2 + OH ;
% J41 : C617OOH = C617O + OH ;
% J41 : C618CO3H = C618O2 + OH ;
% J41 : C618OOH = C618O + OH ;
% J41 : C619OOH = C619O + OH ;
% J41 : C620OOH = C620O + OH ;
% J41 : C622CO3H = C622O2 + OH ;
% J41 : C621OOH = C621O + OH ;
% J41 : C622OOH = C622O + OH ;
% J41 : C623OOH = C623O + OH ;
% J41 : C624CO3H = C624O2 + OH ;
% J41 : C624OOH = C624O + OH ;
% J41 : C625OOH = C625O + OH ;
% J41 : C626CO3H = C626O2 + OH ;
% J41 : C626OOH = C626O + OH ;
% J41 : C627OOH = C627O + OH ;
% J41 : C628OOH = C628O + OH ;
% J41 : C629OOH = C629O + OH ;
% J41 : C67CO3H = C55O2 + OH ;
% J41 : C716OOH = C716O + OH ;
% J41 : C717OOH = C717O + OH ;

% J41 : C718CO3H = C718O2 + OH ;
% J41 : C718OOH = C718O + OH ;
% J41 : C719OOH = C719O + OH ;
% J41 : C720OOH = C720O + OH ;
% J41 : C721CO3H = C721O2 + OH ;
% J41 : C721OOH = C721O + OH ;
% J41 : C722OOH = C722O + OH ;
% J41 : C727CO3H = C727O2 + OH ;
% J41 : C727OOH = C727O + OH ;
% J41 : C728OOH = C728O + OH ;
% J41 : C729CO3H = C729O2 + OH ;
% J41 : C729OOH = C729O + OH ;
% J41 : C730OOH = C730O + OH ;
% J41 : C731CO3H = C731CO2 + OH ;
% J41 : C731OOH = C731O + OH ;
% J41 : C732CO3H = C732O2 + OH ;
% J41 : C732OOH = C732O + OH ;
% J41 : C733OOH = C733O + OH ;
% J41 : C734OOH = C734O + OH ;
% J41 : C735OOH = C735O + OH ;
% J41 : C810OOH = C810O + OH ;
% J41 : C811CO3H = C811O2 + OH ;
% J41 : C811OOH = C811O + OH ;
% J41 : C812OOH = C812O + OH ;
% J41 : C813OOH = C813O + OH ;
% J41 : C816CO3H = C816O2 + OH ;
% J41 : C816OOH = C816O + OH ;
% J41 : C817CO3H = C817O2 + OH ;
% J41 : C817OOH = C817O + OH ;
% J41 : C818OOH = C818O + OH ;
% J41 : C819OOH = C819O + OH ;
% J41 : C820OOH = C820O + OH ;
% J41 : C821OOH = C821O + OH ;
% J41 : C822CO3H = C822CO2 + OH ;
% J41 : C822OOH = C822O + OH ;
% J41 : C823CO3H = C823O2 + OH ;
% J41 : C823OOH = C823O + OH ;
% J41 : C824OOH = C824O + OH ;
% J41 : C825OOH = C825O + OH ;
% J41 : C826OOH = C826O + OH ;
% J41 : C85CO3H = C85O2 + OH ;
% J41 : C85OOH = C85O + OH ;
% J41 : C86OOH = C86O + OH ;
% J41 : C87CO3H = C87O2 + OH ;
% J41 : C87OOH = C87O + OH ;

% J41 : C88CO3H = C88O2 + OH ;
% J41 : C88OOH = C88O + OH ;
% J41 : C89CO3H = C89CO2 + OH ;
% J41 : C89OOH = C89O + OH ;
% J41 : C8BCOOH = C8BCO + OH ;
% J41 : C914OOH = C914O + OH ;
% J41 : C915OOH = C915O + OH ;
% J41 : C916OOH = C916O + OH ;
% J41 : C917OOH = C917O + OH ;
% J41 : C918CO3H = NOPINONE + HO2 + OH ;
% J41 : C918OOH = C918O + OH ;
% J41 : C919OOH = C919O + OH ;
% J41 : C920CO3H = C920O2 + OH ;
% J41 : C920OOH = C920O + OH ;
% J41 : C921OOH = C921O + OH ;
% J41 : C922OOH = C922O + OH ;
% J41 : C923CO3H = C923O2 + OH ;
% J41 : C923OOH = C923O + OH ;
% J41 : C924OOH = C924O + OH ;
% J41 : C925OOH = C925O + OH ;
% J41 : C926OOH = C926O + OH ;
% J41 : C96OOH = C96O + OH ;
% J41 : C97OOH = C97O + OH ;
% J41 : C98OOH = C98O + OH ;
% J41 : C9DCOOH = C9DCO + OH ;
% J41 : CHOC3COOOH = CHOC3COO2 + OH ;
% J41 : CHOC2CO3H = CHOC2H4O2 + OH ;
% J41 : CHOC2H4OOH = CHOC2H4O + OH ;
% J41 : CO23C4CO3H = BIACETO2 + OH ;
% J41 : CO235C6OOH = CO235C6O + OH ;
% J41 : CO25C6CO3H = C627O2 + OH ;
% J41 : CO2C3CO3H = CH3COCH2O2 + OH ;
% J41 : CO2C4CO3H = MEKAO2 + OH ;
% J41 : CO1M22CO3H = IBUTALCO2 + OH ;
% J41 : H1C23C4OOH = H1C23C4O + OH ;
% J41 : H2M2C3CO3H = TBUTOLO2 + OH ;
% J41 : H3C25C6OOH = H3C25C6O + OH ;
% J41 : H3C25CCO3H = H3C25C6O2 + OH ;
% J41 : H3C2C4CO3H = HMVKO2 + OH ;
% J41 : HC23C4CO3H = H1C23C4O2 + OH ;
% J41 : HCOCH2CO3H = HCOCH2O2 + OH ;
% J41 : HOC2H4CO3H = HOCH2CH2O2 + OH ;
% J41 : HOCH2CO3H = HCHO + HO2 + OH ;
% J41 : HOCO3C4OOH = HO1CO3C4O + OH ;
% J41 : HMVKBCO3H = HMVKO2 + OH ;

```
% J41 : IBUTALO2H = M2PROPAL2O + OH ;
% J41 : LIMALAOOH = LIMALAO + OH ;
% J41 : LIMALBOOH = LIMALBO + OH ;
% J41 : LIMAOOH = LIMAO + OH ;
% J41 : LIMBOOH = LIMBO + OH ;
% J41 : LIMCOOH = LIMCO + OH ;
% J41 : LIMALOOH = LIMALO + OH ;
% J41 : LMKAOOH = LMKAO + OH ;
% J41 : LMKBOOH = LMKBO + OH ;
% J41 : LMLKAOOH = LMLKAO + OH ;
% J41 : LMLKBOOH = LMLKBO + OH ;
% J41 : MEKAOOH = MEKAO + OH ;
% J41 : NAPINAOOH = NAPINAO + OH ;
% J41 : NAPINBOOH = NAPINBO + OH ;
% J41 : NBPINAOOH = NBPINAO + OH ;
% J41 : NBPINBOOH = NBPINBO + OH ;
% J41 : NC101OOH = NC101O + OH ;
% J41 : NC102OOH = NC102O + OH ;
% J41 : NC61CO3H = CO235C5CHO + NO2 + OH ;
% J41 : NC623OOH = NC623O + OH ;
% J41 : NC71OOH = NC71O + OH ;
% J41 : NC728OOH = NC728O + OH ;
% J41 : NC72OOH = NC72O + OH ;
% J41 : NC730OOH = NC730O + OH ;
% J41 : NC826OOH = NC826O + OH ;
% J41 : NC91CO3H = NOPINONE + NO2 + OH ;
% J41 : NLIMALOOH = NLIMALO + OH ;
% J41 : NLIMOOH = NLIMO + OH ;
% J41 : NLMKAOOH = NLMKAO + OH ;
% J41 : NOPINAOOH = NOPINAO + OH ;
% J41 : NOPINBOOH = NOPINBO + OH ;
% J41 : NOPINCOOH = NOPINCO + OH ;
% J41 : NOPINDOOH = NOPINDO + OH ;
% J41 : NORLIMOOH = NORLIMO + OH ;
% J41 : PERPINONIC = C96O2 + OH ;
% J41 : PINALOOH = PINALO + OH ;
% J41 : TBUTOLOOH = TBUTOLO + OH ;
% J51 : CH3NO3 = CH3O + NO2 ;
% J53 : ISOPANO3 = ISOPAO + NO2 ;
% J53 : ISOPCNO3 = ISOPCO + NO2 ;
% J53*2.0 : NISOPNO3 = NISOPO + NO2 ;
% J53 : NMGLYOX = NO2 + HCHO + CO + CO + HO2 ;
% J53 : C823NO3 = C823O + NO2 ;
% J53 : C96NO3 = C96O + NO2 ;
% J53 : C923NO3 = C923O + NO2 ;
```

% J53 : C817NO3 = C817O + NO2 ;
% J53 : C729NO3 = C729O + NO2 ;
% J53 : C512NO3 = C512O + NO2 ;
% J53 : C626NO3 = C626O + NO2 ;
% J53 : C822NO3 = C822O + NO2 ;
% J53 : MEKANO3 = MEKAO + NO2 ;
% J53 : C811NO3 = C811O + NO2 ;
% J53 : C622NO3 = C622O + NO2 ;
% J53 : C517NO3 = C517O + NO2 ;
% J53 : C718NO3 = C718O + NO2 ;
% J53 : C731NO3 = C731O + NO2 ;
% J53 : C732NO3 = C732O + NO2 ;
% J54 : C524NO3 + OH = C524O + NO2 ;
% J54 : IC3H7NO3 = IC3H7O + NO2 ;
% J54 : ISOPDNO3 = ISOPDO + NO2 ;
% J54 : NOPINBNO3 = NOPINBO + NO2 ;
% J54 : NOPINANO3 = NOPINAO + NO2 ;
% J54 : C720NO3 = C720O + NO2 ;
% J54 : C8BCNO3 = C8BCO + NO2 ;
% J54 : C9DCNO3 = C9DCO + NO2 ;
% J54 : C915NO3 = C915O + NO2 ;
% J54 : C717NO3 = C717O + NO2 ;
% J54 : C916NO3 = C916O + NO2 ;
% J54 : C514NO3 = C514O + NO2 ;
% J54 : ISOPDNO3 = ISOPDO + NO2 ;
% J54 : C624NO3 = C624O + NO2 ;
% J55 : ISOPBNO3 = ISOPBO + NO2 ;
% J55 : NC71CO = CO235C6CO3 + NO2 ;
% J55 : MACROHNO3 = MACROHO + NO2 ;
% J55 : C810NO3 = C810O + NO2 ;
% J55 : C919NO3 = C919O + NO2 ;
% J55 : C98NO3 = C98O + NO2 ;
% J55 : C106NO3 = C106O + NO2 ;
% J55 : C89NO3 = C89O + NO2 ;
% J55 : C917NO3 = C917O + NO2 ;
% J55 : NC101CO = C96CO3 + NO2 ;
% J55 : APINCNO3 = APINCO + NO2 ;
% J55 : BPINCNO3 = BPINCO + NO2 ;
% J55 : NOPINCNO3 = NOPINCO + NO2 ;
% J55 : PINALNO3 = PINALO + NO2 ;
% J55 : C108NO3 = C108O + NO2 ;
% J55 : C918NO3 = C918O + NO2 ;
% J55 : C813NO3 = C813O + NO2 ;
% J56 : CHOPRNO3 = PROPALO + NO2 ;
% J56 : CO23C4NO3 = BIACETO + NO2 ;

```
% J56 : CONM2CHO = MGLYOX + NO2 + CO + HO2 + BV ;
% J56 : CONM2CO2H = CO + HO2 + NO2 + CH3COCO2H ;
% J56 : CONM2CO3H = CO + HO2 + NO2 + CH3COCO3H ;
% J56 : CONM2PAN = CO + HO2 + NO2 + CH3COPAN ;
% J56 : HMVKNO3 = HOCH2CHO + NO2 + CO + CO + HO2 ;
% J56 : INANCO = ACETOL + NO2 + NO3CH2CO3 ;
% J56 : INB1CO = ACETOL + NO2 + HOCH2CO3 ;
% J56 : INANCOCO2H = NO3CH2CO3 + CH3COCO2H + NO2 ;
% J56 : INANCOCO3H = NO3CH2CO3 + CH3COCO3H + NO2 ;
% J56 : INANCOPAN = NO3CH2CO3 + CH3COPAN + NO2 ;
% J56 : MMALNACO2H = MGLYOX + NO2 + HCOCO2H + BW ;
% J56 : MMALNACO3H = MGLYOX + NO2 + HCOCO3H + BX ;
% J56 : MMALNAPAN = MGLYOX + NO2 + GLYPAN;
% J56 : MVKNO3 = CH3CO3 + HOCH2CHO + NO2;
% J56 : NOA = CH3COCH2O + NO2 ;
% J56 : NO3CH2CHO = NO2 + HCOCH2O ;
% J57 : CHOPRNO3 = HO2 + CO + CH3CHO + NO2 ;
% J57 : CO23C4NO3 = HCHO + CH3CO3 + NO2 + CO;
% J57*2 : CONM2CHO = MGLYOX + NO2 + CO + HO2;
% J57 : CONM2CO2H = CO + HO2 + NO2 + CH3COCO2H ;
% J57 : CONM2CO3H = CO + HO2 + NO2 + CH3COCO3H ;
% J57 : CONM2PAN = CO + HO2 + NO2 + CH3COPAN ;
% J57 : HMVKNO3 = HOCH2CHO + NO2 + CO + CO + HO2 ;
% J57 : INANCO = ACETOL + NO2 + NO3CH2CO3 ;
% J57 : INANCOCO2H = NO3CH2CO3 + CH3COCO2H + NO2 ;
% J57 : INANCOCO3H = NO3CH2CO3 + CH3COCO3H + NO2 ;
% J57 : INANCOPAN = NO3CH2CO3 + CH3COPAN + NO2 ;
% J57 : INB1CO = ACETOL + NO2 + HOCH2CO3 ;
% J57 : MMALNACO2H = MGLYOX + NO2 + HCOCO2H;
% J57 : MMALNACO3H = MGLYOX + NO2 + HCOCO3H;
% J57 : MMALNAPAN = MGLYOX + NO2 + GLYPAN;
% J57 : MVKNO3 = CH3CO3 + HOCH2CHO + NO2;
% J57 : NOA = CH3CO3 + HCHO + NO2;
% J57 : NO3CH2CHO = HO2 + CO + HCHO + NO2 ;
% J58*0.25 : HPALD = OH + HO2 + ACETOL + GLYOX ;
% J58*0.25 : HPALD = OH + HO2 + ACETOL + HCHO + HCHO ;
% J58*0.25 : HPALD = OH + HO2 + MGLYOX + HOCH2CHO;
% J58*0.25 : HPALD = OH + HO2 + MGLYOX + HCHO + HCHO;
**;
```